MOLECULAR PATHOMECHANISMS OF MUSCULAR DYSTROPHIES

Jaakko Sarparanta

Folkhälsan Institute of Genetics and
Department of Medical Genetics, Haartman Institute

Genetics, Department of Biosciences

Helsinki Graduate Program in Biotechnology and Molecular Biology

University of Helsinki
Helsinki, Finland

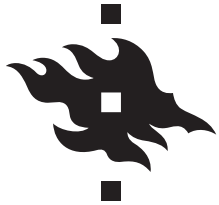

HELSINGIN YLIOPISTO
HELSINGFORS UNIVERSITET
UNIVERSITY OF HELSINKI

folkhälsan

ACADEMIC DISSERTATION

To be presented for public examination, with the permission of
the Faculty of Biological and Environmental Sciences of the University of Helsinki,
in lecture hall 3, Biomedicum Helsinki, on 22 November 2013, at 12 noon.

Helsinki 2013

Supervisors

Professor Bjarne Udd, MD, PhD

Folkhälsan Institute of Genetics and Dept. of Medical Genetics, Haartman Institute, University of Helsinki; Helsinki, Finland

Neuromuscular Research Center, University of Tampere and Tampere University Hospital; Tampere, Finland

Dept. of Neurology, Vaasa Central Hospital; Vaasa, Finland

Docent Peter Hackman, PhD

Folkhälsan Institute of Genetics and Dept. of Medical Genetics, Haartman Institute, University of Helsinki; Helsinki, Finland

Thesis follow-up group

Professor Hannu Kalimo, MD, PhD

Dept. of Pathology, Haartman Institute, University of Helsinki; Helsinki, Finland

Docent Aija Kyttälä, PhD

Institute for Molecular Medicine Finland; Helsinki, Finland

National Institute for Health and Welfare; Helsinki, Finland

Reviewers

Docent Aija Kyttälä, PhD

Institute for Molecular Medicine Finland; Helsinki, Finland

National Institute for Health and Welfare; Helsinki, Finland

Docent Katarina Pelin, PhD

Genetics, Dept. of Biosciences, University of Helsinki; Helsinki, Finland

Opponent

Professor Alan H. Beggs, PhD

Dept. of Pediatrics, Harvard Medical School; Boston, USA

Division of Genetics and Genomics, The Manton Center for Orphan Disease Research, Boston Children's Hospital; Boston, USA

Custos

Professor Minna Nyström, PhD

Genetics, Dept. of Biosciences, University of Helsinki, Helsinki, Finland

ISBN 978-952-10-9418-7 (paperback)
ISBN 978-952-10-9419-4 (PDF)
http://ethesis.helsinki.fi

Unigrafia Oy
Helsinki 2013

To my family

CONTENTS

LIST OF ORIGINAL PUBLICATIONS

This thesis is based on the following original articles, referred to in the text by their Roman numerals. In addition, some unpublished data are presented.

I **Sarparanta J**, Blandin G, Charton K, Vihola A, Marchand S, Milic A, Hackman P, Ehler E, Richard I & Udd B: Interactions with M-band titin and calpain 3 link myospryn (CMYA5) to tibial and limb-girdle muscular dystrophies. *Journal of Biological Chemistry* 2010, 285(39): 30304–30315 (doi:10.1074/jbc.M110.108720)

II **Sarparanta J***, Jonson PH*, Golzio C*, Sandell S, Luque H, Screen M, McDonald K, Stajich JM, Mahjneh I, Vihola A, Raheem O, Penttilä S, Lehtinen S, Huovinen S, Palmio J, Tasca G, Ricci E, Hackman P, Hauser M, Katsanis N & Udd B (*equal contribution): Mutations affecting the cytoplasmic functions of the co-chaperone DNAJB6 cause limb-girdle muscular dystrophy. *Nature Genetics* 2012, 44(4): 450–455 (doi:10.1038/ng.1103)

III Hackman P*, **Sarparanta J***, Lehtinen S, Vihola A, Evilä A, Jonson PH, Luque H, Kere J, Screen M, Chinnery PF, Åhlberg G, Edström L & Udd B (*equal contribution): Welander distal myopathy is caused by a mutation in the RNA-binding protein TIA1. *Annals of Neurology* 2013, 73(4): 500–509 (doi:10.1002/ana.23831)

The topic of the thesis is restricted to the molecular pathomechanisms of muscular dystrophies, and only the studies and results concerning this aspect of the original articles will be discussed in the experimental part of the thesis. Disease genetics, even for the part included in original publications, is considered necessary background information for the functional studies, and will be therefore covered in the Review of the literature.

AUTHOR CONTRIBUTIONS

I	
Titin M10 interaction screen	JS, PH, BU
CAPN3 interaction screen	GB, AM, SM, IR
Pairwise Y2H studies	JS
Coimmunoprecipitation studies	JS
Coexpression studies of titin and CAPN3	KC
Muscle samples and microscopy	JS, AV
Proximity ligation assays	JS
NRC culture and microscopy	EE, JS
Writing the paper	JS, PH, EE, IR, BU
II	
Recruitment and evaluation of patients	BU, SS, JMS, JP, GT, ER, IM
Human genetics	HL, SL, KM, SP, MS, PH
Plasmid constructs	JS, CG, HL, KM
Microscopic analyses of muscle samples	AV, JS, OR, SH
Electron microscopy	SH
Zebrafish experiments	CG
Oligomerization studies	JS, PHJ, HL
Filter trap assays	JS, PHJ, HL
Protein turnover assays	CG
Coimmunoprecipitation studies	JS, PHJ, HL
Proximity ligation assays	JS, HL
Writing the paper	JS, PHJ, CG, MH, NK, BU
III	
Recruitment and evaluation of patients	BU, PFC, GÅ, LE
Human genetics	PH, SL, AE, HL, JK, MS
Microscopic analyses of muscle samples	AV
Plasmid constructs	SL, JS, HL
Western blot analyses	AV, JS, PHJ, HL
Antibody characterization	JS, PHJ, HL
Splicing analyses	JS, HL, PH
Cell biological studies	JS, PHJ, AV, HL
High-content analysis	JS, HL
FRAP	JS
Writing the paper	PH, JS, AV, PHJ, BU

ABBREVIATIONS

5'TOP	5'-terminal oligopyrimidine tract
aa	amino acid(s)
A-band	anisotropic band in the sarcomere
ALS	amyotrophic lateral sclerosis
ARE	adenine/uridine (AU) -rich element
ATP	adenosine triphosphate
BLOC-1	biogenesis of lysosome-related organelles complex 1
CASA	chaperone-assisted selective autophagy
CFP	cyan fluorescent protein
CHX	cycloheximide
CoIP	coimmunoprecipitation
CTD	C-terminal domain (in DNAJB6)
DCM	dilated cardiomyopathy
DGC	dystrophin–glycoprotein complex
eIF	eukaryotic initiation factor
EM	electron microscopy
FHL proteins	four-and-a-half LIM domain proteins
FN3 domain	fibronectin type 3 -like domain
FRAP	fluorescence recovery after photobleaching
FTA	filter trap assay
G/F domain	glycine/phenylalanine-rich domain
GDP	guanosine diphosphate
GFP	green fluorescent protein
GTP	guanosine triphosphate
HA	hemagglutinin
hnRNP	heterogeneous nuclear ribonucleoprotein
HSP	heat shock protein
I-band	isotropic band in the sarcomere
IF	immunofluorescence
Ig domain	immunoglobulin-like domain
is	insertion sequence (in titin)
IS1, IS2	insertion sequences 1 and 2 (in calpain 3)
K8/K18/K19	keratin 8/18/19
kDa	kilodalton
KI	knock-in
KO	knockout
LGMD	limb-girdle muscular dystrophy
M1–M10	M-band domains 1–10 in titin
MAPK	mitogen-activated protein kinase
MARP(s)	muscle ankyrin repeat protein(s)
M-band	structure in the middle of the sarcomere, Mittelscheibe
Mex1–Mex6	M-band exons 1–6 in *TTN*
MFM	myofibrillar myopathy
MIM	Mendelian Inheritance in Man
M-is1–M-is7	M-band insertion sequences 1–7 in titin
MLP	muscle LIM protein

mRNP	messenger ribonucleoprotein (particle)
MURF	muscle RING finger protein
MyBP-C	myosin-binding protein C
N2B-us	unique sequence region of the titin N2B element
NMD	nonsense-mediated decay
NFAT	nuclear factor of activated T-cell
NS	N-terminal sequence (in calpain 3)
PB	processing body
PBS	phosphate-buffered saline
PEVK	titin region rich in proline, glutamate, valine, and lysine
PKA	protein kinase A
PLA	proximity ligation assay
PRD	prion-related domain
RIPA	radioimmunoprecipitation assay buffer
RNAi	RNA interference
RRM	RNA recognition motif
RT-PCR	reverse transcription – polymerase chain reaction
RyR	ryanodine receptor
S.D.	standard deviation
SG	stress granule
snRNP	small nuclear ribonucleoprotein (particle)
SR	sarcoplasmic reticulum
SRF	serum response factor
SUMO	small ubiquitin-like modifier
TA	tibialis anterior muscle
TK	kinase domain of titin
TMD	tibial muscular dystrophy
TRIM	tripartite motif
T-tubule	transverse tubule
UTR	untranslated region
WB	western blotting
WDM	Welander distal myopathy
Y2H	yeast two-hybrid
YFP	yellow fluorescent protein
ZASP	Z-disc alternatively spliced protein (LDB3)
Z-disc	structure at the edge of adjacent sarcomeres, Zwischenscheibe

In addition, standard abbreviations of amino acids and approved symbols of human genes and proteins are used.

ABSTRACT

This study aimed at elucidating molecular pathways behind muscular dystrophies, inherited disorders causing progressive weakness and loss of skeletal muscle, with the perspectives of demonstrating the pathogenicity of newly identified mutations, understanding the biology of muscle diseases, and finding options for their treatment.

Tibial muscular dystrophy (TMD) and limb-girdle muscular dystrophy type 2J (LGMD2J) are caused by mutations in the C-terminal (M-band) part of the sarcomeric protein titin, whereas LGMD2A results from mutations in the muscle-specific protease calpain 3 (CAPN3). In yeast two-hybrid studies aiming at identifying proteins secondarily affected in the diseases, the multifunctional TRIM-related protein myospryn (CMYA5) was identified as a novel binding partner for both M-band titin and CAPN3. The interactions were confirmed by coimmunoprecipitation, and localization of myospryn at the M-band level was supported by multiple methods. Coexpression studies identified myospryn as a proteolytic substrate for CAPN3, and suggested that myospryn may attenuate its autolytic activation. The biological role of the titin–myospryn interaction remained unresolved, and the mouse model of TMD/LGMD2J showed normal myospryn localization. However, since the TMD/LGMD2J mutations disrupt the myospryn binding site in titin, they are likely to have a downstream functional effect on myospryn.

LGMD1D is caused by dominant mutations in the ubiquitous co-chaperone DNAJB6. LGMD1D muscle showed a myofibrillar pathology, with cytoplasmic accumulations of DNAJB6, aggregated Z-disc-associated proteins, and autophagic rimmed vacuoles. Expression of DNAJB6 constructs in zebrafish embryos confirmed a toxic effect of the mutant cytoplasmic DNAJB6b isoform, and cell culture studies demonstrated a slower turnover and impaired anti-aggregation activity of mutant DNAJB6. Protein interaction studies indicated an association of DNAJB6 with the chaperone-assisted selective autophagy (CASA) pathway, and a modulatory effect of BAG3 on DNAJB6 pathogenicity in zebrafish suggested that CASA has active role in the pathogenesis of LGMD1D.

Welander distal myopathy (WDM) results from a dominant mutation in the prion-related domain (PRD) of the RNA-binding protein TIA1, a regulator of splicing and translation, and a component of stress granules (SGs). RT-PCR analysis of selected TIA1 target genes did not show splicing changes in WDM muscle, suggesting that the pathogenesis does not involve extensive mis-splicing. IF microscopy revealed accumulation of TIA1 and other SG proteins in WDM muscle, while image analysis of transfected cells, and fluorescence recovery after photobleaching (FRAP) studies indicated a mild increase in the SG-forming propensity of mutant TIA1. These findings suggest that increased aggregation of the TIA1 PRD causes muscle pathology in WDM, either directly through inappropriate protein aggregation or indirectly by compromising cellular metabolism.

TIIVISTELMÄ

Lihasrappeumat ovat perinnöllisiä sairauksia, jotka johtavat luurankolihasten etenevään heikkouteen ja surkastumiseen. Ne aiheutuvat geenivirheistä useissa lihassyyn rakenneosissa, ja monet sairauteen johtavista molekyylitason mekanismeista tunnetaan huonosti. Tässä väitöskirjassa tutkittiin joidenkin lihasrappeumien tautimekanismeja, tavoitteena osoittaa tunnistettujen geenivirheiden patogeenisuus sekä ymmärtää lihastautien molekyylibiologiaa, esimerkiksi hoitojen kehittämistä ajatellen.

Suomalaiseen tautiperintöön kuuluvat tibiaalinen lihasdystrofia (TMD) ja hartia-lantiotyypin lihasrappeuma 2J (LGMD2J) aiheutuvat virheistä titiinissä, sarkomeerien keskeisessä rakenne- ja säätelyproteiinissa. Tutkimuksessa tunnistettiin titiinin viallisen osan sitoutumiskumppaniksi myospryyni (myospryn, CMYA5), joka toimii solun kalvoliikenteessä ja viestinvälityksessä. TMD/LGMD2J-hiirimallin lihaksessa ei havaittu poikkeavaa myospryynin sijoittumista, mutta toiminnallinen vaikutus myospryyniin on todennäköinen. Myospryyni tunnistettiin myös LGMD2A-lihasrappeuman taustalla olevan kalpaiini 3 -proteaasin substraatiksi ja mahdolliseksi säätelijäksi. Kuvatut proteiinivuorovaikutukset lisäävät lihaksen molekyylibiologian perustuntemusta ja voivat jatkossa auttaa TMD/LGMD2J- ja LGMD2A-tautien synnyn ymmärtämisessä.

Hartia-lantiotyypin lihasrappeuma 1D (LGMD1D) aiheutuu proteiinien laadunvalvontakoneistoon kuuluvan kaitsijaproteiini DNAJB6:n geenivirheistä, joiden seurauksena lihassyihin kertyy proteiinisakkautumia. DNAJB6:n virheellisen muodon todettiin aiheuttavan lihastautia seeprakalan alkiossa tuotettuna, mikä sopii yhteen LGMD1D:n vallitsevan periytymismallin kanssa. Soluviljelmissä havaittiin, että geenivirheet hidastavat DNAJB6:n hajotusta sekä haittaavat kaitsijaproteiinin kykyä estää proteiinien aggregaatiota. Tutkimuksissa onnistuttiin myös vahvistamaan DNAJB6:n epäilty vuorovaikutus hiljattain kuvatun ja lihaksen toiminnalle tärkeäksi todetun CASA-mekanismin (chaperone-assisted selective autophagy, kaitsijaproteiiniavusteinen selektiivinen autofagia) kanssa sekä saatiin viitteitä tämän autofagiareitin suorasta osallisuudesta LGMD1D:n synnyssä.

Ruotsissa ja Suomessa melko yleinen Welanderin distaalinen myopatia (WDM) aiheutuu geenivirheistä TIA1:ssä, joka on lähetti-RNA:n silmukoinnin ja proteiinitranslaation säätelijä sekä soluihin stressitilanteissa muodostuvien stressijyvästen (stress granule) rakenneosa. Tutkittujen TIA1:n kohdegeenien silmukoinnissa ei todettu muutoksia WDM-lihaksessa. Sen sijaan lihasnäytteissä nähtiin TIA1:n ja muiden proteiinien kasaumia, ja soluviljelmissä tehdyissä toiminnallisissa kokeissa havaittiin virheellisen TIA1:n muodostavan stressijyväsiä hieman normaaliproteiinia tehokkaammin. Tulosten perusteella WDM vaikuttaa siis johtuvan poikkeavasta stressijyväsproteiinien käyttäytymisestä, joka on viime aikoina havaittu merkittäväksi ilmiöksi myös hermorappeumasairauksien synnyssä.

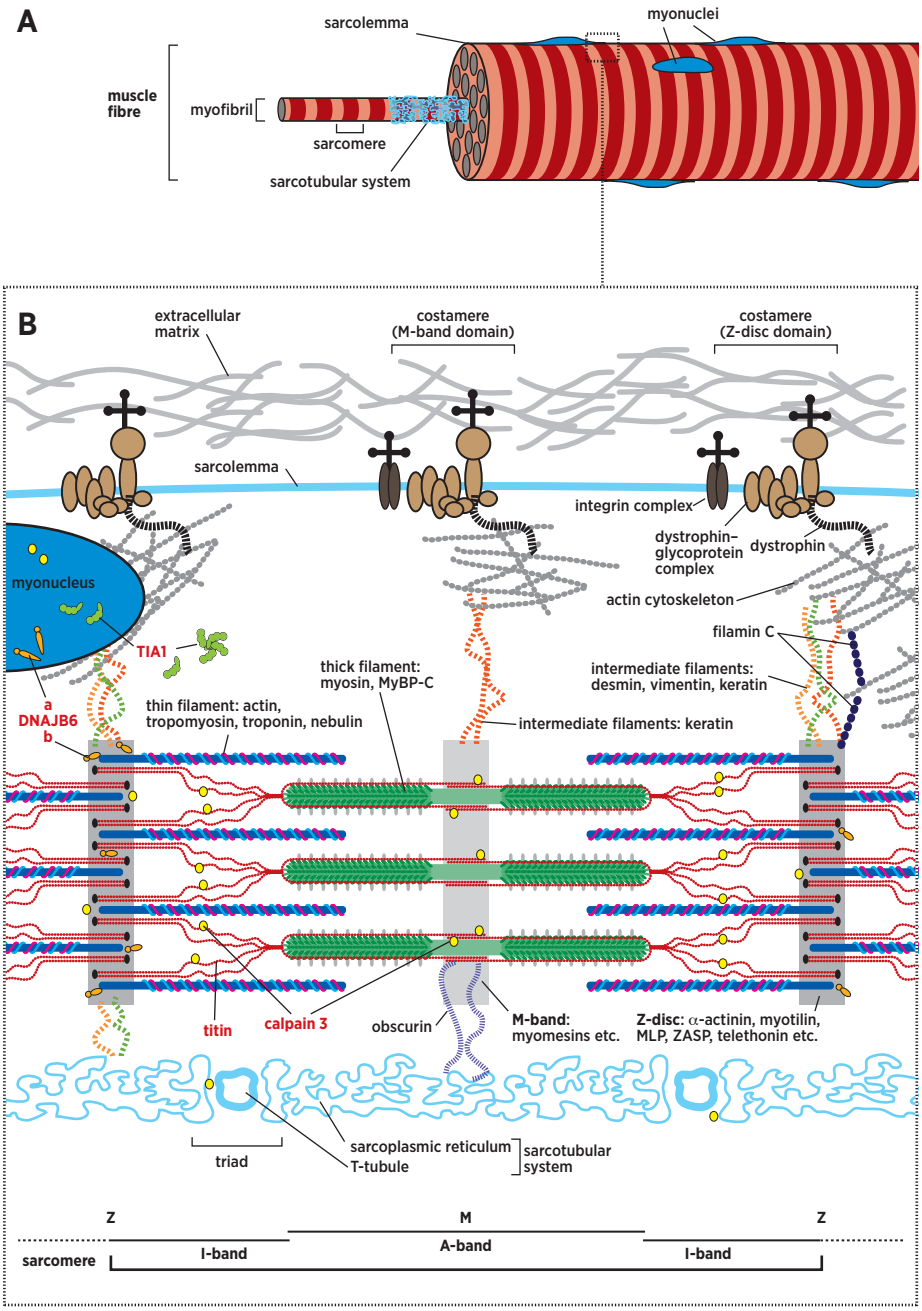
A
sarcolemma
myonuclei
muscle fibre
myofibril
sarcomere
sarcotubular system
B
extracellular matrix
costamere (M-band domain)
costamere (Z-disc domain)
sarcolemma
integrin complex
dystrophin–glycoprotein complex
dystrophin
myonucleus
actin cytoskeleton
filamin C
TIA1
thick filament: myosin, MyBP-C
intermediate filaments: desmin, vimentin, keratin
a
DNAJB6
b
thin filament: actin, tropomyosin, troponin, nebulin
intermediate filaments: keratin
titin
calpain 3
obscurin
M-band: myomesins etc.
Z-disc: α-actinin, myotilin, MLP, ZASP, telethonin etc.
triad
sarcoplasmic reticulum
T-tubule
sarcotubular system
Z
M
Z
sarcomere
I-band
A-band
I-band

1 INTRODUCTION

Muscular dystrophies are a large group of inherited disorders affecting the *skeletal muscles* and causing progressive weakness and loss of muscle mass. The disease group is heterogeneous both genetically and clinically: Muscular dystrophies can be inherited in a recessive or dominant manner. The symptoms may be evident at birth, or appear as late as middle age. The diseases can affect most groups of skeletal muscles or show striking selectivity of muscle involvement. Some muscular dystrophies may be associated with symptoms in other organs such as the heart or the brain. A common denominator in the diseases is gradual death of the *muscle fibres* or *myofibres*—the long, multinucleated muscle cells (Fig. 1A)—in the affected muscles (Mercuri & Muntoni 2013, Rahimov & Kunkel 2013).

Muscular dystrophies have been traditionally classified into a few major categories based on the mode of inheritance and the pattern of muscle involvement (Walton & Nattrass 1954). During the past twenty years, however, mapping of disease genes and identification of the gene defects at an ever-accelerating pace has revealed a surprising genetic diversity underlying the diseases. For example, *limb-girdle muscular dystrophies* (LGMD), characterized by preferential involvement of proximal limb muscles, are currently known to exist in at least eight dominant (LGMD1) and 17 recessive (LGMD2) genetic subtypes (Kaplan & Hamroun 2012). In total, mutations causing muscular dystrophy have been found in over fifty genes, whose protein products have diverse functions and reside in virtually all compartments of the muscle fibre (Kaplan & Hamroun 2012).

A major group of proteins affected by dystrophy-causing mutations are those constituting the dystrophin–glycoprotein complex (DGC) on the *sarcolemma*—the plasma membrane of the muscle fibre (Fig. 1B). Mutations in dystrophin, underlying the archetypal Duchenne muscular dystrophy, and in other DGC components impair the function of the entire complex and compromise the integrity of the

Figure 1. The muscle fibre (facing page)

A Skeletal muscle cells or muscle fibres are elongated cells comprised of myofibrils, parallel bundles of contractile filaments. The repeating functional units of the myofibrils are the sarcomeres, whose regular organization gives rise to the cross-striated appearance of the fibres. Each myofibril is surrounded by membranes of the sarcotubular system. Multiple myonuclei are normally situated at the fibre periphery, beneath the plasma membrane or sarcolemma.

B A close-up of the region boxed in (A) illustrates schematically the central structures of the muscle fibre. The myofibrils are composed of the thin (actin) filaments, thick (myosin) filaments, the titin filaments, and the associated proteins, arranged into serially connected sarcomeres. The thin filaments are anchored to the Z-discs at the ends of the sarcomere, while the thick filaments are bound together by the M-band in the middle of the sarcomere. The titin filaments span over the half-sarcomere from Z-disc to M-band, overlapping at both ends. Costameres link the subsarcolemmal cytoskeleton to the extracellular matrix at the Z-disc and M-band levels. The sarcotubular system comprises the T-tubules (transverse tubules; invaginations of the sarcolemma) and the sarcoplasmic reticulum (SR), junctioning at the triads. The proteins underlying the disorders investigated in this study—titin, calpain 3, DNAJB6, and TIA1—are highlighted in red.

sarcolemma by a mechanism that is not yet entirely known. Adverse downstream effects such as perturbed signalling and increased proteolysis are at least partly due to an increased influx of calcium ions into the muscle fibre (Hopf *et al.* 2007, Rahimov & Kunkel 2013).

Another common theme in many muscular dystrophies is *aggregation* of proteins within the muscle fibres. The *myofibril*, comprised of *sarcomeres*—basic contractile units of the muscle—is a highly ordered structure (Fig. 1B), and mutations disrupting the structural protein interactions or interfering with the correct turnover of the proteins frequently lead to aggregation of the mutant protein itself or other myofibrillar components (Goebel & Müller 2006, Schröder & Schoser 2009).

For many of the muscular dystrophies, however, the detailed molecular mechanisms by which mutations in the underlying genes lead to disease are largely unknown. The studies presented in this thesis aimed at shedding light on the molecular pathomechanisms behind a few of these diseases—the distal myopathies tibial muscular dystrophy (TMD) and Welander distal myopathy (WDM), and the limb-girdle muscular dystrophies of types 1D, 2A, and 2J. These muscular dystrophies are caused by mutations in four very different proteins. Titin, underlying both TMD and LGMD2J, is a gigantic filamentous protein of the sarcomere with structural, mechanical, and regulatory functions. Calpain 3 (CAPN3), mutated in LGMD2A, is a proteolytic enzyme predominantly expressed in skeletal muscle. DNAJB6, mutated in LGMD1D, is a ubiquitously expressed co-chaperone of the J-protein family, and hence a part of the protein quality control machinery. Finally, TIA1, responsible for WDM, is a ubiquitous RNA-binding protein involved in the regulation in splicing and protein expression.

2 REVIEW OF THE LITERATURE

2.1 M-band titinopathies TMD and LGMD2J

Tibial muscular dystrophy (TMD, MIM #600334) and limb-girdle muscular dystrophy type 2J (LGMD2J, MIM #608807) are muscular dystrophies caused by mutations in the C-terminus of titin. As the affected part of the titin protein is situated in the M-band of the sarcomere, the diseases can be described as M-band titinopathies. TMD is the autosomal dominant distal myopathy phenotype caused by heterozygous titin mutations, whereas the recessive limb-girdle phenotype seen in the few described patients homozygous for TMD-causing mutations is designated LGMD2J (Hackman *et al.* 2002, Udd *et al.* 2005). For simplicity, the collective term TMD/LGMD2J will be used here for the whole spectrum of M-band titinopathies caused by extreme C-terminal titin mutations, although the dominant and recessive phenotypes may partly depend on distinct pathomechanisms.

2.1.1 Genetics of TMD/LGMD2J

Mutations so far reported to cause TMD/LGMD2J are located in the two last exons of *TTN*, Mex5 (exon 362) and Mex6 (exon 363), encoding the is7 region and M10 domain of the titin protein (Hackman *et al.* 2002, Van den Bergh *et al.* 2003, Hackman *et al.* 2008, Pollazzon *et al.* 2010, Suominen *et al.* 2012). The Finnish founder mutation FINmaj is a deletion–insertion of 11 base pairs in Mex6, causing the exchange of four amino acid residues (EVTW→VKEK) in the M10 domain (Hackman *et al.* 2002). The other reported mutations, summarized in Table 1, include missense changes, truncations due to frameshift or nonsense mutations, and a small in-frame deletion.

The FINmaj mutation, accounting for most of the known TMD/LGMD2J cases, is common in the Finnish population, where the estimated prevalence of TMD is

Table 1. TMD/LGMD2J-causing mutations in titin

Mutation	Protein change	Domain	Reference
French C	p.S33315QfsX10	is7	Hackman *et al.* 2008
FINmaj	p.E33359_W33362delinsVKEK	M10	Hackman *et al.* 2002
Italian	p.H33378P	M10	Pollazzon *et al.* 2010
Belgian	p.I33379N	M10	Van den Bergh *et al.* 2003
French A	p.L33388P	M10	Hackman *et al.* 2002
Spanish	p.K33395NfsX9	M10	Hackman *et al.* 2008
French B	p.Q33396X	M10	Hackman *et al.* 2008
Swiss	p.Q33396_G33398delinsH	M10	Suominen *et al.* 2012

Sequence numbers refer to the RefSeq record NP_596869.4.

20/100,000 (Udd 2013). While families with other mutations have been identified in other European countries, the only mutations thus far encountered in the homozygous state in LGMD2J patients are FINmaj (six cases in Finland) and Q33396X (one case in France) (Pénisson-Besnier *et al.* 2010, Suominen *et al.* 2012).

Of note, the TMD/LGMD2J-causing mutations are concentrated in the extreme C-terminus of the titin protein. Mutations in other parts of titin are known to cause hypertrophic and dilated cardiomyopathies, hereditary myopathy with early respiratory failure (HMERF), and early onset myopathy with fatal cardiomyopathy (Salih myopathy) (Satoh *et al.* 1999, Gerull *et al.* 2002, Lange *et al.* 2005a, Carmignac *et al.* 2007, Ohlsson *et al.* 2012, Pfeffer *et al.* 2012).

2.1.2 Clinical pictures of TMD and LGMD2J

TMD belongs to distal myopathies, muscular dystrophies preferentially affecting the distal muscles of the limbs. Typical TMD has late onset, the symptoms starting on the fourth decade or later with impaired ankle dorsiflexion. The weakness progresses slowly, leading to foot drop and mild difficulties in walking and climbing the stairs. The disease affects selectively the muscles of the anterior compartment of the lower leg—*tibialis anterior* (TA), *extensor digitorum longus*, and *extensor hallucis longus*—although weakness of thigh and hip muscles can develop later in life. Walking is usually preserved until a very late age or throughout the life (Udd *et al.* 1993, 2005, Udd 2013). Approximately 10% of TMD patients heterozygous for the FINmaj mutation, as well as patients with other mutations, may show a disease different from the typical TMD phenotype. Atypical manifestations can include abnormally early onset, marked involvement of posterior or proximal lower-limb muscles, upper limbs, or bulbar muscles, or persistent asymmetric weakness (Udd *et al.* 1993, 2005, Hackman *et al.* 2008).

Due to the small number of confirmed cases, the natural history of LGMD2J is not well characterized. The onset is early, usually in the first decade. The disease leads to generalized dystrophy involving most groups of skeletal muscles, and eventually to loss of ambulation within 20–30 years of disease onset. Although the diaphragm is among the least affected muscles, fatal respiratory failure may develop in the late course of the disease. Clinically manifest cardiomyopathy has not been diagnosed, but autopsy did reveal mild left ventricular cardiac hypertrophy in one patient (Udd *et al.* 1991, 2005, Udd 1992, Pénisson-Besnier *et al.* 2010).

2.1.3 Muscle pathology in TMD and LGMD2J

Affected muscles in both TMD and LGMD2J show myopathic–dystrophic changes—fibre size variation, central nuclei, split fibres, and fibrosis. At the end stage, the affected muscles are entirely replaced by fatty and fibrous infiltration (Udd *et al.* 1992, 1993, 2005). Myonuclear apoptosis has been found in both diseases (Haravuori *et al.* 2001). Rimmed vacuoles, while present in the affected muscles in TMD, have not been found in muscle biopsies from LGMD2J patients

(Udd *et al.* 1992, 1993). The normal or mildly elevated serum creatine kinase level, and normal appearance of dystrophin in immunofluorescence (IF) microscopy indicate that sarcolemmal integrity is not primarily compromised (Udd *et al.* 1992).

Electron microscopy (EM) of TMD muscles has not revealed alterations in the sarcomere ultrastructure, whereas autophagic vesicles, myeloid figures, filamentous inclusions, and cellular debris are found at the rimmed-vacuolar regions (Udd *et al.* 1998).

2.1.4 Mouse model for TMD/LGMD2J

A knock-in (KI) mouse carrying the FINmaj mutation in the *Ttn* gene has been generated for studying the pathomechanisms of TMD/LGMD2J (Charton *et al.* 2010). The mouse model recapitulates the central clinical features of human TMD/LGMD2J. Mice heterozygous for the FINmaj mutation develop a mild myopathy with late onset (~9 months of age) and selective muscle involvement, TA being most severely affected. The homozygotes have an early onset disease (~1 month) and more widespread muscle involvement, with the *soleus* muscle first and most severely affected. Specific force production is reduced in the *soleus* of homozygous mice, and the same trend is observed in heterozygotes (Charton *et al.* 2010). In contrast to human TMD/LGMD2J patients, the homozygous FINmaj KI mice develop, in addition to skeletal muscle defects, a progressive dilated cardiomyopathy with myocardial fibrosis and systolic dysfunction (Charton *et al.* 2010).

The skeletal muscle pathology in FINmaj KI mice is of myopathic–dystrophic type and generally comparable to that in humans, although fibrosis is only seen in the most severely affected muscles of FINmaj homozygous animals. The absence of rimmed vacuoles in light microscopy and the corresponding changes in EM in both heterozygous and homozygous mice, however, contrasts the human pathology. The sarcomere ultrastructure is normal, similarly to human TMD/LGMD2J. In addition, EM reveals in FINmaj homozygotes vacuolar changes proposed to represent enlarged sarcoplasmic reticulum (SR) or T-tubules, and mitochondrial disorganization (Charton *et al.* 2010).

The original FINmaj KI mouse strain on the 129 background exhibited embryonic lethality, starting around embryonic day 12 and leading to prenatal death in ~50% of heterozygotes and ~90% of homozygotes. However, the surving mutant mice did not show increased mortality postnatally (Charton *et al.* 2010). The embryonic lethality was prevented in FINmaj KI mice heterozygous for CAPN3 knockout (KO) (see 2.1.5.2) and, according to preliminary results, by backcrossing the FINmaj mutation to the C57BL/6 background, suggesting that it was caused by a genetic modifier specific to the 129 strain (Charton *et al.* 2010) and possibly related to developmental CAPN3 expression.

2.1.5 Molecular pathomechanism of TMD/LGMD2J

2.1.5.1 Effect of TMD/LGMD2J mutations on titin

Western blotting studies with the antibody M10-1, raised against a peptide epitope in the titin M10 domain, indicate loss of this epitope in muscle extracts of TMD/LGMD2J patients and FINmaj KI mice. TMD patients and heterozygous FINmaj mice show a ~50% reduction in C-terminal titin fragments reacting with this antibody, whereas in LGMD2J patients and homozygous mice, the loss is pronounced or complete (Hackman *et al.* 2008, Charton *et al.* 2010). Findings are similar in cardiac samples from the mouse model (Charton *et al.* 2010). This loss of immunoreactivity suggests that the FINmaj mutation leads to breakdown of C-terminal titin, possibly via proteolysis (Charton *et al.* 2010).

Absence of C-terminal titin is corroborated by IF microscopy showing a complete loss of M10 signal in skeletal and cardiac muscles of homozygous FINmaj KI mice (Charton *et al.* 2010). Moreover, IF studies indicate that the effect extends beyond the mutated M10 domain: staining for domains M8–M9 is also negative in LGMD2J and homozygous FINmaj KI skeletal muscles. In contrast, staining of the domains A169–A170 at the A-band/M-band boundary (Hackman *et al.* 2002, Charton *et al.* 2010) and the M-is4 region (Anna Vihola, personal communication) are normal, suggesting that most of M-band titin remains intact. Also the major M-band crosslinking protein myomesin stains normally in LGMD2J and FINmaj KI muscles (Hackman *et al.* 2002, Fukuzawa *et al.* 2008, Charton *et al.* 2010).

Comparison with Salih myopathy, caused by mutations leading to premature titin termination at M5 and is6 (Carmignac *et al.* 2007), may be useful for estimating the degree of titin truncation in TMD/LGMD2J. The more benign phenotype of LGMD2J could suggest that FINmaj leads to less extensive truncation of titin than seen in Salih myopathy, and this would place the breakage point C-terminally from the is6 region. However, since other factors such as overall reduction of titin expression could add to the severity of Salih myopathy (discussed in 2.3.5.7), this comparison may not provide an accurate prediction either.

Even without knowledge on the exact cleavage site, IF evidence suggests that FINmaj—and possibly other TMD/LGMD2J mutations—disrupt at least the extreme C-terminal domains M9–is7–M10 of titin, and consequently affect the protein interactions of this titin region. As pointed out by Charton *et al.* (2010), the loss of titin C-terminus is in itself unlikely to be pathogenic, as titin shows similar behaviour both in affected and in non-affected muscles of FINmaj KI mice.

2.1.5.2 Role of calpain 3 in TMD/LGMD2J

The titin region disrupted by the TMD/LGMD2J mutations contains M-is7, the M-band binding site of the protease calpain 3 (CAPN3) (Sorimachi *et al.* 1995) (see 2.4.3.1 for further discussion on the interaction). Accordingly, secondary reduction of the CAPN3 protein is evident in LGMD2J muscles, and minor CAPN3

deficiency of variable degrees has also been seen in some TMD cases (Haravuori *et al.* 2001, Pénisson-Besnier *et al.* 2010). This is replicated in FINmaj KI mice, with CAPN3 levels decreased moderately in heterozygotes and markedly in homozygotes (Charton *et al.* 2010). The unchanged *Capn3* transcript levels in FINmaj KI mice indicate that the lower steady-state level of the protein is due to its increased turnover (Charton *et al.* 2010). The activability of CAPN3, reflecting the ratio of proteolytic activity of CAPN3 to its expression level, is similar or increased in FINmaj homozygotes (Charton *et al.* 2010).

Titin has been suggested to regulate the activity of CAPN3 by preventing its autolytic activation (Sorimachi *et al.* 1995), but the specific roles of the binding sites in the M-band and I-band are not understood. The CAPN3 deficiency and absence of C-terminal titin in TMD/LGMD2J and FINmaj KI suggest that the mutations inhibit the binding of CAPN3 to its M-band binding site, possibly by changing the conformation of the titin C-terminus, thus leading to dysregulation of CAPN3 and inappropriate proteolysis of its substrates, including titin itself (Charton *et al.* 2010).

An active adverse role of CAPN3 deregulation in the pathogenesis of TMD/LGMD2J is indicated by the fact that crossing the FINmaj KI mouse to CAPN3 KO ameliorated the phenotype caused by the titin mutation: mice heterozygous for both FINmaj and CAPN3 null allele showed markedly less severe pathology compared to FINmaj alone. Such improvement by CAPN3 reduction was not evident in skeletal or cardiac muscles of FINmaj homozygotes, suggesting that the severe recessive phenotype may be caused by another, CAPN3-independent pathomechanism (Charton *et al.* 2010).

As mentioned above, heterozygosity for CAPN3 KO also prevented the death of FINmaj heterozygous and homozygous mouse embryos *in utero* (Charton *et al.* 2010), suggesting that the embryonic lethality is CAPN3-mediated. The observed onset of lethality at E12 is well compatible with the onset of CAPN3 expression in mouse embryos between E11.5 and E12.5 (Herasse *et al.* 1999, Charton *et al.* 2010). Problems in cardiac development would be an obvious explanation for embryonic lethality due to a titin mutation; however, CAPN3 may not be expressed in the murine heart during the development (Fougerousse *et al.* 2000b).

2.1.5.3 Role of the obscurin proteins in TMD/LGMD2J

Obscurin (OBSCN) and its homologue obscurin-like 1 (OBSL1) interact with the M10 domain and mediate its interaction with myomesin (discussed in more detail in 2.3.5.6.). In addition to the indirect effect through titin cleavage, these interactions can be directly disrupted or weakened by TMD/LGMD2J mutations (Fukuzawa *et al.* 2008). Although obscurin is localized at the M-band in the muscles of LGMD2J patients and FINmaj KI mice, its sharp colocalization with myomesin is lost, demonstrating that the titin mutations do have some kind of an effect on obscurin (Fukuzawa *et al.* 2008, Charton *et al.* 2010). This could have adverse

functional or structural downstream consequences on the link between myofibrils and the surrounding membrane systems. As proposed by Charton *et al.* (2010), the vacuolar changes observed in FINmaj KI mice could represent SR disorganization possibly caused by the obscurin defect.

2.2 Limb-girdle muscular dystrophy 2A (LGMD2A)

Limb-girdle muscular dystrophy type 2A (LGMD2A, MIM #253600) results from recessive mutations in the protease calpain 3 (CAPN3) (Richard *et al.* 1995). The clinical course of LGMD2A is highly variable. The age of onset can vary from early childhood to the middle age, and the severity of the symptoms ranges from the typical pelvifemoral phenotype to isolated hyper-CK-emia. The muscle weakness is typically symmetrical and involves first the muscles of the pelvic girdle and later the shoulder girdle, although a subset of patients show a scapulohumeral phenotype with preferential involvement of shoulder girdle muscles (Angelini & Fanin 2012).

The Leiden Open Variation Database (Fokkema *et al.* 2011) lists around 400 possibly pathogenic sequence variants in *CAPN3*, localized throughout the gene. These include all kinds of mutations—missense, nonsense, and truncating changes and large rearrangements (reviewed by Kramerova *et al.* 2007). Most mutations lead to the loss of CAPN3 activity in muscle by inactivating the enzyme or preventing its expression. However, some missense mutations, predicted or demonstrated not to affect the proteolytic activity, have been shown to disturb the interaction of CAPN3 with titin, affecting one or both of its binding regions (discussed in 2.4.3) (Ono *et al.* 1998, Kramerova *et al.* 2004, 2007). Some mutations may also affect the proposed non-proteolytic functions of CAPN3 at the triads, leading to altered calcium signalling (Kramerova *et al.* 2012).

2.3 Titin

Titin (TTN, also known as connectin) is the largest polypeptide known in nature (Maruyama 1976, Wang *et al.* 1979, Bang *et al.* 2001a). The human *TTN* gene contains 363 exons, with a total of 114.4 kb of coding sequence. The overall protein-coding capacity is 38,138 amino acid residues, corresponding to a molecular weight of 4.2 MDa (Bang *et al.* 2001a). However, titin isoforms containing all the exons are not known to exist, the largest reported variants being 3.7–3.8 MDa in size (Vikhlyantsev *et al.* 2004, Guo *et al.* 2010).

Titin is expressed in all striated muscles, where it has essential functions in muscle development, structure, mechanics, and signalling. With single molecules spanning over the half-sarcomere from Z-disc and to M-band, titin forms an elastic filament system—sometimes referred to as the “third filament”—alongside the thick myosin filaments and thin actin filaments (Fürst *et al.* 1988). Titin filaments

restore the sarcomere length after muscle stretch and contraction, distribute forces evenly between sarcomeres, and keep the thick filaments centred in the sarcomere, ensuring symmetric force generation (Horowits & Podolsky 1987, Horowits *et al.* 1989, Helmes *et al.* 1996).

Titin is one of the first muscle-specific proteins expressed in differentiating myoblasts (Fürst *et al.* 1989). As the sole structure that spans the whole half-sarcomere, it can act as a molecular blueprint that determines the localization of other sarcomeric components, and as a building scaffold for the sarcomere. In the developing myofibres, Z-discs and M-bands are assembled independently, and as titin interacts with both the nascent thin and thick filaments, it is thought to co-ordinate their integration into mature sarcomeres (Trinick 1994, Whiting *et al.* 1989, Kontrogianni-Konstantopoulos *et al.* 2006a, 2009).

The sensory and signalling functions of titin are concentrated in the signalling hubs located at Z-disc, the N2A and N2B elements of the I-band, and the M-band. Titin-based protein complexes in these regions are thought to sense the stress and strain of the sarcomeres and transduce signals to pathways regulating gene expression, protein turnover, and cell survival (Voelkel & Linke 2011).

The following review will mainly focus on the role of titin in mature skeletal muscle, and on the functions of its M-band part harbouring the TMD/LGMD2J-causing mutations.

2.3.1 Overall structure of titin

Titin is modular in structure: most of the protein is comprised of repeated immunoglobulin-like (Ig) and fibronectin type 3 -like (FN3) domains, often allegorized as beads on a string. These are interspersed by unique insertion sequences (is) that show little or no similarity to other proteins. The unique sequences are enriched in the titin regions with specialized functions: the Z-disc, N2A and N2B elements of the I-band, and the M-band (Labeit *et al.* 1992, Labeit & Kolmerer 1995, Bang *et al.* 2001a).

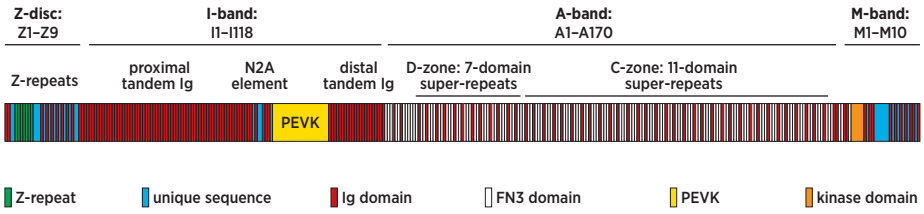

Figure 2. Modular structure of titin

A schematic view of the titin protein (skeletal muscle N2A isoform). I-band titin is comprised of tandemly repeated Ig domains, split into proximal and distal tandem Ig regions by the N2A element and the PEVK region. A-band titin contains both Ig and FN3 domains, most of them arranged into super-repeats of 7 and 11 domains. Unique sequence regions are enriched in the Z-disc and M-band parts of the protein.

In the widely used domain nomenclature by Bang *et al.* (2001a), the Ig and FN3 domains are labelled with a letter prefix indicating the sarcomeric region (Z, I, A, M) followed by the ordinal number of the domain within that region according to the entire genomic sequence (*e.g.* A168 denotes the 168th domain in the A-band region of titin). Similar nomenclature is applied to the insertion sequences in Z-disc and M-band titin, although the prefix can be omitted depending on the context (*e.g.* M-is7 or is7).

The modular structure of skeletal muscle titin is schematically shown in Fig. 2.

2.3.2 Z-disc titin

The N-terminal parts of titin molecules from adjacent sarcomeres span through the Z-disc, overlapping in an antiparallel fashion. The most N-terminal Ig domains Z1 and Z2 are located on Z-disc periphery, on the side of the adjacent sarcomere (Gregorio *et al.* 1998). These domains interact with telethonin (TCAP; also known as titin-cap or T-cap) that glues together the N-termini of two parallel titin molecules with a tight β-sheet sandwich, and has importance for both Z-disc structure and signalling (Kontrogianni-Konstantopoulos & Bloch 2003, Zou *et al.* 2006, Knöll *et al.* 2011). The same titin domains interact with the small ankyrin isoform (sAnk) of the SR, and may regulate SR organization surrounding the Z-disc (Kontrogianni-Konstantopoulos & Bloch 2003).

The width of the Z-disc is spanned by Z-is1, located between domains Z2 and Z3. This long insertion sequence contains unique sequence and up to seven alternatively spliced Z-repeats of 45 amino acids. The Z-repeats and the adjacent unique sequence region bind α-actinin, which crosslinks titin to the thin filaments (Sorimachi *et al.* 1997, Gregorio *et al.* 1998, Young *et al.* 1998). Z-is1 also interacts with the C-terminal SH3 domain of nebulin, the ruler protein of thin filaments (Witt *et al.* 2006), and with filamin C that may connect titin to the cortical actin cytoskeleton (Labeit *et al.* 2006).

The Ig domains Z3–Z9 and the interspersed unique sequences Z-is2–Z-is7 are located at the Z-disc/I-band transition zone, extending ~100 nm from the Z-disc centre. This titin region binds actin and associates with the thin filament in an inextensible fashion, in contrast to the elastic I-band titin (Fürst *et al.* 1988, Linke *et al.* 1997, Trombitás & Granzier 1997).

2.3.2.1 Signalling functions of Z-disc titin

In the Z-disc, key players in titin-based signalling are telethonin and MLP (muscle LIM protein; officially CSRP3, cysteine-rich protein 3), thought to constitute a mechanosensory signalling module on Z-disc titin together with ZASP (Z-disc alternatively spliced protein; officially LDB3, LIM-domain binding protein 3) and myozenins (Knöll *et al.* 2002, Frey & Olson 2002). Telethonin interacts with several proteins with signalling roles (Faulkner *et al.* 2000, Frey & Olson 2002, Knöll *et al.* 2002, Nicholas *et al.* 2002, Kontrogianni-Konstantopoulos & Bloch 2003, Kojic

et al. 2004, Witt *et al.* 2005, Tian *et al.* 2006, Nakano *et al.* 2007, Mihatsch *et al.* 2009, Knöll *et al.* 2011). In cells subjected to biomechanical and oxidative stress, telethonin can localize to nuclei where it has an antiapoptotic function through modulation of p53 turnover (Knöll *et al.* 2011). MLP, interacting with titin through telethonin and α-actinin, is required for targeting of calcineurin (protein phosphatase 2B) and myozenin 2 to the Z-disc and for stretch-induced activation of calcineurin–NFAT (nuclear factor of activated T-cell) signalling (Knöll *et al.* 2002, Heineke *et al.* 2005). MLP can act as a transcriptional coactivator of myogenic regulatory factors (Kong *et al.* 1997), and its translocation to nuclei in response to mechanical stimulation is essential for the hypertrophic response and sarcomeric remodelling (Boateng *et al.* 2009).

2.3.3 I-band titin

I-band titin is largely composed of tandemly repeated Ig domains, divided into proximal (Ig domains I1–I83) and distal (I84–I118) tandem Ig regions (Bang *et al.* 2001a). The two tandem Ig regions are separated by a repetitive sequence region, termed PEVK for its high content of proline (P), glutamate (E), valine (V) and lysine (K) residues (Labeit & Kolmerer 1995). The PEVK region, composed of repeated PPAK motifs (named after the first four residues in the motif) and glutamate-rich PolyE segments, folds into short interconverting polyproline II helices, β-turns, and random coils, and seems to lack a tertiary structure (Greaser 2001, Ma *et al.* 2001, Ma & Wang 2003).

I-band titin undergoes extensive alternative splicing, with the number of proximal Ig domains and the length of the PEVK region accounting for most of the variation in titin size. In addition, I-band titin contains two alternatively spliced sequence elements, named N2A and N2B due to their originally presumed localization near the sarcomeric N2 line. The cardiac-specific N2B element, encoded by a single exon in the middle of the proximal tandem Ig region, comprises three Ig domains (I24–I26) and a unique sequence region N2B-us. The N2A element contains the last Ig domains of the proximal tandem Ig region interspersed by unique sequence stretches (Labeit & Kolmerer 1995, Bang *et al.* 2001a).

Titin isoforms can be classified into three major groups based on I-band structure. The shortest (~3 MDa) isoforms are the cardiac-specific N2B titins that contain only N2B of the two N2 elements and have very short proximal tandem Ig and PEVK regions. Cardiac N2BA forms (~3.3 MDa) contain both N2B and N2A elements separated by a variable number of Ig domains, and also have a longer PEVK region compared to the N2B forms. The N2A titins, expressed in skeletal muscle, contain exclusively the N2A element; in these isoforms, both the proximal Ig and PEVK regions are longer than in cardiac titins. Their length varies considerably between muscle types, the size of the whole molecule ranging from ~3.4 MDa in fast muscles to ~3.7 MDa in slow muscles.

In contrast to the alternatively spliced proximal Ig and PEVK regions, the distal tandem Ig region is constitutively expressed (Freiburg *et al.* 2000). This part of I-band titin hexamerizes in a side-by-side fashion, likely forming the end-filaments, rod-like structures seen in electron microscopy at the ends of the thick filaments (Houmeida *et al.* 2008).

2.3.3.1 Biomechanical functions of I-band titin

The elastic behaviour of titin is conferred by the I-band part of the protein. The tandem Ig region, the PEVK region, and in heart the N2B-us, act as serially coupled springs that have different biomechanical properties and extend independently. Upon sarcomere stretch, the linkers between the Ig domains straighten first, followed by unravelling of the PEVK region and finally by the N2B-us (Linke *et al.* 1998, 1999). Although unfolding of domains was first thought to contribute to titin elasticity (Soteriou *et al.* 1993, Erickson 1994), large-scale unfolding–refolding does not seem to take place in physiological conditions (Linke *et al.* 1999, Minajeva *et al.* 2001).

Lengths of the spring elements affect the overall elasticity of the titin molecule, and titin-based passive tension can be controlled by adjusting the ratio of stiffer short isoforms and more compliant longer isoforms (Freiburg *et al.* 2000, Trombitás *et al.* 2001). In the heart, N2B and N2BA isoforms can be coexpressed in the same sarcomere (Trombitás *et al.* 2001). In skeletal muscle, single fibres can coexpress titin isoforms of different lengths (Prado *et al.* 2005), but coexpression on sarcomere level has not been reported. Adaptive changes in titin isoforms occur during cardiac development and disease (Lahmers *et al.* 2004, Neagoe *et al.* 2002), and in response to altered loading of skeletal muscle (Kasper & Xun 2000).

In addition to long-term changes achieved by alternative splicing, titin elasticity can be modulated in a time frame of seconds to meet the physiological demands. In the heart, phosphorylation of the N2B-us and the PEVK region by a number of kinases reduces titin-based passive tension (Yamasaki *et al.* 2002, Krüger *et al.* 2009, Hidalgo *et al.* 2009, 2013), whereas binding of Ca^{2+} to the PEVK PolyE segments increases tension especially in skeletal muscle titins (Labeit *et al.* 2003). Transient interactions of the proximal tandem Ig and PEVK regions with actin and tropomyosin of the thin filament also modulate sarcomere mechanics (Kulke *et al.* 2001, Yamasaki *et al.* 2001, Raynaud *et al.* 2004).

2.3.3.2 Signalling functions of I-band titin

At the cardiac-specific N2B element, titin-based signalling involves members of the FHL (four-and-a-half LIM domain protein) family, localizing to multiple subcellular compartments and linked to a plethora of signalling pathways (Johannessen *et al.* 2006, Shathasivam *et al.* 2010). FHL1 interacts with the N2B-us of titin and with components of MAPK (mitogen-activated protein kinase) cascade—with a proposed role in stretch-induced hypetrophic MAPK signalling—and modulates

compliance of titin by inhibiting its phosphorylation by ERK2 (extracellular-signal-regulated kinase 2) (Sheikh *et al.* 2008, Raskin *et al.* 2012). FHL2 interacts directly with the N2B-us, and can also dimerize with FHL1 (Lange *et al.* 2002). While the binding of FHL2 to titin can mediate compartmentalization of metabolic enzymes (Lange *et al.* 2002), its importance in titin-based signalling has not been established. Stretching of the N2B-us has been proposed to increase binding of FHL proteins, thereby potentiating hypertrophic signalling (Granzier *et al.* 2009), but this awaits experimental confirmation.

N2A-based signalling, involving CAPN3 and the muscle ankyrin repeat proteins, will be discussed in 2.4.7.

2.3.3.3 Novex-3 titin

A special feature of I-band titin is the novex-3 exon, encoding an alternative titin C-terminus composed of Ig domains and unique sequence stretches. The resulting short (~625 kDa) titin isoform designated "novex-3 titin" is expressed on a low level in both skeletal and cardiac muscle, but its functions are not characterized. The N-terminus of novex-3 titin integrates to the Z-disc normally, but the protein extends only 100–200 nm to the I-band where it interacts with obscurin through its C-terminus (Bang *et al.* 2001a).

2.3.4 A-band titin

The largest part of titin is located at the sarcomeric A-band. This constitutively expressed region of ~2 MDa comprises a total of 170 repeated Ig and FN3 domains, most of which are organized into six super-repeats of seven domains and 11 super-repeats of 11 domains (Labeit *et al.* 1992, Bang *et al.* 2001a). A-band titin is tightly associated with the thick filaments, each thick filament binding six titin molecules (Fürst *et al.* 1988, Whiting *et al.* 1989, Liversage *et al.* 2001). This involves direct interactions of titin FN3 domains with the S1 subfragment of heavy meromyosin, and likely another separate interaction of titin with light meromyosin (Labeit *et al.* 1992, Houmeida *et al.* 1995, Muhle-Goll *et al.* 2001). Titin interacts with myosin also indirectly through myosin binding protein C (MyBP-C) that binds the first Ig domain in each of the 11-domain super-repeats (Freiburg & Gautel 1996).

2.3.5 Structure and functions of M-band titin

The C-terminal 250 kDa of titin are located at the M-band. This part, encoded by *TTN* exons Mex1–Mex6 (358–363), comprises the kinase domain (TK), Ig domains M1–M10, and the unique sequences M-is1–M-is7 (is1–is7) (Gautel *et al.* 1993, Obermann *et al.* 1996, Kolmerer *et al.* 1996). According to the ultrastructural localization of titin epitopes, this part of titin spans through the entire M-band, with TK located at the M-band periphery and the C-terminal M10 domain extending ~60 nm over the M-band centre. Titin C-termini from adjacent half-sarcomeres thus overlap in an antiparallel fashion (Obermann *et al.* 1996). Of note,

this arrangement of titin molecules places the extreme C-terminus and the TK domain of the antiparallel titin molecules in spatial proximity with each other at the M-band periphery (Fig. 3), and functional interactions between these parts of M-band titin could hence be possible.

The structures and functions of the M-band unique sequences are mostly unknown. The is3, is5, and is7 regions (the last of which mediates the interaction with CAPN3; see 2.3.5.4. and 2.4.3.1.) have been suggested to act as flexible linkers between Ig domains (Gautel *et al.* 1993). The long is2, situated between domains M3 and M4, is likely to show an extended conformation, resulting in a substantial overlap of the antiparallel is2 regions at the M-band centre. As the secondary structure of is2 is predicted to be α-helical with a potential for coiled coils, it has been proposed to mediate dimerization or multimerization of titin molecules (Gautel *et al.* 1993, Obermann *et al.* 1996), which could involve either parallel or antiparallel titin strands.

The ten Ig domains of M-band titin show more sequence variation than the highly similar A-band domains, likely reflecting their specialized interactions in M-band structure and functions (Gautel *et al.* 1993). However, surprisingly few protein interactions have been established for this titin region.

Fig. 3 shows schematically the structure of C-terminal titin and its overlapping arrangement in the M-band, and summarizes the known protein interactions.

2.3.5.1 MURF proteins and M-band titin

M-band titin associates with at least two of the muscle RING finger (MURF) proteins. The three members in this subfamily of the TRIM (tripartite motif) proteins—MURF1 (TRIM63), MURF2 (TRIM55), and MURF3 (TRIM54)—are predominantly expressed in striated muscle where they show characteristic expression patterns. In skeletal muscle, MURF1 predominates in fast fibres and MURF2 in slow fibres, whereas MURF3 is expressed in both fibre types (Spencer *et al.* 2000, Centner *et al.* 2001, Perera *et al.* 2012). MURFs are thought to form homo- and heterodimers by their coiled-coil motifs, and interactions have been detected between all the family members (Centner *et al.* 2001, Mrosek *et al.* 2007).

The MURF proteins show variable localization within myofibres. MURF1 is predominantly localized at the M-band, where also MURF2 and MURF3 have been detected. In addition, MURFs can localize at the Z-disc (MURF1 and 3), microtubules (MURF2 and 3), and nuclei (MURF1 and 2), and as a diffuse cytoplasmic pool (Spencer *et al.* 2000, Centner *et al.* 2001, Pizon *et al.* 2002, McElhinny *et al.* 2004, Gregorio *et al.* 2005, Hirner *et al.* 2008).

The functions of the three proteins are partly overlapping. This is especially evident for MURF1 and MURF2 in their role of regulating muscle trophic state: the two proteins share many of their interaction partners, and knockout of both genes in mice is necessary for producing the phenotype characterized by dramatic hypertrophy of heart and skeletal muscles (Witt *et al.* 2005, 2008, Willis *et al.*

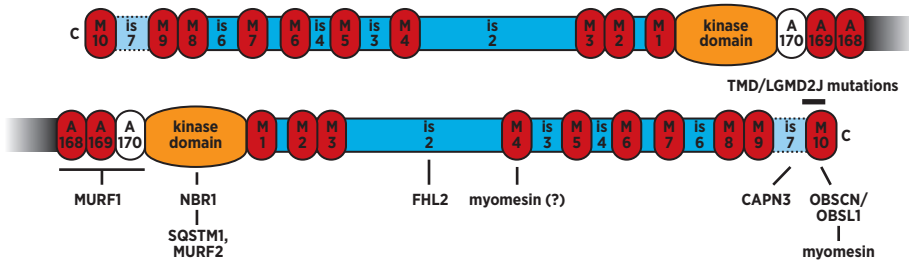

Figure 3. M-band titin

A schematic view of the C-terminal part of titin, situated in the sarcomeric M-band. M-band titin is comprised of the kinase domain, the Ig domains M1–M10, and the unique sequence regions is1–is7. Also the domains A168–A170 at the A-band/M-band boundary are functionally included in M-band titin. All the known TMD/LGMD2J mutations are located in is7 and M10, in the extreme C-terminus of the protein. The alternatively spliced is7 region is indicated by dashed outlines and the lighter blue colour. Protein interactions reported in the myofibrillar context are summarized below the diagram. Two overlapping, antiparallel molecules are shown to illustrate the layout of titin in the M-band; the exact relationship of the molecules is unknown.

2013). On the other hand, MURF2 and MURF3 appear to have redundant functions in microtubule dynamics and myofibrillogenesis (Spencer *et al.* 2000, Pizon *et al.* 2002, McElhinny *et al.* 2004, Perera *et al.* 2011). All three MURFs have E3 ubiquitin ligase activity, accounting for some of their cellular functions (Bodine *et al.* 2001, Kedar *et al.* 2004, Koyama *et al.* 2008), and MURF1 has also been connected to the SUMO (small ubiquitin-like modifier) modification machinery (Dai & Liew 2001, McElhinny *et al.* 2002).

The MURF proteins, notably MURF1 and MURF2, are considered as key regulators of muscle mass, trophic state, and metabolism. Upregulated in atrophy-causing conditions, they promote catabolism of muscle proteins while inhibiting anabolic processes and carbohydrate metabolism (Bodine *et al.* 2001, Witt *et al.* 2005, 2008, Hirner *et al.* 2008, Koyama *et al.* 2008). Through polyubiquitination, MURFs can directly mediate turnover of myofibrillar proteins and metabolic enzymes. While ubiquitination of some proteins (such as troponin I, actin, myosin heavy chain, and creatine kinase) has been demonstrated, others (such as titin and nebulin) have been implied as substrates by protein interactions (Bodine *et al.* 2001, Kedar *et al.* 2004, Polge *et al.* 2011, Witt *et al.* 2005, Clarke *et al.* 2007, Koyama *et al.* 2008). Increased protein synthesis levels in MURF1/MURF2 double KO mice have suggested that MURFs also suppress production of new proteins, partly by their interactions with the translation machinery (Witt *et al.* 2008, Koyama *et al.* 2008). Furthermore, by modulating the levels and localization of transcription factors and signalling proteins, MURFs can affect signalling and gene expression programs regulating muscle hypertrophy and atrophy (McElhinny *et al.* 2002, Arya *et al.* 2004, Koyama *et al.* 2008, Willis *et al.* 2013). Absence of overt

muscle atrophy in MURF1-overexpressing mice, however, indicates tight regulation of these processes also by other factors (Hirner *et al.* 2008).

Interaction with M-band titin was first characterized for MURF1 that binds the titin domains A168–A170 at the A-band/M-band boundary. The three domains form a rigid tandem structure with a surface groove likely to accommodate one MURF1 dimer (Centner *et al.* 2001, Mrosek *et al.* 2007). MURF2 can also bind titin directly within the same region (Pizon *et al.* 2002, Witt *et al.* 2005), and the roles of these interactions could be similar. In addition, MURF2 interacts with the kinase domain of titin through NBR1 and SQSTM1 (Lange *et al.* 2005a); this interaction will be further discussed below.

The function of the interaction between MURF1 (and MURF2) with the titin domains A168–A170 is currently unknown. As overexpression of MURF1 or the interacting titin domains in cultured cardiomyocytes disrupts the M-band and thick filament structures, binding of MURF1 to titin was proposed to destabilize the sarcomeric structure and thereby facilitate the turnover of myofibrillar proteins (McElhinny *et al.* 2002, Kedar *et al.* 2004). This view is, however, challenged by the normal sarcomeric ultrastructure observed in mice overexpressing MURF1 in skeletal muscles (Hirner *et al.* 2008).

The interaction with titin could involve the ubiquitin ligase activity of MURF1. In addition to mediating titin degradation, ubiquitination could have a regulatory function on titin, for example by modifying its protein interactions (Witt *et al.* 2005). In line with this possibility, Witt *et al.* (2005) detected ubiquitin in the M-band in immuno-EM and showed immunoreactivity of titin with ubiquitin antibodies in western blot. Ubiquitination of titin by MURF1 has not, however, been directly demonstrated.

Proximity of the titin kinase domain has prompted a link between MURF1 and TK signalling. In this line of thought, Centner *et al.* (2001) proposed that MURF1 could present substrates to TK, or regulate its activity. Another possibility is regulation of MURF1 by TK, possibly in a strain-dependent manner (Witt *et al.* 2005, 2008). Binding to titin A168–A170 could also serve to concentrate MURFs in the vicinity of TK, hence facilitating their recruitment to the TK-based signalosome (see below).

With regard to M-band titinopathies, the reported binding of MURF1 and MURF2 with titin domains M8–M10 (Witt *et al.* 2008) is of high interest. These interactions were detected in pairwise yeast two-hybrid studies, but their biochemical confirmation has not been published nor their functional importance addressed. Of note, the overlapping arrangement of titin in the M-band (Obermann *et al.* 1996) may place the C-terminal domains M8–M10 close in space to the MURF-binding site at A168–A170. The interactions of MURFs with the two titin sites could thus be functionally related, extending the possible consequences of TMD/LGMD2J mutations to the MURF proteins.

2.3.5.2 Kinase domain of titin

The kinase domain of titin (TK) is a serine/threonine kinase related to myosin light chain kinases (Labeit *et al.* 1992). TK has a dual autoinhibitory mechanism, its activation requiring removal of the C-terminal regulatory tail blocking the ATP binding pocket, and phosphorylation of a tyrosine side chain blocking the catalytic residue (Mayans *et al.* 1998, Puchner *et al.* 2008). The conformational changes relieving the autoinhibition are induced mechanically: physiological levels of strain expose the ATP binding site and allow autophosphorylation of the autoinhibitory tyrosine residue. This mechanical activation was predicted by molecular dynamics simulations (Gräter *et al.* 2005), and experimentally demonstrated by single-molecule measurements with atomic force microscopy (Puchner *et al.* 2008, Puchner & Gaub 2010). The phospho-mimickry mutant TK can also be activated by Ca^{2+}/calmodulin, but this may not be physiologically relevant (Mayans *et al.* 1998, Puchner *et al.* 2008). In addition, TK constructs are transphosphorylated by extracts of differentiating C2C12 myoblasts (Mayans *et al.* 1998), suggesting that alternative modes of activation are possible.

In mature muscle, TK exerts its functions through a signalosome complex composed of the zinc-finger protein NBR1 (next-to-BRCA1), SQSTM1 (sequestosome 1, also known as p62), and MURF2—of these, NBR1 and SQSTM1 are *in vitro* substrates of TK (Lange *et al.* 2005a). Binding of the complex to titin is mediated by NBR1 and requires a semiopen conformation of TK, mimicking the mechanically activated state. In mechanically arrested cardiomyocytes and denervated muscle, the complex dissociates from the M-band and MURF2 relocates to nuclei. This displaces SRF (serum response factor) from the nuclei by a yet uncharacterized mechanism and represses transcription of SRF target genes (Lange *et al.* 2005a). TK can hence modulate gene expression in response to mechanical activity of muscle. Whether TK also regulates direct effects of MURFs, NBR1, and SQSTM1 on protein turnover is currently unknown (Lange *et al.* 2005a, Braun & Gautel 2011). The importance of TK-based signalling is demonstrated by a TK missense mutation disrupting the interaction with NBR1. In muscles of HMERF (hereditary myopathy with early respiratory failure) patients carrying this mutation, normal localization of NBR1 to Z-discs and M-bands is disrupted, and MURF2 shows prominent nuclear localization (Lange *et al.* 2005a).

Also MURF1 has been reported to interact with SQSTM1 (Witt *et al.* 2008). While nuclear localization of MURF1 was not seen by Lange *et al.* (2005a) in HMERF patients, it was reported by Ochala *et al.* (2011) in immobilized rats (a model for critical illness myopathy). Although suggested by the similarity of the proteins, interchangeability of MURF1 and MURF2 in TK-based signalling has not been experimentally demonstrated.

TK seems to have functions also during muscle development. The observations that TK phosphorylates telethonin in differentiating C2C12 myoblasts and that expression of constitutively active TK disrupts myofibrillogenesis suggested that TK

plays a key role in early muscle development (Mayans *et al.* 1998). However, normal initial formation of cardiac sarcomeres in mouse embryos lacking TK argues against this idea (Weinert *et al.* 2006), and the importance of telethonin phosphorylation remains elusive. In light of recent findings emphasizing the signalling role and mobility of telethonin (Knöll *et al.* 2011), shuttling of telethonin to M-band for phosphorylation is also a possibility.

2.3.5.3 FHL2 and metabolic enzymes in the M-band

The M-is2 region, as well as the cardiac-specific N2B element, interact with FHL2 and target it to the sarcomere. As the metabolic enzymes creatine kinase, phosphofructokinase, and adenylate kinase also bind FHL2 and co-localize with it, titin and FHL2 were suggested to concentrate these enzymes to the sarcomeric regions of high metabolic activity (Lange *et al.* 2002). Given the multiple functions of FHL2 in signalling and gene regulation (reviewed by Johannessen *et al.* 2006), its interaction with M-band titin could have additional signalling functions. These mechanisms are likely to be relevant only in the heart, as the expression of FHL2 in skeletal muscle is very low (Chan *et al.* 1998, Chu *et al.* 2000, Scholl *et al.* 2000).

2.3.5.4 Alternatively spliced M-is7

The M-is7 region (hereafter is7) is situated between the two C-terminal Ig domains, M9 and M10 (Fig. 3) (Gautel *et al.* 1993). This unique sequence region, 101 amino acid residues in length, has a remarkably high content of serine (32 residues) and methionine (10 residues). It has been predicted to be an unstructured linker (Gautel *et al.* 1993), but nothing is known about its three-dimensional organization in the M-band.

The *TTN* exon Mex5 (362), coding for is7, undergoes alternative splicing. This results in the expression of M-band titin as Mex5$^+$ (is7$^+$) and Mex5$^-$ (is7$^-$) isoforms (Kolmerer *et al.* 1996). Detailed knowledge on the expression and functions of the two isoforms is, however, lacking.

Kolmerer *et al.* (1996) reported exclusive expression of is7$^+$ in human heart and some is7$^-$ forms in rabbit and mouse hearts. Northern blotting and RT-PCR analyses of rabbit skeletal muscles showed variable levels of Mex5 inclusion. The isoform ratio correlated with muscle type, with fast-twitch muscles showing a higher proportion of is7$^-$ titin (Kolmerer *et al.* 1996). This was supported by RT-PCR studies by Ojima *et al.* (2007), showing approximately equal amounts of is7$^+$ and is7$^-$ forms in mouse *quadriceps femoris* and exclusive is7$^+$ expression in *soleus*. However, there is no information on is7 expression differences on the single-fibre-level. During development, the expression of is7$^-$ forms is negligible, as indicated by *in situ* hybridization on mouse embryos and RT-PCR analysis of cultured mouse myotubes (Kolmerer *et al.* 1996, Ojima *et al.* 2007). On the RNA level, Mex5 skipping may be promoted by the splicing regulator MBNL1 (Muscleblind-like 1), as

suggested by increased proportion of is7^{+} titin in the *Mbnl1* knockout mouse and in the *HSA*^{LR} mouse, a model of myotonic dystrophy with secondarily distrurbed MBNL1 function (Lin *et al.* 2006).

The is7 region mediates the interaction of M-band titin with CAPN3 (Kinbara *et al.* 1997). This interaction, discussed in more detail in 2.4.3.1., is likely of major importance for regulation of CAPN3 in muscle (Haravuori *et al.* 2001, Charton *et al.* 2010). The variable inclusion of is7 may hence indicate a need to adjust the titin–CAPN3 interaction in a muscle-specific manner. The exclusive expression of is7^{+} isoforms in heart, where CAPN3 is practically absent (Kolmerer *et al.* 1996, Fougerousse *et al.* 1998), suggests that the is7 region is likely to have other functions apart from CAPN3 binding.

2.3.5.5 M-band titin and the myomesin proteins

Proteins of the myomesin family—myomesin (MYOM1), myomesin 2 (MYOM2; also known as M-protein), and myomesin 3 (MYOM3)—form elastic filaments that crosslink the M-band through their interactions with myosin and titin (Obermann *et al.* 1995, Lange *et al.* 2005b, Schoenauer *et al.* 2005, 2008, Fukuzawa *et al.* 2008). The exact organization of the myomesin proteins in the M-band is still poorly known; despite their identical domain structures, the three proteins seem to have distinct layouts and functions (Obermann *et al.* 1996, Fukuzawa *et al.* 2008, Schoenauer *et al.* 2008). While myomesin 1 is a constitutive M-band component in all striated muscles, the fibre-type-dependent expression of myomesins 2 and 3, and EH-myomesin (a splice variant of MYOM1) may modulate the mechanical properties of the M-band (Agarkova *et al.* 2000, Schoenauer *et al.* 2005, 2008).

Myomesins are mainly composed of Ig and FN3 domains (Vinkemeier *et al.* 1993, Schoenauer *et al.* 2008). Antiparallel homodimerization through the C-terminal Ig domains has been shown for MYOM1 and MYOM3 (Lange *et al.* 2005b, Pinotsis *et al.* 2008, Schoenauer *et al.* 2008), whereas myosin binding through the N-terminal parts has been demonstrated for MYOM1 and MYOM2 (Obermann *et al.* 1997, 1998). Myomesins interact with M-band titin at least indirectly, as demonstrated by co-purification of myomesins 1 and 2 with titin (Nave *et al.* 1989).

Obermann *et al.* (1997) identified direct binding of myomesin to the titin M4 domain in membrane overlay assays with purified protein fragments; this interaction was found to involve the central FN3 domains My4–My6 of myomesin and to be prevented by phosphorylation of the linker region between My4–5 (Obermann *et al.* 1997). The interaction was, however, not corroborated by pulldown and yeast two-hybrid (Y2H) assays by Fukuzawa *et al.* (2008), who demonstrated the involvement of the same myomesin region in obscurin binding. The phosphorylation-regulated interaction of myomesin with titin M4 was hence proposed to be insignificant in mature muscle but of potential relevance during sarcomere assembly (Fukuzawa *et al.* 2008).

2.3.5.6 M-band titin and the obscurin proteins

C-terminal titin and myomesin 1 are engaged in ternary interactions with the obscurin protein (OBSCN) and its shorter homologue obscurin-like 1 (OBSL1) (Fukuzawa *et al.* 2008). The two obscurin proteins, highly alike in their N-termini, will be here referred to as OBSCN/OBSL1.

The ternary complex between titin, myomesin, and OBSCN/OBSL1 is formed through independent interactions of myomesin and titin with OBSCN/OBSL1, with no direct binding occurring between myomesin and titin. The third Ig domain (Ig3) in OBSCN/OBLS1 interacts with the linker region My4–My5 of myomesin. This interaction is specific for MYOM1 and is unaffected by myomesin phosphorylation. The N-terminal Ig domain (Ig1) of OBSCN/OBSL1, on the other hand, interacts with the titin M10 domain. Y2H and pulldown studies indicated this interaction to be abolished or severely impaired by two of the TMD/LGMD2J-causing mutations (FINmaj and L33388P), whereas the I33379N mutation was reported to have no effect (Fukuzawa *et al.* 2008).

Interactions with titin M10 and myomesin are required for the correct localization of OBSCN/OBSL1 to the M-band. This was shown in cultured cardiomyocytes, where expression of various constructs comprising the above-mentioned interaction sites had dominant negative effects on the localization of endogenous OBSCN and OBSL1, and in C2C12 cells, where the constructs inhibited sarcomere formation (Fukuzawa *et al.* 2008). The importance of titin for the organization of this complex is further demonstrated by the altered obscurin–myomesin colocalization in M-band titinopahies (Fukuzawa *et al.* 2008, Charton *et al.* 2010).

The diverse functions of obscurin and OBSL1 have only recently begun to unravel. During myofibrillogenesis, obscurin is highly expressed, shows variable localization to Z-discs and M-bands, and seems to have both structural and signalling functions. Although some studies have suggested that obscurin has an essential role in myofibrillogenesis, knockout mice have proven the dispensability of the protein (Young *et al.* 2001, Borisov *et al.* 2004, 2006, Kontrogianni-Konstantopoulos *et al.* 2006b, Raeker *et al.* 2006, Ackermann *et al.* 2009, Lange *et al.* 2009). In mature muscle, obscurin is mostly found at the M-band level (Young *et al.* 2001, Bagnato *et al.* 2003, Bowman *et al.* 2007). Interacting with titin through its N-terminus and with ankyrins through its C-terminus, it links myofibrils to the surrounding sarcoplasmic reticulum (SR) and sarcolemma. This has been shown to be important for the organization of the SR, the subsarcolemmal microtubular network, and the dystrophin–glycoprotein complex, and for sarcolemmal integrity (Bagnato *et al.* 2003, Kontrogianni-Konstantopoulos *et al.* 2003, 2006b, Cunha & Mohler 2008, Lange *et al.* 2009, 2012, Randazzo *et al.* 2013). Obscurin also targets a variant form of MyBP-C to the M-band at the myofibril periphery in skeletal muscles, with yet uncharacterized importance for M-band structure and function (Ackermann *et al.* 2009).

OBSL1 is expressed in multiple isoforms with presumably different localizations to cytoskeletal structures. Lacking the ankyrin-binding and signalling domains of obscurin, it has been suggested to have a structural role as a cytoskeletal adaptor (Geisler *et al.* 2007, Fukuzawa *et al.* 2008).

2.3.5.7 Developmental and structural effects of M-band titin deletions

To study the functions of M-band titin *in vivo*, Gotthardt and colleagues have employed a series of mouse models with constitutive or tissue-specific conditional deletions of exons Mex1–Mex2 (Gotthardt *et al.* 2003, Peng *et al.* 2005, 2007, Weinert *et al.* 2006, Ottenheijm *et al.* 2009). Although the primary goal has been to study the importance of the titin kinase, the in-frame deletion of 1974 amino acid residues spans the domains from A169 to M7, removing most of M-band titin.

Constitutive deletion of Mex1–2 in all tissues (Weinert *et al.* 2006) and an early developmental conditional deletion in the heart (Gotthardt *et al.* 2003) have similar outcomes, both leading to early embryonic lethality due to cardiac dysfunction. In constitutive knockouts, the heart develops normally up to E9.0 and initiates beating. Unaltered localization of titin epitopes at the Z-disc, N2B element, and I-band/A-band boundary indicate that cardiac sarcomeres develop and incorporate mutant titin normally. In contrast, domains M8–M9 fail to show periodic localization, suggesting that titin C-terminus is not properly assembled into the M-band. After normal sarcomere formation, myofibrils lacking M-band titin show impaired lateral growth and are disassembled (Weinert *et al.* 2006).

A conditional Mex1–2 KO targeting cardiac and skeletal muscle later in development through the muscle creatine kinase promoter avoids embryonic lethality (Gotthardt *et al.* 2003). The mice develop generalized muscle weakness and wasting, and die around the age of five weeks. Sarcomeres show first normal ultrastructure in EM, but upon gradual replacement of wild-type titin by the deleted protein, they develop pale M-bands and undergo disassembly that progresses from M-band to Z-disc (Gotthardt *et al.* 2003, Peng *et al.* 2005). In contrast to the constitutive deletion model, mutant titin seems to be incorporated to the sarcomeres all the way to the M-band level, possibly due to a stabilizing effect of other M-band proteins in pre-existing sarcomeres or due to different expression of titin-binding proteins in embryonic and adult sarcomeres (Gotthardt *et al.* 2003, Weinert *et al.* 2006). Increased separation of the M8/M9 epitope doublets suggests, however, that the deleted titin C-termini do not overlap in the M-band (Gotthardt *et al.* 2003).

Sarcomere disassembly seen in late stage pathology of all Mex1–2 knockout models has been suggested to result from structural instability of the M-band resulting from a disturbed interaction of titin with myomesin (Gotthardt *et al.* 2003, Weinert *et al.* 2006). In the constitutive knockout model, myomesin—although it does localize to the M-band—shows abnormally diffuse staining that was suggested to reflect the absence of myomesin-binding M4 domains of titin (Weinert *et al.* 2006). Abnormal myomesin organization could also be explained

by altered localization of the M10 domain that interacts with myomesin through obscurin/OBSL1 (Fukuzawa *et al.* 2008).

The studies by Miller *et al.* (2003a) and Musa *et al.* (2006) both utilized deletion models encompassing the entire titin C-terminus starting from the kinase domain. In murine myoblasts, the deletion was found to interfere with myogenic differentiation already in the heterozygous state (Miller *et al.* 2003a). The cells showed impaired fusion and formed poorly ordered myofibrils, with Z-discs and M-bands out of register. Titin, α-actinin, myosin, MURF2, and obscurin were disorganized, while myomesin localization was relatively well preserved (Miller *et al.* 2003a).

In mouse embryonic stem cells induced to differentiate into cardiomyocytes, the heterozygous deletion only caused subtle differences in M-band structure (Musa *et al.* 2006). In the homozygous state, however, a total disruption of myofibrillogenesis was observed, with all the analyzed sarcomeric components— including α-actinin and telethonin— showing abnormal localization. This demonstrated that M-band titin is essential for myofibrillogenesis, and suggested the proper formation of M-band regulates also Z-disc assembly, possibly through TK-based signalling. The difference to skeletal myoblasts, where a single deleted allele had deleterious effects, was proposed to reflect differences in the efficacy of TK signalling between the cell types (Musa *et al.* 2006).

The difference between the total C-terminal deletion that abolishes the myofibrillogenesis completely, and the Mex1–2 deletion that allows the development of beating cardiomyocytes, is noteworthy, as it suggests an important role for the domains M8–M10 in myofibrillogenesis (Gotthardt *et al.* 2003, Musa *et al.* 2006, Weinert *et al.* 2006).

A complementary view on the importance of M-band titin comes from Salih myopathy, a human disease caused by homozygous absence of the titin C-terminus (Carmignac *et al.* 2007). The two described mutations are frameshift-causing deletions in Mex1 and Mex3, leading to premature termination codons and truncation of C-terminal titin at M5 and is6, respectively. Heterozygotes are symptomless, presumably explained by mutant transcripts undergoing nonsense-mediated decay (NMD). In homozygotes, all titin protein, translated from mutant transcripts escaping NMD, lacks the most C-terminal domains (Carmignac *et al.* 2007).

The patients present with congenital skeletal myopathy of moderate severity and slow progression, followed in the childhood by rapidly progressive dilated cardiomyopathy and arrhythmia that ultimately lead to heart failure. Skeletal muscle pathology shows minicore-type lesions, predominance of type 1 fibres, and central nuclei, and later dystrophic changes. EM reveals sarcomeric disruption, with changes in the M-band more pronounced than in the Z-disc (Carmignac *et al.* 2007).

The truncated titin molecules in Salih myopathy are integrated to the sarcomere, and they allow seemingly normal sarcomere development, demonstrating

that the extreme C-terminal titin domains are not required for this process. The mutations remove the M-band binding site of CAPN3, and muscles show secondary CAPN3 deficiency similar to that seen in TMD/LGMD2J (discussed in 2.1.5.2). Lack or dysregulation of CAPN3 may contribute to the skeletal-muscle phenotype, but it is unlikely to explain the cardiomyopathy, given the low level of CAPN3 expression in postnatal heart (Carmignac *et al.* 2007).

Sarcomeric disarray in Salih myopathy resembles that seen in Mex1–2 knockout mice, and it was suggested that mechanical instability of the M-band, resulting from incomplete overlap of the titin molecules, could underlie the phenotype in both cases (Carmignac *et al.* 2007). It is also possible that the pathogenesis of Salih myopathy is partly due to impaired titin production capacity. If most of the transcribed mRNAs are degraded by NMD, insufficient translation of new titin molecules may lead to a reduction in total titin expression and hamper the fibre's ability to renew myofibrils.

2.3.6 Titin in smooth muscle and non-muscle cells

In addition to their established central role in striated muscles, products of the *TTN* gene have been reported in other tissues and cell types. Adult smooth muscles express short titin isoforms of ~1 MDa, containing exons from all titin regions but apparently excluding TK and the extreme C-terminus. Fetal smooth muscles express titin isoforms similar in size and composition to skeletal muscle forms (Labeit *et al.* 2006).

Expression of titin on a low level has been detected also in several non-muscle cell types (Eilertsen & Keller 1992, Cavnar *et al.* 2007, Qi *et al.* 2008, Mikelsaar *et al.* 2010, 2012). The non-muscle isoforms, termed "cellular titin" or c-titin, utilize unique exon patterns and are at least partly distinct from both striated and smooth muscle titins (Cavnar *et al.* 2007). In non-muscle cells, titin has been suggested to participate in the organization of cytoskeletal structures such as stress fibres and to provide them with passive tension, to participate in biomechanical sensing, and to modify the mechanical properties of the tissue (Eilertsen & Keller 1992, Eilertsen *et al.* 1994, 1997, Cavnar *et al.* 2007, Schwarz *et al.* 2008).

2.3.6.1 Nuclear titin

A growing body of evidence suggests that titin has functions also in the nucleus. After the initial description of nuclear titin by Machado and colleagues (1998), titin has been detected in association with chromosomes, the nuclear matrix and envelope, the mitotic spindle, and the centrioles (Machado & Andrew 2000, Zastrow *et al.* 2006, Mikelsaar *et al.* 2010, 2012), and biochemically purified from isolated nuclei (King & Jhou 2010). Furthermore, N-terminal titin constructs have been found to activate β-catenin signalling in transfected cells, suggesting a signalling role for nuclear titin (Qi *et al.* 2008).

With regard to M-band titinopathies, the findings of Zastrow *et al.* (2006) are of potential interest. This study identified an interaction of C-terminal titin with lamins, intermediate filaments of the nuclear matrix and lamina. Each of the domains M7–M10 as well as M-is7 were found to have affinity for lamins, and functional importance of this interaction was supported by disrupted nuclear morphology in HeLa cells transfected with a nuclear-targeted M-is7 construct. An antibody against M-is6 exhibited a diffuse or punctate nuclear localization pattern in HeLa cells, whereas in *Caenorhabditis elegans* two antibodies against the worm titin orthologue stained the nuclear envelope and the mitotic spindle. By interacting with lamins, titin was proposed to participate in the organization of nuclear architecture, condensation of the chromosomes, and assembly and disassembly of the nuclear envelope (Zastrow *et al.* 2006). Interestingly, mutations in lamins can, among other diseases, cause muscular dystrophy and cardiomyopathy (reviewed by Schreiber & Kennedy 2013).

The diverse results of the aforementioned studies regarding the composition, localization and functions of titin in nucleus are difficult to consolidate, and the whole concept of nuclear titin is under debate. Indeed, negative findings obtained in some studies challenge the existence of nuclear titin altogether: Expression analyses on a titin exon microarray did not show any detectable titin transcript in HeLa and HL cells (Labeit *et al.* 2006, Takata *et al.* 2007), whereas proteomics studies have failed to reveal titin in chromosomes and centrosomes (Andersen *et al.* 2003, Takata *et al.* 2007).

2.4 Calpain 3 (CAPN3)

Calpain 3 (CAPN3; also known as p94) is an intracellular protease belonging to the family of calpains, Ca^{2+}-activated papain-like cysteine proteases (Sorimachi *et al.* 1989). Members of this protease family are regarded as modulator proteases, involved in regulation of their substrates through specific proteolytic processing events, rather than in degradation (Ono & Sorimachi 2012).

2.4.1 Structure of CAPN3

CAPN3 contains the domains common to classical calpains: the cysteine protease core domain split into subdomains PC1 and PC2 (previously designated as IIa and IIb), a Ca^{2+}- and phospholipid-binding C2-like domain (C2L, domain III), and a penta-EF-hand domain (PEF, domain IV). In addition, it contains three CAPN3-specific sequences, the N-terminal sequence (NS), and insertion sequences IS1 and IS2 (Sorimachi *et al.* 1989, 1990, Ono & Sorimachi 2012). IS1, located within the PC2 subdomain, acts as an internal propeptide (Sorimachi *et al.* 1993, Diaz *et al.* 2004). IS2, located between the C2L and PEF domains, modulates the activation properties of CAPN3, is involved in titin binding, and contains an apparently func-

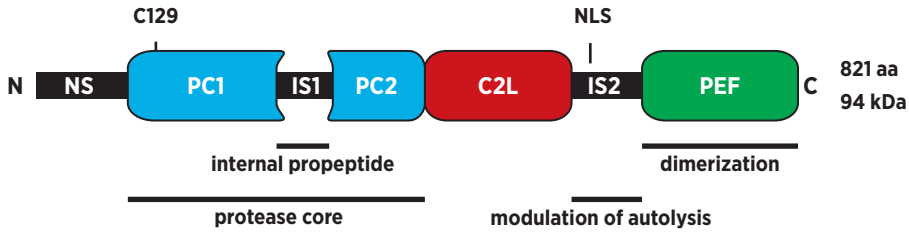

Figure 4. Structure of calpain 3

A schematic view of the CAPN3 protein, comprised of the protease core (subdomains PC1 and PC2), a C2-like domain (C2L), a penta-EF-hand (PEF) domain, and the CAPN3-specific insertions NS, IS1, and IS2. Positions of the catalytic residue C129 and the nuclear localization signal (NLS) are shown.

tional nuclear localization signal (encoded by exon 15) (Sorimachi *et al.* 1989, 1993, 1995). The structure of CAPN3 is schematically presented in Fig. 4.

In contrast to the canonical calpains CAPN1 (μ-calpain) and CAPN2 (m-calpain), CAPN3 does not heterodimerize with the calpain small subunit (Sorimachi *et al.* 1995, Ono & Sorimachi 2012). CAPN3 can homodimerize through the PEF domain and it is purified as a dimer (Kinbara *et al.* 1998, Ravulapalli *et al.* 2005), but whether it within myofibres exists as monomers or dimers is unknown.

Alternative splicing produces several isoforms of CAPN3. The full-length canonical form of 821 amino acids and 94 kDa (RefSeq NP_000061), designated isoform a, is the only form present in significant amounts in mature skeletal myofibres (Richard *et al.* 1995, Herasse *et al.* 1999, Ojima *et al.* 2007). Isoforms lacking exons 6 (encoding IS1) and 15–16 (together encoding most of IS2) in different combinations are expressed in myoblasts and during skeletal muscle development (Richard *et al.* 1995, Herasse *et al.* 1999, Ojima *et al.* 2007). In addition, a variety of minor CAPN3 isoforms, some of which utilize exons not included in the canonical form, have been shown to be expressed in lymphocytes, rodent eyes, or ubiquitously (Fougerousse *et al.* 2000b, Fukiage *et al.* 2002, Kawabata *et al.* 2003, De Tullio *et al.* 2003).

2.4.2 Expression and localization of CAPN3

CAPN3 is predominantly expressed in skeletal muscle, and as mentioned above, tissue-specific or ubiquitous isoforms exist at low levels (Sorimachi *et al.* 1989, Fougerousse *et al.* 1998, 2000b, Fukiage *et al.* 2002, Kawabata *et al.* 2003, De Tullio *et al.* 2003). Importantly, although CAPN3 is expressed during cardiac development, and its transcripts have been detected in adult human heart, the level of CAPN3 protein in the mature heart is very low (Sorimachi *et al.* 1989, Fougerousse *et al.* 1998, 2000a, Taveau *et al.* 2002). The expression within pig skeletal muscles has been reported to show a difference between fibre types, with isolated fast fibres showing an approximately threefold level of CAPN3 in WB compared to slow fibres (Jones *et al.* 1999). However, a recent large-scale proteomics

study did not report differential CAPN3 expression between murine slow and fast muscles (Drexler *et al.* 2012).

Within skeletal myofibres, most of CAPN3 is tightly associated with myofibrils (Murphy & Lamb 2009). Endogenous CAPN3 and transfected constructs have been detected in three sarcomeric regions: I-band, M-band, and Z-disc. Different studies have shown variable distribution of CAPN3 between these regions, variability remaining mostly unexplained (Keira *et al.* 2003, Taveau *et al.* 2003, Ojima *et al.* 2005, 2007, 2010, Murphy & Lamb 2009). In cultured mouse myotubes, CAPN3 was found to show predominant M-band localization during late myofibrillogenesis, whereas the typical pattern in fully mature myotubes and muscles consists of a major doublet band at the I-band region and a minor band at the M-band (Keira *et al.* 2003, Ojima *et al.* 2007, 2010, Murphy & Lamb 2009).

The variable amount of CAPN3 detected at the Z-disc may represent an N-terminal fragment rather than the full-length protein. This was suggested by Ojima *et al.* (2007), who showed stronger Z-disc labelling with a CAPN3 antibody raised against the NS region, and detected an interaction between CAPN3 NS and α-actinin. The biological role for this possible Z-disc targeting of calpain fragments is yet unknown.

Some CAPN3 is found in myonuclei (Baghdiguian *et al.* 1999, Keira *et al.* 2003). This may depend on a lysine-rich motif in IS2, as CAPN3 constructs lacking the IS2 region do not show nuclear localization in transfected cells (Sorimachi *et al.* 1993). Tissue fractionation experiments by Murphy and coworkers (2011) indicated that ≤10% of total CAPN3 in human and rat muscles is nuclear, and this does not change in response to eccentric exercise. CAPN3 in the nuclear pool was found to be mostly in the autolyzed (*i.e.* activated) state, in contrast to the myofibril-bound pool (Murphy *et al.* 2011).

2.4.3 Interactions between CAPN3 and titin

In line with its predominant localization at the I-band and M-band, interactions of CAPN3 with titin have been described at these sarcomeric regions (Sorimachi *et al.* 1995, Hayashi *et al.* 2008).

2.4.3.1 Interaction of CAPN3 with M-band titin

The interaction of CAPN3 with the extreme C-terminus of titin (domains M9–is7–M10) was identified in a yeast two-hybrid screen (Sorimachi *et al.* 1995). In further Y2H studies, M9–is7, but not M9 alone, showed binding to CAPN3, demonstrating that at least is7 is required for the interaction (Kinbara *et al.* 1997). Studies addressing the importance of M9 for CAPN3 binding have not been reported. The interaction seems to require the whole three-dimensional structure of CAPN3, as none of the calpain deletion constructs tested by Kinbara *et al.* (1997) showed binding to C-terminal titin in Y2H. The interaction of CAPN3 and C-terminal titin has been later confirmed in a solid-phase binding assay (Kramerova *et al.* 2004).

Y2H studies by Herasse *et al.* (1999) indicated that developmental CAPN3 isoforms show different interactions with C-terminal titin. CAPN3 isoforms lacking the exon 16, and hence most of the IS2 segment (*i.e.* ex6$^-$15$^-$16$^-$ and ex15$^-$16$^-$), showed dramatically stronger interaction signals with M-band titin, whereas exclusion of exons 6 or 15 alone or together resulted in slightly or clearly weaker binding compared to the full-length form. This suggests that IS2 modulates the interaction with C-terminal titin, but given the low and temporally restricted expression of the CAPN3 ex16$^-$ isoforms (Herasse *et al.* 1999, Ojima *et al.* 2007), the importance of this phenomenon is unclear.

The exact biological function of the CAPN3–titin interaction in the M-band is unknown, but the secondary CAPN3 deficiency seen in TMD/LGMD2J patients and the FINmaj knock-in mouse (Haravuori *et al.* 2001, Charton *et al.* 2010) suggests that C-terminal titin plays a key role in regulating the functions and stability of CAPN3. Moreover, the differential localization of CAPN3 to the M-band and N2A regions, with the apparent correlation to sarcomere length (Ojima *et al.* 2007, 2010) (discussed in 2.4.5.), highlights the dynamic nature of the interaction.

In addition to regulation of CAPN3, the interaction could indicate that C-terminal titin is a substrate for CAPN3. In line with this, the ability of CAPN3 to cleave C-terminal titin has been demonstrated in coexpression experiments. In studies by Taveau *et al.* (2003) on mouse myoblasts, a novel band of 18 kDa was produced in cotransfections of a titin construct with active CAPN3 but not with the C129S mutant. However, small amounts of the fragment were also detected in co-transfections of the titin construct with the CAPN3 ex6$^-$ isoform and the activation-incompetent Y274A mutant (Taveau *et al.* 2003), indicating possible contribution by endogenous CAPN3 or other proteases. Kramerova *et al.* (2004) showed that the titin construct M6–M10 is cleaved by active CAPN3 when coexpressed in insect cells, producing a C-terminal fragment of ~40 kDa. This would place the cleavage in the M-is6 region, N-terminally from the described binding site.

2.4.3.2 Interactions of CAPN3 with I-band titin

CAPN3 binds I-band titin at three identified binding sites. The "primary" binding site, identified in the same Y2H screen that revealed the M-band interaction, encompasses the domains I82–I83 of the N2A element (Sorimachi *et al.* 1995, Ono *et al.* 2004). CAPN3 binds this titin site through a short peptide (V573–L580) at the beginning of the IS2 region. The binding peptide is included in the CAPN3 ex15$^-$16$^-$ isoforms that lack most of IS2, and these developmental CAPN3 variants accordingly bind the N2A element with a similar efficiency as the full-length isoform (Herasse *et al.* 1999, Ono *et al.* 2006).

Two additional CAPN3 binding sites in I-band titin, termed "secondary" sites, were later identified in CoIP studies by Hayashi *et al.* (2008), and regions mediating the interactions were defined with deletion constructs. One such site encompasses the I80 domain and the N2A unique sequence region, thus overlapping

titin's binding site for muscle ankyrin repeat proteins (see 2.4.7.), and the other is found within the PEVK region. The whole structure of CAPN3 seems to be needed for the former interaction, whereas the latter is mediated by a short peptide in early IS2, adjacent to the site binding the N2A Ig domains (Hayashi *et al.* 2008).

2.4.4 Activation of CAPN3

The active site of CAPN3 is blocked by an internal autoinhibitory propeptide formed by the IS1 region; to activate the enzyme, this must be removed by an autolytic mechanism (Rey & Davies 2002, Taveau *et al.* 2003, Diaz *et al.* 2004). The autolytic activation is responsible for the rapid degradation of CAPN3—occurring in many heterologous expression systems and upon muscle homogenization—that has complicated biochemical studies on the native protein (Sorimachi *et al.* 1993, Kinbara *et al.* 1998). The proteolytically inactive C129S mutant is incapable of autolysis (Sorimachi *et al.* 1993), and it has been widely used in molecular studies on CAPN3.

Molecular mechanisms of CAPN3 activation have been extensively studied *in vitro* with CAPN3 constructs containing point mutations or truncations, and with CAPN3 isoforms showing altered autolytic properties. These studies have revealed that the autolysis involves sequential cleavages at several sites in the IS1 and NS regions. The exact cleavage sites identified in different studies differ somewhat, likely indicating slightly different structures of the utilized deletion mutant constructs (Rey & Davies 2002, Taveau *et al.* 2003, Diaz *et al.* 2004, Ono *et al.* 2006, 2008, 2010). The autolysis can proceed through both intramolecular and intermolecular reactions. The initial cleavage events have been regarded as strictly intramolecular (Rey & Davies 2002, García Díaz *et al.* 2006), but the ability of wild-type CAPN3 to autolyse the inactive C129S mutant suggests that intermolecular autolysis could be possible from the beginning (Taveau *et al.* 2003).

Key events in CAPN3 activation are cleavages within the IS1 region, resulting in the disappearance of the full-length protein and producing the characteristic C-terminal fragments of 55–60 kDa in WB. These cleavages lead to detachment of IS1, while the N- and C-terminal moieties constituting the active enzyme remain non-covalently associated (Kinbara *et al.* 1998, Rey & Davies 2002, Taveau *et al.* 2003, Diaz *et al.* 2004, Ono *et al.* 2006). Autolytic cleavages occur also within the NS sequence, resulting in loss of the original N-terminus from the protein. However, the timing of these N-terminal cleavages relative to other autolytic events is unclear due to conflicting results, and their biological importance is unknown (Rey & Davies 2002, Diaz *et al.* 2004, Ono *et al.* 2006). Another autolytic cleavage, producing a C-terminal fragment of ~32 kDa, has been reported in the N-terminal part of IS2. This was suggested to cause dissociation and inactivation of CAPN3 (Ono *et al.* 2006), but conclusive evidence for this is still lacking.

In contrast to the ubiquitous calpains that require Ca^{2+} at micro- or millimolar concentrations for activity, CAPN3 was first described to be calcium-independent

(Kinbara *et al.* 1998). This apparent Ca^{2+}-independence is due to the extremely high Ca^{2+} sensitivity of CAPN3: submicromolar Ca^{2+} concentrations (in the order of 200 nM) are sufficient for its activation *in vitro* (Branca *et al.* 1999, García Díaz *et al.* 2006, Murphy & Lamb 2009). Similarly to ubiquitous calpains, the activation involves realignment of the catalytic triad induced by binding of two Ca^{2+} ions to the protease core, but the presence of IS2 in CAPN3 increases the calcium sensitivity by a yet unknown mechanism (Sorimachi *et al.* 1993, García Díaz *et al.* 2006, Ono *et al.* 2008). A recent report by Ono *et al.* (2010) suggested that CAPN3 can also be activated by Na^{+}, likely through one of the Ca^{2+} binding sites in the protease core. Na^{+} binding was proposed to enhance the responsiveness of CAPN3 to physiological Ca^{2+} concentrations or to modulate the substrate specificity (Ono *et al.* 2010). However, since significant amounts of contaminant Ca^{2+} can be present in reagents (notably, NaCl) and containers (García Díaz *et al.* 2006), the suggested Na^{+} dependency could be artefactual.

In a physiological setting, detectable autolysis of CAPN3 has only been demonstrated to occur following eccentric exercise—a condition known to cause a small but prolonged increase in the resting Ca^{2+} concentration inside myofibres (Murphy *et al.* 2007, 2011, Ojima *et al.* 2010). CAPN3 activation has not been detected after vigorous or prolonged concentric exercise, nor after tetanic stimulation known to cause very high but short-lived Ca^{2+} peaks in myofibres (Murphy *et al.* 2006, 2009).

The presence of intact CAPN3 in the myofibrillar fraction isolated from muscle and its rapid autolysis upon purification have suggested that binding to titin protects CAPN3 from autolysis (Sorimachi *et al.* 1993, 1995, Kinbara *et al.* 1998). In support of this idea, coexpression of the titin fragment I81–I83, encompassing one of the CAPN3 binding sites in the N2A region, was shown to suppress the autolysis of a CAPN3 construct in a yeast-based reporter gene assay, whereas a C-terminal titin construct containing the M-band CAPN3 binding site did not show such an effect (Ono *et al.* 2006). Since CAPN3 can be successfully produced in cells lacking myofibrils and it may, in the absence of Ca^{2+}, remain inactive in solution for hours, titin binding is not a prerequisite for its stabilization (Branca *et al.* 1999, Murphy & Lamb 2009). Interaction with titin through IS2 could, however, modulate the Ca^{2+} sensitivity of CAPN3 activation or limit the mobility of activated CAPN3 molecules, thus inhibiting the propagation of the activation through intermolecular autolysis (suggested by Taveau *et al.* 2003).

In vivo additional factors, possibly coordinated by titin, are likely to regulate the activation of CAPN3. The autolysis of CAPN3 in single-fibre preparations is significantly attenuated in the absence of ATP, however in a manner independent of rigor. This could be explained by binding of ATP to CAPN3 or to one of its myofibrillar partners, or by a phosphorylation event (Murphy & Lamb 2009). In line with the latter possibility, CAPN3 isolated from the myofibrillar fraction may be phosphorylated, as indicated by staining with a phosphate-reactive dye (Ermolova *et al.* 2011).

2.4.5 Dynamics of CAPN3 localization and activity

The relationship between the activity and localization of CAPN3 has been addressed in recent studies, but the results have been somewhat conflicting.

Based on a correlation between sarcomere length and CAPN3 staining pattern in fixed muscle samples, Ojima and coworkers (2007, 2010) proposed that the myofibrillar localization of CAPN3 changes with sarcomere length. A more pronounced staining of the I-band in longer sarcomeres was concluded to reflect relocation of CAPN3 from M-band to the N2A element upon sarcomere stretch. This shuttling appeared to be partly dependent on protease activity, as the inactive CAPN3 C129S showed a slightly higher degree of M-band localization at a given sarcomere length. Similar results were obtained with CAPN3 constructs in cultured myocytes (Ojima *et al.* 2007) and with the endogenous proteins in muscles of wild type and C129S KI mice (Ojima *et al.* 2010). Also FRAP (fluorescence recovery after photobleaching) experiments with GFP-tagged CAPN3 constructs suggested altered mobility of the C129S mutant protein at the M-band (Ojima *et al.* 2010). Moreover, eccentric exercise was reported to cause the translocation of CAPN3 from the myofibrillar to the soluble fraction in mice. As this was not seen in C129S KI, detachment from myofibrils was suggested to depend on the activation of CAPN3 (Ojima *et al.* 2010). The connection between the mobility of CAPN3 and its proteolytic activity was proposed to depend on conformational changes induced by autolysis (Ojima *et al.* 2010), but the different behaviour of the wild-type and C129S proteins could also reflect a difference in their biochemical or biophysical properties unrelated to the protease activity.

The findings by Murphy and colleagues (Murphy & Lamb 2009, Murphy *et al.* 2011) argue against some of the aforementioned notions. In experiments performed on skinned myofibres, stretching was found not to cause autolysis of CAPN3 nor its mobilization from myofibrils. Furthermore, activation of CAPN3 in isolated myofibres and human muscles—induced by Ca^{2+} treatment or eccentric exercise, respectively—did not cause its translocation to the cytosol. The majority of CAPN3 was reported to remain myofibril-associated even after autolysis, and conversely, most of the cytosolic CAPN3 was full-length (Murphy & Lamb 2009, Murphy *et al.* 2011). These studies did not directly address the effect of sarcomere length on the spatial distribution of CAPN3 within the sarcomere. According to Murphy and Lamb (2009), the sarcomere-length-dependent localization differences observed by Ojima *et al.* (2007) in cultured myotubes could reflect local increases in Ca^{2+} concentration, causing both the observed sarcomere hypercontraction (and a corresponding hyperextension in the vicinity) and CAPN3 autolysis. This mechanism is, however, unlikely to explain the similar, albeit less dramatic, effect seen in mouse muscles.

2.4.6 Substrates and proteolytic functions of CAPN3

In contrast to many proteases and similarly to the ubiquitous calpains, CAPN3 does not have a strict requirement for the cleavage site. The substrate specificity of calpains is considered to depend largely on structural features, with a preference for unstructured protein segments such as interdomain linkers (Ono & Sorimachi 2012). However, based on sequence analysis of reported substrates, de Morrée and colleagues (2010) reported the primary sequence motif [LIMV]X_4[LIMV] X_2[LIMV][DE] to mediate recognition and cleavage by CAPN3. Introducing the motif to reporter constructs was shown to transform them to CAPN3 substrates, whereas mutagenesis of key residues inhibited the cleavage. As the motif was also able to predict novel substrates from a sequence database, it may prove a powerful tool for identifying substrates of CAPN3 and studying its functions (de Morrée *et al.* 2010).

Different strategies have been employed for identifying CAPN3 substrates experimentally. Several studies have tested and confirmed the cleavage of candidate substrates by coexpressing them with CAPN3 (Baghdiguian *et al.* 1999, Guyon *et al.* 2003, Taveau *et al.* 2003, Kramerova *et al.* 2004, Hayashi *et al.* 2008, Huang *et al.* 2008), whereas proteomics analyses of cells and muscles overexpressing CAPN3 have been used for identification of novel substrates (Cohen *et al.* 2006, Ono *et al.* 2006). While these studies have identified a number proteins that can be cleaved by CAPN3, it is yet unknown which substrates are physiologically relevant. Among both confirmed and predicted substrates, cytoskeletal and sarcomeric proteins are a significant group, and remodelling of these structures is hence considered to be a major function of CAPN3 in mature muscle (Kramerova *et al.* 2005, Cohen *et al.* 2006, Duguez *et al.* 2006, Beckmann & Spencer 2008, de Morrée *et al.* 2010). Also the association of activated CAPN3 with the myofibrils, suggesting that its physiological substrates are in the vicinity, supports a primary function in cytoskeletal and sarcomeric processing (Beckmann & Spencer 2008, Murphy *et al.* 2011). Moreover, CAPN3 KO mice show impaired sarcomeric remodelling in response to muscle unloading and reloading. The failure of CAPN3 KO muscles to accumulate ubiquitinated protein conjugates during the remodelling process suggests that CAPN3 is required for releasing proteins components from the myofibrils, a prerequisite for their further turnover by the ubiquitin–proteasome pathway (Kramerova *et al.* 2005).

In addition to its apparent major function in cytoskeletal remodelling, the identified substrates of CAPN3 suggest its involvement in the regulation of processes such as muscle development and regeneration, membrane repair, SUMOylation, fat and energy metabolism, and apoptosis (Baghdiguian *et al.* 1999, Cohen *et al.* 2006, Kramerova *et al.* 2006, Huang *et al.* 2008, de Morrée *et al.* 2010, Stuelsatz *et al.* 2010). Furthermore, the protease activity of CAPN3 is suggested to modulate signalling mediated by the titin N2A element and the muscle ankyrin repeat proteins, discussed below.

2.4.7 CAPN3, MARPs, and the titin N2A element in signalling

The muscle ankyrin repeat proteins (MARPs)—ANKRD1 (MARP1; CARP, cardiac ankyrin repeat protein), ANKRD2 (MARP2; ARPP, ankyrin repeat protein with PEST and proline-rich region), and ANKRD23 (MARP3; DARP, diabetes-related ankyrin repeat protein)—are a group of ankyrin repeat domain (ANKRD) proteins predominantly expressed in skeletal and cardiac muscles with characteristic expression patterns. Upregulation of MARPs has been reported in various muscle diseases and in response to immobilization, denervation, eccentric contractions, strenuous exercise, and metabolic challenge, suggesting their importance in muscle remodelling (reviewed by Kojic *et al.* 2011).

MARPs are suggested to have dual roles as structural and regulatory proteins. Myofibres from mice lacking all three MARPs have altered mechanical properties (Barash *et al.* 2007), and MARPs have been proposed to mechanically stabilize the contractile machinery (Tee & Peppelenbosch 2010). The regulatory role of MARPs, probably representing the more important aspect of their functions, is demonstrated by their nuclear localization, DNA binding (shown for ANKRD1), and interactions with a multitude of signalling proteins and transcription factors, and supported by wide-spread changes in gene expression following MARP overexpression or knockdown (Chu *et al.* 1995, Kojic *et al.* 2004, Laure *et al.* 2010, Belgrano *et al.* 2011, Kojic *et al.* 2011).

MARPs show dual localization to the sarcomeric I-band and nuclei, and ANKRD23 can also localize to intercalated discs (Bang *et al.* 2001b, Miller *et al.* 2003b). All three bind the N2A element of titin (Miller *et al.* 2003b), as well as myopalladin, a muscle-restricted Ig-domain protein showing either Z-disc or I-band localization (Bang *et al.* 2001b, Miller *et al.* 2003b). Although MARPs, CAPN3, and myopalladin were suggested to constitute a mechanosensory complex at the titin N2A element a decade ago (Miller *et al.* 2003b), not much is known about the relationships of the proteins, and no mechanosensory function for the proposed complex has been demonstrated. Recent studies have, however, provided some insight into the intricate system (Hayashi *et al.* 2008, Laure *et al.* 2010).

Both ANKRD1 (Laure *et al.* 2010) and ANKRD2 (Hayashi *et al.* 2008) are proteolytic substrates of CAPN3. Cleavage of ANKRD1 may increase its binding to titin and reduce its nuclear shuttling, thereby inhibiting the effects of ANKRD1 on gene expression (Laure *et al.* 2010). The cleavage of ANKRD2 is, on the other hand, possibly enhanced by titin binding (Hayashi *et al.* 2008). Unlike ANKRD1, the cleavage of ANKRD2 does not seem to affect its affinity towards titin (Hayashi *et al.* 2008), suggesting that the myofibrillar association of the two proteins is not regulated in a similar fashion. The possible cleavage site in ANKRD2 is close to a serine residue whose phosphorylation promotes nuclear translocation of the protein (Cenni *et al.* 2011), and phosphorylation has been proposed to cooperate with CAPN3-mediated cleavage in regulating the localization of ANKRD2 (Belgrano *et al.* 2011). These functions may also be modulated by competitive interactions of

the MARPs and CAPN3 with their common binding site in the titin N2A element (Hayashi *et al.* 2008).

Additional clues about the N2A-based functions come from the murine *mdm* (muscular dystrophy with myositis) mutation, a rearrangement ultimately deleting 83 amino acids from the titin N2A element (Garvey *et al.* 2002). Mice homozygous for the mutation develop a severe dystrophy of skeletal muscles, whereas the heterozygotes only exhibit gait abnormalities (Garvey *et al.* 2002, Huebsch *et al.* 2005). The *mdm* mice show a reduction in CAPN3 levels, and before the identification of the gene defects at different parts of titin, *mdm* was suggested to be a natural mouse model for TMD/LGMD2J (Haravuori *et al.* 2001, Garvey *et al.* 2002). The *mdm* deletion disrupts the binding of CAPN3 at titin domains I82–I83 and prevents the suppressive effect of this titin region on CAPN3 autolysis (Witt *et al.* 2004, Ono *et al.* 2006). However, the overall defect may involve more complex changes in the titin–CAPN3–MARP system, possibly involving impaired interactions of ANKRD1 and ANKRD2 with titin and altered proteolysis of I-band titin by CAPN3 and other calpains (Hayashi *et al.* 2008). Interestingly, dysregulated CAPN3 activity does not seem to mediate the primary pathogenesis of *mdm*, as knockout of CAPN3 was reported not to affect the *mdm* phenotype. On the other hand, CAPN3 overexpression was shown to exacerbate the muscular dystrophy in *mdm* homozygotes, but to correct the gait abnormality in heterozygotes (Huebsch *et al.* 2005).

2.4.8 Non-proteolytic functions of CAPN3

The CAPN3 KO mice have a more severe dystrophic phenotype than the knock-in model expressing the proteolytically inactive C129S form of CAPN3, indicating that CAPN3 has functions not requiring its proteolytic activity (Richard *et al.* 2000, Kramerova *et al.* 2004, Ojima *et al.* 2010). One such non-proteolytic role was suggested by recent studies that identified interactions of CAPN3 with aldolase A (AldoA) ryanodine receptor (RyR), and other protein components of the triads, contact points between T-tubules and SR (Kramerova *et al.* 2008, Ojima *et al.* 2011) (Fig. 1). Association with the triads was also supported by the presence of CAPN3 in membrane fractions isolated from mouse muscles (Kramerova *et al.* 2008); however Murphy *et al.* (2011) failed to detect CAPN3 in enriched or purified SR vesicles.

CAPN3 KO mice showed impaired localization of AldoA to triads and a decreased amount of RyR, resulting in a diminished Ca^{2+} release, blunted CaMKII (Ca^{2+}/calmodulin protein kinase II) signalling, and impaired adaptation to exercise (Kramerova *et al.* 2008, 2012). Such changes were not observed in C129S KI mice, implying that CAPN3 has a structural rather than proteolytic role in stabilizing the triad-associated protein complex (Kramerova *et al.* 2008, Ojima *et al.* 2011). However, the majority of CAPN3 in single-fibre preparations is bound to myofibrils, and resistant to detergent extraction in conditions that cause a nearly complete washout of triad proteins (Murphy & Lamb 2009, Murphy *et al.* 2011). Hence, the

proportion of CAPN3 localized to triads is very low, or triad-associated CAPN3 is simultaneously bound to myofibrils. In line with the latter possibility, CAPN3 was proposed by Ojima *et al.* (2011) to provide a structural connection between myofibrils and triads by interacting with both the titin N2A element and triad proteins.

Based on thick filament misalignment observed in CAPN3 KO mouse but not in C129S KI (Kramerova *et al.* 2004, Ojima *et al.* 2010), a structural role was proposed for CAPN3 also in the myofibrils (Ojima *et al.* 2011).

2.5 Limb-girdle muscular dystrophy 1D (LGMD1D)

LGMD1D or DNAJB6 myopathy is an autosomal dominant limb-girdle muscular dystrophy, identified as a distinct 7q36-linked disease entity by Speer and colleagues (1999) in two families from the USA. The nomenclature for this disease entity has been confusing: the HUGO Gene Nomenclature Committee lists 7q36-linked LGMD as LGMD1D (ID 6576; HGNC Database). The MIM database has used both designations LGMD1D and 1E, and currently lists the disease as LGMD1E (MIM #603511). Here, the term LGMD1D will be used.

Before this study, mutations underlying LGMD1D were unknown. Causative mutations in the *DNAJB6* gene (DnaJ homolog, subfamily B, member 6), described in publication II, were first identified in Finnish families, and also found in Italian and the original American families. Additional mutations have been reported in LGMD1D families from the USA and Japan (Harms *et al.* 2012, Sato *et al.* 2013). All the known mutations are missense changes affecting the glycine/phenylalanine-rich (G/F) domain of the protein (Table 2, Fig. 5). The mutations show marked clustering: all five reported mutations are located within a range of eight amino acid residues, three of them affecting the same residue, F93 (II, Harms *et al.* 2012, Sato *et al.* 2013).

2.5.1 Clinical picture of LGMD1D

LGMD1D typically presents with a limb-girdle phenotype—slowly progressive muscle weakness and atrophy, most prominent in the proximal parts of the limbs. Both pelvic and shoulder girdle muscles are affected, the lower limbs usually showing earlier onset and greater severity of symptoms. Of distal leg muscles, *soleus* and medial *gastrocnemius* are most severely affected (Sandell *et al.* 2010, Hackman *et al.* 2011, Harms *et al.* 2012, Sato *et al.* 2013). In a few patients carrying the P96R mutation, Harms *et al.* (2012) described onset of symptoms in distal legs and arms, followed by progression to proximal muscles. Bulbar symptoms, apart from infrequent dysphagia, have not been reported, nor are there cardiac or respiratory problems (Speer *et al.* 1995, Sandell *et al.* 2010, Hackman *et al.* 2011, Harms *et al.* 2012, Sato *et al.* 2013).

The age of onset varies considerably, from the 3rd to the 6th decade, and some cases with a possible childhood onset have been reported. The symptoms begin

Table 2. LGMD1D-causing mutations in *DNAJB6*

cDNA change	Protein change	Reference
c.265T>A	p.Phe89Ile	II
c.277T>C	p.Phe93Leu	II, Harms *et al.* 2012
c.277T>A	p.Phe93Ile	Sato *et al.* 2013
c.279C>G	p.Phe93Leu	II, Sato *et al.* 2013
c.287C>G	p.Pro96Arg	Harms *et al.* 2012

Sequence numbers refer to the RefSeq records NM_005494.2 (cDNA) and NP_005485.1 (protein).

with difficulties in walking, running, climbing stairs, or getting up from the floor. Weakness progresses slowly, and walking ability is usually preserved until a late age (Sandell *et al.* 2010, Hackman *et al.* 2011, Harms *et al.* 2012, Sato *et al.* 2013).

2.5.2 Muscle pathology in LGMD1D

Muscles affected by LGMD1D show myopathic and later dystrophic changes: atrophic and regenerating fibres, fibre size variation, and internal nuclei. Rimmed vacuoles are variably present, ranging from infrequent to abundant (Sandell *et al.* 2010, Hackman *et al.* 2011, Harms *et al.* 2012, Sato *et al.* 2013).

Muscle fibres contain eosinophilic protein inclusions, sometimes in the rimmed-vacuolar regions. These have been shown to stain positive for DNAJB6, as well as several proteins typically accumulating in myofibrillar myopathies (myotilin, αB-crystallin, desmin, ectopic dystrophin, and TARDBP), and components of the chaperone-assisted selective autophagy (CASA) pathway (BAG3, STUB1, HSPA8, and HSPB8) (Sandell *et al.* 2010, Hackman *et al.* 2011, Harms *et al.* 2012, Sato *et al.* 2013). Subsarcolemmal accumulation of DNAJB6 (Harms *et al.* 2012), and nuclear DNAJB6 staining (Sato *et al.* 2013) has also been reported in some affected fibres.

Electron microscopy shows myofibrillar disorganization starting with Z-disc disintegration—a typical finding in myofibrillar myopathies. Rimmed vacuoles are correlated on the EM level by autophagic vacuoles with myeloid bodies, small vesicles, and debris material. Tubulofilamentous inclusions may be found in the sarcoplasm and infrequently in myonuclei (Sandell *et al.* 2010, Hackman *et al.* 2011, Harms *et al.* 2012, Sato *et al.* 2013).

Sarcolemmal markers such as dystrophin and sarcoglycans appear normal in LGMD1D muscle, consistent with the mild to moderate elevation of serum creatine kinase levels in patients (Sandell *et al.* 2010, Hackman *et al.* 2011).

2.5.2.1 Myofibrillar myopathies

Based on muscle pathology alone, LGMD1D can be classified to the group of myofibrillar myopathies (MFM). These diseases, showing clinical and genetic heterogeneity, share common pathological features: myofibrillar disintegration begin-

ning at the Z-disc and accumulation of proteins—especially Z-disc material—within the muscle fibres, characteristic dark and hyaline changes on trichrome stain, and vacuolar degeneration (Selcen 2011, Udd 2013). MFMs can be regarded as diseases of the Z-disc as most of the mutated proteins are structural components of the Z-disc (myotilin, desmin, filamin C, and ZASP) or are involved in Z-disc maintenance (BAG3 and αB-crystallin) (Selcen 2011).

2.6 DNAJB6

DNAJB6 belongs to the DNAJ family of co-chaperones, also known as the J-protein or heat shock protein 40 (Hsp40) family (Seki *et al.* 1999, Qiu *et al.* 2006). The protein was first described as MRJ (mammalian relative of DnaJ) (Seki *et al.* 1999), and this name has been widely used especially in the earlier literature. Also the alias HSJ2 has been used (Hanai & Mashima 2003), although this term can also refer to DNAJA1.

2.6.1 J-proteins and the HSPA chaperone system

J-proteins are essential cofactors or co-chaperones for the HSPA (Hsp70) proteins, a family of ubiquitous molecular chaperones with central roles in the regulation of protein folding and turnover (Kampinga & Craig 2010). The main cytosolic members of the HSPA family are the stress-induced Hsp70 (encoded by the *HSPA1A* and *HSPA1B* genes with nearly identical protein products), and the constitutively expressed HSPA8 (also known as Hsc70, heat-shock cognate 70; Hsp73) (Daugaard *et al.* 2007).

Functions of the HSPA chaperones are based on the recognition of exposed hydrophobic protein stretches characteristic of unfolded proteins. In the ATP-bound open state, HSPAs bind and release their client proteins rapidly, whereas the ADP-bound closed state is needed for high-affinity binding that promotes refolding of the client protein. As the inherent ATPase activity of HSPAs is very low, the conformation switch depends on J-proteins that interact with HSPAs with their J-domains and stimulate ATP hydrolysis, thus stabilizing the binding of HSPAs to their client proteins. J-proteins can also recognize and bind the client proteins before presenting them to the HSPA component, conferring specificity to the otherwise unselective HSPA machinery (Kampinga & Craig 2010).

The classical role of the HSPA chaperones is to prevent the aggregation of unfolded proteins and promote their folding to the native conformation. However, association of different sets of co-chaperones with the core chaperone can affect the fate of the client proteins, targeting them to the proteasomal or autophagic turnover pathways (Esser *et al.* 2004). An example of such a mechanism is the recently described chaperone-assisted selective autophagy (CASA) pathway (Arndt *et al.* 2010).

2.6.2 Structure of DNAJB6

The N-terminal part of DNAJB6 harbours a J-domain of ~70 amino acid residues. This domain, a defining feature of J-proteins, is required for the interaction with HSPA chaperones and stimulation of their ATPase activity (Seki *et al.* 1999, Qiu *et al.* 2006).

The J-domain is followed by a G/F-domain, harbouring all the described mutations causing LGMD1D. This domain of ~45 amino acids, rich in glycine and phenylalanine residues, is present in all type I (DNAJA) and type II (DNAJB) J-proteins (Chuang *et al.* 2002, Qiu *et al.* 2006). The function of the G/F-domain in DNAJB6 has not been characterized, but in bacterial and yeast homologues it has been suggested to participate in recognition of partially unfolded client proteins (Wall *et al.* 1995, Yan & Craig 1999, Perales-Calvo *et al.* 2010). The G/F-domain may also contribute to the interaction of DNAJB6 with HSPA8 (see 2.6.5.1.), since a construct containing the G/F-domain shows a stronger interaction signal in a yeast two-hybrid assay compared to J-domain alone (Izawa *et al.* 2000).

The C-terminal domain (CTD) shows less similarity to other J-proteins. Its most notable feature is the serine-rich region, termed the SSF–SST domain based on its sequence boundaries in the closely related DNAJB8 protein (Hageman *et al.* 2010). Two DNAJB6 isoforms, differing in the C-terminal regions, are generated by alternative splicing. The long isoform DNAJB6a [RefSeq NP_490647; also known as MRJ(L)] contains 326 amino acids and has a molecular weight of 36 kDa, whereas the short isoform DNAJB6b [RefSeq NP_005485; also known as MRJ(S)] contains 241 amino acids and has a molecular weight of 27 kDa. The two isoforms share their 231 N-terminal amino acid residues, which are followed by unique C-terminal tails (Hanai & Mashima 2003).

A schematic view of DNAJB6 is shown in Fig. 5.

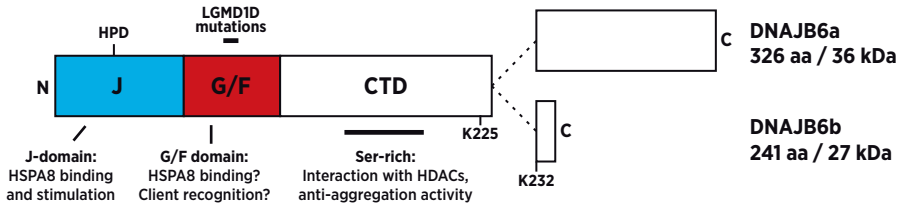

Figure 5. Structure of DNAJB6

The DNAJB6 protein comprises an N-terminal J-domain, a glycine/phenylalanine-rich (G/F) domain harbouring the LGMD1D-causing mutations, and a C-terminal domain (CTD) containing a serine-rich region. Alternative splicing results in two isoforms DNAJB6a and DNAJB6b, with different C-termini. The location of the known LGMD1D-causing mutations, the HPD tripeptide mediating the interaction with HSPA8, and the lysine residues K225 and K232 corresponding to the acetylatable residues in DNAJB8 are indicated.

Adapted from Sarparanta *et al*. Mutations affecting the cytoplasmic functions of the co-chaperone DNAJB6 cause limb-girdle muscular dystrophy. *Nature Genetics*, 2012; 44: 450–455. © 2012 Nature America, Inc.

2.6.3 Tissue distribution of DNAJB6

The expression of DNAJB6 is widespread, if not ubiquitous. Seki *et al.* (1999) detected expression of DNAJB6b by RT-PCR in all human tissues analyzed, whereas nothern blotting experiments by Chuang *et al.* (2002) revealed variable levels of the DNAJB6b transcripts in different bovine and human tissues, with highest expression in brain and retina. Western blotting of rat tissue extracts, while supporting the enrichment of DNAJB6b in the central nervous system, showed detectable levels of the protein only in a subset of rat tissues (Chuang *et al.* 2002). The tissue distribution of the DNAJB6a isoform has not been reported.

2.6.4 Subcellular localization of DNAJB6

Most of the knowledge on the subcellular localization of DNAJB6 has been obtained from overexpression experiments in cell cultures. Based on such transfection studies, DNAJB6a is exclusively localized to the nucleus; this localization depends on the strong nuclear localization signal near the C-terminus of the protein (Hanai & Mashima 2003, Mitra *et al.* 2008). DNAJB6b constructs show mainly diffuse cytoplasmic localization, but they can also exhibit nuclear localization of different degrees, ranging from minor to predominant (Chuang *et al.* 2002, Hanai & Mashima 2003, Dai *et al.* 2005, Andrews *et al.* 2012, Gillis *et al.* 2013).

The few published studies are insufficient for reliably establishing the localization of endogenous DNAJB6. The studies by Izawa *et al.* (2000) and Watson *et al.* (2007) have both indicated cytoplasmic localization—albeit with somewhat differing staining patterns—and this is in line with the substantial amount of evidence supporting the roles of DNAJB6b in the cytoplasm (discussed below). In contrast to the aforementioned results, Dey *et al.* (2009) showed DNAJB6 tightly associated with nucleoli of HeLa cells during interphase and dispersed between the chromosomes in mitotic cells. Both cytoplasmic and nucleolar localization of DNAJB6b have gained support from transfection studies (Chuang *et al.* 2002, Hanai & Mashima 2003, Dai *et al.* 2005, Andrews *et al.* 2012).

2.6.4.1 Nuclear relocation of DNAJB6b

DNAJB6b relocates to the nucleus following heat shock and hypoxia, and returns to the cytoplasm within hours after the removal of the stress stimulus (Dai *et al.* 2005, Andrews *et al.* 2012). However, the localization within the nucleus is not established, as transfection studies with different DNAJB6b constructs have shown either homogeneous nuclear staining with apparent exclusion from the nucleoli (Dai *et al.* 2005), or nucleolar enrichment (Andrews *et al.* 2012).

The mechanism for the nuclear localization of DNAJB6b is unknown, but in the absence of a nuclear localization signal, it is likely to depend on cotransport with another protein. HSPA seems to play a role in the process, since partial J-domain deletions and the H31Q mutation, preventing the interaction with HSPA, have been reported to disrupt the nuclear localization of DNAJB6b in both baseline and

heat-shock situations (Dai *et al.* 2005). Also the twenty C-terminal amino acid residues of DNAJB6b, containing a putative nuclear export signal, are required for the stress-induced relocation, although deletion of these residues does not prevent the nuclear localization in unstressed cells (Andrews *et al.* 2012).

2.6.5 Functions of DNAJB6

As a member of the J-protein family, DNAJB6 is a HSPA co-chaperone. It also has HSPA-independent chaperonal activity, reflected by its ability to suppress protein aggregation. In addition, both DNAJB6 isoforms have been shown to have various functions in cellular signalling. The reported functions of DNAJB6 are reviewed below.

2.6.5.1 HSPA co-chaperone activity

As expected for a J-protein, DNAJB6 interacts with HSPA chaperones in a pull-down system, and a specific interaction with HSPA8 (Hsc70) has been demonstrated in a yeast two-hybrid assay. The J-domain alone is sufficient for HSPA8 binding, but presence of the G/F domain may promote the interaction (Izawa *et al.* 2000). Consistent with the interaction with HSPA8, DNAJB6 can stimulate the ATPase activity of this HSPA chaperone *in vitro* (Chuang *et al.* 2002). In addition to full-length and N-terminal constructs, also a C-terminal construct lacking the J-domain has shown ATPase stimulatory activity (Chuang *et al.* 2002), but this has been suggested to reflect the presence of contaminant bacterial DnaJ in the protein preparations rather than a true function of the C-terminal part (Fayazi *et al.* 2006). While HSPA8 is the only HSPA chaperone directly demonstrated to interact with DNAJB6, it is possible that DNAJB6 could act as a co-chaperone also for other HSPAs.

2.6.5.2 Anti-aggregation activity

Among a wide range of heat shock proteins studied by Hageman and colleagues (2010), members of the DNAJB6-like cluster in the DNAJB family were unique in their ability to counteract protein aggregation, with DNAJB6 and its closely related paralogue DNAJB8 showing the highest anti-aggregation activity. As the expression of DNAJB8 is testis-specific (Hageman *et al.* 2010), DNAJB6 could be one of the most important suppressors of protein aggregation in our body.

The anti-aggregation activity of DNAJB6 is demonstrated by its effects on aggregation-prone proteins containing polyglutamine (polyQ) stretches (Chuang *et al.* 2002, Hageman *et al.* 2010). Aggregation of such proteins is inhibited by DNAJB6b overexpression in cell cultures and *in vivo* in *Xenopus* tadpoles, and increased by DNAJB6 knockdown (Chuang *et al.* 2002, Hageman *et al.* 2010). While most of the experiments have utilized huntingtin fragments containing expansions of 119–150 glutamine residues, anti-aggregation activity has also been demonstrat-

ed against polyQ-containing ataxin 3 and androgen receptor, as well as isolated polyQ peptides (Chuang *et al.* 2002, Hageman *et al.* 2010, Gillis *et al.* 2013).

The anti-aggregation mechanisms of DNAJB6 and DNAJB8 have been characterized by Hageman *et al.* (2010) and Gillis *et al.* (2013). Although some of the experimentation has only been performed with DNAJB8, the same mechanisms are inferred to apply for both of the proteins. DNAJB6 and DNAJB8 suppress aggregation of polyQ proteins by two mechanisms. A minor, HSPA-dependent component was concluded to reflect proteasomal degradation of the client proteins, and will be discussed later (Hageman *et al.* 2010). The major part of the anti-aggregation activity is, however, HSPA-independent, as it is unaffected by deletion of the J-domain or by a point mutation inactivating its functional interaction with HSPA (Hageman *et al.* 2010, Gillis *et al.* 2013). This major anti-aggregation activity is mediated by the C-terminal part of the proteins and, as shown for DNAJB8, depends on deacetylation of lysine residues located near the C-terminus (Hageman *et al.* 2010). The critical residues are K216 and K223, the former having a greater impact on the activity. Substituting these lysines with alanines abolishes the anti-aggregation activity, whereas substitution to arginines, mimicking the deacetylated state, retains it (Hageman *et al.* 2010). The corresponding residues in DNAJB6b are K225 and K232, the latter one specific to the DNAJB6b isoform.

The serine-rich region, required for the anti-aggregation activity, mediates the interaction of DNAJB8 with the histone deacetylases (HDACs) sirtuin 2, HDAC4, and HDAC6 (Hageman *et al.* 2010). Same HDACs interact also with DNAJB6, and a region overlapping with the serine-rich region has been shown to be important for HDAC4 binding (Dai *et al.* 2005, Hageman *et al.* 2010). The activity of DNAJB8 is impaired by the HDAC inhibitor trichostatin A (TSA), and by knockdown of HDAC4 (but not of HDAC6 or sirtuin 2), demonstrating that the deacetylation needed for the anti-aggregation activity is mediated by HDAC4. Also DNAJB6 is inhibited by TSA, but the contribution of the different HDACs has not been reported (Hageman *et al.* 2010).

DNAJB8 assembles into polydisperse oligomeric complexes, as demonstrated by its wide distribution in density gradient centrifugation (Hageman *et al.* 2010). This oligomerization and colocalization of DNAJB8 with huntingtin aggregates are abolished by deletion of the serine-rich region but not affected by HDAC inhibition or substitution of the acetylated lysines (Hageman *et al.* 2010). Based on these observations, Hageman *et al.* (2010) suggested that oligomerization increases the binding area and affinity of DNAJB8 and DNAJB6 towards their client proteins—in a fashion similar to small heat shock proteins—and deacetylation takes place after client binding to activate the anti-aggregation function. The importance of the serine-rich region for client binding was directly demonstrated by Gillis *et al.* (2013), who showed that deletion of this region abolishes the strong interaction DNAJB6b and DNAJB68 with polyQ peptides observed in a FLIM (Fluorescence Lifetime Imaging Microscopy) assay. Interestingly, localization of DNAJB6b and

DNAJB8 in polyQ aggregates was reported by Gillis *et al.* (2013) to be unaffected by the deletions, in contrast to the findings of Hageman *et al.* (2010) on polyQ-huntingtin.

DNAJB6 and DNAJB8 are not able to dissolve existing aggregates—their anti-aggregation activity reflects the ability to keep polyQ proteins in a soluble state (Hageman *et al.* 2010). Coexpression of either DNAJB6 or DNAJB8 decreases the amount of polyQ peptides in aggregates while increasing it in the soluble fraction, suggesting interference with aggregate formation at an early stage (Gillis *et al.* 2013). In line with this, nuclear DNAJB6a is able to prevent also cytoplasmic aggregation of polyQ peptides, indicating that it keeps the peptides soluble and thus capable of moving between the two compartments (Gillis *et al.* 2013). Notably, in contrast to the freely distributing polyQ peptides, aggregation of cytoplasmic polyQ-huntingtin is exclusively suppressed by the DNAJB6b isoform, whereas DNAJB6a is effective towards polyQ-huntingtin targeted to the nucleus (Hageman *et al.* 2010).

In addition to polyQ-proteins, DNAJB6 may also possess anti-aggregation activity towards other proteins. Supporting this notion, DNAJB6b has been shown to suppress the aggregation of heat-denatured luciferase (Hageman *et al.* 2011) and an aggregation-prone point mutant of parkin (Rose *et al.* 2011). While it was not studied whether these effects are due to the HSPA-independent anti-aggregation activity or an HSPA-mediated process, the fact that a similar effect of DNAJB2 on parkin required a functional J-domain supports the involvement of HSPA at least in the latter case (Rose *et al.* 2011).

2.6.5.3 HSPA-dependent degradation of client proteins

Although the anti-aggregation activity of DNAJB6 is mostly independent of the J-domain and hence of HSPA, a functional interaction of DNAJB6 with HSPA is required for the maximal effect of DNAJB6 on the aggregation of polyQ-proteins. The contribution of HSPA was reported by Hageman *et al.* (2010) to be more important for a long polyQ-huntingtin construct (119Q), while it had little effect on a shorter (74Q) construct. The HSPA-dependent component of the anti-aggregation effect was similarly inhibited by deletion of the entire DNAJB6b J-domain, the H31Q mutation disrupting the interaction with HSPAs, and coexpression of co-chaperones antagonizing the ATPase cycle of HSPA (BAG1 and STUB1) (Hageman *et al.* 2010). As the effect was retained in macroautophagy-deficient cells but inhibited by proteasomal inhibition, the lower amount of huntingtin aggregates was concluded to indicate the ability of DNAJB6 and HSPA to together promote degradation of polyQ-huntingtin through the ubiquitin–proteasome pathway. DNAJB6 has also been proposed to promote proteasomal degradation of keratin (Watson *et al.* 2007), but this is not supported by adequate experimental evidence.

DNAJB6 does not support refolding of heat-denatured luciferase, suggesting that its general function as an HSPA co-chaperone is to promote degradation of the client proteins rather than refolding (Hageman *et al.* 2011).

2.6.5.4 Inhibition of aggregate cytotoxicity

In addition to inhibiting the aggregation of polyQ-huntingtin, DNAJB6 suppresses its cytotoxic effects in cultured cells, as indicated by increased cell viability and reduced caspase 3 activation (Chuang *et al.* 2002, Hageman *et al.* 2010). Since increased viability was seen even upon prolonged polyQ expression, where aggregation was no more efficiently suppressed, the cytoprotective effect was suggested to be independent from the anti-aggregation activity (Chuang *et al.* 2002). Consistent with this idea, overexpression of the *Drosophila* DNAJB6 orthologue dMRJ has been reported to decrease polyQ toxicity in the fly eye and central nervous system without a clear effect on aggregate formation (Fayazi *et al.* 2006).

DNAJB6 shows irreversible localization into the core of polyQ aggregates (Chuang *et al.* 2002, Fayazi *et al.* 2006, Hageman *et al.* 2010, Gillis *et al.* 2013), and it has also been found in the core of Lewy bodies in Parkinson's disease (Durrenberger *et al.* 2009). While this was suggested by Gillis *et al.* (2013) to reflect the trapping of DNAJB6 molecules failed in their anti-aggregation function, localization into aggregates could be also related to the role of DNAJB6 in toxicity suppression.

The toxic effects of polyQ depend partly on sequestration of essential proteins into the aggregates (Chai *et al.* 1999, McCampbell *et al.* 2000, Shimohata *et al.* 2000, Donaldson *et al.* 2003). HSPA8 and DNAJB1 can together modulate the aggregation of polyQ-huntingtin, promoting the formation of SDS-soluble amorphous aggregates instead of insoluble amyloid inclusions. These unstructured aggregates may be more readily degraded, and show lower cytotoxicity due to less efficient sequestration of other proteins (Muchowski *et al.* 2000). Although DNAJB1 lacks the HSPA-independent anti-aggregation activity seen in the DNAJB6-like cluster (Hageman *et al.* 2010), the cytoprotective effects of DNAJB1 and DNAJB6 could partly be based on a similar HSPA-dependent mechanism.

The cytoprotective effect of DNAJB6 has been suggested to involve its interaction with MLF1 (myeloid leukemia factor 1) (Li *et al.* 2008). Overexpression of *Drosophila* and human MLF1 orthologues suppresses polyQ toxicity in neurons, reduces the number of inclusions, and diminishes the recruitment of CBP (CREB-binding protein; a transcriptional coactivator often sequestered to polyQ aggregates) and HSPA to them (Kim *et al.* 2005a). When overexpressed in mouse muscles or COS-7 cells, MLF1 forms large intracellular aggregates that also recruit DNAJB6. The MLF1-overexpressing mice do not show any signs of myopathy, in line with a

neutral or protective role rather than a harmful role for MLF1-containing aggregates (Li *et al.* 2008). The molecular details of the DNAJB6–MLF1 interaction and its exact function in neutralizing aggregate toxicity remain to be elucidated.

2.6.5.5 Maintenance of the keratin cytoskeleton

The C-terminal half of DNAJB6b interacts with keratin 18 (K18), a major acidic (type I) keratin in epithelial cells (Izawa *et al.* 2000), and DNAJB6 is essential for the maintenance of the keratin cytoskeleton. Overexpression of either N- or C-terminal half of DNAJB6b causes a collapse of K18-containing filaments (Izawa *et al.* 2000). Also the DNAJB6-deficient mouse trophoblasts show disruption of the keratin cytoskeleton, affecting both K8/K18 and K8/K19 filaments, and contain perinuclear filamentous keratin aggregates. The aggregates are toxic to the placental cells and they are considered to underlie the embryonic lethality of DNAJB6 knockout in mice (Watson *et al.* 2007).

The molecular details of how DNAJB6 works to maintain the keratin filaments are unclear. Based on its colocalization with the 20S proteasome subunits and the observation that proteasome inhibition mimics the effect of DNAJB6 knockout on keratin cytoskeleton, DNAJB6 was suggested to mediate proteasomal degradation of keratin (Watson *et al.* 2007). However, no direct evidence exists to support this hypothesis. Moreover, microinjection of a DNAJB6 antibody in HeLa cells causes a collapse of keratin filaments already within one hour (Izawa *et al.* 2000). The half-life of soluble keratin in unstressed cells has been reported to be 10 h (Jaitovich *et al.* 2008), whereas the keratin cycle, or continuous recycling of keratin subunits by disassembly and assembly of keratin filaments, is a considerably quicker process (Kölsch *et al.* 2010). The rapid effect of DNAJB6 blocking could hence suggest participation of DNAJB6 also in keratin recycling instead of, or in addition to, proteasomal degradation.

Importance of DNAJB6 for keratin maintenance in muscle is unknown. Expression of K18 has not been detected in striated muscle, but K19 forms keratin filaments with K8 at the costameric regions (Abe & Oshima 1990, O'Neill *et al.* 2002, Ursitti *et al.* 2004). While an interaction of DNAJB6 with K19 has not been demonstrated, the disruption of K19-containing filaments in DNAJB6 knockout cells suggests that DNAJB6 could regulate also this type of keratin (Watson *et al.* 2007). Of note, yeast two-hybrid and co-sedimentation analyses by Izawa and coworkers (2000) failed to show an interaction of DNAJB6 with desmin, the most abundant intermediate filament protein in muscle.

Based on the observation that DNAJB6 is upregulated and assumes a localization reminiscent of cytokeratins in mitotic cells, Dey and colleagues (2009) proposed that DNAJB6 could play a role in the reorganization of the intermediate filament cytoskeleton during mitosis.

2.6.5.6 Functions of DNAJB6 in signalling and gene regulation

In addition to the deacetylation of DNAJB6 required for the anti-aggregation function, the interaction of DNAJB6 and HDACs seems to play a role in transcriptional regulation. By interacting with HDAC4 (and other type II HDACs) and NFATc3 through its C-terminal domain, DNAJB6b recruits HDACs to NFAT-regulated promoters and induces chromatin remodelling, repressing calcineurin/NFATc3-dependent gene expression (Dai *et al.* 2005). DNAJB6b has been shown to block calcineurin-induced hypertrophy in cultured cardiomyocytes (Dai *et al.* 2005), and it could also affect the targets of calcineurin signalling, such as hypertrophic response and fibre type transition, in skeletal muscle. The histone demethylase ALKBH1 (Ougland *et al.* 2012) also interacts with the C-terminal domain of DNAJB6 and competes with HDAC4 for DNAJB6 binding (Pan *et al.* 2008). It could thus functionally antagonize the repressive function of both by displacing HDAC4 from DNAJB6 (Pan *et al.* 2008) and through its own chromatin remodelling activity. A role in transcriptional regulation is also suggested by the binding of DNAJB6b to BRMS1 (breast cancer metastasis suppressor 1), a member of the mSin3/HDAC transcription co-repressor complex (Hurst *et al.* 2006), but the importance of this interaction has not been further studied.

In T-cells, DNAJB6 mediates the nuclear localization of the transcription factor Schlafen 1 (Slfn1), required for maintaining T-cells in a quiescent state. This involves an interaction of Slfn1 with the C-terminal domain of DNAJB6. The effect is reproduced by constructs of the DNAJB6b isoform, but constructs sequestered to the cytoplasm are inefficient in this respect, suggesting that Slfn1 piggybacks to the nucleus with DNAJB6b (Zhang *et al.* 2008). DNAJB6b-overexpressing T-cells also show higher levels of Slfn1; this was stated by Zhang *et al.* (2008) to indicate that the co-chaperone activity of DNAJB6b stabilizes Slfn1 and inhibits its degradation, but the presented data were insufficient for excluding other explanations.

The only functional role so far demonstrated for DNAJB6a is the regulation of Wnt/β-catenin signalling, with implications on cancer biology. Advanced breast cancers show loss of DNAJB6a, and restoration of its expression in cancerous cell lines results in a phenotype shift from mesenchymal to epithelial, and diminished malignancy (Mitra *et al.* 2008, 2010). This depends at least partly on the ability of DNAJB6a to suppress Wnt/β-catenin signalling, important in maintaining the mesenchymal phenotype (Mitra *et al.* 2010, 2012). DNAJB6a interacts with glycogen synthase kinase 3β (GSK3β) and promotes its dephosphorylation by protein phosphatase 2A (PP2A). This keeps GSK3β in an active state, capable of inducing the proteasomal degradation of β-catenin. As the effect is lost upon deletion of the DNAJB6a J-domain or mutation of the HPD tripeptide, and as also HSPA8 complexes with both PP2A and GSK3β, it was proposed to reflect co-chaperone activity of DNAJB6a on HSPA8 (Mitra *et al.* 2012).

The significance of the stress-induced nuclear relocation of DNAJB6b (discussed in 2.6.4.1) is not known. Increase in the nuclear DNAJB6b concentration

could have an effect on the reported functions of this isoform in the regulation of gene expression. It has also been suggested to boost the nuclear functions of DNAJB6a in stress situations (Andrews *et al.* 2012), but the apparently opposing effects of the two isoforms argue against this hypothesis. While DNAJB6a suppresses malignancy (Mitra *et al.* 2008, 2010, 2012), constitutive nuclear targeting of DNAJB6b with an added nuclear localization signal causes increased clonogenicity and proliferation, and invasive morphology in cultured cancer cells (Andrews *et al.* 2012).

DNAJB6 knockout mouse embryos show neural tube defects, and a reduction in the number and proliferation of neural stem cells, indicating that DNAJB6 is required for efficient self-renewal of neural stem cells (Watson *et al.* 2009). The molecular mechanism for this function and the identity of the relevant DNAJB6 isoform remain unknown, but based on phenotypic similarities and gene expression changes, defective Notch signalling was proposed as a possible mechanism (Watson *et al.* 2009). As β-catenin signalling is also involved in stem cell self-renewal (Kalani *et al.* 2008), its deregulation could be a plausible explanation for the observed effect of DNAJB6 deficiency. Of note, GSK3β—acting through both β-catenin and NFATc3—affects also the self-renewal and differentiation of muscle satellite cells (Perez-Ruiz *et al.* 2008, van der Velden *et al.* 2008), and DNAJB6 could thus play a role in muscle development and regeneration.

2.6.5.7 Functions of DNAJB6 in muscle

No specific functions in striated muscle have been previously established for DNAJB6. In a recent yeast two-hybrid study by Blandin and coworkers (2013), aiming to elucidate the interactome network of proteins underlying LGMDs, high-confidence interactions were identified between DNAJB6 and several muscle proteins. Novel interaction partners included ANKRD1, myosin-binding protein C, myomesin 1, phosphoglucomutase 1, titin, dysferlin, and γ-sarcoglycan (Blandin *et al.* 2013); these could represent DNAJB6 clients or proteins involved in the regulation of DNAJB6 in muscle.

2.7 Welander distal myopathy (WDM)

Welander distal myopathy (WDM, MIM #604454) is an autosomal dominant distal myopathy described by Lisa Welander in 72 Swedish families (Welander 1951). Linkage to 2p13 was established in 1999 (Åhlberg *et al.* 1999), but before this study the causative mutation remained unknown.

The mutation underlying WDM was identified by our group in the RNA-binding protein TIA1 and reported in publication III. The only known mutation, accounting for all the described cases in Sweden and Finland, is the missense change c.1150G>A (RefSeq NM_022173.2) located in exon 13 of *TIA1* (III). The mutation affects the third last amino acid of TIA1, causing a p.E384K (RefSeq NP_071505.2) change

of a conserved glutamate residue in the prion-related domain of the protein (III). The mutation has a semi-dominant effect: heterozygotes develop typical WDM, whereas homozygotes are more severely affected (III, Welander 1957, Åhlberg *et al.* 1999).

WDM is most prevalent in central and northern parts of Sweden. The frequency in Sweden is 1/10,000, and regionally as high as 1/70 (Åhlberg *et al.* 1999), whereas the approximate frequency in Finland is >2/100,000 (Bjarne Udd, personal communication). Outside Sweden and Finland, one family in Great Britain has been confirmed with the same mutation (III). From the length of linkage disequilibrium, Klar *et al.* (2013) estimated the age of the WDM mutation to be ~1050 years.

2.7.1 Clinical picture of WDM

WDM has a late onset, typically after 40 years of age. The symptoms start usually with weakness of finger extensor muscles, causing first clumsiness in fine motor tasks and then inability to extend the fingers. Symptoms progress slowly to other distal muscles, finally involving all small muscles in hands and feet, and long extensor muscles in forearms and legs. Weakness in the lower leg, *tibialis anterior* in particular, impairs ankle dorsiflexion and causes difficulty in walking. Involvement of posterior muscles in the lower leg is frequently identified on muscle MRI, but is usually subclinical. Proximal muscles are rarely affected, and cardiomyopathy, dysphagia, or respiratory failure never occur (Welander 1951, Borg *et al.* 1998, Udd 2013). The few described homozygous patients show a more severe disease with early onset (around 30 years), clear proximal involvement, and faster progression leading to loss of walking ability (Welander 1957, Åhlberg *et al.* 1999).

Some studies have suggested neural involvement in WDM (Borg *et al.* 1987, 1989, 1991a). However, nerve conduction velocities are normal, and clear electrophysiological signs of a neuropathy are absent even in homozygous patients (Bjarne Udd, personal communication), indicating that the muscle pathology in WDM is of myogenic origin.

2.7.2 Muscle pathology in WDM

Histopathology of WDM muscle shows typical myopathic changes such as internal nuclei, split fibres, fibre size variation, and fibre atrophy affecting both slow and fast fibres. Rimmed vacuoles are a typical finding, and they are present in both normal-sized and atrophic fibres (Åhlberg *et al.* 1994, Borg *et al.* 1998).

Electron microscopy of WDM muscle reveals autophagic vacuoles—ultrastructural correlates of rimmed vacuoles. Tubulofilamentous inclusions composed of randomly dispersed or parallel filaments of 15–20 nm are found in association with the autophagic vacuoles, and less frequently in nuclei. Also fingerprint bodies, honeycomb structures, dense accumulations of Z-disc material, Z-disc streaming, and mitochondrial abnormalities have been reported (Borg *et al.* 1991b, 1993, 1998).

2.8 TIA1

TIA1 is an RNA-binding protein with multiple functions in regulation of splicing, RNA metabolism, and protein expression. It was initially described as "T-cell restricted intracellular antigen", a component of cytolytic granules of T-cells (Anderson *et al.* 1990). This was, however, based on misinterpretation of GMP-17 as "p15-TIA1", a splice variant or proteolytic product of the full-length "p40-TIA1" (Anderson *et al.* 1990, Medley *et al.* 1996). TIA1 immunoreactivity is still persistently utilized in T-cell classification; such literature most likely irrelevant to the true functions of TIA1 will be excluded from the following review.

TIA1 shares its domain structure and many of its functions with its close homologue TIAL1 (TIA1-like; also known as TIAR, TIA1-related protein) (Kawakami *et al.* 1992). The two will be here collectively referred to as the "TIA proteins".

2.8.1 Structure of the TIA proteins

The TIA1 protein (shown schematically in Fig. 6) is composed of three RNA-binding domains (RNA recognition motifs, RRM), followed by a C-terminal glutamine-rich prion-related domain (PRD) (Tian *et al.* 1991, Kedersha *et al.* 1999). Two variants are generated through alternative splicing. The long isoform TIA1a (designated splice variant 2; RefSeq NP_071505) contains 386 amino acids and has a theoretical molecular weight of 43.0 kDa. Exclusion of 11 amino acids, encoded by exon 5 between the first two RRMs produces the short isoform TIA1b of 375 amino acids / 41.8 kDa (splice variant 1; RefSeq NP_071320) (Tian *et al.* 1991, Kawakami *et al.* 1994).

TIA1 and TIAL1 are highly similar in sequence, showing amino acid identity of ~80% in the whole sequence and ~50% in the prion-related domains. The two TIAL1 isoforms, TIAL1a of 392 amino acids (RefSeq NP_001029097) and TIAL1b of 375 amino acids (RefSeq NP_003243), are distinguished by a 17-amino-acid insertion within the first RRM (Kawakami *et al.* 1992, Izquierdo & Valcárcel 2007a).

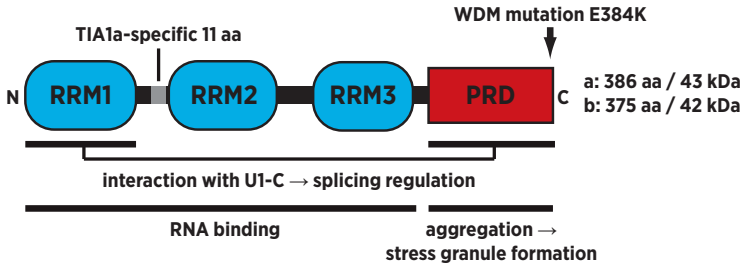

Figure 6. Structure of TIA1

The TIA1 protein comprises three RNA-binding motifs (RRM1–3) followed by a glutamate-rich prion-related domain (PRD). The WDM-causing mutation is located in the C-terminus of PRD. The region encoded by TIA1 exon 5, excluded from the TIA1b isoform, is shown in grey.

2.8.2 Expression and localization of TIA1

2.8.2.1 Tissue distribution

By western blotting of proteins immunoprecipitated with a TIA1/TIAL1 antibody from mouse tissue extracts, Beck *et al.* (1996) showed strong TIA1 expression in brain, spleen, and testis, while other analyzed tissues—including skeletal muscle—showed very low or absent signal. In contrast, WB analysis of human tissues (Izquierdo & Valcárcel 2007a) indicated a wider distribution: TIA1 protein was detected, at different levels, in virtually all analyzed tissues. In skeletal muscle, protein expression was moderate. On the mRNA level, northern blotting and RT-PCR have shown TIA1 expression in several murine and human tissues, with no good correlation to protein expression levels. Both methods detected relatively low levels of TIA1 mRNA in skeletal muscle (Beck *et al.* 1996, Izquierdo & Valcárcel 2007a). Given the universal functions of TIA1, and the observation that either TIA1 or TIAL1 is required for cell viability (see 2.8.3.), expression of TIA1 at least on a basal level is likely to be more or less ubiquitous.

In most tissues and cells, the two TIA1 isoforms have been detected in a rough 1:1 ratio (Beck *et al.* 1996, Izquierdo & Valcárcel 2007a). A notable exception is made by the HeLa cells, reported to predominantly express the TIA1a isoform (Izquierdo & Valcárcel 2007a).

2.8.2.2 TIA1 in muscle

The expression of TIA1 in muscle has not been specifically characterized. Masuda *et al.* (2009) studied the expression of RNA-binding proteins in different human tissues by immunohistochemistry on tissue microarrays. TIA1 expression was reported to be relatively high in fetal skeletal muscle but decline during aging. Both the number of TIA1-expressing cells and the relative expression level in these cells showed a decrease, and less than 10% of cells in middle-aged and old subjects were scored as TIA1-positive. However, as the published results only included numerical expression scoring based on automated image analysis, the reliability of these data cannot be evaluated.

A study comparing the gene expression patterns in human *post mortem* muscle samples (Kang *et al.* 2005) reported *TIA1* as a part of the expression signature of *tibialis anterior* (TA) in paediatric samples —*i.e.* TA showed higher *TIA1* expression compared to the other analyzed muscles (*gastrocnemius*, *quadriceps femoris*, and *deltoideus*). Although the detailed expression patterns in other muscles remain to be elucidated, the result indicates that TIA1 expression may vary significantly between muscles. The differential expression could have pathological relevance for WDM, and it could also explain the variability of the published results concerning TIA1 expression in muscle.

2.8.2.3 Subcellular localization

TIA1 shuttles continuously between the nucleus and the cytoplasm (Kedersha *et al.* 1999, Zhang *et al.* 2005). The localization in unstressed cells is primarily nuclear, but in response to cellular stress TIA1 quickly moves to the cytoplasm (Kedersha *et al.* 1999, 2000). The nuclear import requires RRM2 and the N-terminal half of PRD and is mediated by a Ran-GTP-dependent mechanism, whereas nuclear export is mediated by binding to target RNAs via RRM3 (Zhang *et al.* 2005). The relocation to cytoplasm has been proposed to result from inactivation of nuclear import (Kedersha *et al.* 1999), but the exact mechanisms have not been reported.

2.8.3 Importance of the TIA proteins for life

TIA1 knockout mice show partial embryonic lethality, but the surviving mice have normal life span and fertility (Piecyk *et al.* 2000). Of TIAL1 knockout mice, a higher proportion dies *in utero*, and survivors are sterile due to defective germ cell development affecting both sexes (Beck *et al.* 1998). The fact that single knockouts have deleterious effects with somewhat different phenotypes indicates that the functions of the two TIA proteins are at least partly separate, and loss of one cannot totally be compensated by the other (Piecyk *et al.* 2000).

In contrast to partly viable single knockouts, mice lacking both TIA proteins show early embryonic lethality (Piecyk *et al.* 2000). Similarly, chicken DT40 cells expressing either TIA1 or TIAL1 are viable, but disruption of both genes causes cell death unless TIA1 is ectopically expressed. This demonstrates that the proteins are partly redundant, and also suggests that the double knockout causes lethality in mice through a direct effect on cell viability rather than through interfering with developmental functions of the TIA proteins (Le Guiner *et al.* 2003).

2.8.4 Stress granules

TIA1 and TIAL1 are key components of stress granules (SGs)—cytoplasmic foci of mRNPs (messenger ribonucleoprotein particles)—that coordinate RNA metabolism and protein synthesis in situations of cellular stress. SG formation can occur in various types of stress such as heat shock, oxidative stress, starvation, ER stress, UV irradiation, ischemia, and cold stress. In experimental setups, an established tool for SG induction is oxidative stress caused by sodium arsenite treatment (Anderson & Kedersha 2008, Buchan & Parker 2009, Thomas *et al.* 2011, Hofmann *et al.* 2012). Microscopically visible SGs appear in 15–30 minutes after stress onset, and they gradually fuse into larger granules, typically a few micrometers in diameter. During recovery from stress, SGs dissolve within 60–90 minutes (Kedersha *et al.* 2000, Anderson & Kedersha 2008).

The defining components of SGs are non-translating preinitiation complexes, containing mRNA, small ribosomal subunits, early initiation factors, and poly-A binding protein 1 (PABP1). Beyond that, molecular composition of SGs can vary over time and in different types of stress. In total tens of different proteins have

been observed in SGs, many of them involved in regulation of mRNA stability and translation (Anderson & Kedersha 2008, Buchan & Parker 2009, Thomas *et al.* 2011).

Rather than static RNP aggregates, SGs are highly dynamic: proteins and mRNA continuously shuttle between SGs and the cytosol. Fluorescence recovery after photobleaching (FRAP) studies have indicated SG residence times of seconds to minutes for many of the protein components, as well as for reporter mRNAs (Kedersha *et al.* 2000, 2005, Mollet *et al.* 2008, Buchan & Parker 2009). TIA1 is among the most mobile SG proteins, showing ~90% fluorescence recovery within 10 s after bleaching (Kedersha *et al.* 2000).

The dynamic nature of SGs is reflected in their ultrastructure lacking clear boundaries or defined internal structure. In electron microscopy, SGs appear as loosely organized, moderately electron-dense areas with fibrillo-granular fine structure that can be intermingled with cytoplasmic patches (Souquere *et al.* 2009). IF microscopy has also indicated that individual SGs are heterogeneous in structure, with different components localizing to partially separate microdomains (Baguet *et al.* 2007).

2.8.4.1 Stress granule assembly and disassembly

A dynamic equilibrium exists between actively translated polysome-associated mRNPs, and SG-associated untranslated ones. SG formation is hence driven by any factor that causes cytoplasmic accumulation of non-translating (stalled) mRNPs (Kedersha *et al.* 2000, Anderson & Kedersha 2008). Stalling is usually due to reduced availability of the eIF2–GTP–$tRNA_i^{Met}$ ternary complex, required for normal translation initiation. This can be caused indirectly through phosphorylation of eIF2α in response to cellular stress, or possibly as a direct consequence of reduced GTP/GDP ratio in energy depletion (Kedersha *et al.* 1999, 2002, Anderson & Kedersha 2002a). In the absence of the active ternary complex, translation initiation is inhibited, ribosomes run off the transcripts after completing their round of translation, and transcripts are stalled as non-canonical 48S* preinitiation complexes devoid of eIF2 (Kedersha *et al.* 2002). SG formation can be also triggered independently of eIF2 phosphorylation by inhibiting translation initiation at a later stage, *e.g.* by interfering with functions of eIF4s (Dang *et al.* 2006, Mazroui *et al.* 2006). In either case, untranslated mRNPs accumulate as stalled preinitiation complexes that are then assembled into SGs (Anderson & Kedersha 2008).

SG assembly is mediated by RNA-binding proteins capable of controlled aggregation, among them the TIA proteins. According to a model proposed by Anderson & Kedersha (2008), SG formation is initiated by recognition of stalled mRNPs by various of such SG-nucleating proteins, each binding preferentially to a subset of transcripts. Homotypic aggregation of the proteins assembles mRNPs into submicroscopic aggregates, which are then clustered into larger, microscopically visible SGs by heterotypic interactions between SG-nucleating proteins, and

by association of some RBPs with multiple classes of transcripts (Anderson & Kedersha 2008). Other proteins needed for SG functions are recruited by their interactions with RNA and the protein components (Anderson & Kedersha 2008). SG assembly and disassembly depend partly on active transport mediated by molecular motors: both processes are perturbed by disruption of microtubule or microfilament cytoskeleton, or by depletion of motor proteins (Loschi *et al.* 2009, Thomas *et al.* 2011).

2.8.4.2 TIA1 in stress granules

TIA1 is the most extensively studied, and perhaps the most important, of SG-nucleating proteins. The TIA1 self-assembly driving SG nucleation is mediated by homotypic aggregation of its prion-like domain, demonstrated by the fact that TIA1 lacking the PRD is incapable of SG formation (Gilks *et al.* 2004). On the other hand, overexpressed PRD—capable of oligomerization but not of RNA binding—inhibits SG formation in arsenite-treated cells, likely by sequestering endogenous TIA proteins into insoluble microaggregates. (Kedersha *et al.* 1999, Gilks *et al.* 2004). The finding that PRD overexpression, while not affecting the solubility of other SG markers, inhibits formation of all eIF3-containing SGs (rather than a TIA1-dependent subset) suggests a critical role for the TIA proteins in arsenite-induced SG formation (Gilks *et al.* 2004).

Although TIA1 and TIAL1 have been considered as invariant SG components (Kedersha *et al.* 1999), it is now known that neither protein is absolutely necessary for SG formation. Cells depleted of TIA1 by RNAi can still assemble SGs in response to arsenite, heat shock, or the eIF4F inhibitor pateamine A (López de Silanes *et al.* 2005, Dang *et al.* 2006). Studies on embryonic fibroblasts derived from TIA1 knockout mice have, on the other hand, indicated impaired SG formation, with majority of the cells showing morphologically abnormal small SGs (Gilks *et al.* 2004, Dang *et al.* 2006). In yeast, the TIA1 orthologue Pub1 is required for SG assembly in response to glucose deprivation but not to heat shock (Buchan *et al.* 2008, Groušl *et al.* 2009). With regard to SG formation, TIAL1 seems to be less important than TIA1: Embryonic fibroblasts from TIAL1 knockout mouse show even enhanced SG formation, likely due to the compensatory TIA1 upregulation seen in the cells (Gilks *et al.* 2004).

The mechanisms by which different types of stress trigger TIA1 aggregation are not completely known. Aggregation could partly depend on the stress-induced increase of the cytoplasmic TIA1 concentration. However, SG formation can take place without a parallel change in the TIA1 distribution, demonstrating the importance of other factors (López de Silanes *et al.* 2005). Possible mechanisms proposed to regulate TIA1 aggregation are based on the observation that HSPA1 inhibits aggregation of the TIA1 PRD (Gilks *et al.* 2004). In energy depletion, a shortage of ATP could decrease the ATP-dependent chaperone activity of HSPA1 and lead to TIA1 aggregation (Gilks *et al.* 2004). On the other hand, in cellular stress situations

causing protein denaturation such as heat shock or oxidative stress, cytoplasmic accumulation of unfolded proteins has been suggested to allow SG formation by diverting HSPA1 away from TIA1 (Anderson & Kedersha 2008).

2.8.4.3 Other central proteins in stress granule formation

In addition to TIA1 and TIAL1, a number of other proteins can nucleate SGs and modulate their assembly. Many of these are interaction partners of the TIA proteins.

The SMN (survival of motor neurons) protein interacts with TIA1 at least indirectly, as demonstrated by coimmunoprecipitation of the two proteins. SMN has been proposed to initiate SG assembly, since its recruitment to SGs following stress precedes TIA1, and SMA (spinal muscular atrophy) cells lacking the functional full-length protein show impaired SG formation (Hua & Zhou 2004).

RSK2 (ribosomal S6 kinase 2) interacts with the PRD of TIA1 in a manner dependent on its kinase activity. As RSK2 is stably localized to SGs in stressed breast cells, and as knockdown of RSK2 or inhibition of its kinase activity decreases SG formation, it has been suggested to act as an important regulator of SG formation and a scaffolding protein for other SG components (Eisinger-Mathason *et al.* 2008).

The helicase/endoribonuclease G3BP1 (RasGAP-binding protein 1; often referred to as G3BP), whose oligomerization is regulated by stress-induced Ras-dependent dephosporylation, has been considered a central SG nucleator, as its overexpression causes SG formation (Tourrière *et al.* 2003). However, the recent results of Aulas *et al.* (2012) indicate a role for G3BP1 in SG fusion rather than nucleation. The homologous G3BP2 protein hetero-oligomerizes with G3BP1, and depletion of both severely impairs SG formation, suggesting that the two proteins have overlapping functions (Matsuki *et al.* 2013).

TARDBP (TAR DNA-binding protein, also known as TDP-43) associates with SGs in several cell types (Colombrita *et al.* 2009, Liu-Yesucevitz *et al.* 2010, McDonald *et al.* 2011). It binds TIA1 in an overexpression setup, but with physiological protein concentrations the interaction may be RNA-dependent (Liu-Yesucevitz *et al.* 2010). TARDBP depletion has been reported to inhibit SG formation in HeLa and SK-N-SH cells, resulting in smaller, less defined SGs that fail to fuse and dissolve more quickly. This effect of TARDBP knockdown seems to be partly mediated by its negative effect on G3BP expression, but the protein may also play a direct role in SG formation (McDonald *et al.* 2011, Aulas *et al.* 2012). In the NSC34 motoneuronal cell line, TARDBP knockdown was not found to affect SG formation (Colombrita *et al.* 2009), suggesting differences in SG assembly between cell types.

2.8.4.4 Functions of stress granules

As SG formation parallels stress-induced translational repression, SGs were first thought to mediate this silencing (Kedersha *et al.* 1999). However, general stress-induced repression does not require SG formation, and translation can be

restored without SG disassembly (Buchan *et al.* 2008, Loschi *et al.* 2009). Moreover, TIA1 silences translation of ARE (AU-rich element) -containing mRNAs both in unstressed and stressed cells (López de Silanes *et al.* 2005), and the silencing of 5'TOP (5'-terminal oligopyrimidine tract) mRNAs by TIA1 is not dependent on its aggregation capacity (Damgaard & Lykke-Andersen 2011). SGs are hence not the effectors of TIA1-mediated translation repression, a process discussed in more detail below.

SGs are intimately connected to processing bodies (P-bodies; PB), RNP granules involved in mRNA decapping and 5'–3' decay. As SGs and PBs share many of their components and intermediates can exist in some organisms, they have been suggested to constitute a continuum of mRNP granules (Buchan & Parker 2009, Thomas *et al.* 2011). PBs frequently form juxtaposed to existing SGs and vice versa, and the two types of granules can transiently dock with each other (Kedersha *et al.* 2005, Buchan *et al.* 2008, Mollet *et al.* 2008). Similarly to SGs, proteins move rapidly between PBs and cytoplasm (Kedersha *et al.* 2005).

The dynamic nature and the physical connection of the mRNP granules have led to the idea of a cytoplasmic mRNA cycle, or shuttling of mRNAs between polysomes, SGs, and PBs. In this model, the rates of translation initiation and termination, and association with SG and PB components affect the distribution of mRNAs between the different compartments, and remodelling taking place in the SGs and PBs determines whether the mRNP is returned to translation, stored, or degraded (Parker & Sheth 2007, Buchan & Parker 2009).

The roles of SGs and PBs and the directions of mRNP movement in the mRNA cycle are not established. Anderson & Kedersha (2002a, 2008) have proposed that SGs function as triage centres, where fates of untranslated mRNAs are determined by their interactions with stabilizing or destabilizing proteins. As the association of SGs and PBs is increased by overexpression of the mRNA-decay-promoting proteins TTP (tristetraprolin) and BRF1 (butyrate response factor 1), the docking has been suggested to mediate mRNA transfer from SGs for degradation in PBs (Kedersha *et al.* 2005).

On the other hand, Buchan & Parker (2009) have favoured a view where the triage takes place in PBs, and the primary movement of mRNPs is from PBs to SGs. In such a model, the function of SGs could be to modulate local concentrations of mRNAs and proteins, thereby affecting their interactions and reaction rates. High concentrations of mRNPs and associated proteins would promote their reactions in SGs, whereas depletion of selected molecules from the cytosol would inhibit some reactions and retarget the limited resources, *e.g.* initiation factors, to the most essential reactions (Parker & Sheth 2007, Buchan & Parker 2009). Specifically, SGs have been proposed to function as regions of enhanced translation initiation, as suggested by high concentrations of preinitiation complex components (Parker & Sheth 2007, Buchan & Parker 2009). Localization of silenced mRNAs into SGs

(López de Silanes *et al.* 2005, Damgaard & Lykke-Andersen 2011), however, argues against their role in translation initiation.

SGs have also functions unrelated to RNA metabolism, primarily acting through sequestration of proteins involved in stress signalling. Hence, SGs have been suggested to integrate and modulate stress response pathways (Anderson & Kedersha 2008). Sequestration of TRAF2 (TNF-α receptor associated factor 2) and ROCK1 (Rho-associated, coiled-coil containing protein kinase 1) into SGs blocks their association with downstream effectors, inhibiting proinflammatory and pro-apoptotic signalling (Kim *et al.* 2005b, Tsai & Wei 2010). Nuclear localization of RSK2 depends on its interaction with TIA1, and tight association with SGs inhibits its nuclear functions involved in regulation of cell proliferation and survival (Eisinger-Mathason *et al.* 2008). Finally, a recent study identified a role for SGs in redox regulation: the antioxidant activity of USP10 (ubiquitin-specific protease 10) is inhibited in unstressed cells by G3BP1, but localization of both proteins into SGs lifts the inhibition (Takahashi *et al.* 2013).

2.8.5 TIA1 as a translation regulator

TIA1 and TIAL1 are potent translation repressors, acting generally on most or all mRNA species, and specifically on mRNAs containing certain target sequence elements on their untranslated regions. As discussed above, this repressive activity is not dependent on stress granules, although silenced transcripts can localize to SGs.

The general translation-repressing function of TIA1 is demonstrated by its ability to inhibit the expression of cotransfected reporter genes (Kedersha *et al.* 2000). The repressive activity is thought to reflect functional antagonism with eIF2, association of TIA1 with the mRNA 5' region producing a translationally incompetent initiation complex. TIA1 has been suggested to compete for mRNA binding with initiation factors, possibly the eIF2–GTP–$tRNA_i^{Met}$ ternary complex. The same competitive binding would hence account for TIA1-mediated repression, and recruitment of untranslated mRNAs to SGs (Anderson & Kedersha 2002a). In line with translation suppression occurring at the initiation stage, TIA1 is excluded from polysomes (Kedersha *et al.* 2000), and TIA1 depletion increases the polysome-associated fraction of its target mRNAs (Piecyk *et al.* 2000, Damgaard & Lykke-Andersen 2011).

2.8.5.1 TIA1 target sequences

AREs (adenine/uridine-rich elements) are regulatory sequence elements that control gene expression by decreasing the stability and translation efficiency of the mRNA transcript. They are typically composed of overlapping tandem repeats of the AUUUA pentamer present on 3'UTRs. Up to 10% of human genes contain AREs, but they are enriched in mRNAs requiring tight and rapid regulation such as those encoding cytokines (Halees *et al.* 2008). The TIA proteins bind AREs and suppress the translation of the respective transcripts; an effect first described for TNFα

(tumor necrosis factor α) and COX-2 (cyclooxygenase 2; PTGS2, prostaglandin-endoperoxide synthase 2) (Gueydan *et al.* 1999, Piecyk *et al.* 2000, Dixon *et al.* 2003). The preferential silencing of ARE-containing transcripts implicates the TIA proteins in the regulation of genes involved in processes like apoptosis, inflammation, and proliferation. Indeed, TIA1 knockout mice have a hyperinflammatory phenotype with increased cytokine production, and they develop arthritis (Piecyk *et al.* 2000, Phillips *et al.* 2004). TIA1 is also established as an apoptosis regulator; this function will be addressed in 2.8.7.

Sequence analysis of transcripts coimmunoprecipitated with TIA1 (López de Silanes *et al.* 2005) identified a recognition motif on TIA1 target mRNAs. This motif of 30–37 nucleotides—termed URSL (uridine-rich stem-loop) by Yamasaki *et al.* (2007)—has a U-rich 5' segment and an AU-rich 3' segment, and forms a bent stem-loop structure. The URSL allows TIA1 binding to reporter mRNAs, and TIA1 depletion increases expression of endogenous mRNAs containing the motif (López de Silanes *et al.* 2005). Whether the URSL alone is sufficient to induce silencing of the transcript, has not been investigated. The URSL was reported to exist on ~3% of transcripts in UniGene database, with enrichment in 3'UTRs. As it was present only on a subset of the analyzed TIA1-binding transcripts, other similar recognition motifs may exist (López de Silanes *et al.* 2005). The URSL was also found on TNFα and COX-2 transcripts. However, its relationship with the ARE elements was not discussed (López de Silanes *et al.* 2005), and it is unclear whether the URSL-containing transcripts represent a subset of the ARE mRNAs, or a partially overlapping group of TIA1 target transcripts.

The silencing effect of 3'UTR sequences has been proposed to be mechanistically similar to the general TIA1-mediated repression: association of TIA1 with the 3'UTR could increase its likelihood of binding to the initiation site, thereby enhancing its repressive activity (Anderson & Kedersha 2002b).

Another group of target mRNAs for TIA1-mediated silencing are those containing a 5'TOP (5'-terminal oligopyrimidine tract). These mRNAs, encoding ribosomal proteins and translation factors, are highly expressed in unstressed cells. Their translation is selectively repressed during amino acid starvation or cell cycle arrest, allowing the cell to drive down energetically demanding protein biosynthesis when resources are limited. TIA1 and TIAL1 were recently identified as effectors of this starvation-induced silencing (Damgaard & Lykke-Andersen 2011). Starvation increases binding of the TIA proteins to the characteristic oligopyrimidine tracts on the 5'UTRs of the transcripts, inhibiting translation initiation. This leads to polysome dissociation and assembly of the untranslated target mRNAs to SGs. The detailed molecular mechanism of increased TIA1/TIAL1 binding is not known, but it requires activation of GCN2 and inactivation of the mTOR (mammalian target of rapamycin) pathway. Effects of TIA1 and TIAL1 on the 5'TOP mRNAs are redundant, but the effect of TIA1 is somewhat stronger (Damgaard & Lykke-Andersen 2011).

2.8.5.2 Multiple levels of regulation

The repressive action of TIA1 takes typically place at the translation level, as demonstrated by unaltered mRNA levels of its target genes (Piecyk *et al.* 2000, Dixon *et al.* 2003). However, TIA1-mediated silencing and polysome disassembly have also been reported to promote rapid decay of a subset of target mRNAs and TIA1-tethered reporter mRNA. This was proposed to depend on simultaneous or sequential action of proteins regulating RNA stability, such as TTP, but the molecular determinants for mRNA destabilization are not known (Yamasaki *et al.* 2007). Moreover, RNAi knockdown of both TIA proteins has been shown to cause changes both in steady-state levels and turnover rates of mRNAs (Reyes *et al.* 2009). In addition, TIA1 and TIAL1 have been suggested to regulate gene expression by suppressing transcription, based on increased steady-state levels of many mRNAs and enhanced reporter gene induction in HeLa cells depleted of both proteins (Reyes *et al.* 2009)

The activity of TIA1 can be modulated by its interactions with other proteins. Interactions of SRC-3 (steroid receptor cofactor 3) with the PRDs of TIA1 and TIAL1 enhance their binding to AREs and promote their repressive function (Yu *et al.* 2007). FASTK (Fas-activated serine/threonine kinase; also known as FAST, Fas-activated serine/threonine phosphoprotein), an interaction partner of TIA1 PRD, increases expression of cotransfected and endogenous genes. As this effect is mediated by the TIA1-interacting N-terminal part of the protein and inhibited by TIA1 cotransfection, binding to FASTK was proposed to inhibit the translation repression activity of TIA1 (Li *et al.* 2004). However, a recent study identified FASTK as an eIF4E-binding protein, suggesting that FASTK, eIF4E, and TIA1 actually form a translation-inhibiting complex that prevents recruitment of eIF4G to the preinitiation complex, and at the same time stabilizes mRNA by inhibiting its decapping. The apparent antagonistic effects of overexpressed FASTK and TIA1 could be explained by altered assembly or regulation of this complex (Li *et al.* 2013).

2.8.6 TIA1 as a splicing regulator

In the nucleus, both TIA proteins have been established to act as splicing regulators. As the two proteins bind to the same intronic regions, their functions in splicing have been suggested to be largely redundant (Wang *et al.* 2010).

TIA1 exerts its effects on splicing by multiple mechanisms. The first and best characterized is its ability to activate weak 5' splice sites (5'ss) immediately followed by a U-rich sequence stretch (Del Gatto-Konczak *et al.* 2000, Le Guiner *et al.* 2001, Förch *et al.* 2002, Gesnel *et al.* 2007). Binding of TIA1 to the U-rich sequence recruits U1 snRNP to the 5'ss, thus promoting the inclusion of the weakly defined upstream exon. Binding of TIA1 and U1 snRNP to the mRNA is cooperative: association of TIA1 with the U-rich sequence is enhanced by an adjacent 5'ss or tethering U1 snRNP to the vicinity, and impaired by depletion of U1 snRNA (Del Gatto-Konczak *et al.* 2000, Gesnel *et al.* 2007). The binding of TIA1 to U1 snRNP depends

on a direct interaction between the TIA1 PRD and U1-C, a protein component of the snRNP, and also RRM1 contributes to U1-C binding and enhances U1 snRNP recruitment (Förch *et al.* 2002).

FASTK-mediated phosphorylation of TIA1 enhances U1 snRNP recruitment without affecting the RNA-binding properties of TIA1 (Izquierdo & Valcárcel 2007b). Phosphorylation is known to occur during proapoptotic signalling (Tian *et al.* 1995), with implications on apoptosis regulation (discussed below), but its importance in other situations has not been reported.

While first studies focused on the effect of the TIA proteins on specific exons, more recent studies have suggested widespread involvement of the TIA proteins in the splicing of both alternative and constitutive exons (Aznarez *et al.* 2008, Wang *et al.* 2010). A large-scale bioinformatics analysis of intron sequences revealed enrichment of U-rich motifs downstream of constitutive and alternative exons, particularly those where other splicing signals are weak (Aznarez *et al.* 2008). This was corroborated by transcriptome-wide mapping of RNA sequences immunoprecipitated with TIA proteins, directly showing extensive association of TIA1 and TIAL1 with U-rich sequences in 5' ends of introns (Wang *et al.* 2010). The proportion of alternatively spliced cassette exons regulated by TIA proteins has been estimated to be 5–15% (Aznarez *et al.* 2008, Wang *et al.* 2010).

Knockdown experiments have supported the widespread functional significance of TIA proteins in splicing. Depletion of TIA1 and TIAL1 in HeLa cells causes increased skipping in a majority of those alternative cassette exons that are followed by a U-rich downstream sequence (Aznarez *et al.* 2008, Wang *et al.* 2010). The effect of TIA is correlated with the uridine content of the downstream sequence and the distance of the U-rich motifs from the 5' splice site (Aznarez *et al.* 2008).

Analysis of TIA-depleted cells with a splice-junction microarray demonstrated that TIA proteins can also regulate variable-length exons by affecting the choice of alternative splice sites, and suppress the inclusion of the downstream alternative exons (Wang *et al.* 2010). The suppressive effect was suggested to reflect altered splicing kinetics, with enhanced splicing of the upstream exon leaving less time for defining the downstream exon (Wang *et al.* 2010). Changes in intron retention in TIA-depleted cells indicated that the TIA proteins can also enhance the splicing fidelity of constitutive exons (Wang *et al.* 2010).

In addition to direct recruitment of U1 snRNP, other yet unknown mechanisms are involved in the splice-regulating activity of the TIA proteins. For example, it is unclear how overall U-richness extending beyond the immediate vicinity of the 5'ss enhances splicing. It has been suggested that U-richness can increase the likelihood of TIA binding close to the splice site, or facilitate cooperative binding of multiple TIA proteins on the mRNA (Aznarez *et al.* 2008). In the *SMN2* gene, TIA1 promotes the inclusion of exon 7 by binding two U-rich clusters separated from the 5'ss by a negative *cis* element. In this case, TIA1 has been proposed to induce a contextual change in the mRNA that inhibits recruitment of negative splicing regu-

lators such as hnRNPA1. This effect requires the N-terminal half of PRD in combination with any of the RNA-binding domains (Singh *et al.* 2011). Furthermore, the TIA1 construct lacking the RRM1 and PRD, and thus incapable of U1-C binding, retains some of its splice-promoting activity towards the K-SAM exon of *FGFR2*, and this activity must thus depend on yet another mechanism (Gesnel *et al.* 2007).

The activity of the TIA proteins in splicing can be modulated by their other interactions. TIA1 and TIAL1, together with U1 snRNP and other splicing factors, are physically associated with RNA polymerase II. This interaction with the transcription machinery is suggested to enhance cotranscriptional recruitment of splicing factors to the pre-mRNA (Das *et al.* 2007). TIA1 has also been shown to interact with genomic DNA in intronal regions of the *COL2A1* gene—this was proposed to enhance alternative splicing by slowing down transcription or by enhancing recruitment of TIA1 to the transcript introns (McAlinden *et al.* 2007).

2.8.7 TIA1 in apoptosis

TIA1 is linked to regulation of apoptosis through many lines of evidence, related to its functions both in splicing regulation and in stress granules.

A direct proapoptotic function for TIA1 was suggested by the early finding that purified recombinant TIA1 induces DNA fragmentation when introduced to permeabilized thymocytes. This nucleolytic effect has been demonstrated for the full-length TIA1b and a 15-kDa C-terminal fragment comprising the PRD (Tian *et al.* 1991), and for TIAL1 (Kawakami *et al.* 1992). TIA1 secretion was proposed to mediate induction of apoptosis in cells targeted by cytotoxic T lymphocytes (Tian *et al.* 1991), but this is now known not to be the case since TIA1 does not reside in cytolytic granules. The biological importance of the nucleolytic activity is unclear, but given the widespread functions of the TIA proteins, it may simply be a consequence of misregulated RNA metabolism or protein expression.

Proapoptotic functions of TIA1 are modulated by its interaction with FASTK by complex mechanisms. FASTK was first described as a kinase activated during Fas-mediated apoptosis, an apoptotic pathway initiated by trimerization of the Fas receptor (CD95) on the cell surface. Following Fas ligation, FASTK is dephosphorylated and activated, and it in turn phosphorylates TIA1 (but not TIAL1) on a serine residue located within the C-terminal ~15 kDa of the protein (Tian *et al.* 1995). Phosphorylation enhances the ability of TIA1 to recruit U1 snRNP to the splice sites, hence stimulating exon inclusion (Izquierdo & Valcárcel 2007b). An experimentally demonstrated consequence is increased inclusion of *FAS* exon 6, leading to the production of the membrane-bound Fas receptor instead of the soluble decoy receptor. This implies a positive feedback loop, where proapoptotic signalling further increases the expression of Fas on the plasma membrane (Izquierdo & Valcárcel 2007b). The cytoplasmic pool of FASTK normally resides on mitochondrial outer membrane in complex with BCL-X_L, but during proapoptotic signalling it is released into the cytoplasm, allowing binding to TIA1 (Li *et al.* 2004).

As FASTK overexpression increases the expression of antiapoptotic proteins and inhibits Fas-induced apoptosis, FASTK was suggested to antagonize with TIA1 in translation regulation (Li *et al.* 2004). However, the molecular details remain unresolved, with the recent results suggesting synergistic functions of FASTK and TIA1 in regulating translation and mRNA turnover (Li *et al.* 2013). With the current knowledge, it is unclear whether the role of FASTK in this case is pro- or antiapoptotic.

Also stress granules play a role in the regulation of apoptosis. In sublethal stress, transient SG formation enhances cell survival by sequestration of proapoptotic signalling proteins (Kim *et al.* 2005b, Arimoto *et al.* 2008, Tsai & Wei 2010), and by inhibiting the production of reactive oxygen species (Takahashi *et al.* 2013). On the other hand, SGs persist in cells exposed to lethal stress (Kedersha *et al.* 1999); whether this plays a role in regulating entry into apoptosis in physiological conditions is not known.

2.8.8 Autoregulation of the TIA proteins

The TIA proteins can regulate their own expression and activity through intricate feedback loops acting on multiple levels, suggesting that their tightly controlled activity is essential for cellular homeostasis (Le Guiner *et al.* 2001, Izquierdo & Valcárcel 2007a, Pullmann *et al.* 2007).

TIA1 and TIAL1 activate weak 5' splice sites followed by U-rich stretches also on their own mRNAs, promoting the inclusion of non-productive exons that introduce in-frame stop codons or nonsense-causing frameshifts to *TIA1* and *TIAL1* transcripts. As this leads to nonsense-mediated mRNA decay or production of nonfunctional truncated proteins, TIA proteins are expected to negatively regulate their own expression (Le Guiner *et al.* 2001).

TIA1 exon 5, encoding the TIA1a-specific insert, is also regulated by TIAL1. Depletion of TIAL1 increases skipping of this exon, leading to enhanced production of the short TIA1b isoform (Izquierdo & Valcárcel 2007a). TIA1b activates splicing more efficiently than TIA1a, and adjusting the isoform ratio has been proposed to fine tune splice-regulating activity of the TIA proteins. The two TIA1 isoforms show similar localization and RNA-binding; the higher activity of TIA1b is based on more efficient U1 snRNP recruitment (Izquierdo & Valcárcel 2007a). As other functional differences between TIA1a and TIA1b have not been reported, the two isoforms may exist to allow regulation of the splicing activity independently of other TIA1 functions.

Yet another autoregulatory mechanism functions at the level of translation. Both TIA proteins associate with their own mRNAs, and RNAi knockdown of one increases the protein level of the other. Depletion of TIAL1 has been shown to increase both the translation rate of endogenous TIA1, and the steady-state level of a GFP construct bearing the *TIA1* 3'UTR, demonstrating a suppressive effect on TIA1 translation (Pullmann *et al.* 2007).

3 AIMS OF THE STUDY

This study aimed at elucidating the molecular mechanisms by which mutations in four different proteins with diverse functions—titin, calpain 3, DNAJB6, and TIA1—cause hereditary muscular dystrophies.

The specific objectives in each of the subprojects were:

I to identify proteins interacting with the extreme C-terminal part of titin and with calpain 3, to characterize the biological functions of the interactions, and to investigate their possible involvement in the pathogeneses of TMD/LGMD2J and LGMD2A.

II to obtain functional evidence for the pathogenicity of the LGMD1D-causing mutations newly identified by our research group in the co-chaperone DNAJB6, to characterize the role of DNAJB6 in skeletal muscle, and to understand how its functions are affected by disease mutations.

III to obtain functional evidence for the pathogenicity of the E384K mutation in the RNA-binding protein TIA1—newly identified by our research group—and to elucidate the ensuing molecular events leading to Welander distal myopathy.

4 MATERIALS AND METHODS

4.1 Plasmid constructs (I–III, unpublished)

Plasmid constructs used in the studies are listed in Table 3.

4.2 Antibodies (I–III, unpublished)

Primary antibodies used in the studies are listed in Table 4. Commercial primary antibodies were acquired from Abcam plc (Cambridge, UK), Abnova (Taipei, Taiwan), Calbiochem / Merck Millipore (Darmstadt, Germany), Cell Signaling Technology (Danvers, MA, USA), Covance Research Products (Berkeley, CA, USA), Dako Denmark A/S (Glostrup, Denmark), Developmental Studies Hybridoma Bank (DSHB, Iowa City, IA, USA), Epitomics (Burlingame, CA, USA), Invitrogen / Life Technologies (Carlsbad, CA, USA), Novocastra / Leica Biosystems Newcastle Ltd. (Newcastle, UK), Novus Biologicals LLC (Littleton, CO, USA), Proteintech Group (Chicago, IL, USA), Roche Applied Science (Penzberg, Germany), Santa Cruz Biotechnology, Inc. (Santa Cruz, CA, USA), Sigma-Aldrich (St. Louis, MO, USA), Southern Biotech (Birmingham, AL, USA), Thermo Fisher Scientific (Waltham, MA, USA), and Triple Point Biologics, Inc. (Forest Grove, OR, USA).

4.3 Muscle material (I–III, unpublished)

Muscle biopsies used in microscopic, western blotting, and RT-PCR analyses were taken from various muscles of LGMD2J (I), LGMD1D (II), and WDM (III) patients, and healthy control individuals (I–III). Human *tibialis anterior* control muscle for stretch-fixed immunofluorescence samples (I) was obtained from an amputated leg. All samples were obtained with informed consent according to the Helsinki declaration.

Normal muscle tissue was collected from C57BL/6 mice (I) and Wistar rats (II) sacrificed for other experimental purposes. The effects of FINmaj mutation (unpublished) were studied on muscles from heterozygous and homozygous FINmaj KI mice (Charton *et al.* 2010) and wild-type littermates. Samples were collected from lower leg muscles (*tibialis anterior*, *soleus*, and *gastrocnemius*).

Table 3. Plasmid constructs

Construct	Versions	Vector	Insert	Fusion	Producer / reference	Publ.
pGBKT7-M10	wt, FINmaj	pGBKT7	human titin (132 C-term. aa of is7^{-} isoform)	N-term. GAL4 DBD		I
pB27-CAPN3$^{T417-S643}$		pB27	human CAPN3 (aa 417–643)	N-term. LexA DBD		I
pGADT7-CMYA5$^{3811-CT}$		pGADT7	human CMYA5 (aa 3811–4069)	N-term. GAL4 AD		I
pGADT7-CMYA5$^{3860-CT}$		pGADT7	human CMYA5 (aa 3860–4069)	N-term. GAL4 AD		I
pGADT7-CMYA5$^{3811-3941}$		pGADT7	human CMYA5 (aa 3811–3941)	N-term. GAL4 AD		I
pGADT7-CMYA5$^{3862-CT}$		pGADT7	human CMYA5 (aa 3862–4069)	N-term. GAL4 AD		I
pGADT7-CMYA5$^{3865-CT}$		pGADT7	human CMYA5 (aa 3865–4069)	N-term. GAL4 AD		I
pGADT7-CMYA5$^{3867-CT}$		pGADT7	human CMYA5 (aa 3867–4069)	N-term. GAL4 AD		I
pGADT7-CMYA5$^{3875-CT}$		pGADT7	human CMYA5 (aa 3875–4069)	N-term. GAL4 AD		I
pGADT7-CMYA5$^{3883-CT}$		pGADT7	human CMYA5 (aa 3883–4069)	N-term. GAL4 AD		I
pGADT7-CMYA5$^{3892-CT}$		pGADT7	human CMYA5 (aa 3892–4069)	N-term. GAL4 AD		I
pGADT7-CMYA5$^{3931-CT}$		pGADT7	human CMYA5 (aa 3931–4069)	N-term. GAL4 AD		I
pGBKT7-53		pGBKT7	p53	N-term. GAL4 DBD	Clontech Corp.	I
pGADT7-T		pGADT7	SV40 large T antigen	N-term. GAL4 AD	Clontech Corp.	I
is6–M8-V5		pEF6-V5/His-TOPO	human titin is6–M8	C-term. V5/His_6		I
is6–M9-V5		pEF6-V5/His-TOPO	human titin is6–M9	C-term. V5/His_6		I, II
is6–is7-V5		pEF6-V5/His-TOPO	human titin is6–is7	C-term. V5/His_6		I
is6–M10-V5 is7^{+}	wt, FINmaj	pEF6-V5/His-TOPO	human titin is6–M10 (is7^{+} isoform)	C-term. V5/His_6		I
is6–M10-V5 is7^{-}	wt, FINmaj	pEF6-V5/His-TOPO	human titin is6–M10 (is7^{-} isoform)	C-term. V5/His_6		I
is6–M10 is7^{+}		pEF6-V5/His-TOPO	human titin is6–M10 (is7^{+} isoform)	none		I
HA-is6–M10 is7^{+}	wt	pEF6-V5/His-TOPO	human titin is6–M10 (is7^{+} isoform)	N-term. HA		I
GFP-M10	wt	pEGFP-C	human titin domain M10	N-term. GFP	Fukuzawa *et al.* 2008	I
Myc-MD7		pCMV-Myc	mouse CMYA5 (aa 3039–3739)	N-term. Myc	Benson *et al.* 2004	I
Myc-MD9		pAMC	mouse CMYA5 (aa 2731–3739)	N-term. Myc		I
Myc-CMYA5$^{3811-CT}$		pAMC	mouse CMYA5 (aa 3039–3739)	N-term. Myc		I
GFP-MD9		pEGFP-C1	mouse CMYA5 (aa 2731–3739)	N-term. GFP		I
GFP-CMYA5$^{3811-CT}$		pEGFP-C1	human CMYA5 (aa 3811–4069)	N-term. GFP		I
YFP-CAPN3-CFP	wt, C129S	pTOM	rat CAPN3 isoform a	N-term. YFP, C-term. CFP	Taveau *et al.* 2003	I

pSRD-rCAPN3	C129S	pSRD	rat CAPN3 isoform a	none	Ono *et al*. 1998	I
pEF6-DNAJB6a		pEF6-V5/His-TOPO	human DNAJB6a	none		II
pEF6-DNAJB6b	wt, F93L	pEF6-V5/His-TOPO	human DNAJB6b	none		II
pEF6-DNAJB6a-V5	wt, F93L	pEF6-V5/His-TOPO	human DNAJB6a	C-term. V5/His_6		II
pEF6-DNAJB6b-V5	wt, F93L	pEF6-V5/His-TOPO	human DNAJB6b	C-term. V5/His_6		II
HA-DNAJB6a	wt, F93L	pCMV-HA	human DNAJB6a	N-term. HA		II
HA-DNAJB6b	wt, F89I, F93L	pCMV-HA	human DNAJB6b	N-term. HA		II
pCS2-DNAJB6a	wt, F89I, F93L	pCS2	human DNAJB6a	none		II
pCS2-DNAJB6b	wt, F89I, F89G, F93L, F93G, F93A	pCS2	human DNAJB6b	none		II
GFP-DNAJB6b	wt, F93L	pCDNA6.2/N-EmEGFP-DEST	human DNAJB6b	N-term. EmGFP		II
pCDNA5/TO-DNAJB6a-V5	wt	pCDNA5/TO	human DNAJB6a	C-term. V5/His_6		II
pCDNA5/TO-DNAJB6b-V5	wt, F89I, F93L	pCDNA5/TO	human DNAJB6b	C-term. V5/His_6		II
pCS2-BAG3	wt, P209L	pCS2	human BAG3	none		II
pEGFP/HD-120Q		pEGFP-N1	human HTT exon 1 with 120Q	C-term. GFP	Hasholt *et al.* 2003	II
pCDNA3.1/Myc-His-STUB1		pCDNA3.1/Myc-His	human STUB1	C-term. Myc/His_6	Qian *et al.* 2006	II
GFP-TIA1a	wt, E384K	pEGFP-C1	human TIA1a	N-term. GFP		III, u
GFP-TIA1b	wt, E384K	pEGFP-C1	human TIA1b	N-term. GFP		III, u
HA-TIA1a	wt, E384K	pAHC	human TIA1a	N-term. HA		III
HA-TIA1b	wt, E384K	pAHC	human TIA1b	N-term. HA		III
HT-TIA1a	wt, E384K	pHTN	human TIA1a	N-term. HaloTag		III
HT-TIA1b	wt, E384K	pHTN	human TIA1b	N-term. HaloTag		III
HA-TIA1a-V5	wt, E384K	pEF6-V5/His-TOPO	human TIA1a	N-term. HA, C-term. V5/His_6		III

AD, activation domain; DBD, DNA-binding domain; EmGFP, emerald green fluorescent protein; u, unpublished

Table 4. Antibodies

Target	Clone / product	Host	Type	Producer / reference	Application	Publ.
α-tubulin	YL1/2	rt	mAb	Abcam	WB	II
α-tubulin	T6074	ms	mAb	Sigma-Aldrich	WB	II
αB-crystallin	G2JF	ms	mAb	Novocastra	IHC	II
actin	A2066	rb	pAb	Sigma-Aldrich	WB	I
BAG3	10599-1-AP	rb	pAb	Proteintech	IF, PLA, WB	II
calpain 3	RP2	rb	pAb	Triple Point Biologics	WB	I
desmin	Y66	rb	mAb	Epitomics	IF	II
DNAJB6	2C11-C1	ms	mAb	Abnova	IF, WB	II
DNAJB6	H00010049-A01	ms	pAb	Abnova	WB, PLA	II
dystrophin	Dy4/6D3	ms	mAb	Novocastra	IF	I
eIF3	sc-16377	gt	pAb	Santa Cruz	IF	III
filamin	F1888	ms	mAb	Sigma-Aldrich	IF	II
G3BP	ab56574	ms	mAb	Abcam	IF	III
GFP	ab6556	rb	pAb	Abcam	WB	I
GFP	66002-1-Ig	ms	mAb	Proteintech	WB	III
GFP	SC-8334	rb	pAb	Santa Cruz	WB	II
GFP	G1544	rb	pAb	Sigma-Aldrich	WB	II
HA	M4439	ms	mAb	Sigma-Aldrich	WB	II
HA tag	HA.11	ms	mAb	Covance	IF, WB	III
HA tag	3F10	rt	mAb	Roche Applied Science	IF	I
Hsp90	SC-7947	rb	pAb	Santa Cruz	WB	II
HSPA8	ab1427	rb	pAb	Abcam	IF, PLA	II
HSPB8	ab79784	rb	pAb	Abcam	PLA	II
HSPB8	3059	rb	pAb	Cell Signaling	WB	II
HuR	3A2	ms	mAb	Invitrogen	IF	III
KRT18	ab52948	rb	pAb	Abcam	IF	II
LAMP2	H4B4	ms	mAb	Southern Biotech	IF	III
LC3	NB100-2331	rb	pAb	Novus Biologicals	IF	II
LC3b	#2775	rb	pAb	Cell Signaling	IF	III
MLF1	ab70211	rb	pAb	Abcam	IF	II
Myc tag	9E10	ms	mAb	Abcam	IF, WB	I, II
Myc tag	R950-CUS	ms	mAb	Invitrogen	WB	I
Myc tag	9E10	ms	mAb	Roche Applied Science	IF, WB	I, II
Myc tag	9E10	ms	mAb	Santa Cruz	IF, WB	I, II
Myc tag	E6654	rb	agar.	Sigma-Aldrich	IP	I
Myc tag	NB600-342	gt	agar.	Novus Biologicals	IP	I
myosin heavy chain	F59	ms	mAb	DSHB	IF	II
myospryn	Des122	rb	pAb	Benson *et al.* 2004	IF, PLA, WB	I, u
myotilin	151	rb	pAb	Mologni *et al.* 2005	IF	II
PGM1	15161-1-AP	rb	pAb	Proteintech		u
sarcomeric α-actinin	EA-53	ms	mAb	Sigma-Aldrich	IF	I, u
sarcomeric α-actinin	653	rb	pAb	van der Ven *et al.* 2000	IF	I
SQSTM1 (p62)	sc-28359	ms	mAb	Santa Cruz	IF	III
STUB1	PC711	rb	pAb	Calbiochem	IF, PLA, WB	II

TARDBP	2E2-D3	ms	mAb	Sigma-Aldrich	IF	III
TIA1 (C-term.)	ab40693	rb	pAb	Abcam	IF, WB	III
TIA1 (C-term.)	C-20 (sc-1751)	gt	pAb	Santa Cruz	WB	III
TIA1 (central)	ab61700	gt	pAb	Abcam	IF	III
TIA1 (N-term,)	G-3	ms	mAb	Santa Cruz	WB	III
TIAL1	C-18	gt	pAb	Santa Cruz	IF, WB	III
titin (M-is4)	T41	ms	mAb	Obermann *et al.* 1996	PLA	I, u
titin (M10)	M10-1	rb	pAb	Hackman *et al.* 2008	WB	I
titin (M8)	Tm8ra	rb	pAb	Obermann *et al.* 1996	IF	I
titin (M9)	T51	ms	mAb	Obermann *et al.* 1996	IF, PLA	I, u
ubiquitin	Z-0458	rb	pAb	Dako	IF	III
V5 tag	SV5-P-k	ms	mAb	Invitrogen	WB	I, II, III
V5 tag	NB600-387	gt	agar.	Novus Biologicals	IP	I, II
VCP	MA3-004	ms	mAb	Thermo Fisher	IF	III

rt, rat; ms, mouse; rb, rabbit; gt, goat; agar, pAb agarose conjugate; u, unpublished

4.4 Cell culture and transfections (I–III, unpublished)

4.4.1 Cell lines (I–III)

The following mammalian cell lines were used in the study: COS-1 (ATCC, Manassas, VA, USA), human embryonic retinoblast 911 (Fallaux *et al*. 1996), HeLa (ATCC), T-REx 293 (Invitrogen, Life Technologies, Carlsbad, CA, USA), 293FT (Invitrogen), and C2C12 (ATCC). Cells were cultured at 37°C, 5% CO_2 using standard techniques. Transient transfections were performed with FuGENE 6 (Roche Applied Science, Penzberg, Germany; or Promega Corporation, Madison, WI, USA), or with Lipofectamine 2000 (Invitrogen).

4.4.2 Neonatal rat cardiomyocyte (NRC) cultures (I)

Neonatal rat cardiomyocytes (NRCs) were isolated using the Worthington Neonatal Cardiomyocyte Isolation System (Worthington Biochemical Corporation, Lakewood, NJ, USA), and transfected using the Escort III reagent (Sigma-Aldrich, St. Louis, MO, USA) according to manufacturer's instructions. Transfected NRCs were cultured for 1–2 days in maintenance medium (74.7% DMEM, 18.6% medium M199, 3.8% horse serum, penicillin/streptomycin, 4 mM L-glutamine, 100 μM phenylephrine, 10 μM cytosine-β-D-arabinofuranoside) or for 5 days in transfection medium with antibiotics (73% DBSS-K medium, 21% medium M199, 4% horse serum, 4 mM L-glutamine, penicillin/streptomycin).

4.4.3 C2C12 myotube cultures (unpublished)

C2C12 myoblasts were seeded on collagen-coated culture dishes and transfected using Lipofectamine 2000 within 2 h. For differentiation into myotubes, confluent cells were cultured in DMEM with 2% horse serum, L-glutamine, and penicillin/streptomycin for 5–6 days.

4.5 Yeast two-hybrid studies (I)

4.5.1 Yeast two-hybrid screens (I)

The yeast two-hybrid screen for identifying interaction partners of the titin M10 domain was performed at the two-hybrid core facility of Biocentrum Helsinki, University of Helsinki. The bait encoding the wild-type human M10 domain in pGBKT7 was screened against a human skeletal muscle prey library in pACT2 (Clontech Laboratories, Inc., Mountain View, CA, USA). A total of 10.56 million yeast colonies were screened.

The yeast two-hybrid screen for identifying CAPN3 ligands was performed at Hybrigenics S.A. (Paris, France). A pB27 bait construct encoding residues T417–S643 of CAPN3 was screened against a prey library consisting of a 1:1 mixture of human adult and fetal skeletal muscle poly(A) RNAs in pB6. A total of 106 million yeast colonies were screened.

4.5.2 Pairwise yeast two-hybrid analyses (I)

Pairwise yeast two-hybrid studies were performed with the mating strategy using the Matchmaker 3 system (Clontech) according to the manufacturer's instructions. AH109 strains carrying pGBKT7 bait constructs were mated with Y187 strains carrying pGADT7 prey constructs, and activation of *HIS2* and *ADE2* reporter genes was assayed on selection plates lacking histidine and adenine. Activation of the *LacZ* reporter was separately assayed with an X-gal overlay assay.

4.6 SDS-PAGE and western blotting (I–III)

SDS-PAGE was performed with standard methods with self-cast Tris-glycine gels or precast TGX gels (Bio-Rad Laboratories, Hercules, CA, USA). Western blotting was performed with standard methdods, with chemiluminescent detection on film or on a ChemiDoc XRS+ system (Bio-Rad), or with fluorescent detection on an Odyssey Infrared Laser Imaging System (LI-COR Biosciences, Lincoln, NE, USA).

4.7 Coimmunoprecipitation (CoIP) (I–II)

For coimmunoprecipitation studies without crosslinking (I–II), cells were lysed by resuspending in ice-cold hypotonic gentle lysis buffer (10 mM Tris-HCl pH 7.5, 10 mM NaCl, 2 mM EDTA, 0.5% Triton X-100, 1× Complete Protease Inhibitor Mixture [Roche Applied Science]; supplemented to 150 mM NaCl after 10 min of lysis). Insoluble material was pelleted by centrifugation (15 min, 16,000×*g* at 8°C).

For coimmunoprecipitation with crosslinking (II), cells were lysed by resuspending in ice-cold PBS / 0.5% Triton X-100 / 1× Complete, and triturating through a 27G needle. Insoluble material was pelleted by centrifugation as described above. Proteins in the cleared lysates were crosslinked with 1 mM dithiobis(succinimidyl

propionate) (Pierce, Thermo Fisher Scientific, Waltham, MA, USA) for 30 min on ice, and crosslinking was quenched with 20 mM Tris-HCl, pH 7.4 for 15 min on ice.

Lysates were incubated with antibody-conjugated agarose beads 2 h to overnight at 8°C. The beads were washed several times with NET-2 (50 mM Tris-HCl, pH 7.5, 150 mM NaCl, 0.05% Triton X-100; in CoIP without crosslinking) or RIPA (50 mM Tris-HCl, pH 7.5, 150 mM NaCl, 1% NP-40, 0.5% Na-deoxycholate, 0.1% SDS; in CoIP with crosslinking). Bound proteins were eluted in SDS sample buffer by heating 5 min at 95°C and analyzed by western blotting.

4.8 Immunofluorescence microscopy (I–III, unpublished)

4.8.1 Preparation of muscle samples

Tissue samples from human muscle biopsies or dissected mouse muscles were freshly embedded in Tissue-Tek O.C.T (Sakura Finetek Europe B.V., Zoeterwoude, The Netherlands), frozen in isopentane chilled with liquid nitrogen, and stored at –80°C until use.

For preparation of stretched muscle samples (I–II, unpublished), rodent or human muscle pieces were pinned on cork or held with surgical retractors in a stretched position (~1.5× slack length), fixed in 4% PFA for 30 min at RT, and cryoprotected in glucose in PBS (10% for 1 h, 20% for 1 h, 30% overnight). The muscles were then embedded in Tissue-Tek and frozen as described above.

Frozen muscles were cut to transverse or longitudinal cryosections of 8–10 μm. Sections were stored frozen in –20°C (short term) or –80°C (long term) until use.

4.8.2 Immunofluorescent (IF) stainings

For cultured cells and muscle sections, indirect immunofluorescent (IF) stainings were performed with standard techniques, using secondary antibodies labelled with Alexa Fluor (Molecular Probes, Life Technologies) or CyDye dyes (Jackson ImmunoResearch Laboratories, Inc., West Grove, PA, USA).

Zebrafish embryos were fixed in 4% PFA overnight and stored in 100% methanol at –20°C. Embryos were rehydrated with PBS, washed in 0.1% Tween-20, 1% BSA / PBS for 10 min at RT, blocked in 10% fetal calf serum / 1% BSA / PBS for 1 h at RT. Whole-mount indirect IF staining was performed with antibodies diluted in blocking buffer.

4.8.3 Fluorescence microscopy (I–III, unpublished)

Wide-field fluorescence microscopy was performed using Zeiss Axioplan 2 (Carl Zeiss MicroImaging GmbH, Göttingen, Germany) or AZ100 (Nikon Instruments Inc., Melville, NY, USA). Confocal microscopy was performed using LSM 510 Meta or LSM 780 confocal microscopes (Carl Zeiss MicroImaging) with 63× / NA 1.4 and 40× / NA 1.3 objectives.

4.9 *In situ* proximity ligation assay (I–II, unpublished)

Cryosections of stretch-fixed mouse and rat muscles were prepared and permeabilized as for the IF stainings. PLA experiments were performed with the Duolink system and the Duolink fluorescent detection kit 563 (Olink Bioscience, Uppsala, Sweden) with minor modifications to the manufacturer's instructions. Alexa Fluor 488-conjugated phalloidin (Molecular Probes) was added 1:100 to the primary antibody solution as a counterstain.

4.10 DNAJB6 knockdown and expression in zebrafish (II)

Zebrafish (*Danio rerio*) were maintained with standard methods. For knockdown of *dnajb6b*, fish embryos (1- or 2-cell stage) were injected with 6 ng of a splice-blocking morpholino oligonucleotide targeted against the gene. For ectopic expression of human wild-type or mutant DNAJB6, the embryos were injected with 50–100 pg of *in vitro* transcribed, capped mRNA.

Fish embryos at 48 hours post-fertilization were fixed in PFA, and slow myofibres visualized with whole-mount IF staining of slow myosin heavy chain. Based on microscopic evaluation, embryos were categorized as normal (no discernible muscle defects), class I (complete or partial detachment of fibres from the vertical myosepta affecting 1–2 somites) or class II (affecting multiple somites). Phenotype distributions were analysed with the χ^2 test.

4.11 Filter trap assay (FTA) (II)

For testing the anti-aggregation activity of DNAJB6 in filter trap assay (FTA), T-REx 293 cells were co-transfected with pcDNA5/TO-DNAJB6 and pEGFP/HD-120Q (mass ratio 7:1) in duplicate. DNAJB6 expression was induced 7 h post-transfection in one of the duplicate wells with 1 µg/ml tetracycline. Cells were harvested 48 h post-transfection, and FTA was performed according to a protocol adapted from Hageman *et al.* (2010). The cells were lysed in FTA buffer (10 mM Tris-HCl pH 8.0, 150 mM NaCl, 50 mM dithiothreitol) containing 2% SDS and 1× Complete, by triturating through a 27G needle, sonicated for 1 min at RT in a bath sonicator and heated to 98°C. Samples for quantification of SDS-soluble huntingtin were removed form lysates and analysed by western blotting. For the trapping of aggregated huntingtin, samples of remaining lysates were filtered through a cellulose acetate membrane (pore size 0.2 µm, Whatman plc, Maidstone, UK), followed by three washes with 300 µl FTA buffer containing 0.1% SDS.

Immunostaining and fluorescent detection of FTA membranes and western blots of SDS-soluble huntingtin was performed as described elsewhere. Amounts of aggregated (aggr.) huntingtin on FTA membranes and soluble (sol.) huntingtin on WB were quantified with the Odyssey software.

Antiaggregation effect of the DNAJB6 construct was expressed as aggregation score [$(aggr./sol)_{induced}/(aggr./sol.)_{uninduced}$], calculated for each transfection pair. Results were analysed with the two-tailed Mann–Whitney *U*-test using the Bonferroni correction.

4.12 Density gradient centrifugation (II)

The density gradient centrifugation procedure for the analysis of DNAJB6 oligomerization was adapted from Hageman *et al.* (2010). Sucrose gradients in 10 mM Tris-HCl pH 8.0, 50 mM NaCl, 5 mM EDTA were prepared by layering sucrose solutions (80–10%, with 10-% intervals) in ultracentrifuge tubes. Cells were lysed in 10 mM Tris-HCl pH 8.0, 150 mM NaCl, 0.5% NP-40, 3% glycerol, 1× Complete, by triturating through a 27G needle, and centrifuged 15 min at 300×*g*. Supernatants were loaded on sucrose gradients and ultracentrifuged for 18–20 h, 100,000×*g* at 8°C.

After centrifugation, 12 fractions of equal volume were collected from the bottom of the gradients. Proteins were precipitated by mixing 1:1 with 25% trichloroacetic acid and incubating 30 min on ice, pelleted by centrifugation (15 min, 16,000×*g* at 8°C), washed twice with 80% acetone, air dried, dissolved in a 1:1 mixture of 1% SDS / 0.1M NaOH and 2× SDS sample buffer, and analyzed by western blotting.

4.13 Protein turnover assays (II)

The turnover of DNAJB6 was studied with a cycloheximide (CHX) chase assay on 293FT cells. Cells were transfected with HA- or GFP-tagged DNAJB6 constructs, and after 48 h treated with 50 μg/ml CHX to block synthesis of new proteins. Optionally, protein turnover pathways were inhibited by adding 20 μM lactacystin (EMD Millipore, Billerica, MA, USA) or 100 nM bafilomycin A1 (Sigma-Aldrich) together with CHX. After various durations (0–7 h) of drug treatment, cells were washed with PBS and lysed in RIPA buffer. DNAJB6 constructs were quantified from soluble fractions of the cell extracts by western blotting, and normalized to α-tubulin or HSP90, depending on the molecular weight of the construct.

4.14 Stress granule analyses (III)

4.14.1 Induction of stress granules by arsenite treatment (III)

To induce stress granule assembly, HeLa or C2C12 cells were treated with 500 μM sodium arsenite (Sigma-Aldrich) in normal medium for 45 min prior to cell fixation.

4.14.2 High-content analysis of stress granules (III)

HeLa cells were seeded on 24-well plates and transfected with TIA1 constructs (GFP-TIA1, HA-TIA1, or HT-TIA1). For fluorescent labelling, HT-TIA1-transfected cells were treated overnight with HaloTag TMRDirect Ligand (Promega) diluted 1:2000 in normal medium. The next day (18 h after transfection for GFP-TIA1 and HA-TIA1, 20 h after transfection for HT-TIA1), the cells were treated with 500 μM sodium arsenite or control medium for 45 min and fixed with 4% PFA. Cells were permeablized with 0.2% Triton X-100 / PBS, and stained with Hoechst for labelling the nuclei. HA-TIA1 proteins were visualized with an indirect IF staining with an anti-HA antibody as described elsewhere.

Fluorescent images of 200 fields per well were captured with the CellInsight instrument (Thermo Fisher) using a 10× / NA 0.3 objective and fixed exposure times. Automated image analysis for quantification of stress granules was performed with the SpotDetector.V4 BioApplication in vHCS Scan 6.2.3 software (Thermo Fisher). Cells expressing moderate levels of TIA1 constructs were selected for analysis based on mean fluorescence intensity of the whole cell, and fluorescent spots fulfilling empirically determined criteria of size, shape, and intensity were analyzed from a region of interest surrounding the nucleus. The mean results of each well (number of spots and total spot area per analyzed cell) were normalized to the mean of untreated wild-type wells on the same plate.

4.14.3 Fluorescence recovery after photobleaching (FRAP) (III)

HeLa cells, transfected with GFP-TIA1a constructs, were cultured on Lab-Tek II chambered coverglass (Nunc A/S, Roskilde, Denmark) in phenol-red-free medium. Stress granule formation was induced 22–25 h post-transfection with sodium arsenite. FRAP measurements were performed either at 35–36°C or at 37°C, 5% CO_2, within the time window of 30–60 min after arsenite addition.

FRAP was performed with an LSM 510 Duo confocal microscope equipped with an LD C-Apochromat 40× / NA 1.10 water immersion objective (Carl Zeiss MicroImaging). Using an instrument zoom factor of 20× and frame size of 88×88 pixels, a circular target region of 8 pixels (approx. 1 μm) in diameter was centered on a stress granule and bleached by point scanning with 405-nm, 458-nm and 488-nm laser lines. A time series of 60 frames (10 frames before and 50 after bleaching) was captured with maximum acquisition speed and frame interval of 250 ms.

Images were analyzed with ImageJ. Mean fluorescence intensity was measured from the FRAP target region, a reference region containing a non-bleached SG, and a background region from outside the cell. For each frame, background-subtracted intensity of the target region was normalized to that of the reference region (to correct for acquisition bleaching), and these values were expressed relative to the initial prebleach value of the target region. Image series where stress granules moved partly away from measurement regions or bleaching caused a clear intensity drop in the reference region were omitted from analysis.

4.15 Image processing and analysis (I–III)

Image processing and analysis were done using the LSM 510 Meta 3.2 software (Carl Zeiss MicroImaging), Odyssey software (LI-COR), vHCS Scan 6.2.3 software (Thermo Fisher), Adobe Photoshop (various versions; Adobe Systems Inc., San Jose, CA, USA) and ImageJ (various versions; US National Institutes of Health, Bethesda, MD, USA).

4.16 Miscellaneous methods (I–III)

4.16.1 Protein modelling (I)

A structural model for the C-terminal FN3 domain in myospryn was generated at the Swiss-Model workspace (Arnold *et al.* 2006) by homology modelling, using the Protein Data Bank structure 2dmk as template.

4.16.2 Electron microscopy (II)

Transmission electron microscopy of muscle samples was performed using standard techniques.

4.16.3 RNA isolation and RT-PCR (III)

Muscle RNA was isolated with the Dr. P Kit (BioChain Institute, Inc., Newark, CA, USA) and reverse transcribed using SuperScript Reverse Transcriptase (Invitrogen). Regions of interest were PCR-amplified from muscle cDNA, and isoform ratios were assessed from agarose gels visually or quantified from gel images.

4.16.4 Antibody epitope mapping (III)

For epitope mapping of C-terminal TIA1 antibodies, a SPOT peptide array covering the 69 C-terminal amino acid residues of human TIA1 as 15-mers was synthesized at the peptide synthesis unit, Haartman Institute, University of Helsinki. The peptides containing the WDM mutation site were included as both wild-type and E384K mutant forms. The array was probed with TIA1 antibodies using ECL detection, and minimal antibody binding sites were inferred from the sequences of the reactive peptide spots.

4.16.5 In vitro translation (III)

Wild-type and E384K mutant HA-TIA1 were translated *in vitro* from the pAHC-TIA1 constructs with the TnT T7 Quick Coupled Transcription/Translation System (Promega) according to the manufacturer's instructions, and analyzed by western blotting.

5 RESULTS AND DISCUSSION

5.1 Titinopathies TMD/LGMD2J and calpainopathy LGMD2A

5.1.1 Search for novel interaction partners of C-terminal titin and calpain 3

When mutations causing TMD/LGMD2J were first identified in titin (Hackman *et al.* 2002), no proteins were known to interact with the M10 domain harbouring the mutations. For the identification of interaction partners, potentially affected by the disease mutations, a yeast two-hybrid interaction screen was performed using the M10 domain as bait.

The M10 interaction screen yielded 84 positive prey clones coding for 21 different proteins. Six putative interaction partners represented by more than one prey clone (CMYA5, PGM1, RANBP9, RING1, FHOD1, and KTN1) were chosen for further analysis in pairwise Y2H studies: The cDNA inserts were moved to the pGADT7 vector and tested in Y2H against wild-type and FINmaj mutant versions of the original M10 bait construct, as well as the empty bait vector. Four clones, encoding RANBP9, RING1, FHOD1, and KTN1, showed reporter gene activation also in combination with the empty bait vector, and were discarded as false positive hits. Two prey clones encoding phosphoglucomutase 1 (PGM1) also showed autoactivation, but the interaction warranted further studies due to the high number of recovered clones and the biological plausibility of the interaction (discussed below).

The interaction of the titin M10 domain and myospryn (CMYA5) was supported by pairwise Y2H studies. In parallel, myospryn was also identified as a putative interaction partner for the protease calpain 3 (CAPN3) in another yeast two-hybrid screen. This screen was performed as a part of an interactome project for LGMD-associated proteins, coordinated by Dr. Isabelle Richard's laboratory in Généthon, Evry, France. The interactions of myospryn with titin and CAPN3 will be further discussed in 5.1.3.

Since the initation of our interaction study in 2004, the titin M10 domain has been reported to bind the obscurin proteins OBSCN/OBSL1 (Fukuzawa *et al.* 2008) and nuclear lamins (Zastrow *et al.* 2006). In addition, a small C-terminal titin fragment was found to interact with the KY protease, but as the interaction was not reproduced with Y2H constructs containing the entire M10 domain, it was deemed physiologically irrelevant (Beatham *et al.* 2004, 2006). Interactions of MURF1 and MURF2 with the titin domains M8–M10, were identified by Witt *et al.* (2008) in a Y2H system, but further studies have not been reported. None of these confirmed or putative interaction partners were among the clones recovered in our interaction screen. At least for the large obscurin proteins, known to interact with titin through their N-terminal domains (Fukuzawa *et al.* 2008), this is likely to reflect the lack of N-terminal clones from the oligo-dT-primed prey library.

5.1.2 Putative interaction of PGM1 with the titin M10 domain (I, unpublished)

The most frequent hit in the M10 interaction screen, represented by 19 prey clones, was phosphoglucomutase 1 (PGM1), a metabolic enzyme catalyzing the interconversion of glucose 1-phosphate and glucose 6-phosphate. Recovered PGM1 clones spanned 77–107 C-terminal amino acid residues of the protein. Prey constructs encompassing 77 or 89 C-terminal residues were tested in further Y2H studies, where both showed reporter activation with the empty bait vector, strongly suggesting a false positive hit. However, in combination with the FINmaj M10 bait, the longer prey construct showed a lower level of reporter activation compared to either the wild-type bait or the empty vector, which could reflect a true interaction with the M10 domain.

PGM1 has not been reported as a frequent false positive in GAL4-based Y2H screens, which could be expected for a strong autoactivating protein. It was reported as an interaction partner of the Z-disc protein ZASP, based on a Y2H screen utilizing the same Matchmaker 3 system that was used in our experiments (Arimura *et al.* 2009). Also in this screen, PGM1 was the most abundant hit, with the amino acid range of the positive clones (74–162 C-terminal residues) very similar to ours. Testing the recovered prey clones in Y2H against a negative-control bait was not reported, but the interaction with ZASP was supported by mammalian two-hybrid, CoIP, and cell biological studies, suggesting that the finding was not a mere result of prey autoactivation (Arimura *et al.* 2009). On the other hand, PGM1 was also recovered in a Y2H screen with LRRC39 (interestingly, another M-band protein) as bait (Jenniches 2012). Here, PGM1 was classified as a probable false positive due to promiscuity, but experimental evidence behind this judgement was not discussed.

Solely based on the Y2H findings, the putative interaction of PGM1 with titin M10 seems thus questionable. Other pieces of evidence, however, support the possibility of a true interaction. Firstly, other metabolic enzymes (enolase, creatine kinase, adenylate kinase, and phosphofructokinase) are targeted to the M-band, in part by titin and FHL2 (Keller *et al.* 2000, Lange *et al.* 2002). This is suggested to concentrate the enzymes to regions of high metabolic activity, and in this context the interaction of PGM1 with M-band titin would be functionally plausible. Secondly, also PGM1 shows partial localization to the M-band. This was particularly evident in cardiomyocytes transfected with a GFP-tagged C-terminal PGM1 construct (Arimura *et al.* 2009), although the authors did not discuss the M-band localization. Also in our preliminary IF studies on mouse muscle, variable amounts of PGM1 were present at the M-band. This M-band signal did not appear disrupted in homozygous FINmaj knock-in muscle, indicating that the M-band targeting does not depend on the putative interaction with M10 (Fig. 7, unpublished data).

Further CoIP experiments performed in our group have so far failed to provide conclusive evidence for the titin–PGM1 interaction (Anni Evilä, unpublished data). Additional studies would thus be needed for definitively proving or disproving the putative interaction.

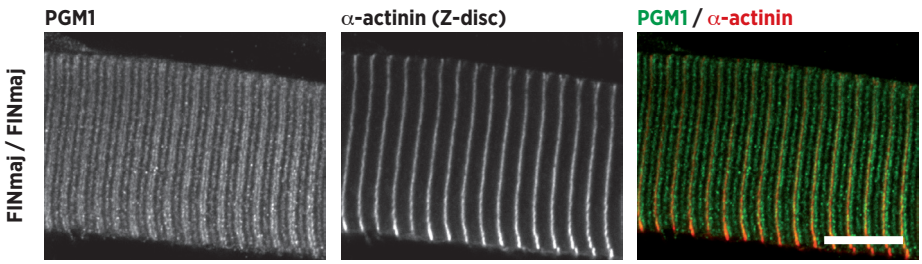

Figure 7. Phosphoglucomutase 1 in muscle

Confocal microscopy of PGM1 and the Z-disc marker α-actinin in mouse muscle. PGM1 was mostly localized around the Z-disc, but it also exhibited variable degrees of M-band localization, ranging from undetectable to prominent (exemplified here), No obvious difference was seen between wild-type (not shown) and homozygous FINmaj KI (FINmaj / FINmaj) muscles. Scale bar, 10 μm.

5.1.3 Novel interaction of myospryn with C-terminal titin and CAPN3

Myospryn (CMYA5, cardiomyopathy-associated 5), identified in the Y2H screens as an interaction partner for C-terminal titin and calpain 3, is a large multifunctional protein related to the tripartite motif (TRIM) family. Its expression on transcript and protein levels was initially characterized as restricted to skeletal and cardiac muscles (Benson *et al.* 2004, Durham *et al.* 2006), but moderate myospryn expression in the brain has been recently reported (Chen *et al.* 2011).

The official symbol CMYA5, suggesting an association with cardiomyopathy, was originally coined on hypothetical grounds, based on coexpression with known cardiomyopathy genes (Walker 2001). Aliases genethonin-3 (Tkatchenko *et al.* 2001) and stretch-responsive 553 or sr553 (McKoy *et al.* 2002) have been used in individual early studies. Although lacking the RING domain present in canonical TRIM proteins, myospryn is also classified as TRIM76 (HGNC Database).

Human myospryn, comprising 4069 amino acid residues, has a predicted molecular weight of 449 kDa (Fig. 8). Its C-terminal region of ~600 amino acids has a domain architecture resembling the TRIM proteins: The region contains a B-Box' domain (a variant of the B-Box zinc finger domain containing two instead of four Zn^{2+}-coordinating residue pairs), a BBC (B-Box C-terminal coiled-coil), two FN3 domains, and a SPRY (SPlA and RYanodine receptor) domain (Benson *et al.* 2004). According to Y2H and CoIP studies, the TRIM-like region is capable of self-association, suggesting that the protein may exist as a homodimer (Benson *et al.* 2004).

The TRIM-like region of myospryn is highly conserved in evolution, with ~90% identity between the human and murine orthologues. Another region showing evolutionary conservation is a stretch of ~100 amino acid residues near myospryn N-terminus, but the domain structure and functions of this part of the protein are currently unknown. Most of myospryn is comprised of repetitive, glutamate-rich sequence without predictable domains (Benson *et al.* 2004); this low-complexity region shows variation in length and repeat composition between myospryn orthologues in different species, and could thus serve as a flexible linker between the conserved N-and C-terminal regions.

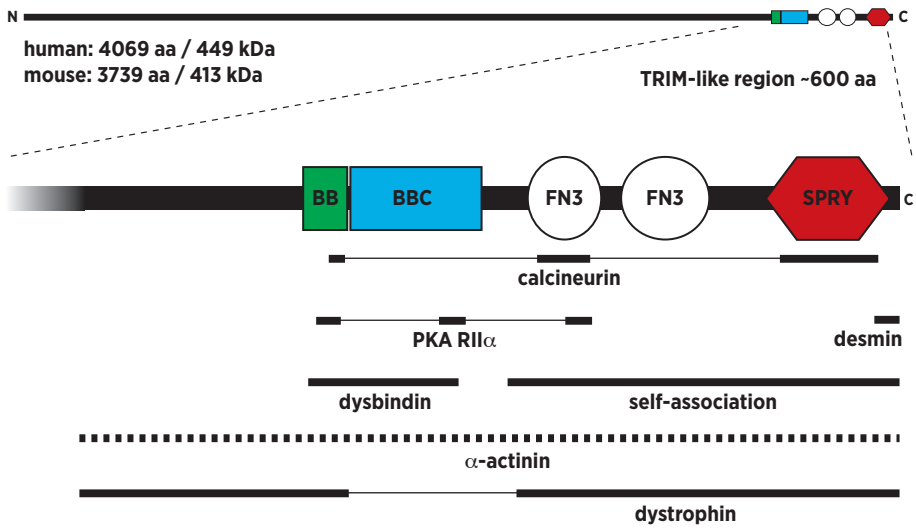

Figure 8. Structure and reported interactions of myospryn

Most of the myospryn (CMYA5) protein is composed of repetitive, acidic sequence with no recognizable domains. The C-terminal part of the protein contains a TRIM-like domain structure with BBox' (BB), coiled-coil (BBC), FN3, and SPRY domains. Sites of reported protein interactions are indicated.

Adapted from Sarparanta J: Biology of Myospryn: What's Known? *Journal of Muscle Research and Cell Motility*, 2008; 29:177–180 with kind permission from Springer Science and Business Media. © 2009 Springer Science and Business Media B.V.

5.1.3.1 Myospryn interacts in Y2H with wild-type but not FINmaj mutant M10 (I)

In the M10 interaction screen, myospryn was represented by two recovered prey clones, spanning 259 (A3811–CT) and 210 (L3860–CT) C-terminal residues of the protein. Pairwise Y2H studies (I: Fig. 2) replicated the interaction of the two recovered myospryn prey clones with the wild-type M10 bait, while no reporter activation was seen with the empty bait vector. Moreover, both myospryn clones failed to cause reporter activation in combination with the FINmaj mutant M10 bait, suggesting that the interaction is specific and requires a correctly folded M10 domain. Additional Y2H experiments with deletion constructs showed that half of the C-terminal FN3 domain and the SPRY domain of myospryn are required for the interaction with titin M10. Progressively weaker reporter signals obtained with a series of deletion constructs starting in the region L3860–Y3875 suggested that this region may contain amino acid residues directly participating in titin binding (I: Fig. 1–2).

5.1.3.2 A larger C-terminal part of titin participates in myospryn binding (I)

To confirm the interaction of myospryn with titin, CoIP experiments were carried out in COS-1 cells. The myospryn constructs utilized in these studies covered three different C-terminal regions: A3811–CT of human myospryn (corresponding to the longer prey clone recovered in the M10 screen), as well as G3039–CT (MD7) and Y2731–CT (MD9) of the murine protein (Benson *et al.* 2004). In contrast to expec-

tations from the Y2H studies, none of the myospryn constructs showed binding to a GFP-tagged M10 construct in the tested CoIP conditions. All were, however, pulled down with a longer (is6–M10-V5 is7^{+}) titin construct, supporting the interaction of the proteins but suggesting that myospryn binding is not limited to the M10 domain (I: Fig. 3).

Additional CoIP studies were performed with the myospryn construct MD9 and a series of V5-tagged titin constructs of different lengths. Either V5 or Myc antibodies were used for immunoprecipitating the titin or myospryn constructs, respectively. In these experiments—in addition to is6–M10-V5 is7^{+}—also titin constructs spanning the regions is6–M10 (is7^{-}) and is6–is7 showed clear binding to myospryn MD9, whereas for is6–M9 and is6–M8, the interaction was weak or undetectable (I: Fig. 3). The difference between is6–M9 and is6–is7 indicates that the is7 region participates in the interaction. The binding seen with is6–M10 is7^{-} but not with M10 alone, on the other hand, demonstrates the contribution of the M9 domain. In conclusion, the whole C-terminal region M9–is7–M10 in titin is involved in myospryn binding (Fig. 9).

In CoIP experiments the FINmaj mutation failed to disrupt the interaction of is6–M10 constructs with myospryn, but rather seemed to increase the binding. This discrepancy between CoIP and Y2H results is likely due to preserved interaction of M9–is7 with myospryn despite the mutation. The apparent increase in binding could be explained by unspecific adhering of proteins to the unfolded M10 domain.

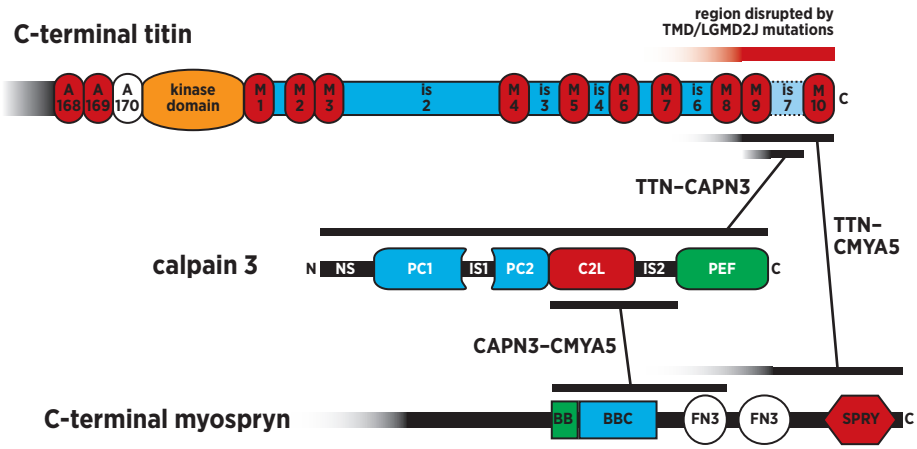

Figure 9. Interactions between myospryn, C-terminal titin, and CAPN3

Summary of the novel and previously reported interactions between myospryn (CMYA5), C-terminal titin (TTN), and CAPN3. Regions participating in the interactions, as defined by Y2H and CoIP assays, are indicated by black bars.

5.1.3.3 The interaction of CAPN3 and myospryn is supported by CoIP (I)

The interaction of myospryn with CAPN3, identified in the Y2H screen for CAPN3 ligands, was confirmed by CoIP studies in COS-1 cells, where both myospryn constructs MD7 and MD9 pulled down the proteolytically inactive CAPN3 C129S construct with comparable efficiencies (I: Fig. 3). Based on the regions covered by the Y2H bait construct and the recovered prey clones, the interaction involves the C2-like domain and IS2 of CAPN3, and a myospryn region encompassing the BBox', coiled-coil, and the first FN3 domain (Fig. 9). As this was not refined further with deletion constructs, the minimal interacting regions could be smaller.

5.1.4 Subcellular localization of myospryn

5.1.4.1 Localization of myospryn in muscle fibres (I, unpublished)

To obtain support for its interaction with M-band titin, the localization of myospryn in muscle fibres was studied by immunofluorescence microscopy. In mouse and human muscle samples fixed in a stretched position, the Des122 antibody revealed myospryn predominantly as broad doublet bands flanking the Z-disc. In addition, fainter striations were sometimes discernible at the M-band level, compatibly with an interaction with C-terminal titin (I: Fig. 4). The M-band staining was most prominent at fibre periphery, whereas the major doublet bands were of similar intensity throughout the fibre. In non-stretched muscle samples fixed as sections, the M-band localization was not detectable, which could be due to lower resolution of sarcomeric regions or poor preservation of the structure in the sample preparation procedure.

In situ proximity ligation assays (PLA) on mouse muscle sections were employed as a complementary method for studying the colocalization of myospryn and M-band titin. This technique, based on oligonucleotide-conjugated antibodies, visualizes the spatial proximity of two primary antibodies *in situ* as fluorescent dots. In wild-type muscles, positive PLA signals demonstrated the proximity of the antibody binding sites in C-terminal titin (antibodies T51 and T41) and myospryn (Des122), consistent with an interaction between the two proteins (I: Fig. 5). The predominant localization of PLA signals at the fibre periphery was in line with the localization of myospryn in IF microscopy.

The subcellular localization of myospryn observed in our studies is consistent with the staining pattern previously seen in skeletal muscle with the same antibody (Matthew Benson and Derek Blake, personal communication). The published reports on myospryn localization, however, rely on three different antibodies, and the results are partly inconsistent (Benson *et al.* 2004, Durham *et al.* 2006, Kouloumenta *et al.* 2007, Reynolds *et al.* 2007).

With the antibody Des122, also utilized in this study, Benson *et al.* (2004) showed myospryn in transverse rat skeletal muscle sections mostly at the myofibre periphery, with weaker staining inside the fibre. While this is in line with the

localization reported by Durham *et al.* (2006) on transverse mouse muscle sections, the patterns obtained with the same antibodies on the longitudinal sections are different: The major cross-striations detected with Des122 flank the Z-disc as doublet bands in skeletal muscle and coincide with the Z-disc in cardiac muscle, thus reflecting the position of T-tubules and terminal cisternae of SR in these tissues (this study and Matthew Benson and Derek Blake, personal communication). The antibody utilized by the Naya group was, on the other hand, reported to produce cross-striations overlapping the Z-discs in both cardiac and skeletal muscle, suggesting a lozalization in the costameric Z-disc domains (Durham *et al.* 2006, Reynolds *et al.* 2007). Costameric localization was also favoured by Kouloumenta *et al.* (2007), who reported Z-disc-overlapping cross-striations present exclusively at the subsarcolemmal level in cardiac muscle, as well as prominent staining of intercalated discs and perinuclear regions. The subcellular localization of myospryn is hence not established, and elucidating the genuine localization would require validation and cross-comparison of the antibodies, ideally on knockout animal tissues.

5.1.4.2 Localization of myospryn in neonatal rat cardiomyocytes (I)

To study the M-band localization of myospryn with an independent method, IF microscopy of endogenous and transfected myospryn was performed in cultured neonatal rat cardiomyocytes (NRCs) (I: Fig. 6). Staining with the Des122 antibody revealed endogenous myospryn in a granular or reticular pattern, and—in cell regions with best-organized sarcomeres—cross-striations overlapping the Z-discs. Less frequently, another set of striations of lower intensity was seen at the M-band level.

Localization of GFP- or Myc-tagged myospryn constructs (human CMYA5$^{3811–CT}$ and mouse MD9) in NRCs was investigated 1–5 d post-transfection. CMYA5$^{3811–CT}$ constructs typically showed strong targeting to Z-discs, stress-fibre-like structures, and intercalated discs. The localization of MD9 was reminiscent of the endogenous protein—a granular–reticular pattern, with cross-striations sometimes present at both Z-disc and M-band levels. Partial localization of both endogenous and transfected myospryn at the M-band level in cardiomyocytes paralleled the findings in skeletal muscle, and was consistent with an interaction with C-terminal titin.

Transfections of HA-tagged titin is6–M10 is7^{+}, alone or together with myospryn constructs, were performed for investigating whether C-terminal titin and myospryn could affect the localization of each other. The titin construct exhibited cytotoxicity in a subset of cells, but in surviving cells it typically showed a diffuse localization without a dramatic effect on the localization of endogenous or transfected myospryn. Interestingly, in cotransfections with CMYA5$^{3811–CT}$, the titin construct gave an impression of increased association with the Z-discs, suggesting that the myospryn construct could modulate its localization. This phenomenon could not, however, be analyzed statistically due to the low number of double-transfected cells.

5.1.4.3 Localization of myospryn is not disrupted by FINmaj (I, unpublished)

To investigate the effect of the FINmaj titin mutation on myospryn localization, IF studies were performed on muscle samples from a LGMD2J patient and the TMD/LGMD2J mouse model (FINmaj KI). In LGMD2J muscle, the major doublet bands seemed normal, but the status of the M-band striation could not be determined on the non-stretched standard biopsy material (I). In stretched and immersion-fixed muscle samples of both heterozygous and homozygous FINmaj KI mice, myospryn localization was indistinguishable from wild-type controls, including a clear striation at the M-band level (Fig. 10; unpublished data)

While the IF results indicated a preserved M-band localization of myospryn in FINmaj KI muscles, a submicroscopic effect on the colocalization of myospryn and titin was not excluded. To investigate this possibility, *in situ* PLA studies were performed with the myospryn antibody Des122 in combination the titin antibody T41, whose epitope in M-is4 is outside the region disrupted in TMD/LGMD2J (Anna Vihola, personal communication). PLA showed similar signals in the muscles of control and FINmaj KI mice (Fig. 10; unpublished data), indicating that the physical proximity of myospryn with the remaining part of C-terminal titin is not dramatically affected by the mutation.

As the titin domains M9–is7–M10, constituting the entire myospryn-binding region defined in our CoIP experiments, are likely absent in homozygote FINmaj KI muscle (Charton *et al.* 2010), the apparently normal myospryn localization suggests that the interaction with titin is not required for targeting of myospryn to the M-band level.

5.1.5 Reported interactions and functions of myospryn

The C-terminal part of myospryn, identified in this study to contain the binding sites for titin and CAPN3, has been previously reported to interact with several other proteins. The reported interactions with α-actinin (Durham *et al.* 2006), desmin (Kouloumenta *et al.* 2007) and dystrophin (Reynolds *et al.* 2008) connect myospryn with cytoskeletal components, whereas the interactions with dysbindin (Benson *et al.* 2004), protein kinase A (Reynolds *et al.* 2007), and calcineurin (Kielbasa *et al.* 2011) relate to the functions of myospryn in membrane trafficking and cellular signalling.

5.1.5.1 Interactions of myospryn with cytoskeletal proteins

Binding of myospryn to α-actinin 2, postulated based on their co-localization in the costameric Z-disc domain, has been demonstrated with CoIP studies of transfected proteins. α-actinin binding was reported for several constructs covering various regions within the C-terminal half of mouse myospryn (Durham *et al.* 2006). This complex interaction has not been confirmed with other methods, nor is its functional significance known.

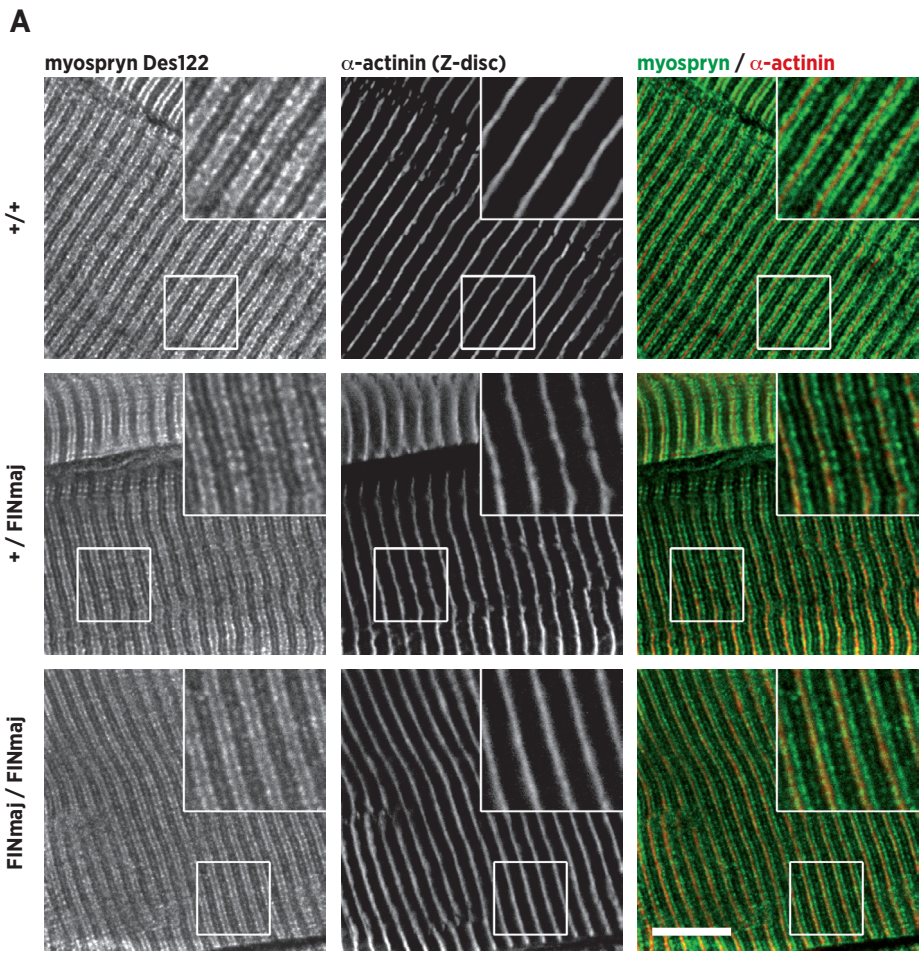

Figure 10. Myospryn in muscles of control and FINmaj knock-in mice

A–B Confocal microscopy of myospryn (antibody Des122), with α-actinin as a Z-disc marker (A) or the titin M9 domain (antibody T51) as an M-band marker (B) in muscles of wild-type (+ / +), and FINmaj knock-in mice heterozygous (+ / FINmaj) or homozygous (FINmaj / FINmaj) for the titin mutation. The faint myospryn signal at the M-band level was not visibly affected by in the FINmaj KI muscles, while negative T51 staining confirmed the absence of C-terminal titin in the homozygous mutant mice. The images show a single optical section. Scale bars, 10 μm. Insets show twofold magnifications of the boxed regions.

C *In situ* proximity ligation assay (PLA) with antibodies against myospryn (Des122) and titin M-is4 (T41) in muscles of wild-type and homozygous FINmaj KI mice. The combination of the two antibodies (Des122 / T41) produced numerous punctate PLA signals indicating spatial proximity of their binding sites, with no difference between wild-type and FINmaj KI. The negative control reaction with the myospryn antibody alone (Des122 / –) produced few background spots on wild-type mouse muscle. The images show maximum-intensity projections through z-stacks of 15 optical sections. Scale bar, 10 μm.

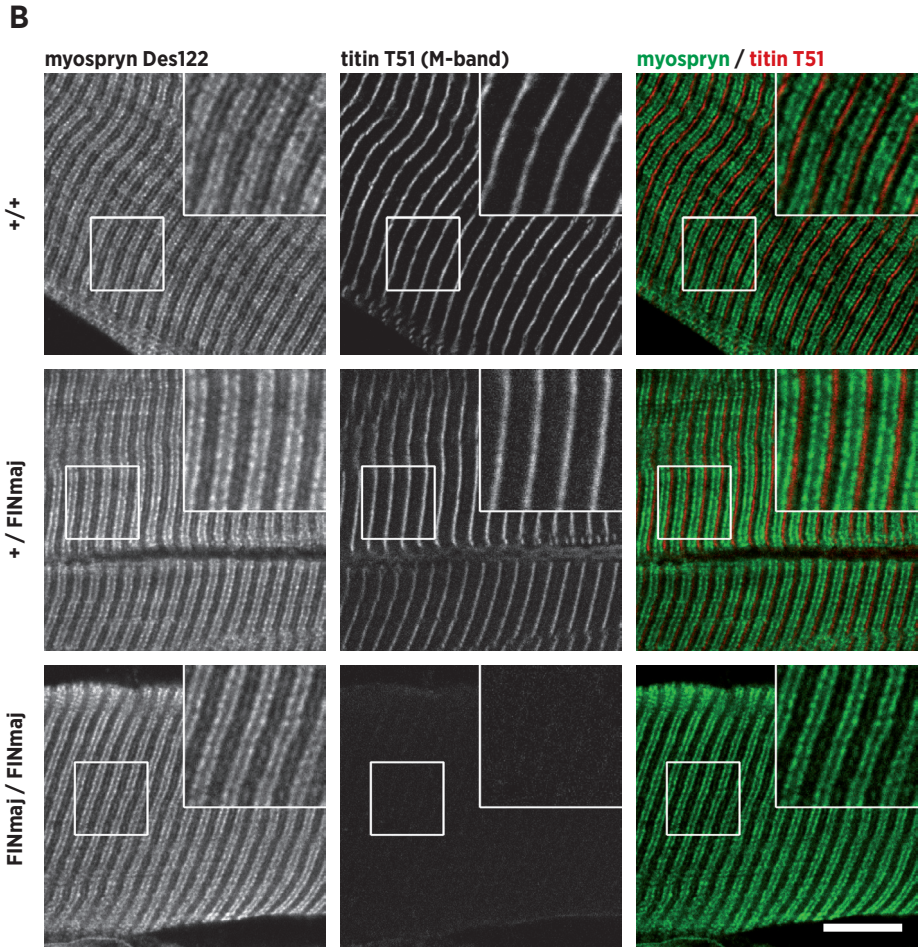
B
myospryn Des122
titin T51 (M-band)
myospryn / titin T51
+/+
+ / FINmaj
FINmaj / FINmaj
C
PLA: myospryn Des122 / –
PLA: myospryn Des122 / titin T41
+ / +
+ / +
FINmaj / FINmaj

Binding of myospryn to the N-terminal domain of desmin has been identified in a Y2H screen for desmin ligands, and defined with deletion constructs to involve the extreme C-terminal 24 amino acids of myospryn (Kouloumenta *et al.* 2007). In support of this interaction, desmin antibodies were shown to coimmunoprecipitate myospryn from heart homogenates. In desmin-deficient cardiomyocytes, myospryn was reported to lose its enrichment in the perinuclear region and to adopt a diffuse cytoplasmic localization, while localization to costameres and intercalated discs was not disrupted (Kouloumenta *et al.* 2007).

Interaction of myospryn and dystrophin has been identified by CoIP of endogenous proteins from a skeletal muscle extract and shown by pulldown experiments to involve two separate regions in C-terminal myospryn and the C-terminal part of dystrophin (Reynolds *et al.* 2008). Of the reported interactions of myospryn with cytoskeletal proteins, the one with dystrophin is supported by the most convincing *in vivo* evidence: In dystrophin-deficient *mdx* mice, proteolytic degradation of myospryn and its selective mislocalization from the subsarcolemmal region suggested that the interaction with dystrophin is responsible for the costameric localization of myospryn (Reynolds *et al.* 2008). The *mdx* mice also showed downstream changes in protein kinase A signalling, in line with the disturbed signalling functions of myospryn, discussed below.

5.1.5.2 Myospryn as a signalling scaffold

By interacting with protein kinase A (PKA) and calcineurin (protein phosphatase 2B, PP2B), myospryn regulates the activity of these signalling molecules in muscle (Reynolds *et al.* 2007, Kielbasa *et al.* 2011). Regulation of PKA is mediated by interaction of the PKA regulatory subunit RIIα with myospryn through three amphipathic helices located in the TRIM-like region (Reynolds *et al.* 2007). Functional relevance of myospryn as an A-kinase anchoring protein (AKAP) is demonstrated in muscles of the dystrophin-deficient *mdx* mice, where both myospryn and PKA RII are mislocalized, PKA activity is reduced although its expression level is normal, and several target genes of the PKA–CREB pathway are dysregulated (Reynolds *et al.* 2008).

The TRIM-like region of myospryn contains also three binding regions for calcineurin (Kielbasa *et al.* 2011). This calcium-activated protein phosphatase activates NFATc and MEF2 (myocyte enhancer factor 2) pathways, playing important roles for example in muscle regeneration, hypertrophy and fibre type determination (Sakuma & Yamaguchi 2010). Binding to myospryn inhibits calcineurin activity both *in vitro* and *in vivo*: Myospryn represses the calcineurin-mediated expression of NFATc reporter construct in cell cultures, and overexpression of the myospryn TRIM-like region in mouse muscles reverses the fast-to-slow fibre type switch caused by constitutively actively calcineurin, as well as attenuates muscle regeneration after cardiotoxin injection (Kielbasa *et al.* 2011).

Importance of highly controlled myospryn-based signalling is highlighted by the fact that myospryn itself is regulated by the same pathways, suggesting the existence of feedback loops. Myospryn is a transcriptional target of MEF2A (Durham *et al.* 2006) and PKA–CREB pathways (Reynolds *et al.* 2008). Its expression is downregulated in *mdx* mice, where PKA activity is reduced (Reynolds *et al.* 2008), as well as in DMD patients (Tkatchenko *et al.* 2001). The N-terminal part of myospryn is also directly phosphorylated by PKA (Reynolds *et al.* 2007), but the importance of this modification is currently unknown.

5.1.5.3 Myospryn and the BLOC-1 complex in vesicle trafficking

Myospryn is linked to vesicle trafficking by its interaction with dysbindin (DTNBP1), a subunit of the BLOC-1 (biogenesis of lysosome-related organelles) complex (Benson *et al.* 2004). This hetero-octameric complex cooperates in membrane trafficking and cargo sorting with the clathrin adaptor protein (AP) complexes and actin cytoskeleton regulators, but its exact molecular function is unclear (Falcon-Perez *et al.* 2002, Setty *et al.* 2007, Sitaram *et al.* 2012, Ryder *et al.* 2013). BLOC-1 is best known for its essential role in the sorting of selected cargo proteins from early endosomes to lysosome-related organelles (LROs)—specialized vesicular organelles that share some lysosomal features but also contain proteins needed for various cell-type-specific functions (Setty *et al.* 2007, Huizing *et al.* 2008). Other demonstrated or inferred functions of BLOC-1 include sorting and transport of cargo from endosomes to ordinary lysosomes, the Golgi apparatus, and synaptic vesicles, and participation in neurite outgrowth (Ghiani *et al.* 2010, Marley & von Zastrow 2010, Larimore *et al.* 2011, Gokhale *et al.* 2012). An apparently unrelated role in redox homeostasis was recently suggested by its interaction with peroxiredoxins and altered redox state in BLOC-1-deficient cells (Gokhale *et al.* 2012). Based on numerous identified protein interactions, dysbindin has been suggested to have additional functions *e.g.* in transcriptional regulation (reviewed by Ghiani & Dell'Angelica 2011, Mullin *et al.* 2011), but the physiological relevance of interactions and functions not validated in the context of BLOC-1 is questionable (Ghiani & Dell'Angelica 2011).

Mutations in dysbindin and other BLOC-1 subunits, leading to the secondary loss of the whole complex, cause the multisystem disorder Hermansky-Pudlak syndrome (HPS) in man and similar phenotypes in mice (Li *et al.* 2003, Morgan *et al.* 2006, Huizing *et al.* 2008, Cullinane *et al.* 2011). The symptoms are due to the defective biogenesis of the different LROs and include hypopigmentation, impaired blood clotting, and subtype-specific features such as pulmonary fibrosis and lipofuscin accumulation (reviewed by Huizing *et al.* 2008). The absence of overt symptoms in other cells and tissues, despite the ubiquitous expression of BLOC-1, suggests that while BLOC-1 is required for LRO biogenesis, its other functions are redundant (Dell'Angelica 2004). In muscle, specialized LROs are not known to exist. Skeletal muscle abnormalities have not been reported in HPS, and specific

efforts have failed to reveal any muscle involvement in the BLOC-1-deficient *sandy* and *pallid* mice (Li *et al.* 2003, Nazarian *et al.* 2006).

Dysbindin was initially characterized as a binding partner of dystrobrevins, cytoplasmic components of the DGC (Benson *et al.* 2001), but its dystrobrevin-binding region was later found to be occupied in interactions with other BLOC-1 components (Li *et al.* 2003, Nazarian *et al.* 2006). A stable association of dysbindin and BLOC-1 is also indicated by their practically complete co-fractionation in several tissues, and the secondary dysbindin deficiency caused by depletion of other BLOC-1 subunits (Li *et al.* 2003, Starcevic & Dell'Angelica 2004, Nazarian *et al.* 2006, Ghiani *et al.* 2010). The existence of a DGC-associated dysbindin pool is hence unlikely, and the interaction with dysbindin most probably links myospryn to BLOC-1. An association of myospryn and BLOC-1 is further supported by co-immunoprecipitation of the BLOC-1 subunits dysbindin and pallidin with desmin and myospryn from heart extract (Kouloumenta *et al.* 2007) and by the possible genetic association of *CMYA5* with schizophrenia—a condition to which dysbindin and other BLOC-1 subunits have been previously linked by genetic and functional evidence (Straub *et al.* 2002, Talbot *et al.* 2004, Morris *et al.* 2008, Chen *et al.* 2011, Li *et al.* 2011, Furukawa *et al.* 2013).

The role of BLOC-1 in muscle has not been characterized, but the absence of muscle symptoms in HPS and in BLOC-1-deficient mice (Li *et al.* 2003, Nazarian *et al.* 2006) indicates that the complex is not required for normal muscle function. The partial co-localization of myospryn with lysosomes in cultured cardiomyocytes, and the altered localization of both myospryn and lysosomes in desmin-deficient cells do, however, suggest a connection between myospryn and the endosomal–lysosomal system in muscle, possibly involving BLOC-1 (Kouloumenta *et al.* 2007).

5.1.6 Functional aspects of the novel interactions

5.1.6.1 Myospryn is a substrate and possible regulator of CAPN3

In order to assess the biological importance of the novel myospryn–CAPN3 interaction, cotransfection studies were performed in 911 cells. Coexpression of active YFP-CAPN3-CFP caused the disappearance of the full-length (115 kDa) form of the myospryn construct MD9 and the appearance of a ~40-kDa N-terminal fragment in western blot (I: Fig. 7). This identified myospryn as an *in vitro* proteolytic substrate for CAPN3, with the cleavage site situated approximately 70–80 kDa from myospryn C-terminus (40–140 amino acid residues N-terminally from the BBox' domain). In contrast, the shorter MD7 construct (80 kDa) was not cleaved by CAPN3, which could indicate that the cleavage occurs just N-terminally to the MD7 region, or that the construct adopts a conformation not accessible to the protease.

Given the role of calpains as modulator proteases (Ono & Sorimachi 2012), proteolytic cleavage by CAPN3 could serve to regulate the localization or interactions of myospryn. However, the physiological significance of the CAPN3 substrates

identified *in vitro* is unclear (see 2.4.6.), and the ability of CAPN3 to proteolyze myospryn in a coexpression setup does not necessarily identify myospryn as a physiological substrate.

In addition to demonstrating the proteolytic cleavage of myospryn, cotransfections suggested that myospryn attenuates the autolytic activation of CAPN3, as the ratio of the full-length YFP-CAPN3-CFP construct to its 80-kDa autolytic fragment was increased in cells cotransfected with MD9 (I: Fig. 7). A simple explanation would be that binding to myospryn through the IS2 segment causes structural changes in CAPN3 directly affecting its autolysis—a conceivable assumption considering the known ability of IS2 to modulate the autolytic properties of CAPN3 (see 2.4.4.). This could either be a physiologically relevant phenomenon or a mere side effect of the coexpression.

The failure of the MD7 construct to attenuate the autolysis similarly to MD9, even though both myospryn constructs showed binding to CAPN3 in CoIP, could, however, favour a more complex mechanism, and imply that myospryn plays a specific role in regulation of CAPN3. This might, for example, involve phosphorylation or dephosphorylation events by PKA and calcineurin (see 5.1.5.2.). Phosphorylation of CAPN3 was suggested by Ermolova *et al.* (2011), but the phosphorylation site, the kinase(s) and phosphatase(s) regulating the modification, and its effect on CAPN3 activity are unknown.

It remains unknown whether both of the suggested functions of the CAPN3–myospryn interaction bear physiological significance. A dual role of myospryn as both a substrate and a regulator of CAPN3 could provide a feedback system for autoregulation of either myospryn or CAPN3 activity.

5.1.6.2 Conclusions on the titin–myospryn interaction

Functional studies for demonstrating the biological importance of the discovered titin–myospryn interaction were beyond the scope of this study. However, the presented results—binding of myospryn to M-band titin in Y2H and CoIP assays, the localization of myospryn at the M-band level, and the physical proximity of the two proteins demonstrated by PLA—strongly support a genuine interaction with likely physiological relevance.

This study adds titin to the list of structural proteins interacting with myospryn. The identified titin-binding region overlaps with all of the previously described binding sites, and at least some of the interactions may be mutually exclusive. Interactions are also limited by the subcellular localizations of the proteins: myospryn can hardly interact with M-band titin and the Z-disc-associated proteins α-actinin and desmin at the same time. A simultaneous interaction of myospryn with titin and dystrophin could, on the other hand, be envisioned to take place at the costameric domains overlying the M-band (Porter *et al.* 1992). Indeed, the localization of myospryn at the M-band level and its interaction with titin seem to be restricted or enriched to the subsarcolemmal region (see 5.1.4.1.), suggesting a

connection between titin molecules in the peripheral myofibrils and myospryn in the costamere. The preserved localization of myospryn in the FINmaj KI mouse (this study) and its mislocalization in the *mdx* mouse (Reynolds *et al.* 2008) suggest that myospryn is targeted to the costameric M-band domains by its interaction with dystrophin—and in this case, the interaction of titin and myospryn is likely to be functional rather than structural.

A functional interaction between C-terminal titin and myospryn could be involved either in transmitting information from the titin filament system to the signalling pathways coordinated by myospryn, or in regulation of titin or other M-band components by these pathways. In line with these possibilities, both PKA RII (Reynolds *et al.* 2007) and calcineurin (Torgan & Daniels 2006) are partly localized at the M-band level.

With the current limited knowledge on the role of myospryn and BLOC-1 in membrane trafficking, a possible role of M-band titin in these functions cannot be excluded. However, vesicles of the endosomal–lysosomal system in muscle fibres are mostly found at the I-band, notably in association with the T-tubules (Kaisto *et al.* 1999), suggesting that, in terms of trafficking, the myospryn pool localized in this region might be more important than the M-band-associated pool.

5.1.6.3 Relationship of the novel interactions

The similar localization of myospryn and CAPN3 at the I-band and M-band regions (this study, Ojima *et al.* 2007) would allow the proteins to interact at either of these locations. However, since C-terminal titin, CAPN3, and myospryn can all interact with each other, the three proteins could conceivably form a ternary complex at the M-band. As triple CoIP experiments performed for addressing this possibility were inconclusive (unpublished results), the existence of a ternary titin–CAPN3–myospryn complex awaits confirmation. This could be achieved for example with crosslinking experiments.

5.1.7 Role of myospryn in muscular dystrophies

CoIP studies demonstrated that the binding of myospryn to titin is not directly prevented by the TMD/LGMD2J-causing FINmaj mutation, and IF microscopy indicated apparently normal targeting of myospryn to the M-band level in muscles of the FINmaj knock-in mouse. However, as FINmaj and other titinopathy mutations ultimately lead to the absence of the entire myospryn-binding region from mutant titin (Hackman *et al.* 2002, 2008, Charton *et al.* 2010), partial or total disruption of the functional titin–myospryn interaction is a likely consequence of the mutations.

The downstream effects of the disrupted titin–myospryn interaction cannot be directly studied before the biological function of the interaction is elucidated. As circumstantial evidence favours the possibility that titin participates in the signalling functions of myospryn (see 5.1.6.2), perturbed PKA and/or calcineurin signal-

ling could be a possible consequence of TMD/LGMD2J mutations. Interestingly, preferential disorganization of the costameric M-band domains (Williams & Bloch 1999), and myospryn mislocalization coupled with compromised PKA signalling (Reynolds *et al.* 2008) in *mdx* mice provide a tentative pathomechanistic link between dystrophinopathies and TMD/LGMD2J.

Although the functions of myospryn in membrane trafficking seem less likely to be important at the M-band, their impairment as a consequence of titin mutations could also potentially contribute to the pathogenesis of titinopathies. For example, the rimmed-vacuolar pathology in TMD might reflect a mild defect in autophagy caused by impaired trafficking.

As far as LGMD2A is concerned, loss of CAPN3 activity is predicted to have widespread downstream effects on the regulation of its proteolytic substrates. If myospryn is a physiological CAPN3 substrate, its processing is likely to be compromised in LGMD2A, which may for its part contribute to the pathogenesis. The importance of myospryn relative to other substrates in this respect cannot be assessed until more is known about the physiological substrates and the effects of CAPN3-mediated cleavage on their functions.

5.2 LGMD1D

Identification of the first LGMD1D-causing *DNAJB6* mutations by our group (II: Table 1, Suppl. Fig. 2) necessitated functional studies for evaluating the pathogenicity of the novel changes and allowed, for the first time, the investigation of the pathways underlying the disease on the molecular level.

5.2.1 Localization of DNAJB6 to the Z-disc and protein aggregates (II)

The subcellular localization of DNAJB6 in muscle had not been reported previously. To characterize DNAJB6 localization in normal muscle and to investigate the pathological changes in LGMD1D, muscle biopsies were studied by IF microscopy. Control muscles showed DNAJB6 predominantly in the Z-discs (II: Fig. 1). This localization was not altered in the regions of LGMD1D muscle having preserved sarcomere structure, but DNAJB6 was also often found in intracellular protein accumulations of variable size and shape. Other proteins detected in the accumulations by IF stainings included binding partners of DNAJB6 (HSPA8 and MLF1), typical components of protein aggregates in myofibrillar myopathies (desmin, filamin, myotilin, and αB-crystallin), and a reported client protein of DNAJB6 (KRT18) (II: Fig. 1, Suppl. Fig. 4). These results were in line with previous findings on light microscopic level (Sandell *et al.* 2010) and IF studies later published by others (Harms *et al.* 2012, Sato *et al.* 2013). Double stainings indicated that the accumulations varied in composition, as all did not stain positive for the same proteins. DNAJB6 was typically detected in the periphery of these structures, colocalizing only partially with the other accumulation components. This was

in contrast to a primary myotilinopathy sample, studied for comparison, where DNAJB6 and myotilin appeared more perfectly colocalized throughout the accumulations (II: Suppl. Fig. 4).

Transmission electron microscopy of LGMD1D muscle revealed regions of disorganized myofibrillar structure, with an increase and dispersion of electron-dense Z-disc material likely corresponding to the accumulations seen in IF microscopy. EM also showed vacuolar changes indicating autophagic pathology, in agreement with regions of LC3 accumulation and rimmed vacuoles seen in immunohistochemistry and light microscopy (II: Fig. 1, Suppl. Fig. 3).

5.2.2 Pathogenicity of DNAJB6 knockdown and mutations in zebrafish (II)

To understand the mode of action of LGMD1D-causing mutations, *in vivo* studies were carried out in zebrafish, an inexpensive model organism well suited for rapid functional screening of mutations.

First, the importance of DNAJB6 in muscle was studied by knocking down the expression of *dnajb6b*, the zebrafish orthologue of the co-chaperone, with splice-blocking morpholino oligonucleotides. Knockdown of *dnajb6b* produced a muscle defect, with ~30% of injected morphant embryos showing detachment of myofibres from vertical myosepta (II: Fig. 2), indicating that *dnajb6b* is required for muscle integrity in developing zebrafish. Specificity of the phenotype was demonstrated by efficient rescue by co-injection of wild-type human DNAJB6b mRNA.

The effects of LGMD1D mutations were then explored by ectopic expression of wild-type and mutant human DNAJB6 in fish embryos. Injection of mRNAs encoding wild-type DNAJB6a or DNAJB6b in the embryos, even at high doses, did not cause any observable muscle phenotype. In contrast, F89I and F93L mutant forms of DNAJB6b led to a muscle defect similar to that seen in *dnajb6b* morphants, consistent with their dominant pathogenic effect in humans (II: Fig. 3). The phenotype was reproduced by DNAJB6b F93A and F93G, suggesting that the loss of phenylalanine residue, rather than the gain of leucine, is the critical pathogenic change. The F89G change in human DNAJB6b, on the other hand, did not cause a phenotype, possibly reflecting the fact that the zebrafish protein has a glycine residue at this position. No muscle defects were observed in embryos expressing the different mutations in DNAJB6a, indicating that the pathogenicity is mediated by the DNAJB6b isoform.

Interestingly, equimolar co-injection of wild-type DNAJB6b with either of the LGMD1D mutant proteins accentuated the muscle defect caused by the mutations, as indicated by a higher proportion of severely affected embryos (II: Fig. 3). This phenomenon was further studied by co-injections of wild-type and F93L DNAJB6b at various ratios. The severity of the muscle defect increased with higher amounts of mutant mRNA, whereas higher amounts of wild-type mRNA rescued the phenotype (II: Suppl. Fig. 5).

5.2.3 Characterization of mutant DNAJB6 in cell cultures (II)

Transfection studies of V5-tagged and untagged DNAJB6 constructs on different cell lines were performed in order to identify differences in the properties of wild-type and mutant DNAJB6. Subcellular localization of the constructs was investigated by IF microscopy, and expression and solubility analyzed by western blotting. This basic characterization did not reveal any obvious differences between the wild-type and mutant proteins. In some experiments, however, mutant DNAJB6b constructs showed increased steady-state levels compared to wild-type.

5.2.3.1 Oligomerization of DNAJB6 is not affected by LGMD1D mutations

Oligomerization of DNAJB6 was suggested by its similarity to DNAJB8, previously shown to from polydisperse complexes (Hageman *et al.* 2010), and interfering with the oligomer formation was thus a potential mechanism for the dominant negative effect of disease mutations. This possibility was tested in CoIP experiments, where V5-tagged and untagged DNAJB6b were coexpressed in COS-1 cells as different combinations of wild-type and F93L mutant, and immunoprecipitated with V5 antibody beads (II: Suppl. Fig. 6). Untagged DNAJB6b was coimmunoprecipitated with the tagged construct, indicating that DNAJB6b is capable of self-association as proposed. However, presence of the F93L mutation in either one or both constructs did not have any effect on coimmunoprecipitation efficiency. Oligomerization was also studied by sucrose density gradient centrifugation of proteins expressed in COS-1 cells, a setup previously used by Hageman and colleagues (2010) for DNAJB8. Similar fractionation of wild-type and F93L DNAJB6b-V5 indicated that, in line with the CoIP results, the size distribution of DNAJB6 oligomers was not affected by the mutation (II: Suppl. Fig. 6). These results indicated that the dominant negative effect of the LGMD1D mutations is not due to altered oligomerization properties.

5.2.3.2 Mutant DNAJB6 reduces the turnover of the entire complex

The higher levels of mutant DNAJB6 constructs seen in some transfection experiments suggested that the mutations might affect the turnover of DNAJB6. This idea was supported by chase assays, where levels of DNAJB6 constructs in 293FT cells were followed while synthesis of new proteins was inhibited with cycloheximide (CHX). F89I and F93L mutant DNAJB6b constructs showed significantly slower turnover than the wild-type construct in CHX-treated cells (II: Fig. 3, Suppl. Fig. 7). The F93L mutation also decreased the turnover rate of DNAJB6a; the effect of F89I on this isoform was not determined.

Interestingly, in cotransfections of GFP- and HA-tagged wild-type and F93L mutant DNAJB6b, both constructs showed decreased turnover compared to single transfections. The effect was similar regardless of the construct carrying the mutation (II: Fig. 3, Suppl. Fig. 7). This finding, consistent with the dominant nega-

tive effect of the mutation, suggested that incorporation of mutant DNAJB6 to the oligomeric complex can affect the turnover of the whole complex.

Inhibitors of the major protein turnover pathways were used for investigating which pathway is responsible for the degradation of DNAJB6. Bafilomycin A1, an inhibitor of lysosomal acidification, efficiently blocked DNAJB6 turnover in CHX-treated cells, indicating the DNAJB6 is turned over by the autophagic-lysosomal pathway. The proteasome inhibitor lactacystin did not increase the DNAJB6 level in CHX-treated cells, but rather decreased it compared to CHX alone, possibly due to autophagic activation following proteasome inhibition (II: Suppl. Fig. 7).

5.2.3.3 Mutations impair the anti-aggregation effect of DNAJB6

The aggregate pathology in LGMD1D suggested that the disease mutations might interfere with the ability of DNAJB6 to suppress protein aggregation, demonstrated in several studies (Chuang *et al.* 2002, Hageman *et al.* 2010, Hageman *et al.* 2011, Rose *et al.* 2011). This possibility was investigated by filter trap assays (FTA) using polyQ-containing huntingtin as an aggregation-prone client protein—a method previously utilized for studying the anti-aggregation activities of DNAJB6 and other proteins (Hageman *et al.* 2010). The different DNAJB6 constructs were co-expressed with GFP-tagged polyQ-huntingtin in T-REx 293 cells, and amounts of soluble and aggregated huntingtin determined from cell extracts by western blotting and filter trap. To minimize the effects of transfection efficiency on the results, a novel robust measure of anti-aggregation activity, termed aggregation score, was established. This was based on a pairwise comparison of the aggregated-to-soluble ratios between induced and uninduced wells from duplicate transfections.

Compared to wild-type DNAJB6b, both F89I and F93L mutant proteins showed significantly impaired anti-aggregation activity, indicated by higher aggregation scores (Fig. 11). This was reflected by both an increase in aggregated huntingtin and a decrease in soluble huntingtin compared to coexpression with wild-type DNAJB6b (II: Suppl. Fig. 8). Both mutants still retained activity, as they performed better than the nuclear DNAJB6a isoform used as a negative control. The impaired anti-aggregation effect did not depend on lower expression of the mutant proteins; on the contrary they showed somewhat higher steady-state levels than the wild-type construct (II: Suppl. Fig. 8).

5.2.4 Association of DNAJB6 with the CASA pathway (II)

Chaperone-assisted selective autophagy (CASA) was recently described as important for sarcomere maintenance (Arndt *et al.* 2010). This autophagic pathway is mediated by HSPA8 together with the co-chaperone BAG3 (BCL2-associated athanogene 3), the small heat shock protein HSPB8, and the E3 ubiquitin ligase STUB1 (STIP1 homology and U-box containing protein; also known as CHIP, C-terminus of Hsc70-interacting protein) (Arndt *et al.* 2010). The only hitherto established clients for CASA are filamins (Arndt *et al.* 2010, Ulbricht *et al.* 2013). In striated

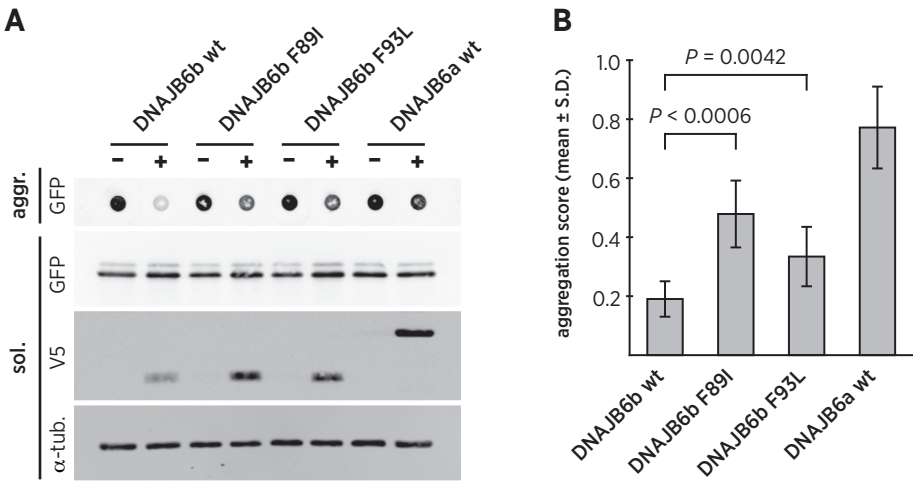

Figure 11. Impaired anti-aggregation activity of mutant DNAJB6

The anti-aggregation activity of DNAJB6 on GFP-tagged polyQ-huntingtin protein was studied in a filter trap assay.

A Filter trap assay. T-REx 293 cells were cotransfected with GFP-tagged huntingtin and V5-tagged DNAJB6 constructs, and DNAJB6 expression was induced (+) or left uninduced (–). Aggregated (aggr.) and soluble (sol.) huntingtin in cell extracts were analyzed on a filter trap membrane and on western blot, respectively. Expression of DNAJB6 constructs (V5) and equal protein loading (α-tubulin) were controlled on western blot.

B Aggregation scores. Aggregated and soluble huntingtin in induced and uninduced cells were quantified from filter traps and western blots, and aggregation scores were calculated as described in Materials and methods. Both mutant DNAJB6b constructs (F89I and F93L) were less efficient in preventing huntingtin aggregation than wild-type (wt) DNAJB6b, as indicated by higher aggregation scores. The nuclear DNAJB6a isoform, ineffective towards the cytoplasmic huntingtin construct, was used as negative control. For each construct, $n = 12$. Statistical significance was tested using the Mann–Whitney *U* test with the Bonferroni correction.

muscle, the predominant member of this protein family is filamin C (FLNC, filamin 2) that links the Z-discs to each other and to the sarcolemma (Arndt *et al.* 2010).

Filamins undergo conformational changes, including reversible unfolding, upon mechanical tension; this has been suggested to expose them to mechanically induced damage, necessitating efficient protein turnover (Arndt *et al.* 2010). The CASA proteins HSPA8, BAG3, and HSPB8—binding cooperatively to a mechano-sensitive filamin region—sense the strain on the molecules and mediate their autophagic degradation (Arndt *et al.* 2010, Ulbricht *et al.* 2013). In mechanically stressed cells, BAG3 facilitates the release of damaged filamin from the cytoskeleton. Following polyubiquitination by STUB1, both filamin and BAG3 are engulfed in autophagosomes for degradation. This involves recruitment of phagophore membranes through the recognition of polyubiquitinated proteins by SQSTM1 and the interaction of BAG3 with synaptopodin 2 (Arndt *et al.* 2010, Ulbricht *et al.* 2013).

BAG3 seems to be the rate-limiting component regulating the activity of the CASA pathway. Induction of the transcription factor HSF1 (heat shock factor 1) by mechanical tension upregulates BAG3 expression and activates CASA (Arndt *et al.* 2010, Ulbricht *et al.* 2013). The importance of BAG3 for skeletal and cardiac muscles is highlighted by its high expression in these tissues (Homma *et al.* 2006) and by the effects of BAG3 depletion and mutations: BAG3 knockout mice develop a severe skeletal and cardiac myopathy characterized by Z-disc disruption, myofibrillar degeneration, and myonuclear apoptosis (Homma *et al.* 2006). The missense mutation P209L causes BAG3 myopathy—a severe dominant form of myofibrillar myopathy (MFM) (Selcen *et al.* 2009)—while several other BAG3 mutations have been reported in dilated cardiomyopathy (DCM) (Norton *et al.* 2011, Villard *et al.* 2011, Arimura *et al.* 2011).

5.2.4.1 DNAJB6 physically interacts with the CASA proteins

An connection of DNAJB6 with the CASA pathway was suggested by the known interaction of DNAJB6 with HSPA8, the colocalization of DNAJB6 and the CASA complex at the Z-disc, as well as the myofibrillar pathology of LGMD1D, indicating defective Z-disc maintenance and sharing pathological features with the BAG3 myopathy.

To test the hypothesis that DNAJB6 and CASA could be linked, CoIP studies were carried out using V5-tagged DNAJB6b constructs overexpressed in COS-1 cells (Fig. 12; III: Suppl. Fig. 9). DNAJB6b-V5 constructs, immunoprecipitated with anti-V5 beads, efficiently pulled down endogenous BAG3, and chemical crosslinking of proteins in cell lysates prior to immunoprecipitation also allowed detection of endogenous HSPB8 in the immunoprecipitates. Furthermore, when BAG3 and Myc-tagged STUB1 were coexpressed with DNAJB6b-V5, both of them could be immunoprecipitated with it. The CASA proteins were not pulled down by anti-V5 beads from cells expressing negative-control bait constructs (a V5-tagged titin is6–M9 construct or an untagged DNAJB6b construct), indicating that the results were not due to unspecific binding of CASA components to irrelevant proteins or the antibody beads. Hence, CoIP supported the postulated association of DNAJB6 and the CASA pathway. The tested F93L mutation did not affect coimmunoprecipitation of CASA proteins with DNAJB6, indicating that the pathomechanism is not likely to involve disrupted interaction with the CASA complex.

Interaction of DNAJB6 and the CASA components gained further support from *in situ* proximity ligation assays on rat muscle. In combination with a DNAJB6 antibody, antibodies against BAG3, HSPB8, and STUB1 showed similar levels of PLA signals as the known DNAJB6 partner HSPA8 (III: Fig. 5).

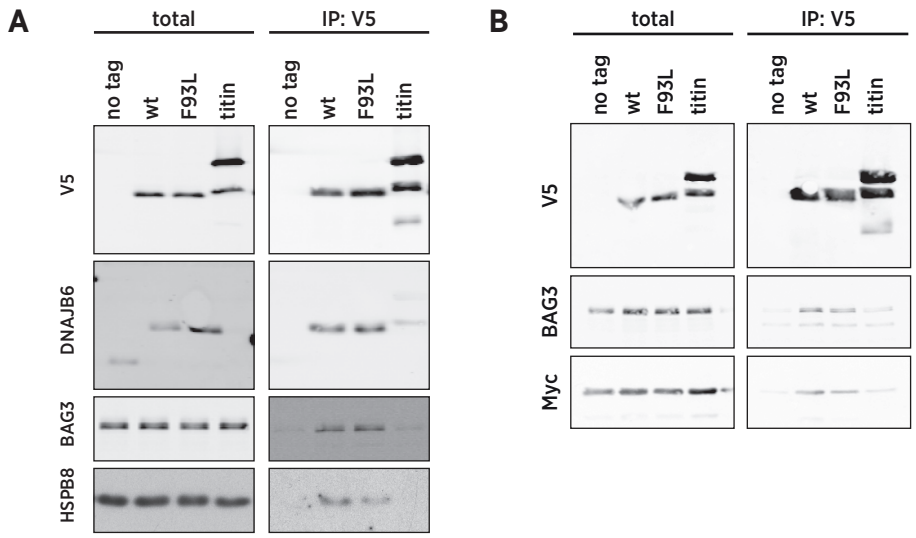

Figure 12. Coimmunoprecipitation of DNAJB6 and the CASA proteins

Wild-type (wt) or F93L mutant DNAJB6b-V5 constructs, or negative control constructs (DNAJB6b with no tag, or titin is6–M9-V5) were expressed in COS-1 cells and immunoprecipitated with V5 antibody beads. Samples taken from cell extracts before immunoprecipitation (total), and proteins bound to the antibody beads (IP) were analyzed by western blotting.

A Proteins in cell extracts were crosslinked prior to CoIP, and endogenous BAG3 and HSPB8 were analyzed from the samples.

B BAG3 and Myc-STUB1 constructs were cotransfected with the different bait proteins, and CoIP was performed without crosslinking.

The CASA proteins BAG3 (A, B), HSPB8 (A), and STUB1 (B) were pulled down with the DNAJB6b-V5 constructs, with no difference between wild-type and F93L.

Adapted from Sarparanta *et al.* Mutations affecting the cytoplasmic functions of the co-chaperone DNAJB6 cause limb-girdle muscular dystrophy. *Nature Genetics*, 2012; 44: 450–455. © 2012 Nature America, Inc.

5.2.4.2 Functional interaction of DNAJB6 and BAG3 demonstrated in zebrafish

A possible functional interaction of DNAJB6 and CASA was investigated by expressing BAG3 and DNAJB6b in zebrafish embryos (III: Fig. 5). While injection of wild-type BAG3 mRNA alone into the embryos had no adverse effects on fish muscles, its co-injection aggravated the pathogenic effect of DNAJB6b F93L, as demonstrated by an increase in the proportion of severely affected embryos. In contrast, the P209L mutant form of BAG3, alone showing a toxic effect comparable to mutant DNAJB6b, did not show an additive effect with DNAJB6b F93L. These findings not only provided evidence for a functional connection between DNAJB6 and BAG3, but also suggested that the BAG3 has plays an active role in the pathogenesis of LGMD1D.

Notably, the different *in vitro* effects of BAG3 mutations causing MFM and DCM have suggested that the diseases are caused by distinct molecular pathways (Arimura *et al.* 2011). When expressed in cultured cardiomyocytes, BAG3 constructs with DCM-associated mutations (R218W or L462P) inhibit Z-disc assembly, show abnormal nuclear localization, and cause increased apoptosis upon

serum starvation, whereas such effects are not seen with the MFM-causing P209L mutation (Arimura *et al.* 2011). The P209L mutant form of BAG3 is, on the other hand, unable to stimulate filamin degradation in smooth muscle cells (Arndt *et al.* 2010). The P209L mutation overlaps with one of the two Ile-Pro-Val motifs that mediate the interaction of BAG3 with HSPB8, and it has been suggested to interfere with HSPB8 binding (Fuchs *et al.* 2010). The faster migration of BAG3 P209L in native PAGE analysis is also consistent with an absent protein interaction (Selcen *et al.* 2009). Together these findings suggest that while other functions of BAG3 are affected by DCM mutations, the MFM-causing P209L mutation specifically interferes with the CASA pathway, possibly by disrupting HSPB8 binding. By extension, the failure of BAG3 P209L to accentuate the toxic effect of mutant DNAJB6 in zebrafish implicates the CASA pathway also in the pathomechanism of LGMD1D.

While the results obtained in this study indicate an association of DNAJB6 with the CASA proteins, they provide little insight into its functional importance in the pathway. Further studies are hence needed for determining the role of DNAJB6 in CASA. The simplest view, consistent with the published functions of DNAJB6b in preventing protein aggregation and promoting their degradation in an HSPA-dependent manner, would be that DNAJB6 recognizes client proteins and presents them to the CASA machinery. However, other modes of action are also possible.

Although the functional link to the CASA pathway is underlined by the effect of the BAG3 P209L mutation, discussed above, the association of DNAJB6 with the CASA proteins could also reflect its participation in other functions of HSPA8, BAG3, STUB1, and HSPB8. In addition to filamin turnover through the HSPA8-dependent CASA pathway, BAG3 and HSPB8 can promote autophagic degradation of polyQ-huntingtin in an HSPA8-independent manner. The induction of autophagy, accompanied by translation suppression, results from stimulation of eIF2α phosphorylation by the BAG3–HSPB8 complex. The activity requires the PXXP domain of BAG3 and is partly mediated by the GCN2 kinase (general control nonderepressible 2), but the molecular mechanism is currently unknown (Carra *et al.* 2008, 2009). Of note, as eIF2α phosphorylation status was not addressed in the studies describing the CASA pathway (Arndt *et al.* 2010, Ulbricht *et al.* 2013), it is possible that the autophagy stimulation by BAG3 in mechanically stressed cells is partly dependent on the same mechanism.

Another role of BAG3 in the Z-disc is to promote the interaction of HSPA8 with the actin-capping protein CapZ (Hishiya *et al.* 2010). This is required for the correct localization and stability of CapZ, and resistance of myofibrils to mechanical stress. BAG3-deficient cells subjected to mechanical stress show myofibrillar disruption, and the protective effect conferred by CapZ overexpression suggests this effect of BAG3 depletion indeed depends on CapZ rather than filamin deficiency due to impaired CASA (Hishiya *et al.* 2010).

5.2.5 Conclusions on the pathomechanism of LGMD1D

Pathological findings in LGMD1D muscle—protein accumulations and rimmed-vacuolar autophagy—point to a defect in protein quality control and turnover. The impaired ability of mutant DNAJB6b to suppress protein aggregation could directly lead to accumulation of unfolded proteins. A simple loss-of-function mechanism is, however, not consistent with the dominant effect of the mutations. It remains thus unclear if the impaired anti-aggregation activity of mutant DNAJB6, demonstrated by the filter trap assays, has a causative role in the pathomechanism or if it simply reflects the otherwise altered properties of DNAJB6.

Observations of the zebrafish studies—the dominant effect of mutant DNAJB6b and its exacerbation by the wild-type protein—are compatible with a model where incorporation of mutant monomers to the oligomeric DNAJB6b complex renders a toxic function to the whole complex. In such a scenario, co-injection of wild-type protein with the mutant, although decreasing the proportion of mutant monomers, would increase the total amount of the toxic complex. Rescue of the phenotype with a further increase in the wild-type protein would imply that significant toxicity results only when the proportion of mutant monomers within the complex exceeds a certain threshold value. While attenuated autophagic turnover seems to be a property of the mutant DNAJB6 complex, it could be either the cause or a consequence of the toxicity. Of note, the mutated DNAJB6a isoform, while not causing toxicity in zebrafish, still exhibited slower turnover. Hence, impaired turnover alone cannot alone explain the toxic effect of DNAJB6b mutations.

The increased severity of the zebrafish muscle defect observed in co-injections of BAG3 and mutant DNAJB6b suggests that the toxic function of the mutant DNAJB6 complex is mediated by BAG3. As the P209L mutation, predicted to interfere with the binding of HSPB8 to BAG3 (Fuchs *et al.* 2010), prevents the additive effect, it is conceivable that recruitment of HSPB8 to the mutant DNAJB6 complex mediates the pathogenesis, either by conferring toxicity to the complex or due to sequestration of HSPB8. Such possibilities could be investigated *e.g.* by studying the combined effect of the DNAJB6 mutations and HSPB8 coexpression or knockdown in zebrafish.

5.3 Welander distal myopathy

The putative WDM-causing mutation was identified by our group in the prion-related domain (PRD) of the RNA-binding protein TIA1 (III: Fig. 2). While the genetic evidence linking the identified E384K change to the disease was convincing, functional studies were initiated to demonstrate that the mutation affects the behaviour of TIA1 and to explore the possible pathogenic mechanisms.

5.3.1 Biochemical characterization of wild-type and mutant TIA1 (III)

To identify any major effects of the E384K mutation on TIA1 behaviour, transfection studies of HA- or GFP-tagged TIA1 constructs were performed in HeLa cells. Cells transfected with wild-type or mutant TIA1a or TIA1b constructs were analyzed by western blotting of total cell extracts, or soluble and insoluble fractions. The wild-type and mutant constructs showed no obvious difference in solubility, and their steady-state levels were similar as judged by antibodies against the N-terminal tag moieties or central TIA1. However, the two commercial antibodies raised against the C-terminal part of TIA1 showed dramatically weaker detection of the mutant constructs. The mutant constructs also tended to show slightly increased mobility in SDS-PAGE, which—together with the difference in antibody detection—suggested a proteolytic cleavage or altered post-translational modification of mutant TIA1. The possibility of proteolytic cleavage was ruled out by analysis of double-tagged constructs, as the bands staining positive for both the N-terminal HA tag and the C-terminal V5 tag still showed a migration difference. Also HA-tagged constructs translated *in vitro* showed the difference in migration, arguing against but not excluding the possibility of protein modifications. The migration difference was thus judged as a likely direct effect of the amino acid change.

5.3.2 Characterization of TIA1 and TIAL1 antibodies (III)

The different recognition of wild-type and mutant constructs by the C-terminal TIA1 antibodies, as well as expected cross-reaction problems due to high similarity of TIA1 and TIAL1, necessitated thorough characterization of the commercial TIA1 and TIAL1 antibodies used in the studies.

The binding of the two C-terminal TIA1 antibodies (ab40693 and C-20) to wild-type and E384K TIA1 was investigated by double labelling of GFP-TIA1a constructs in western blotting. Based on the TIA1/GFP signal ratios, both antibodies labelled the mutant constructs with 25–30% efficiency compared to wild-type. Testing both antibodies on a peptide array confirmed that their epitopes overlapped the mutation site. Both showed weaker reaction with the mutation-containing synthetic peptides, indicating a direct effect of the mutation on antibody binding rather than a biologically relevant secondary change in the protein.

The specificity of the TIA1 and TIAL1 antibodies utilized in muscle WB studies was investigated by comparing their reactions with GFP-tagged TIA1a and TIAL1b constructs. The N-terminal TIA1 antibody G-3 showed similar reactivity towards both proteins, with GFP-normalized relative signals 100% for TIA1 and 112% for TIAL1. The C-terminal TIA1 antibody C-20 proved fairly TIA1-specific, with TIAL1 constructs showing only 4% signal compared to TIA1. Also the TIAL1 antibody C-18 showed high specificity, with the TIA1 constructs showing 6% signal compared to TIAL1.

5.3.3 Expression analysis of the TIA proteins in WDM muscle (III)

To investigate whether the expression levels or isoform ratio of the TIA proteins were altered in WDM muscle, TIA1 and TIAL1 were analyzed from WDM and control samples by western blotting (III: Fig. 3). Both utilized TIA1 antibodies (G-3 and C-20) detected a ~40-kDa band doublet representing the two TIA1 isoforms, as well as some presumably unspecific bands. In line with the impaired binding of C-20 to mutant TIA1, this antibody showed a slight reduction of the TIA1 doublet in WDM patients compared to control samples. The approximate 1:1 intensity ratio of the two doublet bands in both controls and patients indicated no major change in the isoform expression ratio.

With the G-3 antibody, comparison of TIA1b levels was precluded by cross-reaction with the co-migrating TIAL1 band. The TIA1a-specific upper bands did not show any consistent difference between control and WDM samples. The TIAL1 antibody G-18 detected a single strong band at ~40 kDa, again with no difference between WDM and control. As the two TIAL1 isoforms should migrate at different speeds (Beck *et al.* 1996), the detected band presumably represents TIAL1b, reported to predominate on the protein level in many tissues and cells (Beck *et al.* 1996, Li *et al.* 2002).

5.3.4 Microscopic analysis of TIA1 localization and pathology in WDM (III)

IF microscopy was used for studying the subcellular localization of TIA1 in normal and WDM-affected muscle, and for characterizing the pathological changes in WDM. In control muscles, TIA1 showed predominantly nuclear and weaker diffuse cytoplasmic localization. This appeared unchanged in most fibres of WDM sections, but some affected fibres showed an increase in cytoplasmic TIA1, with focal accumulations at the rimmed-vacuolar regions (III: Fig. 4). The stress granule components TARDBP and G3BP1 showed accumulation and partial colocalization with TIA1 in these regions, while eIF3 and HuR did not. Increased LC3b and SQSTM1 staining in the rimmed-vacuolar regions indicated ongoing autophagy and possibly reduced autophagic clearance, and ubiquitinated proteins were detected either at the rimmed vacuoles or throughout the affected fibres (III: Fig. 4). The results on TIA1, TARDBP, G3BP1, and SQSTM1 were later perfectly replicated in immunohistochemical studies by Klar *et al.* (2013).

5.3.5 RT-PCR analysis does not indicate major splicing changes in WDM (III)

The role of TIA1 as a splicing regulator, involving the interaction of U1-C with the PRD (Del Gatto-Konczak *et al.* 2000, Förch *et al.* 2000, 2002, Aznarez *et al.* 2008), suggested splicing defects as a possible pathomechanism for WDM. Splicing changes in WDM muscle were investigated by RT-PCR analysis of a few selected *TIA1* target exons. A well-characterized effect of TIA1 is inclusion of *FAS* exon 6, generating the active isoform of the pro-apoptotic receptor Fas (Förch *et al.* 2000, Izquierdo *et al.* 2005). Among the exons analyzed by Aznarez *et al.* (2008),

exon 13A of the procollagen lysine hydroxylase 2 (*PLOD2*) gene showed the highest (~10-fold) expression difference in response to TIA1 and TIAL1 depletion in HeLa cells, and the gene is also highly expressed in skeletal muscle (Valtavaara *et al.* 1997). Finally, TIA1 promotes the inclusion of stop-codon-containing exons 6A, 6B, and 11A in *TIAL1*, negatively regulating its expression levels (Le Guiner *et al.* 2001). Analysis of isoform ratios on agarose gels did not reveal consistent differences in the inclusion of these exons between control and WDM muscles.

Splicing of *TIA1* itself in muscle biopsies and cultured myoblasts was studied from RT-PCR products spanning different parts of the transcript. In addition, inclusion of non-productive alternative exons (Le Guiner *et al.* 2001) was analyzed with RT-PCR primers overlapping exon boundaries. Neither approach indicated splicing changes in WDM. Analysis of muscle cDNA revealed a novel non-productive *TIA1* splice variant, with the first 214 bases of intron 8 included between exons 8 and 9, but also this product was found in both control and WDM samples.

As this preliminary analysis of selected target exons did not reveal splicing differences, a general splicing defect was considered as an unlikely explanation for WDM pathogenesis, and splicing studies were not continued with more refined methodology. However, using quantitative real-time PCR, Klar and coworkers (2013) later detected in WDM muscle increased skipping of *SMN2* exon 7, another reported target exon of TIA1 (Singh *et al.* 2011), and proposed that perturbed splicing could contribute to the pathomechanism. It remains unclear whether the different outcomes of the two studies depend on the more accurate analysis method used by Klar *et al.*, or gene-specific differences in splicing. It is possible that a different quantification method would have allowed detection of splicing differences also in this study, but an effect as large as the threefold change reported for *SMN2* would have hardly escaped detection even with the currently utilized techniques. On the other hand, the *SMN2* result was based on a rather small dataset of two WDM patients and three controls, and the reported difference could reflect sample-to-sample variation rather than a disease-specific change.

5.3.6 Mutant TIA1 has altered stress-granule-forming properties (III)

Aggregation of the TIA1 PRD mediates the formation of stress granules (SGs) (Gilks *et al.* 2004), suggesting that the WDM mutation located in this domain could affect SG assembly or disassembly. The effects of the mutation on SG formation were studied in transfection experiments using constructs of both TIA1 isoforms N-terminally tagged with GFP, HA tag, or HaloTag. The experiments were performed in HeLa cells, a cell line used in several published SG studies.

In line with published findings (Gilks *et al.* 2004), overexpression of TIA1 constructs induced SG formation in some cells. Oxidative stress caused with sodium arsenite treatment increased the SG number, with nearly all transfected cells containing SGs. Visual inspection by IF microscopy did not reveal differences between wild-type and E384K constructs in the abundance, size, or localization of SGs

(III: Fig. 5). G3BP1, eIF3, and TIAL1 showed similar targeting to SGs containing wild-type and mutant TIA1 constructs. Localization of HuR and TARDBP to the SGs was more variable, but did not show any obvious difference between wild-type and mutant TIA1 SGs (III: Fig. 5, Suppl. Fig. 1).

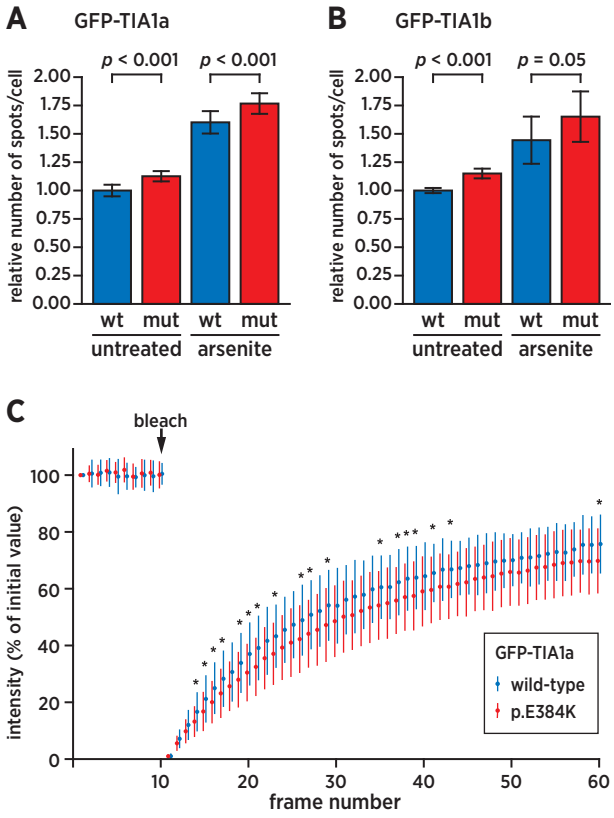

Figure 13. WDM mutation alters stress granule formation and dynamics of TIA1

A–B Quantification of stress granules from HeLa cells transfected with GFP-TIA1a (A) or GFP-TIA1b (B) by high-content image analysis. The E384K mutant constructs (mut) formed a higher number of stress granules compared to wild-type (wt), both in untreated and in arsenite-stressed cells. The graphs show the mean number of spots per analyzed cell (mean ± S.D. of well averages, normalized to the mean of wt untreated on each plate). Data for each group were pooled from 12 wells of 3 plates in A and 9 wells on 2 plates in B, and significance levels calculated with the 2-tailed Mann–Whitney *U* test.

C FRAP analysis of wild-type and E384K mutant GFP-TIA1a in stress granules of arsenite-stressed HeLa cells. After bleaching, mutant GFP-TIA1a showed slightly lower average fluorescence recovery than wild-type, suggesting tighter binding of the mutant protein to the stress granules. The graph shows the fluorescence intensity of the FRAP target region relative to the initial prebleach value (mean ± S.D.). Asterisks indicate statistically significant differences ($p < 0.05$, 2-tailed heteroscedastic *t* test) between wild-type ($n = 26$) and mutant ($n = 29$). Image frames were captured at intervals of 250 ms.

High-content analysis on the CellInsight system was used for quantification of stress granules. To facilitate automated spot detection, analysis was restricted to cells expressing the constructs at moderate levels. The high-content analysis revealed a minor wild-type–mutant difference affecting both TIA1 isoforms: both untreated and arsenite-treated cells expressing mutant TIA1 showed 10–20% more SGs compared to wild-type (Fig. 13). A similar difference was seen in both the number of SGs and their total area per analyzed cell, indicating an increase in SG formation propensity rather than attenuated clustering of small SGs (III: Suppl. Table 2). While GFP- and HaloTag-tagged TIA1 constructs showed similar behaviour, HA-tagged constructs failed to do so. This difference could be explained by lower and more variable expression of HA-TIA1, evident in WB analysis of the different constructs. Alternatively, the indirect immunostaining required for detection of the HA tag might result in an inferior signal-to-noise ratio, interfering with the image analysis.

Fluorescence recovery after photobleaching (FRAP) analysis in HeLa cells was used for investigating if the steady-state difference observed between wild-type and mutant TIA1 in SG number reflected altered dynamics of SG association/dissociation. Fluorescence recovery of bleached SGs indicated rapid shuttling of wild-type GFP-TIA1a between cytosol and stress granules, consistent with previous findings (Kedersha *et al.* 2000), and the E384K construct showed slightly slower average recovery (Fig. 13). Similar results were obtained in FRAP experiments performed at 37°C and at 35–36°C; in the lower temperature, both constructs showed slower recovery but the difference between wild-type and mutant was preserved. The lower recovery rate suggests tighter association of mutant TIA1 to the SGs, possibly indicating increased aggregation propensity of the prion-related domain.

In FRAP analysis of a hundred SGs in non-stressed cells, all analyzed granules exhibited rapid fluorescence recovery, in contrast to GFP-tagged huntingtin aggregates that did not show any recovery during the follow-up period. This indicated that the increased SG number observed in high-content analysis was due to genuine SGs rather than aggregation of mutant TIA1 to insoluble protein inclusions.

5.3.6.1 Stress granule studies in C2C12 myotubes (unpublished)

To investigate SG formation in a biological system more relevant to muscle disease, C2C12 myoblasts were transfected with GFP-TIA1 constructs and differentiated into myotubes. The majority of transfected cells died or lost the plasmid expression during differentiation, but individual myotubes expressing GFP-TIA1 survived. While in unstressed cells the localization of GFP-TIA1 was mostly diffuse cytoplasmic, arsenite-stressed myotubes showed numerous stress granules (Fig. 14). Visual inspection did not show a dramatic difference between wild-type and mutant constructs. However, due to the small number and variable size of transfected myotubes, and the variable expression levels of the constructs in these cells, quantitative analysis of SGs was not possible.

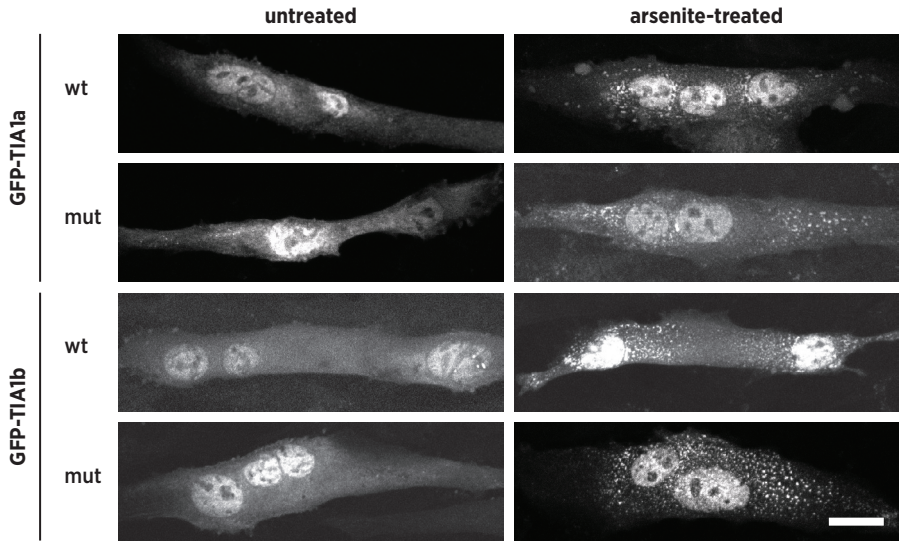

Figure 14. Stress granules in C2C12 myotubes

C2C12 myotubes expressing wild-type (wt) and E384K mutant (mut) GFP-tagged TIA1a and TIA1b constructs were oxidatively stressed with 500 μM sodium arsenite for 45 min and fixed. Arsenite caused a clear recruitment of all TIA1 constructs to stress granules, but quantitative comparison between wild-type and mutant constructs was not possible. Scale bar, 20 μm.

5.3.7 Aggregation of SG proteins is a likely pathomechanism for WDM

The enhanced SG formation observed in high-content analysis and slower fluorescence recovery in FRAP experiments suggest that the E384K mutation, situated in the prion-related domain of TIA1, slightly increases its aggregation propensity. The accumulations of TIA1, TARDBP, and G3BP1 observed in the rimmed-vacuolar regions of WDM muscles support the idea that aggregation of TIA1 plays a role in the pathogenesis of WDM. The relatively weak effect of the mutation on the behaviour of TIA1, observed in the functional studies, is consistent with the very late onset and slow progression of the disease.

The inherent ability of SG proteins to aggregate, while important for their biological functions, makes them also prone to undesired aggregation. Indeed, aggregation of SG components is emerging as an important phenomenon in human diseases, most notably neurogenerative ones (Wolozin 2012, Kim *et al.* 2013). Disease-causing mutations may directly enhance the aggregation of the respective proteins and increase their recruitment to SGs (Johnson *et al.* 2009, Liu-Yesucevitz *et al.* 2010, Kim *et al.* 2013). Such mutations in TARDBP, most of them located in its prion-like domain, cause a familial form of amyotrophic lateral sclerosis (ALS) (Johnson *et al.* 2009, Liu-Yesucevitz *et al.* 2010). ALS-causing mutations have also been identified in FUS (fused in sarcoma), another RNA-binding protein showing SG localization. Rather than affecting the prion-like domain directly, these mutations increase the cytoplasmic aggregation of FUS by interfering with its nuclear localization (Sun *et al.* 2011).

Aggregation-enhancing mutations in the prion-like domains of the heterogeneous nuclear ribonucleoproteins hnRNPA2B1 and hnRNPA1 were recently identified in ALS and multisystem proteinopathy (MSP), a syndrome with protein aggregation pathology involving muscle, brain, motor neurons, and bone (Kim *et al.* 2013). The analogy to WDM is particularly interesting due to the similar muscle pathology with rimmed vacuoles and TARDBP-positive inclusions (Kim *et al.* 2013).

Also normal SG proteins may contribute to inclusion formation by increasing the local concentrations of aggregation-prone proteins and cross-seeding their aggregation (Wolozin 2012). In line with this, SG components have been seen to secondarily colocalize with various types of pathological inclusions. TIA1 and eIF3 were detected in TARDBP inclusions in brain and spinal cord affected with ALS and FTLD-U (ubiquitin-positive frontotemporal lobar degeneration) (Liu-Yesucevitz *et al.* 2010). Brains from tauopathic mice, and from human patients with Alzheimer's disease or FTDP-17 (frontotemporal dementia with parkinsonism 17), showed an increase of TIA1-positive inclusions whose size and colocalization with tau pathology increased with disease severity (Vanderweyde *et al.* 2012). TIA1 and tau have also been demonstrated to promote the aggregation of each other in cell cultures (Vanderweyde *et al.* 2012). Finally, TIA1 is also recruited to polyQ-huntingtin aggregates in cell cultures (Waelter *et al.* 2001).

Pathogenicity of abormal SG formation may depend on sequestration of essential mRNAs and proteins, misregulation of RNA transport and translation, or by direct toxicity of the inclusions (Wolozin 2012), and increased aggregation of TIA1 could cause muscle disease by any of these mechanisms. The simplest explanation is that accumulation of TIA1, possibly seeding the aggregation of other proteins, directly overburdens the protein turnover machinery in muscle fibres. Given the RNA-binding capacity of TIA1, the accumulation pathology could also involve mRNAs. Interestingly, Nakano *et al.* (2005) found accumulation of the SG components HuR and poly(A)-binding protein 1 (PABP1) together with poly(A) RNA at the rimmed-vacuolar regions in sporadic inclusion body myositis, and suggested that the pathomechanism may involve inhibition of mRNA degradation. Whether poly(A) RNA is also accumulating in WDM muscle, should be addressed by further studies.

In addition to a direct effect of the aggregates, increased TIA1 aggregation could lead to disease by interfering with multiple functions of the protein in translation control and RNA metabolism. Abnormal SG function could, for example, mildly impair the cellular response to oxidative or other types of stress, leading to proteotoxic stress due to accumulation of defective proteins. Another possibility would be specific or general suppression of protein expression due to sequestration of mRNAs in TIA1 accumulations.

Given the high degree of alternative splicing in skeletal muscle, defective regulation of splicing could well play a role in the pathogenesis of WDM. While this study did not indicate general splicing abnormality of TIA1 target genes in WDM

muscle, a pathogenic role of specific mis-spliced genes is not excluded. The possibility of splicing effects on individual genes is underlined by the *SMN2* splicing difference later reported by Klar *et al.* (2013). However, as also pointed out by Klar and colleagues (2013), this specific splicing difference is not likely to be relevant in WDM. Impaired expression of SMN would be expected to cause a phenotype in motor neurons rather than in muscle, and splicing efficiency of *SMN2* is in any case unlikely to be of importance in the presence of a functional *SMN1* gene. To understand the role of splicing changes in WDM, splicing of TIA1 target genes in WDM muscle should be systematically studied, for example on a microarray platform.

5.3.7.1 Muscle selectivity in WDM

Data on the tissue distribution of TIA1 are somewhat discordant, but according to WB and RT-PCR studies by Izquierdo and Valcárcel (2007a) TIA1 is widely expressed, and its level in muscle is not particularly high. The selective disease involvement limited to a small group of skeletal muscles, with no symptoms in other tissues, is hence intriguing.

This study compared the SG-forming properties of wild-type and mutant TIA1 only in the cellular context, *i.e.* in the presence of proteins possibly modifying TIA1 behaviour. It is thus possible that the observed difference depends on an interaction with another SG component, and tissue selectivity could arise from differential expression of such a mediating protein. One candidate could be TIAL1 that according to Izquierdo and Valcárcel (2007a) is highly expressed in skeletal muscle. A weak interaction of soluble TIA1 and TIAL1 has been suggested by immunoprecipitation (López de Silanes *et al.* 2005), but studies addressing hetero-oligomerization of the two proteins in SGs have not been reported.

While differential TIA1 expression is unlikely to explain the specific disease involvement of skeletal muscle, expression differences among muscles could contribute to the muscle involvement pattern. The higher TIA1 expression in *tibialis anterior* (TA) compared to *gastrocnemius*, *quadriceps femoris*, and *deltoideus* (Kang *et al.* 2005), is in line with marked involvement of TA in WDM. Expression levels of TIA1 in finger extensor muscles, first affected by WDM, have not been determined.

The muscle specificity could also reflect the unique stress exposure of skeletal muscle. Contractile activity causes thermal, mechanical, and oxidative stress (Close *et al.* 2005, Morton *et al.* 2009) that, together with the high content of fibrous proteins, might make the post-mitotic muscle fibres generally susceptible to defects of protein turnover and accumulation of faulty proteins. Moreover, the aforementioned recurrent stress exposure could cause relatively high levels of SG formation in muscle compared to other tissues, directly predisposing it to accumulation of SG-derived aggregates. Another type of stress potentially contributing to the muscle selectivity could be exposure of distal muscles to cold temperatures, known to cause SG formation in cell culture (Hofmann *et al.* 2012).

6 CONCLUSIONS AND FUTURE WORK

The studies presented in this thesis aimed at elucidating molecular pathomechanisms of muscular dystrophies. While the answers are far from complete, the studies gave important preliminary insight into the processes underlying LGMD1D and WDM, and provided new knowledge on the molecular biology of M-band titin and calpain 3, necessary for understanding the pathomechanisms of TMD/LGMD2J and LGMD2A.

Study I met its goal of finding novel interaction partners of C-terminal titin and calpain 3: myospryn was identified as a ligand for both proteins, and hence potentially involved in the pathomechanisms of TMD/LGMD2J and LGMD2A. Although the FINmaj KI mouse model failed to show a direct downstream effect on myospryn localization, loss of the functional interaction is an expected consequence of titin mutations, and this may be relevant in the pathogenesis of TMD/LGMD2J. While these initial studies did not reveal the biological function of the titin–myospryn interaction, they established a good background for future functional work that is expected to complement the basic understanding of muscle biology and to elucidate the importance of myospryn in muscular dystrophies. Possible future studies could, for example, investigate the role of M-band myospryn in cell signalling by analyzing local PKA and calcineurin activities in wild-type and FINmaj KI muscles and cell cultures.

The proteolytic cleavage of myospryn, and its modulatory effect on CAPN3 autolysis already provide clues about the possible functions of the CAPN3–myospryn interaction, but further studies will be needed for characterization of these effects on a mechanistical level and for determining their biological relevance. Quantification of myospryn levels and turnover in normal and CAPN3-deficient cells and tissues could be used for investigating whether myospryn is a physiological substrate for CAPN3. Possible regulation of CAPN3 activity could, on the other hand, involve phosphorylation or dephosphorylation events coordinated by myospryn. This possibility could be addressed by studying effect of myospryn coexpression on the phosphorylation state of CAPN3.

Study II identified mutations in DNAJB6 as the genetic cause of LGMD1D, unequivocally demonstrating the pathogenicity of the described mutations. The dominant toxic effect shown for mutated DNAJB6b is highly likely to be the major pathogenic factor underlying LGMD1D. It remains unclear whether the observed reduction of DNAJB6 anti-aggregation activity is an independent factor possibly contributing to the pathogenesis, or a direct cause or consequence of the toxicity. For understanding these effects, it should be first clarified whether the mutations affect the HSPA-dependent or -independent component of the anti-aggregation activity. This could be achieved by studying the relative effects of disease mutations on DNAJB6 constructs defective either in the HSPA co-chaperone activity (deletion or inactivating H31Q mutation of the J-domain) or in the acetylation-dependent anti-aggregation pathway (acetylation site mutations).

Confirmation of the postulated link between DNAJB6 and the CASA pathway shed new light on the protein quality control and degradation pathways in muscle, although further studies are needed for characterizing the relationship of DNAJB6 and CASA in healthy muscle and in LGMD1D. In this regard, the potential role of HSPB8 as the mediator of DNAJB6 toxicity is of particular interest and could be studied with overexpression and knockdown approaches in zebrafish. If the CASA machinery is necessary for the toxicity of mutant DNAJB6, its high expression in muscle (Ballinger *et al.* 1999, Kappé *et al.* 2001, Homma *et al.* 2006) is likely to explain the tissue-selective effect of the mutations at least partly. Also muscle-specific interaction partners of the mutated G/F domain or client proteins of DNAJB6 may play a role in the tissue selectivity, and their identification would be important for more complete understanding of the pathomechanism.

Study III demonstrated the TIA1 mutation E384K as the genetic cause of Welander distal myopathy. A slightly increased aggregation propensity was identified for the mutant protein, suggesting altered stress granule dynamics to be a part of the pathomechanism of WDM. While this alone may be a sufficient explanation for the pathogenicity, the possible contribution of splicing changes should be kept in mind and investigated further, despite the negative results for the target genes studied here. Regarding the pathomechanism of WDM, the most important open issue is the selective involvement of a small subset of muscles, which could be elucidated by identification of differentially expressed factors modifying TIA1 aggregation. For assessing the contribution of complex environmental factors such as physical activity and temperature on TIA1 aggregation and WDM pathogenesis, an animal model for WDM would be an informative tool. While WDM itself is relatively benign, detailed characterization of its pathomechanism may also be of interest with regard to other, more severe, diseases involving inappropriate aggregation of prion-like domains.

As a whole, these studies have augmented the knowledge on the molecular mechanisms of normal muscle function and disease pathogenesis. Understanding these mechanisms is a prerequisite for ultimately developing therapies to the studied disorders as well as other muscular dystrophies.

7 ACKNOWLEDGEMENTS

These studies was conducted at the Folkhälsan Institute of Genetics and the Department of Medical Genetics, University of Helsinki, mostly in 2006–2013 (although the titin M10 interaction work was set in motion already during my undergrad years). The heads of these institutes during this period—Anna-Elina Lehesjoki, Per-Henrik Groop, Irma Järvelä, and Päivi Peltomäki—are acknowledged for providing excellent resources and facilities for the research. Thanks to Anna-Elina also for kind support during my years at Folkhälsan.

My work was funded by a fellowship of the Helsinki Graduate School in Biotechnology and Molecular Biology in 2007–2010, and brought to completion with continuing support from the Alfred Kordelin Foundation. Shorter periods have been funded by the University of Helsinki Research Foundation and the Orion Farmos Research Foundation. In addition, I have received support for travel and materials from the European Molecular Biology Organization, the Emil Aaltonen Foundation, Lihastautien tutkimussäätiö, the Magnus Ehrnrooth Foundation, the Oskar Öflund Foundation, the University of Helsinki Funds, and the World Muscle Society. I am grateful for all the financial support that has made this work possible.

Thanks to Aija Kyttälä and Hannu Kalimo, the external members of my thesis follow-up group, for their commitment during my GSBM period and support also afterwards. Aija, together with Katarina Pelin, is also thanked for taking the time for reviewing this thesis—I feel that the manuscript improved a whole lot thanks to your constructive comments.

My postgraduate studies in genetics were done at my "home department", the Dept. of Biosciences, University of Helsinki. Thanks to Tapio Palva and Pekka Heino there for their guidance, and to Minna Nyström for agreeing to act as custos for my defence. Thanks to Pekka Lappalainen, Erkki Raulo, Anne-Maria Pajari, and Anita Tienhaara for both education and extracurricular activities at GSBM.

I am grateful to my PhD supervisor and group leader Bjarne Udd for his contagious enthusiasm towards muscle research, for having confidence in my abilities, and for providing an inspiring, rewarding and educative research environment with a great deal of independence and responsibility for one's own work. I have learnt so much during these years.

Peter Hackman, the co-supervisor of my PhD, deserves my deepest gratitude for welcoming me to the Udd group in the summer 2001 (it became a longer journey together than neither of us expected!) and introducing me to the work in a real lab, for being my nearest boss always there for the daily matters (if not in Transnistria or North Korea), and for the numerous fun and unforgettable moments both in the lab and outside.

Thanks to Anna Vihola, a long-standing colleague and friend, for her expert contribution in the analysis of muscle samples in these studies, for teaching me most of what I know of western blotting and IF microscopy, and for sharing the occasional confusion and frustration with misbehaving experiments.

Thanks to pH Jonson, my inseparable filter trapping and brainstrorming companion in the DNAJB6 project, for his friendship, passion for proteins, and no-nonsense attitude towards science and life.

A million thanks to Helena Luque for the countless western blots, IF stainings, and clonings performed with guaranteed precision and reliability, for keeping the lab book up-to-date when I didn't, and for her always cheerful attitude.

I am also grateful to my other colleagues in the Udd group, many of whom have directly contributed to these studies one way or another. Thanks to Merja Soininen for friendship during our long common years in the group and for helping in the lab; to Marjut Ritala for skilled technical assistance and pretty muscle sections; to Sara Lehtinen for starting the functional work in the WDM project; to Mark Screen for lunch and travel company and alerts on new exciting papers; to Anni Evilä for follow-up work on the titin interactions before tackling the gene hunt challenges with new techniques; to Jeanette Holmlund-Hampf for mutual language tutoring; to Lydia Sagath for continuing with stress granules; to Katri Leinonen for help in the lab; and to Giorgio Tasca for being a good guy.

From the Tampere/Seinäjoki branches of our group, I'm grateful to Yinka Raheem, Sanna Huovinen, Sini Penttilä, Satu Sandell, and Johanna Palmio, for co-authoring the DNAJB6 paper. All of them, as well as Tiina Suominen and Manu Jokela, are also thanked for the fun company during WMS and other conference trips and the legendary summer cottage meetings. Thanks also to all the lab personnel in Tampere, first and foremost Hanna-Liisa Kojo, Jaana Leppikangas, and Satu Luhtasela.

All the co-authors of the original publications outside the Udd group are thanked for their invaluable contributions to the projects. Special thanks to those involved with me in the functional studies: to Karine Charton, Gaëlle Blandin and others in Isabelle Richard's team at Généthon for the calpain side of the myospryn project and for the FINmaj mouse work; to Elisabeth Ehler for welcoming me to London for the NRC experiments and sharing her expertise in cell biology, as well as jolly company in EMC meetings; and to Christelle Golzio and Nico Katsanis for their input that truly brought the DNAJB6 paper to the next level.

Thanks to Derek Blake for fruitful collaboration in the myospryn project; to Mathias Gautel for ideas and conversations; and to Stephan Lange for showing interest in my projects and providing many good pieces of advice. Thanks to Kirsi Mänttäri and Outi Kokkonen for performing the M10 Y2H screen. Thanks also to everyone who has shared constructs and antibodies used in these projects.

Thanks to Rabah Soliymani, Maciej Lalowski, and Marc Baumann for their dedicated help in the endless titin protein chemistry project, and to Mika Kaakinen for electroporation experiments—studies that did not make it to this thesis.

Thanks to my high school biology teacher Kari Kariluoto, without whom I would have probably ended up as a journalist. Thanks to Carina Wallgren-Pettersson and Maija Wessman for their supportive attitude during my FIG years.

Thanks to Marjatta Valkama, Madeleine Avellan, Jaana Welin-Haapamäki, Stephan Keskinen, and Nina Forss for efficiently running the administrative and financial business at FIG.

Thanks to Ann-Liz, the soul of FIG, for lab management and friendship.

Thanks to my past and present officemates at FIG—to dorktor Vilma for ensuring that there's never a dull moment in our office, for hymn singing, and for many late nights in WMS meetings; to Mervi for her friendship, peer support, and enthusiasm to science; and to Reetta, Kaisa, and Jenni for nice atmosphere and conversations, and for making sure that coming to work has always been a pleasure.

Thanks to Saara and Maria S. for our long years together at FIG, and for sharing the final anxiety with the thesis writing and defence preparations over the past year. Congratulations and good luck for both of you! Saara is also thanked for travel company in all the hemispheres as well as many memorable moments back home.

Thanks to my other fellow PhD students at FIG during the years—Anni L., Otto, Inken, Kirsi K., Edu, Minttu, Hanna V., Anne J., Eija, Milja, Maria K., Anna-Kaisa, Kirsi A., Riikka, Kati, Liina N., and Jukka K.—and my other past and present workmates, including but not limited to Tarja J., Outi, Mubashir, Olesya, Adile, Anja, Marilotta, Paula, Teija, Tuula, Sinikka, Juha I., Juha K., Tarja S., Ulla L., Nina A., Maria L., Maria L.-H., Elina, Minnamari, Hanna H., and Hanne—for all the science-related stuff, and especially for our common moments in the lab and the cell room, on lunch, coffee and ice cream breaks, in fitness boxing, in Mountain and Hadanka, in karonkkas, in film shootings, on conference trips, and everywhere else. It has been a pleasure working with you.

Thanks to all my friends for providing distractions from the hard work. Thanks especially to Jaakko, Anna, Rixu, Mikko, Sini, Aapo, Heidi, and Hennis for bird-watching trips and all the other good times together; to the Sunday lunch gang for the guaranteed monthly social event; to the pub quiz team (including my sister Katri and brother-in-law Valtsu) for the relaxing evenings; and to everybody in the Symbioosi choir for pastyme in good company!

I am deeply grateful to my parents Jore and Päkä for supporting me in whatever I do, to my inlaws Ismo and Päivi for being interested in the progress of my thesis (current status: 100%), and to my wonderful extended family for being there in my life. You all mean a lot to me!

Warmest thanks to my wife Mirkka for her love and companionship, for sharing the life with me during the past ten years, for understanding the ups and downs of being a scientist, for proofreading this thesis, and for providing rat muscles. Finally, a million thanks to our dear son Lauri for bringing so much joy and happiness to our lives!

Helsinki, October 2013

Jaakko

8 REFERENCES

Abe M & Oshima RG (1990) A single human keratin 18 gene is expressed in diverse epithelial cells of transgenic mice. *J.Cell Biol.* 111(3): 1197–1206

Ackermann MA *et al.* (2009) Obscurin interacts with a novel isoform of MyBP-C slow at the periphery of the sarcomeric M-band and regulates thick filament assembly. *Mol.Biol.Cell* 20(12): 2963–2978

Agarkova I *et al.* (2000) A novel marker for vertebrate embryonic heart, the EH-myomesin isoform. *J.Biol.Chem.* 275(14): 10256–10264

Andersen JS *et al.* (2003) Proteomic characterization of the human centrosome by protein correlation profiling. *Nature* 426(6966): 570–574

Anderson P *et al.* (1990) A monoclonal antibody reactive with a 15-kDa cytoplasmic granule-associated protein defines a subpopulation of $CD8^+$ T lymphocytes. *J.Immunol.* 144(2): 574–582

Anderson P & Kedersha N (2002) Stressful initiations. *J.Cell.Sci.* 115(16): 3227–3234

Anderson P & Kedersha N (2002) Visibly stressed: the role of eIF2, TIA-1, and stress granules in protein translation. *Cell Stress Chaperones* 7(2): 213–221

Anderson P & Kedersha N (2008) Stress granules: the Tao of RNA triage. *Trends Biochem.Sci.* 33(3): 141–150

Andrews JF *et al.* (2012) Cellular stress stimulates nuclear localization signal (NLS) independent nuclear transport of MRJ. *Exp.Cell Res.* 318(10): 1086–1093

Angelini C & Fanin M (2012) Calpainopathy. In Pagon RA *et al.* (eds.) GeneReviews. University of Washington, Seattle, Seattle, WA, USA. Updated 07/05/2012, accessed 06/20/2013. Available at: http://www.ncbi.nlm.nih.gov/books/NBK1313/

Arimoto K *et al.* (2008) Formation of stress granules inhibits apoptosis by suppressing stress-responsive MAPK pathways. *Nat.Cell Biol.* 10(11): 1324–1332

Arimura T *et al.* (2009) Impaired binding of ZASP/Cypher with phosphoglucomutase 1 is associated with dilated cardiomyopathy. *Cardiovasc.Res.* 83(1): 80–88

Arimura T *et al.* (2011) Dilated cardiomyopathy-associated BAG3 mutations impair Z-disc assembly and enhance sensitivity to apoptosis in cardiomyocytes. *Hum.Mutat.* 32(12): 1481–1491

Arndt V *et al.* (2010) Chaperone-assisted selective autophagy is essential for muscle maintenance. *Curr.Biol.* 20(2): 143–148

Arnold K *et al.* (2006) The SWISS-MODEL workspace: a web-based environment for protein structure homology modelling. *Bioinformatics* 22(2): 195–201

Arya R *et al.* (2004) Muscle ring finger protein-1 inhibits PKCε activation and prevents cardiomyocyte hypertrophy. *J.Cell Biol.* 167(6): 1147–1159

Aulas A *et al.* (2012) Endogenous TDP-43, but not FUS, contributes to stress granule assembly via G3BP. *Mol.Neurodegener.* 7: 54 doi: 10.1186/1750-1326-7-54

Aznarez I *et al.* (2008) A systematic analysis of intronic sequences downstream of 5' splice sites reveals a widespread role for U-rich motifs and TIA1/TIAL1 proteins in alternative splicing regulation. *Genome Res.* 18(8): 1247–1258

Baghdiguian S *et al.* (1999) Calpain 3 deficiency is associated with myonuclear apoptosis and profound perturbation of the IκBα/NF-κB pathway in limb-girdle muscular dystrophy type 2A. *Nat.Med.* 5(5): 503–511

Bagnato P *et al.* (2003) Binding of an ankyrin-1 isoform to obscurin suggests a molecular link between the sarcoplasmic reticulum and myofibrils in striated muscles. *J.Cell Biol.* 160(2): 245–253

Baguet A *et al.* (2007) The exon-junction-complex-component metastatic lymph node 51 functions in stress-granule assembly. *J.Cell.Sci.* 120(16): 2774–2784

Ballinger CA *et al.* (1999) Identification of CHIP, a novel tetratricopeptide repeat-containing protein that interacts with heat shock proteins and negatively regulates chaperone functions. *Mol.Cell.Biol.* 19(6): 4535–4545

Bang ML *et al.* (2001) The complete gene sequence of titin, expression of an unusual approximately 700-kDa titin isoform, and its interaction with obscurin identify a novel Z-line to I-band linking system. *Circ.Res.* 89(11): 1065–1072

Bang ML *et al.* (2001) Myopalladin, a novel 145-kilodalton sarcomeric protein with multiple roles in Z-disc and I-band protein assemblies. *J.Cell Biol.* 153(2): 413–427

Barash IA *et al.* (2007) Structural and regulatory roles of muscle ankyrin repeat protein family in skeletal muscle. *Am.J.Physiol.Cell.Physiol.* 293(1): C218–27

Beatham J *et al.* (2004) Filamin C interacts with the muscular dystrophy KY protein and is abnormally distributed in mouse KY deficient muscle fibres. *Hum.Mol.Genet.* 13(22): 2863–2874
Beatham J *et al.* (2006) Constitutive upregulations of titin-based signalling proteins in KY deficient muscles. *Neuromuscul.Disord.* 16(7): 437–445
Beck AR *et al.* (1996) Structure, tissue distribution and genomic organization of the murine RRM-type RNA binding proteins TIA-1 and TIAR. *Nucleic Acids Res.* 24(19): 3829–3835
Beck AR *et al.* (1998) RNA-binding protein TIAR is essential for primordial germ cell development. *Proc.Natl.Acad.Sci.U.S.A.* 95(5): 2331–2336
Beckmann JS & Spencer M (2008) Calpain 3, the "gatekeeper" of proper sarcomere assembly, turnover and maintenance. *Neuromuscul.Disord.* 18(12): 913–921
Belgrano A *et al.* (2011) Multi-tasking role of the mechanosensing protein Ankrd2 in the signaling network of striated muscle. *PLoS One* 6(10): e25519
Benson MA *et al.* (2001) Dysbindin, a novel coiled-coil-containing protein that interacts with the dystrobrevins in muscle and brain. *J.Biol.Chem.* 276(26): 24232–24241
Benson MA *et al.* (2004) Myospryn is a novel binding partner for dysbindin in muscle. *J.Biol.Chem.* 279(11): 10450–10458
Blandin G *et al.* (2013) A human skeletal muscle interactome centered on proteins involved in muscular dystrophies: LGMD interactome. *Skelet.Muscle* 3(1): 3-5040-3-3
Boateng SY *et al.* (2009) Myocyte remodeling in response to hypertrophic stimuli requires nucleocytoplasmic shuttling of muscle LIM protein. *J.Mol.Cell.Cardiol.* 47(4): 426–435
Bodine SC *et al.* (2001) Identification of ubiquitin ligases required for skeletal muscle atrophy. *Science* 294(5547): 1704–1708
Borg K *et al.* (1987) Sensory involvement in distal myopathy (Welander). *J.Neurol.Sci.* 80(2–3): 323–332
Borg K *et al.* (1989) Neurogenic involvement in distal myopathy (Welander). Histochemical and morphological observations on muscle and nerve biopsies. *J.Neurol.Sci.* 91(1–2): 53–70
Borg K *et al.* (1991) Welander's distal myopathy: clinical, neurophysiological and muscle biopsy observations in young and middle aged adults with early symptoms. *J.Neurol.Neurosurg.Psychiatry.* 54(6): 494–498
Borg K *et al.* (1991) Intranuclear and cytoplasmic filamentous inclusions in distal myopathy (Welander). *Acta Neuropathol.* 82(2): 102–106
Borg K *et al.* (1993) Muscle fibre degeneration in distal myopathy (Welander)—ultrastructure related to immunohistochemical observations on cytoskeletal proteins and Leu-19 antigen. *Neuromuscul.Disord.* 3(2): 149–155
Borg K *et al.* (1998) Welander distal myopathy—an overview. *Neuromuscul.Disord.* 8(2): 115–118
Borisov AB *et al.* (2004) Dynamics of obscurin localization during differentiation and remodeling of cardiac myocytes: obscurin as an integrator of myofibrillar structure. *J.Histochem.Cytochem.* 52(9): 1117–1127
Borisov AB *et al.* (2006) Essential role of obscurin in cardiac myofibrillogenesis and hypertrophic response: evidence from small interfering RNA-mediated gene silencing. *Histochem.Cell Biol.* 125(3): 227–238
Bowman AL *et al.* (2007) Different obscurin isoforms localize to distinct sites at sarcomeres. *FEBS Lett.* 581(8): 1549–1554
Branca D *et al.* (1999) Expression, partial purification and functional properties of the muscle-specific calpain isoform p94. *Eur.J.Biochem.* 265(2): 839–846
Braun T & Gautel M (2011) Transcriptional mechanisms regulating skeletal muscle differentiation, growth and homeostasis. *Nat.Rev.Mol.Cell Biol.* 12(6): 349–361
Buchan JR *et al.* (2008) P bodies promote stress granule assembly in *Saccharomyces cerevisiae*. *J.Cell Biol.* 183(3): 441–455
Buchan JR & Parker R (2009) Eukaryotic stress granules: the ins and outs of translation. *Mol.Cell* 36(6): 932–941
Carmignac V *et al.* (2007) C-terminal titin deletions cause a novel early-onset myopathy with fatal cardiomyopathy. *Ann.Neurol.* 61(4): 340–351
Carra S *et al.* (2008) HspB8 chaperone activity toward poly(Q)-containing proteins depends on its association with Bag3, a stimulator of macroautophagy. *J.Biol.Chem.* 283(3): 1437–1444
Carra S *et al.* (2009) HspB8 participates in protein quality control by a non-chaperone-like mechanism that requires eIF2α phosphorylation. *J.Biol.Chem.* 284(9): 5523–5532
Cavnar PJ *et al.* (2007) Molecular identification and localization of cellular titin, a novel titin isoform in the fibroblast stress fiber. *Cell Motil.Cytoskeleton* 64(6): 418–433

Cenni V *et al.* (2011) Ankrd2/ARPP is a novel Akt2 specific substrate and regulates myogenic differentiation upon cellular exposure to H_2O_2. *Mol.Biol.Cell* 22(16): 2946–2956
Centner T *et al.* (2001) Identification of muscle specific ring finger proteins as potential regulators of the titin kinase domain. *J.Mol.Biol.* 306(4): 717–726
Chai Y *et al.* (1999) Evidence for proteasome involvement in polyglutamine disease: localization to nuclear inclusions in SCA3/MJD and suppression of polyglutamine aggregation in vitro. *Hum.Mol.Genet.* 8(4): 673–682
Chan KK *et al.* (1998) Molecular cloning and characterization of FHL2, a novel LIM domain protein preferentially expressed in human heart. *Gene* 210(2): 345–350
Charton K *et al.* (2010) Removal of the calpain 3 protease reverses the myopathology in a mouse model for titinopathies. *Hum.Mol.Genet.* 19(23): 4608–4624
Chen X *et al.* (2011) GWA study data mining and independent replication identify cardiomyopathy-associated 5 (*CMYA5*) as a risk gene for schizophrenia. *Mol.Psychiatry* 16(11): 1117–1129
Chu PH *et al.* (2000) Expression patterns of FHL/SLIM family members suggest important functional roles in skeletal muscle and cardiovascular system. *Mech.Dev.* 95(1–2): 259–265
Chu W *et al.* (1995) Identification and characterization of a novel cytokine-inducible nuclear protein from human endothelial cells. *J.Biol.Chem.* 270(17): 10236–10245
Chuang JZ *et al.* (2002) Characterization of a brain-enriched chaperone, MRJ, that inhibits Huntingtin aggregation and toxicity independently. *J.Biol.Chem.* 277(22): 19831–19838
Clarke BA *et al.* (2007) The E3 Ligase MuRF1 degrades myosin heavy chain protein in dexamethasone-treated skeletal muscle. *Cell.Metab.* 6(5): 376–385
Close GL *et al.* (2005) Skeletal muscle damage with exercise and aging. *Sports Med.* 35(5): 413–427
Cohen N *et al.* (2006) Identification of putative in vivo substrates of calpain 3 by comparative proteomics of overexpressing transgenic and nontransgenic mice. *Proteomics* 6(22): 6075–6084
Colombrita C *et al.* (2009) TDP-43 is recruited to stress granules in conditions of oxidative insult. *J.Neurochem.* 111(4): 1051–1061
Cullinane AR *et al.* (2011) A BLOC-1 mutation screen reveals that *PLDN* is mutated in Hermansky-Pudlak Syndrome type 9. *Am.J.Hum.Genet.* 88(6): 778–787
Cunha SR & Mohler PJ (2008) Obscurin targets ankyrin-B and protein phosphatase 2A to the cardiac M-line. *J.Biol.Chem.* 283(46): 31968–31980
Dai KS & Liew CC (2001) A novel human striated muscle RING zinc finger protein, SMRZ, interacts with SMT3b via its RING domain. *J.Biol.Chem.* 276(26): 23992–23999
Dai YS *et al.* (2005) The DnaJ-related factor Mrj interacts with nuclear factor of activated T cells c3 and mediates transcriptional repression through class II histone deacetylase recruitment. *Mol.Cell.Biol.* 25(22): 9936–9948
Damgaard CK & Lykke-Andersen J (2011) Translational coregulation of 5'TOP mRNAs by TIA-1 and TIAR. *Genes Dev.* 25(19): 2057–2068
Dang Y *et al.* (2006) Eukaryotic initiation factor 2α-independent pathway of stress granule induction by the natural product pateamine A. *J.Biol.Chem.* 281(43): 32870–32878
Das R *et al.* (2007) SR proteins function in coupling RNAP II transcription to pre-mRNA splicing. *Mol.Cell* 26(6): 867–881
Daugaard M *et al.* (2007) The heat shock protein 70 family: Highly homologous proteins with overlapping and distinct functions. *FEBS Lett.* 581(19): 3702–3710
de Morrée A *et al.* (2010) Calpain 3 is a rapid-action, unidirectional proteolytic switch central to muscle remodeling. *PLoS One* 5(8): e11940
De Tullio R *et al.* (2003) Characterization of a new p94-like calpain form in human lymphocytes. *Biochem.J.* 375(3): 689–696
Del Gatto-Konczak F *et al.* (2000) The RNA-binding protein TIA-1 is a novel mammalian splicing regulator acting through intron sequences adjacent to a 5' splice site. *Mol.Cell.Biol.* 20(17): 6287–6299
Dell'Angelica EC (2004) The building BLOC(k)s of lysosomes and related organelles. *Curr.Opin. Cell Biol.* 16(4): 458–464
Dey S *et al.* (2009) Cell cycle specific expression and nucleolar localization of human J-domain containing co-chaperone Mrj. *Mol.Cell.Biochem.* 322(1–2): 137–142
Diaz BG *et al.* (2004) Insertion sequence 1 of muscle-specific calpain, p94, acts as an internal propeptide. *J.Biol.Chem.* 279(26): 27656–27666
Dixon DA *et al.* (2003) Regulation of cyclooxygenase-2 expression by the translational silencer TIA-1. *J.Exp.Med.* 198(3): 475–481

Donaldson KM *et al.* (2003) Ubiquitin-mediated sequestration of normal cellular proteins into polyglutamine aggregates. *Proc.Natl.Acad.Sci.U.S.A.* 100(15): 8892–8897

Drexler HC *et al.* (2012) On marathons and Sprints: an integrated quantitative proteomics and transcriptomics analysis of differences between slow and fast muscle fibers. *Mol.Cell. Proteomics* 11(6): M111.010801

Duguez S *et al.* (2006) Calpain 3: a key regulator of the sarcomere? *FEBS J.* 273(15): 3427–3436

Durham JT *et al.* (2006) Myospryn is a direct transcriptional target for MEF2A that encodes a striated muscle, α-actinin-interacting, costamere-localized protein. *J.Biol.Chem.* 281(10): 6841–6849

Durrenberger PF *et al.* (2009) DnaJB6 is present in the core of Lewy bodies and is highly up-regulated in parkinsonian astrocytes. *J.Neurosci.Res.* 87(1): 238–245

Eilertsen KJ & Keller TC,3rd (1992) Identification and characterization of two huge protein components of the brush border cytoskeleton: evidence for a cellular isoform of titin. *J.Cell Biol.* 119(3): 549–557

Eilertsen KJ *et al.* (1994) Cellular titin localization in stress fibers and interaction with myosin II filaments in vitro. *J.Cell Biol.* 126(5): 1201–1210

Eilertsen KJ *et al.* (1997) Interaction of alpha-actinin with cellular titin. *Eur.J.Cell Biol.* 74(4): 361–364

Eisinger-Mathason TS *et al.* (2008) Codependent functions of RSK2 and the apoptosis-promoting factor TIA-1 in stress granule assembly and cell survival. *Mol.Cell* 31(5): 722–736

Erickson HP (1994) Reversible unfolding of fibronectin type III and immunoglobulin domains provides the structural basis for stretch and elasticity of titin and fibronectin. *Proc.Natl.Acad. Sci.U.S.A.* 91(21): 10114–10118

Ermolova N *et al.* (2011) Pathogenity of some limb girdle muscular dystrophy mutations can result from reduced anchorage to myofibrils and altered stability of calpain 3. *Hum.Mol.Genet.* 20(17): 3331–3345

Esser C *et al.* (2004) Cooperation of molecular chaperones with the ubiquitin/proteasome system. *Biochim.Biophys.Acta* 1695(1–3): 171–188

Falcon-Perez JM *et al.* (2002) BLOC-1, a novel complex containing the pallidin and muted proteins involved in the biogenesis of melanosomes and platelet-dense granules. *J.Biol.Chem.* 277(31): 28191–28199

Fallaux FJ *et al.* (1996) Characterization of 911: a new helper cell line for the titration and propagation of early region 1-deleted adenoviral vectors. *Hum.Gene Ther.* 7(2): 215–222

Faulkner G *et al.* (2000) FATZ, a filamin-, actinin-, and telethonin-binding protein of the Z-disc of skeletal muscle. *J.Biol.Chem.* 275(52): 41234–41242

Fayazi Z *et al.* (2006) A *Drosophila* ortholog of the human MRJ modulates polyglutamine toxicity and aggregation. *Neurobiol.Dis.* 24(2): 226–244

Fokkema IF *et al.* (2011) LOVD v.2.0: the next generation in gene variant databases. *Hum.Mutat.* 32(5): 557–563

Förch P *et al.* (2000) The apoptosis-promoting factor TIA-1 is a regulator of alternative pre-mRNA splicing. *Mol.Cell* 6(5): 1089–1098

Förch P *et al.* (2002) The splicing regulator TIA-1 interacts with U1-C to promote U1 snRNP recruitment to 5' splice sites. *EMBO J.* 21(24): 6882–6892

Fougerousse F *et al.* (1998) Expression of genes (*CAPN3*, *SGCA*, *SGCB*, and *TTN*) involved in progressive muscular dystrophies during early human development. *Genomics* 48(2): 145–156

Fougerousse F *et al.* (2000) Calpain3 expression during human cardiogenesis. *Neuromuscul. Disord.* 10(4–5): 251–256

Fougerousse F *et al.* (2000) Human-mouse differences in the embryonic expression patterns of developmental control genes and disease genes. *Hum.Mol.Genet.* 9(2): 165–173

Freiburg A & Gautel M (1996) A molecular map of the interactions between titin and myosin-binding protein C. Implications for sarcomeric assembly in familial hypertrophic cardiomyopathy. *Eur.J.Biochem.* 235(1–2): 317–323

Freiburg A *et al.* (2000) Series of exon-skipping events in the elastic spring region of titin as the structural basis for myofibrillar elastic diversity. *Circ.Res.* 86(11): 1114–1121

Frey N & Olson EN (2002) Calsarcin-3, a novel skeletal muscle-specific member of the calsarcin family, interacts with multiple Z-disc proteins. *J.Biol.Chem.* 277(16): 13998–14004

Fuchs M *et al.* (2010) Identification of the key structural motifs involved in HspB8/HspB6-Bag3 interaction. *Biochem.J.* 425(1): 245–255

Fukiage C *et al.* (2002) Characterization and regulation of lens-specific calpain Lp82. *J.Biol.Chem.* 277(23): 20678–20685
Fukuzawa A *et al.* (2008) Interactions with titin and myomesin target obscurin and obscurin-like 1 to the M-band – implications for hereditary myopathies. *J.Cell.Sci.* 121(11): 1841–1851
Fürst DO *et al.* (1988) The organization of titin filaments in the half-sarcomere revealed by monoclonal antibodies in immunoelectron microscopy: a map of ten nonrepetitive epitopes starting at the Z line extends close to the M line. *J.Cell Biol.* 106(5): 1563–1572
Fürst DO *et al.* (1989) Myogenesis in the mouse embryo: differential onset of expression of myogenic proteins and the involvement of titin in myofibril assembly. *J.Cell Biol.* 109(2): 517–527
Furukawa M *et al.* (2013) An association analysis of the cardiomyopathy-associated 5 (*CMYA5*) gene with schizophrenia in a Japanese population. *Psychiatr.Genet.* 23(4):179–180
García Díaz BE *et al.* (2006) Ca^{2+} dependency of calpain 3 (p94) activation. *Biochemistry* 45(11): 3714–3722
Garvey SM *et al.* (2002) The muscular dystrophy with myositis (*mdm*) mouse mutation disrupts a skeletal muscle-specific domain of titin. *Genomics* 79(2): 146–149
Gautel M *et al.* (1993) Phosphorylation of KSP motifs in the C-terminal region of titin in differentiating myoblasts. *EMBO J.* 12(10): 3827–3834
Geisler SB *et al.* (2007) Obscurin-like 1, OBSL1, is a novel cytoskeletal protein related to obscurin. *Genomics* 89(4): 521–531
Gerull B *et al.* (2002) Mutations of *TTN*, encoding the giant muscle filament titin, cause familial dilated cardiomyopathy. *Nat.Genet.* 30(2): 201–204
Gesnel MC *et al.* (2007) Cooperative binding of TIA-1 and U1 snRNP in K-SAM exon splicing activation. *Biochem.Biophys.Res.Commun.* 358(4): 1065–1070
Ghiani CA *et al.* (2010) The dysbindin-containing complex (BLOC-1) in brain: developmental regulation, interaction with SNARE proteins and role in neurite outgrowth. *Mol.Psychiatry* 15(2): 115, 204–15
Ghiani CA & Dell'Angelica EC (2011) Dysbindin-containing complexes and their proposed functions in brain: from zero to (too) many in a decade. *ASN Neuro* 3(2): 10.1042/AN20110010
Gilks N *et al.* (2004) Stress granule assembly is mediated by prion-like aggregation of TIA-1. *Mol. Biol.Cell* 15(12): 5383–5398
Gillis J *et al.* (2013) The DNAJB6 and DNAJB8 Protein Chaperones Prevent Intracellular Aggregation of Polyglutamine Peptides. *J.Biol.Chem.* 288(24): 17225–17237
Goebel HH & Müller HD (2006) Protein Aggregate Myopathies. *Semin.Pediatr.Neurol.* 13(2): 96–103
Gokhale A *et al.* (2012) Quantitative proteomic and genetic analyses of the schizophrenia susceptibility factor dysbindin identify novel roles of the biogenesis of lysosome-related organelles complex 1. *J.Neurosci.* 32(11): 3697–3711
Gotthardt M *et al.* (2003) Conditional expression of mutant M-line titins results in cardiomyopathy with altered sarcomere structure. *J.Biol.Chem.* 278(8): 6059–6065
Granzier HL *et al.* (2009) Truncation of titin's elastic PEVK region leads to cardiomyopathy with diastolic dysfunction. *Circ.Res.* 105(6): 557–564
Gräter F *et al.* (2005) Mechanically induced titin kinase activation studied by force-probe molecular dynamics simulations. *Biophys.J.* 88(2): 790–804
Greaser M (2001) Identification of new repeating motifs in titin. *Proteins* 43(2): 145–149
Gregorio CC *et al.* (1998) The NH_2 terminus of titin spans the Z-disc: its interaction with a novel 19-kD ligand (T-cap) is required for sarcomeric integrity. *J.Cell Biol.* 143(4): 1013–1027
Gregorio CC *et al.* (2005) Functional properties of the titin/connectin-associated proteins, the muscle-specific RING finger proteins (MURFs), in striated muscle. *J.Muscle Res.Cell.Motil.* 26(6–8): 389–400
Groušl T *et al.* (2009) Robust heat shock induces eIF2α-phosphorylation-independent assembly of stress granules containing eIF3 and 40S ribosomal subunits in budding yeast, *Saccharomyces cerevisiae*. *J.Cell.Sci.* 122(12): 2078–2088
Gueydan C *et al.* (1999) Identification of TIAR as a protein binding to the translational regulatory AU-rich element of tumor necrosis factor α mRNA. *J.Biol.Chem.* 274(4): 2322–2326
Guo W *et al.* (2010) Titin diversity—alternative splicing gone wild. *J.Biomed.Biotechnol.* 2010: 753675
Guyon JR *et al.* (2003) Calpain 3 cleaves filamin C and regulates its ability to interact with γ- and δ-sarcoglycans. *Muscle Nerve* 28(4): 472–483

Hackman P *et al.* (2002) Tibial muscular dystrophy is a titinopathy caused by mutations in *TTN*, the gene encoding the giant skeletal-muscle protein titin. *Am.J.Hum.Genet.* 71(3): 492–500
Hackman P *et al.* (2008) Truncating mutations in C-terminal titin may cause more severe tibial muscular dystrophy (TMD). *Neuromuscul.Disord.* 18(12): 922–928
Hackman P *et al.* (2011) Four new Finnish families with LGMD1D; refinement of the clinical phenotype and the linked 7q36 locus. *Neuromuscul.Disord.* 21(5): 338–344
Hageman J *et al.* (2010) A DNAJB chaperone subfamily with HDAC-dependent activities suppresses toxic protein aggregation. *Mol.Cell* 37(3): 355–369
Hageman J *et al.* (2011) The diverse members of the mammalian HSP70 machine show distinct chaperone-like activities. *Biochem.J.* 435(1): 127–142
Halees AS *et al.* (2008) ARED Organism: expansion of ARED reveals AU-rich element cluster variations between human and mouse. *Nucleic Acids Res.* 36(Database issue): D137–40
Hanai R & Mashima K (2003) Characterization of two isoforms of a human DnaJ homologue, HSJ2. *Mol.Biol.Rep.* 30(3): 149–153
Haravuori H *et al.* (2001) Secondary calpain3 deficiency in 2q-linked muscular dystrophy: titin is the candidate gene. *Neurology* 56(7): 869–877
Harms MB *et al.* (2012) Exome sequencing reveals *DNAJB6* mutations in dominantly-inherited myopathy. *Ann.Neurol.* 71(3): 407–416
Hasholt L *et al.* (2003) Antisense downregulation of mutant huntingtin in a cell model. *J.Gene Med.* 5(6): 528–538
Hayashi C *et al.* (2008) Multiple molecular interactions implicate the connectin/titin N2A region as a modulating scaffold for p94/calpain 3 activity in skeletal muscle. *J.Biol.Chem.* 283(21): 14801–14814
Heineke J *et al.* (2005) Attenuation of cardiac remodeling after myocardial infarction by muscle LIM protein-calcineurin signaling at the sarcomeric Z-disc. *Proc.Natl.Acad.Sci.U.S.A.* 102(5): 1655–1660
Helmes M *et al.* (1996) Titin develops restoring force in rat cardiac myocytes. *Circ.Res.* 79(3): 619–626
Herasse M *et al.* (1999) Expression and functional characteristics of calpain 3 isoforms generated through tissue-specific transcriptional and posttranscriptional events. *Mol.Cell.Biol.* 19(6): 4047–4055
HGNC Database. HUGO Gene Nomenclature Committee (HGNC), EMBL Outstation – Hinxton, European Bioinformatics Institute, Hinxton, UK. Accessed 09/2013. Available at: www.genenames.org
Hidalgo C *et al.* (2009) PKC phosphorylation of titin's PEVK element: a novel and conserved pathway for modulating myocardial stiffness. *Circ.Res.* 105(7): 631-8, 17 p following 638
Hidalgo CG *et al.* (2013) The multifunctional Ca^{2+}/calmodulin-dependent protein kinase II delta (CaMKIIδ) phosphorylates cardiac titin's spring elements. *J.Mol.Cell.Cardiol.* 54: 90–97
Hirner S *et al.* (2008) MuRF1-dependent regulation of systemic carbohydrate metabolism as revealed from transgenic mouse studies. *J.Mol.Biol.* 379(4): 666–677
Hishiya A *et al.* (2010) BAG3 and Hsc70 interact with actin capping protein CapZ to maintain myofibrillar integrity under mechanical stress. *Circ.Res.* 107(10): 1220–1231
Hofmann S *et al.* (2012) Translation suppression promotes stress granule formation and cell survival in response to cold shock. *Mol.Biol.Cell* 23(19): 3786–3800
Homma S *et al.* (2006) BAG3 deficiency results in fulminant myopathy and early lethality. *Am.J.Pathol.* 169(3): 761–773
Hopf FW *et al.* (2007) Calcium misregulation and the pathogenesis of muscular dystrophy. *Subcell.Biochem.* 45: 429–464
Horowits R & Podolsky RJ (1987) The positional stability of thick filaments in activated skeletal muscle depends on sarcomere length: evidence for the role of titin filaments. *J.Cell Biol.* 105(5): 2217–2223
Horowits R *et al.* (1989) Elastic behavior of connectin filaments during thick filament movement in activated skeletal muscle. *J.Cell Biol.* 109(5): 2169–2176
Houmeida A *et al.* (1995) Studies of the interaction between titin and myosin. *J.Cell Biol.* 131 (6 Pt 1): 1471–1481
Houmeida A *et al.* (2008) Evidence for the oligomeric state of 'elastic' titin in muscle sarcomeres. *J.Mol.Biol.* 384(2): 299–312
Hua Y & Zhou J (2004) Survival motor neuron protein facilitates assembly of stress granules. *FEBS Lett.* 572(1–3): 69–74

Huang Y *et al.* (2008) Calpain 3 is a modulator of the dysferlin protein complex in skeletal muscle. *Hum.Mol.Genet.* 17(12): 1855–1866
Huebsch KA *et al.* (2005) *Mdm* muscular dystrophy: interactions with calpain 3 and a novel functional role for titin's N2A domain. *Hum.Mol.Genet.* 14(19): 2801–2811
Huizing M *et al.* (2008) Disorders of lysosome-related organelle biogenesis: clinical and molecular genetics. *Annu.Rev.Genomics Hum.Genet.* 9: 359–386
Hurst DR *et al.* (2006) Breast cancer metastasis suppressor 1 (BRMS1) is stabilized by the Hsp90 chaperone. *Biochem.Biophys.Res.Commun.* 348(4): 1429–1435
Izawa I *et al.* (2000) Identification of Mrj, a DnaJ/Hsp40 family protein, as a keratin 8/18 filament regulatory protein. *J.Biol.Chem.* 275(44): 34521–34527
Izquierdo JM *et al.* (2005) Regulation of Fas alternative splicing by antagonistic effects of TIA-1 and PTB on exon definition. *Mol.Cell* 19(4): 475–484
Izquierdo JM & Valcárcel J (2007a) Two isoforms of the T-cell intracellular antigen 1 (TIA-1) splicing factor display distinct splicing regulation activities. Control of TIA-1 isoform ratio by TIA-1-related protein. *J.Biol.Chem.* 282(27): 19410–19417
Izquierdo JM & Valcárcel J (2007b) Fas-activated serine/threonine kinase (FAST K) synergizes with TIA-1/TIAR proteins to regulate Fas alternative splicing. *J.Biol.Chem.* 282(3): 1539–1543
Jaitovich A *et al.* (2008) Ubiquitin-proteasome-mediated degradation of keratin intermediate filaments in mechanically stimulated A549 cells. *J.Biol.Chem.* 283(37): 25348–25355
Jenniches K (2012) Characterisation and functional analysis of novel genes in the striated musculature: LRRC39 and its role for muscle function. Fachbereich Biologie und Chemie, Justus-Liebig-Universität Giessen, Giessen, Germany.
Johannessen M *et al.* (2006) The multifunctional roles of the four-and-a-half-LIM only protein FHL2. *Cell Mol.Life Sci.* 63(3): 268–284
Johnson BS *et al.* (2009) TDP-43 is intrinsically aggregation-prone, and amyotrophic lateral sclerosis-linked mutations accelerate aggregation and increase toxicity. *J.Biol.Chem.* 284(30): 20329–20339
Jones SW *et al.* (1999) Fibre type-specific expression of p94, a skeletal muscle-specific calpain. *J.Muscle Res.Cell.Motil.* 20(4): 417–424
Kaisto T *et al.* (1999) Endocytosis in skeletal muscle fibers. *Exp.Cell Res.* 253(2): 551–560
Kalani MY *et al.* (2008) Wnt-mediated self-renewal of neural stem/progenitor cells. *Proc.Natl.Acad.Sci.U.S.A.* 105(44): 16970–16975
Kampinga HH & Craig EA (2010) The HSP70 chaperone machinery: J proteins as drivers of functional specificity. *Nat.Rev.Mol.Cell Biol.* 11(8): 579–592
Kang PB *et al.* (2005) Variations in gene expression among different types of human skeletal muscle. *Muscle Nerve* 32(4): 483–491
Kaplan J-C & Hamroun D (2012) The 2013 version of the gene table of neuromuscular disorders (nuclear genome). *Neuromuscul.Disord.* 22(12): 1108–1135
Kappé G *et al.* (2001) Characterization of two novel human small heat shock proteins: protein kinase-related HspB8 and testis-specific HspB9. *Biochim.Biophys.Acta* 1520(1): 1–6
Kasper CE & Xun L (2000) Expression of titin in skeletal muscle varies with hind-limb unloading. *Biol.Res.Nurs.* 2(2): 107–115
Kawabata Y *et al.* (2003) Newly identified exons encoding novel variants of p94/calpain 3 are expressed ubiquitously and overlap the α-glucosidase C gene. *FEBS Lett.* 555(3): 623–630
Kawakami A *et al.* (1992) Identification and functional characterization of a TIA-1-related nucleolysin. *Proc.Natl.Acad.Sci.U.S.A.* 89(18): 8681–8685
Kawakami A *et al.* (1994) Intron-exon organization and chromosomal localization of the human TIA-1 gene. *J.Immunol.* 152(10): 4937–4945
Kedar V *et al.* (2004) Muscle-specific RING finger 1 is a bona fide ubiquitin ligase that degrades cardiac troponin I. *Proc.Natl.Acad.Sci.U.S.A.* 101(52): 18135–18140
Kedersha N *et al.* (2000) Dynamic shuttling of TIA-1 accompanies the recruitment of mRNA to mammalian stress granules. *J.Cell Biol.* 151(6): 1257–1268
Kedersha N *et al.* (2002) Evidence that ternary complex (eIF2-GTP-$tRNA_i^{Met}$)-deficient preinitiation complexes are core constituents of mammalian stress granules. *Mol.Biol.Cell* 13(1): 195–210
Kedersha N *et al.* (2005) Stress granules and processing bodies are dynamically linked sites of mRNP remodeling. *J.Cell Biol.* 169(6): 871–884
Kedersha NL *et al.* (1999) RNA-binding proteins TIA-1 and TIAR link the phosphorylation of eIF-2α to the assembly of mammalian stress granules. *J.Cell Biol.* 147(7): 1431–1442

Keira Y *et al.* (2003) Localization of calpain 3 in human skeletal muscle and its alteration in limb-girdle muscular dystrophy 2A muscle. *J.Biochem.(Tokyo)* 133(5): 659–664
Keller A *et al.* (2000) Fibre-type distribution and subcellular localisation of α and β enolase in mouse striated muscle. *Biol.Cell.* 92(7): 527–535
Kielbasa OM *et al.* (2011) Myospryn is a calcineurin-interacting protein that negatively modulates slow-fiber-type transformation and skeletal muscle regeneration. *FASEB J.* 25(7): 2276–2286
Kim HJ *et al.* (2013) Mutations in prion-like domains in hnRNPA2B1 and hnRNPA1 cause multisystem proteinopathy and ALS. *Nature* 495(7442): 467–473
Kim WY *et al.* (2005a) Evidence for sequestration of polyglutamine inclusions by *Drosophila* myeloid leukemia factor. *Mol.Cell.Neurosci.* 29(4): 536–544
Kim WJ *et al.* (2005b) Sequestration of TRAF2 into stress granules interrupts tumor necrosis factor signaling under stress conditions. *Mol.Cell.Biol.* 25(6): 2450–2462
Kinbara K *et al.* (1997) Muscle-specific calpain, p94, interacts with the extreme C-terminal region of connectin, a unique region flanked by two immunoglobulin C2 motifs. *Arch.Biochem. Biophys.* 342(1): 99–107
Kinbara K *et al.* (1998) Purification of native p94, a muscle-specific calpain, and characterization of its autolysis. *Biochem.J.* 335(3): 589–596
King L & Jhou CR (2010) Nuclear titin interacts with histones. *Chang Gung Med.J.* 33(2): 201–210
Klar J *et al.* (2013) Welander distal myopathy caused by an ancient founder mutation in *TIA1* associated with perturbed splicing. *Hum.Mutat.* 34(4): 572–577
Knöll R *et al.* (2002) The cardiac mechanical stretch sensor machinery involves a Z disc complex that is defective in a subset of human dilated cardiomyopathy. *Cell* 111(7): 943–955
Knöll R *et al.* (2011) Telethonin deficiency is associated with maladaptation to biomechanical stress in the mammalian heart. *Circ.Res.* 109(7): 758–769
Kojic S *et al.* (2004) The Ankrd2 protein, a link between the sarcomere and the nucleus in skeletal muscle. *J.Mol.Biol.* 339(2): 313–325
Kojic S *et al.* (2011) Muscle ankyrin repeat proteins: their role in striated muscle function in health and disease. *Crit.Rev.Clin.Lab.Sci.* 48(5–6): 269–294
Kolmerer B *et al.* (1996) Genomic organization of M line titin and its tissue-specific expression in two distinct isoforms. *J.Mol.Biol.* 256(3): 556–563
Kölsch A *et al.* (2010) The keratin-filament cycle of assembly and disassembly. *J.Cell.Sci.* 123(13): 2266–2272
Kong Y *et al.* (1997) Muscle LIM protein promotes myogenesis by enhancing the activity of MyoD. *Mol.Cell.Biol.* 17(8): 4750–4760
Kontrogianni-Konstantopoulos A & Bloch RJ (2003) The hydrophilic domain of small ankyrin-1 interacts with the two N-terminal immunoglobulin domains of titin. *J.Biol.Chem.* 278(6): 3985–3991
Kontrogianni-Konstantopoulos A *et al.* (2003) Obscurin is a ligand for small ankyrin 1 in skeletal muscle. *Mol.Biol.Cell* 14(3): 1138–1148
Kontrogianni-Konstantopoulos A *et al.* (2006a) De novo myofibrillogenesis in C_2C_{12} cells: evidence for the independent assembly of M bands and Z disks. *Am.J.Physiol.Cell.Physiol.* 290(2): C626–37
Kontrogianni-Konstantopoulos A *et al.* (2006b) Obscurin modulates the assembly and organization of sarcomeres and the sarcoplasmic reticulum. *FASEB J.* 20(12): 2102–2111
Kontrogianni-Konstantopoulos A *et al.* (2009) Muscle giants: molecular scaffolds in sarcomerogenesis. *Physiol.Rev.* 89(4): 1217–1267
Kouloumenta A *et al.* (2007) Proper perinuclear localization of the TRIM-like protein myospryn requires its binding partner desmin. *J.Biol.Chem.* 282(48): 35211–35221
Koyama S *et al.* (2008) Muscle RING-finger protein-1 (MuRF1) as a connector of muscle energy metabolism and protein synthesis. *J.Mol.Biol.* 376(5): 1224–1236
Kramerova I *et al.* (2004) Null mutation of calpain 3 (p94) in mice causes abnormal sarcomere formation *in vivo* and *in vitro*. *Hum.Mol.Genet.* 13(13): 1373–1388
Kramerova I *et al.* (2005) Calpain 3 participates in sarcomere remodeling by acting upstream of the ubiquitin-proteasome pathway. *Hum.Mol.Genet.* 14(15): 2125–2134
Kramerova I *et al.* (2006) Regulation of the M-cadherin-β-catenin complex by calpain 3 during terminal stages of myogenic differentiation. *Mol.Cell.Biol.* 26(22): 8437–8447
Kramerova I *et al.* (2007) Molecular and cellular basis of calpainopathy (limb girdle muscular dystrophy type 2A). *Biochim.Biophys.Acta* 1772(2): 128–144

Kramerova I *et al.* (2008) Novel role of calpain-3 in the triad-associated protein complex regulating calcium release in skeletal muscle. *Hum.Mol.Genet.* 17(21): 3271–3280
Kramerova I *et al.* (2012) Impaired calcium calmodulin kinase signaling and muscle adaptation response in the absence of calpain 3. *Hum.Mol.Genet.* 21(14): 3193–3204
Krüger M *et al.* (2009) Protein kinase G modulates human myocardial passive stiffness by phosphorylation of the titin springs. *Circ.Res.* 104(1): 87–94
Kulke M *et al.* (2001) Interaction between PEVK-titin and actin filaments: origin of a viscous force component in cardiac myofibrils. *Circ.Res.* 89(10): 874–881
Labeit D *et al.* (2003) Calcium-dependent molecular spring elements in the giant protein titin. *Proc.Natl.Acad.Sci.U.S.A.* 100(23): 13716–13721
Labeit S *et al.* (1992) Towards a molecular understanding of titin. *EMBO J.* 11(5): 1711–1716
Labeit S & Kolmerer B (1995) Titins: giant proteins in charge of muscle ultrastructure and elasticity. *Science* 270(5234): 293–296
Labeit S *et al.* (2006) Expression of distinct classes of titin isoforms in striated and smooth muscles by alternative splicing, and their conserved interaction with filamins. *J.Mol.Biol.* 362(4): 664–681
Lahmers S *et al.* (2004) Developmental control of titin isoform expression and passive stiffness in fetal and neonatal myocardium. *Circ.Res.* 94(4): 505–513
Lange S *et al.* (2002) Subcellular targeting of metabolic enzymes to titin in heart muscle may be mediated by DRAL/FHL-2. *J.Cell.Sci.* 115(24): 4925–4936
Lange S *et al.* (2005a) The kinase domain of titin controls muscle gene expression and protein turnover. *Science* 308(5728): 1599–1603
Lange S *et al.* (2005b) Dimerisation of myomesin: implications for the structure of the sarcomeric M-band. *J.Mol.Biol.* 345(2): 289–298
Lange S *et al.* (2009) Obscurin determines the architecture of the longitudinal sarcoplasmic reticulum. *J.Cell.Sci.* 122(15): 2640–2650
Lange S *et al.* (2012) Obscurin and KCTD6 regulate cullin-dependent small ankyrin-1 (sAnk1.5) protein turnover. *Mol.Biol.Cell* 23(13): 2490–2504
Larimore J *et al.* (2011) The schizophrenia susceptibility factor dysbindin and its associated complex sort cargoes from cell bodies to the synapse. *Mol.Biol.Cell* 22(24): 4854–4867
Laure L *et al.* (2010) A new pathway encompassing calpain 3 and its newly identified substrate cardiac ankyrin repeat protein is involved in the regulation of the nuclear factor-κB pathway in skeletal muscle. *FEBS J.* 277(20): 4322–4337
Le Guiner C *et al.* (2001) TIA-1 and TIAR activate splicing of alternative exons with weak 5' splice sites followed by a U-rich stretch on their own pre-mRNAs. *J.Biol.Chem.* 276(44): 40638–40646
Le Guiner C *et al.* (2003) TIA-1 or TIAR is required for DT40 cell viability. *J.Biol.Chem.* 278(12): 10465–10476
Li M *et al.* (2011) A common variant of the cardiomyopathy associated 5 gene (*CMYA5*) is associated with schizophrenia in Chinese population. *Schizophr.Res.* 129(2–3): 217–219
Li W *et al.* (2002) Cell proteins TIA-1 and TIAR interact with the 3' stem-loop of the West Nile virus complementary minus-strand RNA and facilitate virus replication. *J.Virol.* 76(23): 11989–12000
Li W *et al.* (2003) Hermansky-Pudlak syndrome type 7 (HPS-7) results from mutant dysbindin, a member of the biogenesis of lysosome-related organelles complex 1 (BLOC-1). *Nat.Genet.* 35(1): 84–89
Li W *et al.* (2004) FAST is a survival protein that senses mitochondrial stress and modulates TIA-1-regulated changes in protein expression. *Mol.Cell.Biol.* 24(24): 10718–10732
Li W *et al.* (2013) Fas-activated Ser/Thr phosphoprotein (FAST) is a eukaryotic initiation factor 4E-binding protein that regulates mRNA stability and cell survival. *Translation* 1: e24047
Li ZF *et al.* (2008) Non-pathogenic protein aggregates in skeletal muscle in MLF1 transgenic mice. *J.Neurol.Sci.* 264(1–2): 77–86
Lin X *et al.* (2006) Failure of MBNL1-dependent post-natal splicing transitions in myotonic dystrophy. *Hum.Mol.Genet.* 15(13): 2087–2097
Linke WA *et al.* (1997) Actin-titin interaction in cardiac myofibrils: probing a physiological role. *Biophys.J.* 73(2): 905–919
Linke WA *et al.* (1998) Characterizing titin's I-band Ig domain region as an entropic spring. *J.Cell.Sci.* 111(11): 1567–1574

Linke WA *et al.* (1999) I-band titin in cardiac muscle is a three-element molecular spring and is critical for maintaining thin filament structure. *J.Cell Biol.* 146(3): 631–644
Liu-Yesucevitz L *et al.* (2010) Tar DNA binding protein-43 (TDP-43) associates with stress granules: analysis of cultured cells and pathological brain tissue. *PLoS One* 5(10): e13250
Liversage AD *et al.* (2001) Titin and the sarcomere symmetry paradox. *J.Mol.Biol.* 305(3): 401–409
López de Silanes I *et al.* (2005) Identification and functional outcome of mRNAs associated with RNA-binding protein TIA-1. *Mol.Cell.Biol.* 25(21): 9520–9531
Loschi M *et al.* (2009) Dynein and kinesin regulate stress-granule and P-body dynamics. *J.Cell. Sci.* 122(21): 3973–3982
Ma K *et al.* (2001) Polyproline II helix is a key structural motif of the elastic PEVK segment of titin. *Biochemistry* 40(12): 3427–3438
Ma K & Wang K (2003) Malleable conformation of the elastic PEVK segment of titin: non-co-operative interconversion of polyproline II helix, β-turn and unordered structures. *Biochem.J.* 374(3): 687–695
Machado C *et al.* (1998) Human autoantibodies reveal titin as a chromosomal protein. *J.Cell Biol.* 141(2): 321–333
Machado C & Andrew DJ (2000) D-Titin: a giant protein with dual roles in chromosomes and muscles. *J.Cell Biol.* 151(3): 639–652
Marley A & von Zastrow M (2010) Dysbindin promotes the post-endocytic sorting of G protein-coupled receptors to lysosomes. *PLoS One* 5(2): e9325
Maruyama K (1976) Connectin, an elastic protein from myofibrils. *J.Biochem.* 80(2): 405–407
Masuda K *et al.* (2009) Tissue- and age-dependent expression of RNA-binding proteins that influence mRNA turnover and translation. *Aging* 1(8): 681–698
Matsuki H *et al.* (2013) Both G3BP1 and G3BP2 contribute to stress granule formation. *Genes Cells* 18(2): 135–146
Mayans O *et al.* (1998) Structural basis for activation of the titin kinase domain during myofibrillogenesis. *Nature* 395(6705): 863–869
Mazroui R *et al.* (2006) Inhibition of ribosome recruitment induces stress granule formation independently of eukaryotic initiation factor 2α phosphorylation. *Mol.Biol.Cell* 17(10): 4212–4219
McAlinden A *et al.* (2007) Nuclear protein TIA-1 regulates COL2A1 alternative splicing and interacts with precursor mRNA and genomic DNA. *J.Biol.Chem.* 282(33): 24444–24454
McCampbell A *et al.* (2000) CREB-binding protein sequestration by expanded polyglutamine. *Hum.Mol.Genet.* 9(14): 2197–2202
McDonald KK *et al.* (2011) TAR DNA-binding protein 43 (TDP-43) regulates stress granule dynamics via differential regulation of G3BP and TIA-1. *Hum.Mol.Genet.* 20(7): 1400–1410
McElhinny AS *et al.* (2002) Muscle-specific RING finger-1 interacts with titin to regulate sarcomeric M-line and thick filament structure and may have nuclear functions via its interaction with glucocorticoid modulatory element binding protein-1. *J.Cell Biol.* 157(1): 125–136
McElhinny AS *et al.* (2004) Muscle-specific RING finger-2 (MURF-2) is important for microtubule, intermediate filament and sarcomeric M-line maintenance in striated muscle development. *J.Cell.Sci.* 117(15): 3175–3188
McKoy G *et al.* (2002) Identification of a novel stretch-sensitive SPRY domain-coding gene in skeletal muscle. In Abstracts: 31st Annual Meeting of the European Society for Muscle Research – Lunteren, The Netherlands 14–17 September 2002. *J.Muscle Res.Cell Motil.* 23(1):44
Medley QG *et al.* (1996) Characterization of GMP-17, a granule membrane protein that moves to the plasma membrane of natural killer cells following target cell recognition. *Proc.Natl.Acad. Sci.U.S.A.* 93(2): 685–689
Mercuri E & Muntoni F (2013) Muscular dystrophies. *The Lancet* 381(9869): 845–860
Mihatsch K *et al.* (2009) Proapoptotic protein Siva binds to the muscle protein telethonin in cardiomyocytes during coxsackieviral infection. *Cardiovasc.Res.* 81(1): 108–115
Mikelsaar AV *et al.* (2010) Titin A-band-specific monoclonal antibody Tit1 5H1.1. Cellular Titin as a centriolar protein in non-muscle cells. *Hybridoma (Larchmt)* 29(5): 391–401
Mikelsaar AV *et al.* (2012) Epitope of titin A-band-specific monoclonal antibody Tit1 5 H1.1 is highly conserved in several Fn3 domains of the titin molecule. Centriole staining in human, mouse and zebrafish cells. *Cell.Div.* 7(1): 21-1028-7-21
Miller G *et al.* (2003a) A targeted deletion of the C-terminal end of titin, including the titin kinase domain, impairs myofibrillogenesis. *J.Cell.Sci.* 116(23): 4811–4819

Miller MK *et al.* (2003b) The muscle ankyrin repeat proteins: CARP, ankrd2/Arpp and DARP as a family of titin filament-based stress response molecules. *J.Mol.Biol.* 333(5): 951–964
MIM database. Mendelian Inheritance in Man, OMIM. McKusick-Nathans Institute of Genetic Medicine, Johns Hopkins University, Baltimore, MD, USA. Available at: http://omim.org/
Minajeva A *et al.* (2001) Unfolding of titin domains explains the viscoelastic behavior of skeletal myofibrils. *Biophys.J.* 80(3): 1442–1451
Mitra A *et al.* (2008) Large isoform of MRJ (DNAJB6) reduces malignant activity of breast cancer. *Breast Cancer Res.* 10(2): R22
Mitra A *et al.* (2010) DNAJB6 induces degradation of β-catenin and causes partial reversal of mesenchymal phenotype. *J.Biol.Chem.* 285(32): 24686–24694
Mitra A *et al.* (2012) DNAJB6 chaperones PP2A mediated dephosphorylation of GSK3β to downregulate β-catenin transcription target, osteopontin. *Oncogene* 31(41): 4472–4483
Mollet S *et al.* (2008) Translationally repressed mRNA transiently cycles through stress granules during stress. *Mol.Biol.Cell* 19(10): 4469–4479
Mologni L *et al.* (2005) Characterization of mouse myotilin and its promoter. *Biochem.Biophys. Res.Commun.* 329(3): 1001–1009
Morgan NV *et al.* (2006) A germline mutation in BLOC1S3/reduced pigmentation causes a novel variant of Hermansky-Pudlak syndrome (HPS8). *Am.J.Hum.Genet.* 78(1): 160–166
Morris DW *et al.* (2008) Dysbindin (DTNBP1) and the biogenesis of lysosome-related organelles complex 1 (BLOC-1): main and epistatic gene effects are potential contributors to schizophrenia susceptibility. *Biol.Psychiatry* 63(1): 24–31
Morton JP *et al.* (2009) The exercise-induced stress response of skeletal muscle, with specific emphasis on humans. *Sports Med.* 39(8): 643–662
Mrosek M *et al.* (2007) Molecular determinants for the recruitment of the ubiquitin-ligase MuRF-1 onto M-line titin. *FASEB J.* 21(7): 1383–1392
Muchowski PJ *et al.* (2000) Hsp70 and Hsp40 chaperones can inhibit self-assembly of polyglutamine proteins into amyloid-like fibrils. *Proc.Natl.Acad.Sci.U.S.A.* 97(14): 7841–7846
Muhle-Goll C *et al.* (2001) Structural and functional studies of titin's fn3 modules reveal conserved surface patterns and binding to myosin S1–a possible role in the Frank-Starling mechanism of the heart. *J.Mol.Biol.* 313(2): 431–447
Mullin AP *et al.* (2011) Cell biology of the BLOC-1 complex subunit dysbindin, a schizophrenia susceptibility gene. *Mol.Neurobiol.* 44(1): 53–64
Murphy RM *et al.* (2006) μ-Calpain and calpain-3 are not autolyzed with exhaustive exercise in humans. *Am.J.Physiol.Cell.Physiol.* 290(1): C116–22
Murphy RM *et al.* (2007) Calpain-3 is autolyzed and hence activated in human skeletal muscle 24 h following a single bout of eccentric exercise. *J.Appl.Physiol.* 103(3): 926–931
Murphy RM & Lamb GD (2009) Endogenous calpain-3 activation is primarily governed by small increases in resting cytoplasmic [Ca^{2+}] and is not dependent on stretch. *J.Biol.Chem.* 284(12): 7811–7819
Murphy RM *et al.* (2011) Activation of skeletal muscle calpain-3 by eccentric exercise in humans does not result in its translocation to the nucleus or cytosol. *J.Appl.Physiol.* 111(5): 1448–1458
Musa H *et al.* (2006) Targeted homozygous deletion of M-band titin in cardiomyocytes prevents sarcomere formation. *J.Cell.Sci.* 119(20): 4322–4331
Nakano N *et al.* (2007) Interaction of BMP10 with Tcap may modulate the course of hypertensive cardiac hypertrophy. *Am.J.Physiol.Heart Circ.Physiol.* 293(6): H3396–403
Nakano S *et al.* (2005) Messenger RNA degradation may be inhibited in sporadic inclusion body myositis. *Neurology* 65(3): 420–425
Nave R *et al.* (1989) Visualization of the polarity of isolated titin molecules: a single globular head on a long thin rod as the M band anchoring domain? *J.Cell Biol.* 109(5): 2177–2187
Nazarian R *et al.* (2006) Reinvestigation of the dysbindin subunit of BLOC-1 (biogenesis of lysosome-related organelles complex-1) as a dystrobrevin-binding protein. *Biochem.J.* 395(3): 587–598
Neagoe C *et al.* (2002) Titin isoform switch in ischemic human heart disease. *Circulation* 106(11): 1333–1341
Nicholas G *et al.* (2002) Titin-cap associates with, and regulates secretion of, Myostatin. *J.Cell. Physiol.* 193(1): 120–131
Norton N *et al.* (2011) Genome-wide studies of copy number variation and exome sequencing identify rare variants in *BAG3* as a cause of dilated cardiomyopathy. *Am.J.Hum.Genet.* 88(3): 273–282

Obermann WM *et al.* (1995) Purification and biochemical characterization of myomesin, a myosin-binding and titin-binding protein, from bovine skeletal muscle. *Eur.J.Biochem.* 233(1): 110–115

Obermann WM *et al.* (1996) The structure of the sarcomeric M band: localization of defined domains of myomesin, M-protein, and the 250-kD carboxy-terminal region of titin by immunoelectron microscopy. *J.Cell Biol.* 134(6): 1441–1453

Obermann WM *et al.* (1997) Molecular structure of the sarcomeric M band: mapping of titin and myosin binding domains in myomesin and the identification of a potential regulatory phosphorylation site in myomesin. *EMBO J.* 16(2): 211–220

Obermann WM *et al.* (1998) Mapping of a myosin-binding domain and a regulatory phosphorylation site in M-protein, a structural protein of the sarcomeric M band. *Mol.Biol.Cell* 9(4): 829–840

Ochala J *et al.* (2011) Preferential skeletal muscle myosin loss in response to mechanical silencing in a novel rat intensive care unit model: underlying mechanisms. *J.Physiol.* 589(8): 2007–2026

Ohlsson M *et al.* (2012) Hereditary myopathy with early respiratory failure associated with a mutation in A-band titin. *Brain* 135(6): 1682–1694

Ojima K *et al.* (2005) Possible functions of p94 in connectin-mediated signaling pathways in skeletal muscle cells. *J.Muscle Res.Cell.Motil.* 26(6–8): 409–417

Ojima K *et al.* (2007) Myogenic stage, sarcomere length, and protease activity modulate localization of muscle-specific calpain. *J.Biol.Chem.* 282(19): 14493–14504

Ojima K *et al.* (2010) Dynamic distribution of muscle-specific calpain in mice has a key role in physical-stress adaptation and is impaired in muscular dystrophy. *J.Clin.Invest.* 120(8): 2672–2683

Ojima K *et al.* (2011) Non-proteolytic functions of calpain-3 in sarcoplasmic reticulum in skeletal muscles. *J.Mol.Biol.* 407(3): 439–449

O'Neill A *et al.* (2002) Sarcolemmal organization in skeletal muscle lacking desmin: evidence for cytokeratins associated with the membrane skeleton at costameres. *Mol.Biol.Cell* 13(7): 2347–2359

Ono Y *et al.* (1998) Functional defects of a muscle-specific calpain, p94, caused by mutations associated with limb-girdle muscular dystrophy type 2A. *J.Biol.Chem.* 273(27): 17073–17078

Ono Y *et al.* (2004) Possible regulation of the conventional calpain system by skeletal muscle-specific calpain, p94/calpain 3. *J.Biol.Chem.* 279(4): 2761–2771

Ono Y *et al.* (2006) Suppressed disassembly of autolyzing p94/CAPN3 by N2A connectin/titin in a genetic reporter system. *J.Biol.Chem.* 281(27): 18519–18531

Ono Y *et al.* (2008) The importance of conserved amino acid residues in p94 protease sub-domain IIb and the IS2 region for constitutive autolysis. *FEBS Lett.* 582(5): 691–698

Ono Y *et al.* (2010) Skeletal muscle-specific calpain is an intracellular Na^+-dependent protease. *J.Biol.Chem.* 285(30): 22986–22998

Ono Y & Sorimachi H (2012) Calpains: an elaborate proteolytic system. *Biochim.Biophys.Acta* 1824(1): 224–236

Ottenheijm CA *et al.* (2009) Altered contractility of skeletal muscle in mice deficient in titin's M-band region. *J.Mol.Biol.* 393(1): 10–26

Ougland R *et al.* (2012) ALKBH1 is a histone H2A dioxygenase involved in neural differentiation. *Stem Cells* 30(12): 2672–2682

Pan Z *et al.* (2008) Impaired placental trophoblast lineage differentiation in $Alkbh1^{-/-}$ mice. *Dev.Dyn.* 237(2): 316–327

Parker R & Sheth U (2007) P bodies and the control of mRNA translation and degradation. *Mol. Cell* 25(5): 635–646

Peng J *et al.* (2005) Muscle atrophy in Titin M-line deficient mice. *J.Muscle Res.Cell.Motil.* 26(6–8): 381–388

Peng J *et al.* (2007) Cardiac hypertrophy and reduced contractility in hearts deficient in the titin kinase region. *Circulation* 115(6): 743–751

Pénisson-Besnier I *et al.* (2010) Myopathies caused by homozygous titin mutations: limb-girdle muscular dystrophy 2J and variations of phenotype. *J.Neurol.Neurosurg.Psychiatry.* 81(11): 1200–1202

Perales-Calvo J *et al.* (2010) Role of DnaJ G/F-rich domain in conformational recognition and binding of protein substrates. *J.Biol.Chem.* 285(44): 34231–34239

Perera S *et al.* (2011) Developmental regulation of MURF ubiquitin ligases and autophagy proteins nbr1, p62/SQSTM1 and LC3 during cardiac myofibril assembly and turnover. *Dev.Biol.* 351(1): 46–61
Perera S *et al.* (2012) Developmental regulation of MURF E3 ubiquitin ligases in skeletal muscle. *J.Muscle Res.Cell.Motil.* 33(2): 107–122
Perez-Ruiz A *et al.* (2008) β-Catenin promotes self-renewal of skeletal-muscle satellite cells. *J.Cell.Sci.* 121(9): 1373–1382
Pfeffer G *et al.* (2012) Titin mutation segregates with hereditary myopathy with early respiratory failure. *Brain* 135(6): 1695–1713
Phillips K *et al.* (2004) Arthritis suppressor genes TIA-1 and TTP dampen the expression of tumor necrosis factor α, cyclooxygenase 2, and inflammatory arthritis. *Proc.Natl.Acad.Sci.U.S.A.* 101(7): 2011–2016
Piecyk M *et al.* (2000) TIA-1 is a translational silencer that selectively regulates the expression of TNF-α. *EMBO J.* 19(15): 4154–4163
Pinotsis N *et al.* (2008) Molecular basis of the C-terminal tail-to-tail assembly of the sarcomeric filament protein myomesin. *EMBO J.* 27(1): 253–264
Pizon V *et al.* (2002) Transient association of titin and myosin with microtubules in nascent myofibrils directed by the MURF2 RING-finger protein. *J.Cell.Sci.* 115(23): 4469–4482
Polge C *et al.* (2011) Muscle actin is polyubiquitinylated *in vitro* and *in vivo* and targeted for breakdown by the E3 ligase MuRF1. *FASEB J.* 25(11): 3790–3802
Pollazzon M *et al.* (2010) The first Italian family with tibial muscular dystrophy caused by a novel titin mutation. *J.Neurol.* 257(4): 575–579
Porter GA *et al.* (1992) Dystrophin colocalizes with β-spectrin in distinct subsarcolemmal domains in mammalian skeletal muscle. *J.Cell Biol.* 117(5): 997–1005
Prado LG *et al.* (2005) Isoform diversity of giant proteins in relation to passive and active contractile properties of rabbit skeletal muscles. *J.Gen.Physiol.* 126(5): 461–480
Puchner EM *et al.* (2008) Mechanoenzymatics of titin kinase. *Proc.Natl.Acad.Sci.U.S.A.* 105(36): 13385–13390
Puchner EM & Gaub HE (2010) Exploring the conformation-regulated function of titin kinase by mechanical pump and probe experiments with single molecules. *Angew.Chem.Int.Ed Engl.* 49(6): 1147–1150
Pullmann R,Jr *et al.* (2007) Analysis of turnover and translation regulatory RNA-binding protein expression through binding to cognate mRNAs. *Mol.Cell.Biol.* 27(18): 6265–6278
Qi J *et al.* (2008) Nuclear localization of the titin Z1Z2Zr domain and role in regulating cell proliferation. *Am.J.Physiol.Cell.Physiol.* 295(4): C975–85
Qian SB *et al.* (2006) CHIP-mediated stress recovery by sequential ubiquitination of substrates and Hsp70. *Nature* 440(7083): 551–555
Qiu XB *et al.* (2006) The diversity of the DnaJ/Hsp40 family, the crucial partners for Hsp70 chaperones. *Cell Mol.Life Sci.* 63(22): 2560–2570
Raeker MO *et al.* (2006) Obscurin is required for the lateral alignment of striated myofibrils in zebrafish. *Dev.Dyn.* 235(8): 2018–2029
Rahimov F & Kunkel LM (2013) The cell biology of disease: cellular and molecular mechanisms underlying muscular dystrophy. *J.Cell Biol.* 201(4): 499–510
Randazzo D *et al.* (2013) Obscurin is required for ankyrinB-dependent dystrophin localization and sarcolemma integrity. *J.Cell Biol.* 200(4): 523–536
Raskin A *et al.* (2012) A novel mechanism involving four-and-a-half LIM domain protein-1 and extracellular signal-regulated kinase-2 regulates titin phosphorylation and mechanics. *J.Biol.Chem.* 287(35): 29273–29284
Ravulapalli R *et al.* (2005) Homodimerization of calpain 3 penta-EF-hand domain. *Biochem.J.* 388(2): 585–591
Raynaud F *et al.* (2004) Evidence for a direct but sequential binding of titin to tropomyosin and actin filaments. *Biochim.Biophys.Acta* 1700(2): 171–178
RefSeq database. US National Institutes of Health, Bethesda, MD, USA. Available at: http://www.ncbi.nlm.nih.gov/refseq/
Rey MA & Davies PL (2002) The protease core of the muscle-specific calpain, p94, undergoes Ca^{2+}-dependent intramolecular autolysis. *FEBS Lett.* 532(3): 401–406
Reyes R *et al.* (2009) Depletion of T-cell intracellular antigen proteins promotes cell proliferation. *Genome Biol.* 10(8): R87

Reynolds JG *et al.* (2007) Identification and mapping of protein kinase A binding sites in the costameric protein myospryn. *Biochim.Biophys.Acta* 1773(6): 891–902
Reynolds JG *et al.* (2008) Deregulated protein kinase A signaling and myospryn expression in muscular dystrophy. *J.Biol.Chem.* 283(13): 8070–8074
Richard I *et al.* (1995) Mutations in the proteolytic enzyme calpain 3 cause limb-girdle muscular dystrophy type 2A. *Cell* 81(1): 27–40
Richard I *et al.* (2000) Loss of calpain 3 proteolytic activity leads to muscular dystrophy and to apoptosis-associated IκBα/nuclear factor κB pathway perturbation in mice. *J.Cell Biol.* 151(7): 1583–1590
Rose JM *et al.* (2011) Molecular chaperone-mediated rescue of mitophagy by a Parkin RING1 domain mutant. *Hum.Mol.Genet.* 20(1): 16–27
Ryder PV *et al.* (2013) The WASH Complex, an Endosomal Arp2/3 Activator, Interacts with the Hermansky-Pudlak Syndrome Complex BLOC-1 and its Cargo Phosphatidylinositol-4-kinase Type II Alpha. *Mol.Biol.Cell* 24(14):2269–2284
Sakuma K & Yamaguchi A (2010) The functional role of calcineurin in hypertrophy, regeneration, and disorders of skeletal muscle. *J.Biomed.Biotechnol.* 2010: 721219
Sandell S *et al.* (2010) The enigma of 7q36 linked autosomal dominant limb girdle muscular dystrophy. *J.Neurol.Neurosurg.Psychiatry.* 81(8): 834–839
Sarparanta J (2008) Biology of myospryn: what's known? *J.Muscle Res.Cell.Motil.* 29(6–8): 177–180
Sato T *et al.* (2013) DNAJB6 myopathy in an Asian cohort and cytoplasmic/nuclear inclusions. *Neuromuscul.Disord.* 23(3): 269–276
Satoh M *et al.* (1999) Structural analysis of the titin gene in hypertrophic cardiomyopathy: identification of a novel disease gene. *Biochem.Biophys.Res.Commun.* 262(2): 411–417
Schoenauer R *et al.* (2005) Myomesin is a molecular spring with adaptable elasticity. *J.Mol.Biol.* 349(2): 367–379
Schoenauer R *et al.* (2008) Myomesin 3, a novel structural component of the M-band in striated muscle. *J.Mol.Biol.* 376(2): 338–351
Scholl FA *et al.* (2000) DRAL is a p53-responsive gene whose four and a half LIM domain protein product induces apoptosis. *J.Cell Biol.* 151(3): 495–506
Schreiber KH & Kennedy BK (2013) When lamins go bad: nuclear structure and disease. *Cell* 152(6): 1365–1375
Schröder R & Schoser B (2009) Myofibrillar myopathies: a clinical and myopathological guide. *Brain Pathol.* 19(3): 483–492
Schwarz ML *et al.* (2008) Titin expression in human articular cartilage and cultured chondrocytes: a novel component in articular cartilage biomechanical sensing? *Biomed.Pharmacother.* 62(5): 339–347
Seki N *et al.* (1999) Cloning, tissue expression, and chromosomal assignment of human MRJ gene for a member of the DNAJ protein family. *J.Hum.Genet.* 44(3): 185–189
Selcen D *et al.* (2009) Mutation in *BAG3* causes severe dominant childhood muscular dystrophy. *Ann.Neurol.* 65(1): 83–89
Selcen D (2011) Myofibrillar myopathies. *Neuromuscul.Disord.* 21(3): 161–171
Setty SR *et al.* (2007) BLOC-1 is required for cargo-specific sorting from vacuolar early endosomes toward lysosome-related organelles. *Mol.Biol.Cell* 18(3): 768–780
Shathasivam T *et al.* (2010) Genes, proteins and complexes: the multifaceted nature of FHL family proteins in diverse tissues. *J.Cell.Mol.Med.* 14(12): 2702–2720
Sheikh F *et al.* (2008) An FHL1-containing complex within the cardiomyocyte sarcomere mediates hypertrophic biomechanical stress responses in mice. *J.Clin.Invest.* 118(12): 3870–3880
Shimohata T *et al.* (2000) Expanded polyglutamine stretches interact with TAFII130, interfering with CREB-dependent transcription. *Nat.Genet.* 26(1): 29–36
Singh NN *et al.* (2011) TIA1 prevents skipping of a critical exon associated with spinal muscular atrophy. *Mol.Cell.Biol.* 31(5): 935–954
Sitaram A *et al.* (2012) Differential recognition of a dileucine-based sorting signal by AP-1 and AP-3 reveals a requirement for both BLOC-1 and AP-3 in delivery of OCA2 to melanosomes. *Mol.Biol.Cell* 23(16): 3178–3192
Sorimachi H *et al.* (1989) Molecular cloning of a novel mammalian calcium-dependent protease distinct from both m- and μ-types. Specific expression of the mRNA in skeletal muscle. *J.Biol.Chem.* 264(33): 20106–20111

Sorimachi H *et al.* (1990) A novel member of the calcium-dependent cysteine protease family. *Biol.Chem.Hoppe Seyler* 371 Suppl: 171–176
Sorimachi H *et al.* (1993) Muscle-specific calpain, p94, is degraded by autolysis immediately after translation, resulting in disappearance from muscle. *J.Biol.Chem.* 268(14): 10593–10605
Sorimachi H *et al.* (1995) Muscle-specific calpain, p94, responsible for limb girdle muscular dystrophy type 2A, associates with connectin through IS2, a p94-specific sequence. *J.Biol. Chem.* 270(52): 31158–31162
Sorimachi H *et al.* (1997) Tissue-specific expression and α-actinin binding properties of the Z-disc titin: implications for the nature of vertebrate Z-discs. *J.Mol.Biol.* 270(5): 688–695
Soteriou A *et al.* (1993) Titin folding energy and elasticity. Proc.Biol.Sci. 254(1340): 83–86
Souquere S *et al.* (2009) Unravelling the ultrastructure of stress granules and associated P-bodies in human cells. *J.Cell.Sci.* 122(20): 3619–3626
Speer MC *et al.* (1995) Evidence for locus heterogeneity in autosomal dominant limb-girdle muscular dystrophy. *Am.J.Hum.Genet.* 57(6): 1371–1376
Speer MC *et al.* (1999) Identification of a new autosomal dominant limb-girdle muscular dystrophy locus on chromosome 7. *Am.J.Hum.Genet.* 64(2): 556–562
Spencer JA *et al.* (2000) Regulation of microtubule dynamics and myogenic differentiation by MURF, a striated muscle RING-finger protein. *J.Cell Biol.* 150(4): 771–784
Starcevic M & Dell'Angelica EC (2004) Identification of snapin and three novel proteins (BLOS1, BLOS2, and BLOS3/reduced pigmentation) as subunits of biogenesis of lysosome-related organelles complex-1 (BLOC-1). *J.Biol.Chem.* 279(27): 28393–28401
Straub RE *et al.* (2002) Genetic variation in the 6p22.3 gene *DTNBP1*, the human ortholog of the mouse dysbindin gene, is associated with schizophrenia. *Am.J.Hum.Genet.* 71(2): 337–348
Stuelsatz P *et al.* (2010) Down-regulation of MyoD by calpain 3 promotes generation of reserve cells in C2C12 myoblasts. *J.Biol.Chem.* 285(17): 12670–12683
Sun Z *et al.* (2011) Molecular determinants and genetic modifiers of aggregation and toxicity for the ALS disease protein FUS/TLS. *PLoS Biol.* 9(4): e1000614
Suominen T *et al.* (2012) Udd Distal Myopathy. In Pagon RA *et al.* (eds.) GeneReviews. University of Washington, Seattle, Seattle, WA, USA. Updated 08/23/2012, accessed 06/11/2103. Available at: http://www.ncbi.nlm.nih.gov/books/NBK1323/
Takahashi M *et al.* (2013) Stress granules inhibit apoptosis by reducing reactive oxygen species production. *Mol.Cell.Biol.* 33(4): 815–829
Takata H *et al.* (2007) A comparative proteome analysis of human metaphase chromosomes isolated from two different cell lines reveals a set of conserved chromosome-associated proteins. *Genes Cells* 12(3): 269–284
Talbot K *et al.* (2004) Dysbindin-1 is reduced in intrinsic, glutamatergic terminals of the hippocampal formation in schizophrenia. *J.Clin.Invest.* 113(9): 1353–1363
Taveau M *et al.* (2002) Quantification of splice variants using molecular beacon or scorpion primers. *Anal.Biochem.* 305(2): 227–235
Taveau M *et al.* (2003) Calpain 3 is activated through autolysis within the active site and lyses sarcomeric and sarcolemmal components. *Mol.Cell.Biol.* 23(24): 9127–9135
Tee JM & Peppelenbosch MP (2010) Anchoring skeletal muscle development and disease: the role of ankyrin repeat domain containing proteins in muscle physiology. *Crit.Rev.Biochem.Mol. Biol.* 45(4): 318–330
Thomas MG *et al.* (2011) RNA granules: the good, the bad and the ugly. *Cell.Signal.* 23(2): 324–334
Tian LF *et al.* (2006) MDM2 interacts with and downregulates a sarcomeric protein, TCAP. *Biochem.Biophys.Res.Commun.* 345(1): 355–361
Tian Q *et al.* (1991) A polyadenylate binding protein localized to the granules of cytolytic lymphocytes induces DNA fragmentation in target cells. *Cell* 67(3): 629–639
Tian Q *et al.* (1995) Fas-activated serine/threonine kinase (FAST) phosphorylates TIA-1 during Fas-mediated apoptosis. *J.Exp.Med.* 182(3): 865–874
Tkatchenko AV *et al.* (2001) Identification of altered gene expression in skeletal muscles from Duchenne muscular dystrophy patients. *Neuromuscul.Disord.* 11(3): 269–277
Torgan CE & Daniels MP (2006) Calcineurin localization in skeletal muscle offers insights into potential new targets. *J.Histochem.Cytochem.* 54(1): 119–128
Tourrière H *et al.* (2003) The RasGAP-associated endoribonuclease G3BP assembles stress granules. *J.Cell Biol.* 160(6): 823–831
Trinick J (1994) Titin and nebulin: protein rulers in muscle? *Trends Biochem.Sci.* 19(10): 405–409

Trombitás K & Granzier H (1997) Actin removal from cardiac myocytes shows that near Z line titin attaches to actin while under tension. Am.*J.Physiol.* 273(2 1): C662–70
Trombitás K *et al.* (2001) Cardiac titin isoforms are coexpressed in the half-sarcomere and extend independently. *Am.J.Physiol.Heart Circ.Physiol.* 281(4): H1793–9
Tsai NP & Wei LN (2010) RhoA/ROCK1 signaling regulates stress granule formation and apoptosis. *Cell.Signal.* 22(4): 668–675
Udd B *et al.* (1991) Muscular dystrophy with separate clinical phenotypes in a large family. *Muscle Nerve* 14(11): 1050–1058
Udd B (1992) Limb-girdle type muscular dystrophy in a large family with distal myopathy: homozygous manifestation of a dominant gene? *J.Med.Genet.* 29(6): 383–389
Udd B *et al.* (1992) Nonvacuolar myopathy in a large family with both late adult onset distal myopathy and severe proximal muscular dystrophy. *J.Neurol.Sci.* 113(2): 214–221
Udd B *et al.* (1993) Tibial muscular dystrophy. Late adult-onset distal myopathy in 66 Finnish patients. *Arch.Neurol.* 50(6): 604–608
Udd B *et al.* (1998) Tibial muscular dystrophy—from clinical description to linkage on chromosome 2q31. *Neuromuscul.Disord.* 8(5): 327–332
Udd B *et al.* (2005) Titinopathies and extension of the M-line mutation phenotype beyond distal myopathy and LGMD2J. *Neurology* 64(4): 636–642
Udd B (2013) Distal myopathies and myofibrillar myopathies. In Hilton-Jones D & Turner M (eds.) Neuromuscular Disorders (Oxford Textbooks in Clinical Neurology). Oxford University Press, Oxford, UK. In press.
Ulbricht A *et al.* (2013) Cellular mechanotransduction relies on tension-induced and chaperone-assisted autophagy. *Curr.Biol.* 23(5): 430–435
Ursitti JA *et al.* (2004) Cloning and characterization of cytokeratins 8 and 19 in adult rat striated muscle. Interaction with the dystrophin glycoprotein complex. *J.Biol.Chem.* 279(40): 41830–41838
Valtavaara M *et al.* (1997) Cloning and characterization of a novel human lysyl hydroxylase isoform highly expressed in pancreas and muscle. *J.Biol.Chem.* 272(11): 6831–6834
Van den Bergh PY *et al.* (2003) Tibial muscular dystrophy in a Belgian family. *Ann.Neurol.* 54(2): 248–251
van der Velden JL *et al.* (2008) Glycogen synthase kinase 3 suppresses myogenic differentiation through negative regulation of NFATc3. *J.Biol.Chem.* 283(1): 358–366
van der Ven PF *et al.* (2000) Characterization of muscle filamin isoforms suggests a possible role of γ-filamin/ABP-L in sarcomeric Z-disc formation. *Cell Motil.Cytoskeleton* 45(2): 149–162
Vanderweyde T *et al.* (2012) Contrasting Pathology of the Stress Granule Proteins TIA-1 and G3BP in Tauopathies. *J.Neurosci.* 32(24): 8270–8283
Vikhlyantsev IM *et al.* (2004) New titin isoforms in skeletal muscles of mammals. *Dokl.Biochem.Biophys.* 395: 111–113
Villard E *et al.* (2011) A genome-wide association study identifies two loci associated with heart failure due to dilated cardiomyopathy. *Eur.Heart J.* 32(9): 1065–1076
Vinkemeier U *et al.* (1993) The globular head domain of titin extends into the center of the sarcomeric M band. cDNA cloning, epitope mapping and immunoelectron microscopy of two titin-associated proteins. *J.Cell.Sci.* 106 (1)(1): 319–330
Voelkel T & Linke WA (2011) Conformation-regulated mechanosensory control via titin domains in cardiac muscle. *Pflugers Arch.* 462(1): 143–154
Waelter S *et al.* (2001) Accumulation of mutant huntingtin fragments in aggresome-like inclusion bodies as a result of insufficient protein degradation. *Mol.Biol.Cell* 12(5): 1393–1407
Walker MG (2001) Pharmaceutical target identification by gene expression analysis. *Mini Rev.Med.Chem.* 1(2): 197–205
Wall D *et al.* (1995) The conserved G/F motif of the DnaJ chaperone is necessary for the activation of the substrate binding properties of the DnaK chaperone. *J.Biol.Chem.* 270(5): 2139–2144
Walton JN & Nattrass FJ (1954) On the classification, natural history and treatment of the myopathies. *Brain* 77(2): 169–231
Wang K *et al.* (1979) Titin: major myofibrillar components of striated muscle. *Proc.Natl.Acad.Sci.U.S.A.* 76(8): 3698–3702
Wang Z *et al.* (2010) iCLIP predicts the dual splicing effects of TIA-RNA interactions. *PLoS Biol.* 8(10): e1000530

Watson ED *et al.* (2007) The Mrj co-chaperone mediates keratin turnover and prevents the formation of toxic inclusion bodies in trophoblast cells of the placenta. *Development* 134(9): 1809–1817
Watson ED *et al.* (2009) Neural stem cell self-renewal requires the Mrj co-chaperone. *Dev.Dyn.* 238(10): 2564–2574
Weinert S *et al.* (2006) M line-deficient titin causes cardiac lethality through impaired maturation of the sarcomere. *J.Cell Biol.* 173(4): 559–570
Welander L (1951) Myopathia distalis tarda hereditaria; 249 examined cases in 72 pedigrees. *Acta Med.Scand.Suppl.* 265: 1–124
Welander L (1957) Homozygous appearance of distal myopathy. *Acta Genet.Stat.Med.* 7(2): 321–325
Whiting A *et al.* (1989) Does titin regulate the length of muscle thick filaments? *J.Mol.Biol.* 205(1): 263–268
Williams MW & Bloch RJ (1999) Extensive but coordinated reorganization of the membrane skeleton in myofibers of dystrophic (*mdx*) mice. *J.Cell Biol.* 144(6): 1259–1270
Willis MS *et al.* (2013) Muscle ring finger 1 and muscle ring finger 2 are necessary but functionally redundant during developmental cardiac growth and regulate E2F1-mediated gene expression in vivo. *Cell Biochem.Funct.* DOI: 10.1002/cbf.2969
Witt CC *et al.* (2004) Induction and myofibrillar targeting of CARP, and suppression of the Nkx2.5 pathway in the MDM mouse with impaired titin-based signaling. *J.Mol.Biol.* 336(1): 145–154
Witt CC *et al.* (2006) Nebulin regulates thin filament length, contractility, and Z-disk structure in vivo. *EMBO J.* 25(16): 3843–3855
Witt CC *et al.* (2008) Cooperative control of striated muscle mass and metabolism by MuRF1 and MuRF2. *EMBO J.* 27(2): 350–360
Witt SH *et al.* (2005) MURF-1 and MURF-2 target a specific subset of myofibrillar proteins redundantly: towards understanding MURF-dependent muscle ubiquitination. *J.Mol.Biol.* 350(4): 713–722
Wolozin B (2012) Regulated protein aggregation: stress granules and neurodegeneration. *Mol. Neurodegener.* 7: 56-1326-7-56
Yamasaki R *et al.* (2001) Titin-actin interaction in mouse myocardium: passive tension modulation and its regulation by calcium/S100A1. *Biophys.J.* 81(4): 2297–2313
Yamasaki R *et al.* (2002) Protein kinase A phosphorylates titin's cardiac-specific N2B domain and reduces passive tension in rat cardiac myocytes. *Circ.Res.* 90(11): 1181–1188
Yamasaki S *et al.* (2007) T-cell intracellular antigen-1 (TIA-1)-induced translational silencing promotes the decay of selected mRNAs. *J.Biol.Chem.* 282(41): 30070–30077
Yan W & Craig EA (1999) The glycine-phenylalanine-rich region determines the specificity of the yeast Hsp40 Sis1. *Mol.Cell.Biol.* 19(11): 7751–7758
Young P *et al.* (1998) Molecular structure of the sarcomeric Z-disk: two types of titin interactions lead to an asymmetrical sorting of α-actinin. *EMBO J.* 17(6): 1614–1624
Young P *et al.* (2001) Obscurin, a giant sarcomeric Rho guanine nucleotide exchange factor protein involved in sarcomere assembly. *J.Cell Biol.* 154(1): 123–136
Yu C *et al.* (2007) An essential function of the SRC-3 coactivator in suppression of cytokine mRNA translation and inflammatory response. *Mol.Cell* 25(5): 765–778
Zastrow MS *et al.* (2006) Nuclear titin interacts with A- and B-type lamins in vitro and in vivo. *J.Cell.Sci.* 119(2): 239–249
Zhang T *et al.* (2005) Identification of the sequence determinants mediating the nucleo-cytoplasmic shuttling of TIAR and TIA-1 RNA-binding proteins. *J.Cell.Sci.* 118(23): 5453–5463
Zhang Y *et al.* (2008) The Hsp40 family chaperone protein DnaJB6 enhances Schlafen1 nuclear localization which is critical for promotion of cell-cycle arrest in T-cells. *Biochem.J.* 413(2): 239–250
Zou P *et al.* (2006) Palindromic assembly of the giant muscle protein titin in the sarcomeric Z-disk. *Nature* 439(7073): 229–233
Åhlberg G *et al.* (1994) Distribution of muscle degeneration in Welander distal myopathy—a magnetic resonance imaging and muscle biopsy study. *Neuromuscul.Disord.* 4(1): 55–62
Åhlberg G *et al.* (1999) Genetic linkage of Welander distal myopathy to chromosome 2p13. *Ann.Neurol.* 46(3): 399–404